UNIVERSIDADE ESTADUAL DE CAMPINAS

INSTITUTO DE BIOLOGIA

FLÁVIA MARIA LEME

"FLORAL DEVELOPMENT AND LATICIFERS IN SPECIES OF CANNABACEAE MARTINOV AND ULMACEAE MIRB."

"DESENVOLVIMENTO FLORAL E LATICÍFEROS EM ESPÉCIES DE CANNABACEAE MARTINOV E ULMACEAE MIRB. "

CAMPINAS

2018

FLÁVIA MARIA LEME

"FLORAL DEVELOPMENT AND LATICIFERS IN SPECIES OF CANNABACEAE MARTINOV AND ULMACEAE MIRB."

"DESENVOLVIMENTO FLORAL E LATICÍFEROS EM ESPÉCIES DE CANNABACEAE MARTINOV E ULMACEAE MIRB."

Thesis presented to the Institute of Biology of the University of Campinas in partial fulfillment of the requirements for the degree of doctor in Plant Biology.

Tese apresentada ao Instituto de Biologia da Universidade Estadual de Campinas como parte dos requisitos exigidos para a obtenção do Título de doutora em Biologia Vegetal.

ESTE ARQUIVO DIGITAL CORRESPONDE À VERSÃO FINAL DA TESE DEFENDIDA PELA ALUNA FLÁVIA MARIA LEME E ORIENTADA PELA SIMONE DE PÁDUA TEIXEIRA.

Orientador: Profa. Dra. Simone de Pádua Teixeira

CAMPINAS

2018

Agência(s) de fomento e nº(s) de processo(s): CAPES; CNPq, 156025/2017-5; FAPESP, 2014/07453-3

Ficha catalográfica
Universidade Estadual de Campinas
Biblioteca do Instituto de Biologia
Mara Janaina de Oliveira - CRB 8/6972

Leme, Flávia Maria, 1986-
L542f Floral development and laticifers in species of Cannabaceae Martinov and Ulmaceae Mirb. / Flávia Maria Leme. – Campinas, SP : [s.n.], 2018.

Orientador: Simone de Pádua Teixeira.
Tese (doutorado) – Universidade Estadual de Campinas, Instituto de Biologia.

1. Flores - Anatomia. 2. Flores - Morfologia. 3. Plantas – Ontogenia. 4. Estruturas secretoras. 5. Rosales. I. Teixeira, Simone de Pádua. II. Universidade Estadual de Campinas. Instituto de Biologia. III. Título.

Informações para Biblioteca Digital

Título em outro idioma: Desenvolvimento floral e laticíferos em espécies de Cannabaceae Martinov e Ulmaceae Mirb.
Palavras-chave em inglês:
Flowers - Anatomy
Flowers - Morphology
Plants - Ontogeny
Secretory structures
Rosales
Área de concentração: Biologia Vegetal
Titulação: Doutora em Biologia Vegetal
Banca examinadora:
Simone de Pádua Teixeira [Orientador]
Silvia Rodrigues Machado
Sandra Maria Carmello Guerreiro
Ângela Lúcia Bagnatori Sartori
Diego Demarco
Data de defesa: 02-08-2018
Programa de Pós-Graduação: Biologia Vegetal

Campinas, 2 de agosto de 2018.

COMISSÃO EXAMINADORA

Profa. Dra. Simone de Pádua Teixeira (Orientadora)

Profa. Dra. Silvia Rodrigues Machado

Profa. Dra. Sandra Maria Carmello Guerreiro

Profa Dra. Ângela Lúcia Bagnatori Sartori

Prof. Dr. Diego Demarco

Os membros da Comissão Examinadora acima assinaram a Ata de Defesa, que se encontra no processo de vida acadêmica do aluno.

Dedicatória

Dedico este meu trabalho de doutorado à Maria Aparecida Pereira da Cruz (D. Cida da Botânica/UFMS).

"Ainda que eu falasse línguas, as dos homens e dos anjos, se eu não tivesse o amor, seria como sino ruidoso ou como címbalo estridente. Ainda que eu tivesse o dom da profecia, o conhecimento de todos os mistérios e de toda a ciência; ainda que eu tivesse toda a fé, a ponto de transportar montanhas, se não tivesse o amor, eu não seria nada.

[....]

Agora, portanto, permanecem estas três coisas: a fé, a esperança e o amor. A maior delas, porém, é o amor."

Bíblia, I Coríntios 13

Agradecimentos

À UFMS e aos meus colegas de trabalho que concederam meu afastamento das atividades do laboratório de Botânica (INBIO/UFMS) para o desenvolvimento desta tese.

À UNICAMP e ao Programa de Pós-Graduação em Biologia Vegetal do Instituto de Biologia, pelo apoio e oportunidades concedidos.

À USP e à Faculdade de Ciências Farmacêuticas de Ribeirão Preto por conceder a infraestrutura necessária à realização do trabalho.

À FAPESP (processo 2014/07453-3), Cnpq (processo 156025/2017-5) e CAPES pelo apoio financeiro a este trabalho. À CAPES (processo 88881.133681/2016-01) pela bolsa de doutorado sanduíche no exterior concedida.

À Simone de Pádua Teixeira, pelo aceite de orientação, inspiração, paciência, e pelo auxílio e incentivo à participação em eventos e estágios no exterior. Muito Obrigado por esses quatro anos de orientação e amizade!

A todos que, de uma forma ou outra, contribuíram para as coletas realizadas durante meu doutorado: Aloysio de Pádua Teixeira, Lucélia Berbert, Francisco de Jesus, Fabio Junior Kochanovski, Sebastião Leme, Edimárcio da Silva Campos, Juliana Paulino, João Paulo Basso Alves, Thais Curry de Barros, Juca San Martin, Yannick Staedler, Antônio Carlos Moro, Maria de Lourdes Tani Leme e Luan Rodolfo Leme dos Santos.

Ao Edimárcio da Silva Campos (FCFRP/USP), José Augusto Maulin (FMRP-USP), Rodrigo Ferreira Silva (DQ-FFCLRP/USP), Maria Dolores Seabra Ferreira (FMRP/USP), Susanne Sontag (UNIVIE), e Susanne Pamperl (UNIVIE) pelo apoio técnico e solicitude.

À Maria Roseli de Melo e Líliam A. Senne, pela ajuda nos trâmites institucionais da Unicamp.

À Universidade de Viena pela infraestrutura durante o estágio no exterior (PDSE). Aos pesquisadores Dr. Yannick Staedler e Dr. Jürg Schönenberger por contribuírem nas análises de reconstrução 3D e excelentes sugestões aos capítulos de desenvolvimento floral.

Aos doutores Juliana Lischka Sampaio Mayer, André Simões e Aline Oriani, membros da banca de qualificação; e doutoras Silvia Rodrigues Machado, Rosani Arruda e Juliana Lischka Sampaio Mayer, membros da pré-banca; pelas críticas e sugestões.

Aos membros titulares e suplentes da banca examinadora, pela disponibilidade e disposição em contribuir com o trabalho.

Aos amigos do Laboratório de Botânica, Aline Rejane, Ana Paula Caetano, Carimi Cortez, Cristina Marinho, Edimárcio Campos, Giseli Pedersoli, Isabel Nascimento, Juca San Martin, Marina Costa, Pedro H. Borella, Thais de Barros e Viviane Leite, pelo auxílio e companheirismo ao longo desses anos de trabalho. Agradeço em especial à Isabel Nascimento, Cristina Marinho e Carimi Cortez pelas longas conversas e apoio em todas as horas.

Aos amigos da Unicamp, em especial Edimar Lopes, Ana Cláudia Alencar da Silva Santos e Elimar Alves de Lima, por estarem presentes nas disciplinas e auxílio durante as estadias em Barão Geraldo.

Aos meus pais, Sebastião e Maria de Lourdes, por me ensinarem que tudo é possível atráves do trabalho e esforço, e apoio em todos os momentos. Aos meus irmãos Simone e Adriano, ao meu querido sobrinho Luan Rodolfo, ao meu namorado Antônio Carlos, e ao amigo Jorge Luiz, pela amizade e bons momentos. Obrigada, família!

Abstract

Cannabaceae and Ulmaceae together with Moraceae and Urticaceae form the Urticalean rosid clade, comprised in the Rosales order. Their flowers are wind-pollinated, reduced, monochlamydeous, diclinous, with a pseudomonomerous gynoecium. The presence of laticifers was only reported to Moraceae and Urticaceae, constituting synapomorphies for these families. For Ulmaceae, no laticifers were reported and for Cannabaceae, observations are restricted to *Cannabis sativa* and *Humulus lupulus*. Thus, our objective was to study the morphology of developing flower in species of Cannabaceae and Ulmaceae, in order to understand the processes involved in the floral reduction and to check the breeding system (if andromonoecy, monoecy or dioecy). Beyond that, we extended the study to laticifer morphology and distribution in order to review the synapomorphies raised for the Urticalean clade. Nine species of Cannabaceae and two of Ulmaceae were analysed: *Cannabis sativa, Celtis brasiliensis, C. ehrembergiana, C. iguanaea, C. occidentalis*, *C. pubescens*, *C. sinensis, Pteroceltis tatarinowii, Trema micrantha* (Cannabaceae), *Ampelocera glabra* and *Zelkova serrata* (Ulmaceae). Floral buds and flowers were processed for surface (scanning electron microscopy) and histological (light microscopy) examinations, and carry out 3D reconstructions of flower vasculature (High Resolution X-Ray Computed Tomography). Samples of shoot apex, floral apex, stems, leaves and flowers were also processed for laticifer anatomy, distribution, histochemistry, ultrastructure and cytochemical locatization of pectinase and cellulase. *Celtis* species (Cannabaceae) and *Ampelocera glabra* (Ulmaceae) are monoecious, and *Cannabis sativa* and *Trema micrantha* (Cannabaceae) are dioecious. All species have two floral morph types, pistillate and staminate. In pistillate flowers, the staminodes have no pollen or have unviable pollen. In staminate flower, the pistillode can be inflated and participates in an interesting mechanism of explosive release of pollen. The main processes that lead to the floral reduction in Cannabaceae and Ulmaceae are: (1) absence of organs or whorls from inception, resulting in apetalous and diclinous flowers and low number of organs per whorl, and (2) abortion of all stamens, all carpels or at least one carpel, resulting in diclinous flowers with a pseudomonomerous gynoecium. The aborted carpel exhibits reduced vascularization and does not form an ovule. In Ulmaceae, the flowers of *Ampelocera glabra* have no hypanthium and the atypical merism is associated to the space left by reduction of the whorls and of organs. Laticifers are of the articulated type and are found in all analysed species, a novelty for Ulmaceae and for *Celtis*,

Pteroceltis and *Trema*, genera of Cannabaceae. The wide distribution of laticifers and occurrence of starch and terpenes in the latex are by the first time described for these families. The laticifer of *Cannabis sativa, Celtis pubescens* and *Trema micrantha* are similar in ultrastructure and, probably, produces the same chemical classes of compounds, playing an important role in the protection of floral organs in this group of plants. The cellulase and pectinase activities were identified in the cell walls of the laticifers indicating their importance during the formation of the laticifer. Concluding, the laticifers widely occur in the Urticalean clade and can be considered a synapomorphy of the clade. Ontogenic processes leading to floral reduction in Cannabaceae and in Ulmaceae can be interpreted as products of selective pressures imposed by anemophyly.

Key words: *Ampelocera, Cannabis*, *Celtis*, floral morphology, floral ontogeny, pseudomonomerous gynoecium, *Trema*, vascularization, *Zelkova*.

Resumo

Cannabaceae e Ulmaceae juntamente com Moraceae e Urticaceae formam o clado Urticoide, da ordem Rosales. Suas flores são polinizadas pelo vento, reduzidas, monoclamídeas, díclinas, com gineceu pseudomonômero. A presença de laticíferos foi registrada para Moraceae e Urticaceae, constituindo sinapomorfia, para estas famílias. Para Ulmaceae, não há registros de laticíferos e, em Cannabaceae, as observações são restritas a *Cannabis sativa* e *Humulus lupulus*. Assim, o objetivo deste trabalho foi estudar a morfologia da flor em desenvolvimento em espécies de Cannabaceae e Ulmaceae, a fim de entender os processos envolvidos na redução floral e verificar o sistema reprodutivo (se andromonoico, monoico ou dioico). Além disto, estendemos o estudo aos laticíferos a fim de revisar as sinapomorfias consideradas para o clado urticoide. Nove espécies de Cannabaceae e duas de Ulmaceae foram analisadas: *Cannabis sativa, Celtis brasiliensis, C. ehrembergiana, C. iguanaea, C. occidentalis*, *C. pubescens, C. sinensis, Pteroceltis tatarinowii, Trema micrantha* (Cannabaceae), *Ampelocera glabra* e *Zelkova serrata* (Ulmaceae). Botões florais e flores foram processados para análises de superfície (microscopia eletrônica de varredura) e histológicas (microscopia de luz), e realizadas reconstruções 3D da vascularização (tomografia computadorizada de alta resolução em raio X). Amostras de gemas vegetativas, gemas florais, caule, folhas e flores de algumas das espécies também foram processadas para análises anatômicas, histoquímicas, ultraestruturais e citoquímicas (atividade da pectinase e celulase) dos laticiferos. As espécies de *Celtis* (Cannabaceae) e *A. glabra* (Ulmaceae) são monoicas, e *Cannabis sativa* e *Trema micrantha* (Cannabaceae) são dioicas. Todas as espécies possuem dois morfotipos florais, o pistilado e o estaminado. Nas flores pistiladas, os estaminódios não tem pólen ou os grãos de pólen são atípicos. Nas flores estaminadas o pistilódio pode ser inflado e participar de um interessante mecanismo de liberação explosiva do pólen. Os principais processos que levam à redução floral em Cannabaceae e Ulmaceae são: (1) ausência de órgãos ou de verticilos inteiros desde o início do desenvolvimento, resultando em flores apétalas e díclinas, com número baixo de órgãos por verticilo, e (2) aborto do androceu, do gineceu ou de um dos carpelos, resultando em flores díclinas com gineceu pseudomonômero. O carpelo abortado possui vascularização reduzida e não forma óvulo. Em Ulmaceae, as flores de *Ampelocera glabra* não exibem hipanto e o merisma atípico está associado com o espaço deixado pela ausência de verticilos e órgãos. Os laticíferos são do tipo articulado e estão presentes em todas as espécies analisadas, uma novidade para

Ulmaceae e para *Celtis*, *Pteroceltis* e *Trema*, gêneros de Cannabaceae. Sua ampla distribuição e ocorrência de grãos de amido e terpenos no látex são, pela primeira vez, descritos para essas famílias. Os laticíferos de *Cannabis sativa*, *Celtis pubescens* e *Trema micrantha* são similares em ultraestrutura e, provavelmente, produzem a mesma classe de compostos químicos, e parecem ter uma função importante na proteção dos órgãos florais. As atividades da celulase e pectinase foram identificadas na parede celular dos laticíferos indicando sua importância durante a formação do laticífero. Conclui-se que laticíferos ocorrem amplamente no clado Urticoide e sua presença pode ser considerada uma sinapomorfia do clado. Os processos ontogênicos que levam à redução floral em Cannabaceae e em Ulmaceae podem ser interpretados como produtos de pressões seletivas impostas pela anemofilia.

Palavras-chave: *Ampelocera*, *Cannabis*, *Celtis*, gineceu pseudomonômero, morfologia floral, ontogenia floral, *Trema*, vascularização, *Zelkova*.

Summary

Introduction

Cannabaceae and Ulmaceae belong to the Urticalean clade of the Rosales order (APG IV 2016) (Fig. 1). Rosales comprises nine families (APG IV 2016) that are widely distributed in tropical and temperate regions. Its economic importance is well-known, illustrated by the aesthetic use of Rosaceae species (Judd et al. 2009) and medicinal and recreational use of Cannabaceae species (Schultes 1976; Fleming and Clarke 1998; Ashton 2001; Zanoli and Zavatti 2008; Judd et al. 2009; Small 2017).

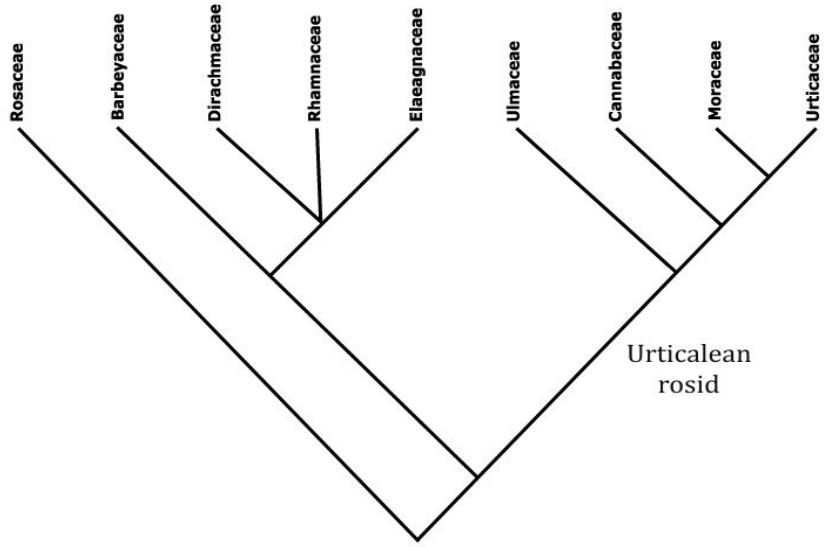

Figure 1 Representation of the phylogenetic tree of Rosales, evidencing the relationship among the families and the Urticalean rosids (= Urticalean clade). Fonte: http://www.mobot.org/mobot/research/apweb/orders/rosalesweb.

Cannabaceae, Moraceae, Ulmaceae and Urticaceae form the Urticalean clade (Sytsma et al. 2002) that together with Rosaceae are considered the two species-richest groups of Rosales (ca. of 2.586 species and c.a. of 4.828 species, respectively, The Plant List 2013). Rosaceae holds the type-genus *Rosa* with exuberant flowers in structure and colors (Judd et al. 2009). Flowers are pentamerous, with two perianth whorls, two whorls of stamens or more and gynoecium with three or more carpels (Judd et al. 2009). Urticalean clade is characterized by having globose cystoliths and leaves with urticoid teeth (Judd et al. 2009). Unlike Rosaceae, flowers of Urticalean rosids are inconspicuous, usually green, with three or two whorls (a perianth and an androecium and/or gynoecium), usually with five or fewer stamens, two carpels and

unilocullate or bilocullate ovary with a single apical ovule (Bechtel 1921; Berg 1977, 1989; Judd et al. 2009).

Cannabaceae comprises 109 species distributed in 10 genera (Yang et al. 2013). *Cannabis sativa* L. and *Humulus lupulus* L. are the most known species with high economic values, used mainly in the medicine and recreation (Measham et al. 1994; Miligan et al. 1999; Ashton 2001; Honório et al. 2006; Zanoli & Zavatti 2008; Hill et al. 2010). The other eight genera (*Aphananthe, Celtis, Chaetachme, Gironniera, Lozanella, Parasponia, Pteroceltis* and *Trema*) belonged to Ulmaceae but were inserted in Cannabaceae in 2002 after many morphological and molecular studies (Oginuma et al. 1990; Tobe and Takaso 1996; Zavada and Kim 1996; Ueda et al. 1997; Sytsma et al. 2002). The flowers of Cannabaceae are diclinous, inconspicuous, with four or five lobes of the perianth, four or five stamens and two connate carpels (Bechtel 1921; Judd et al. 2009), interpreted as pseudomonomerous gynoecium (gynoecium formed of two carpels but with only one single locule and one ovule suggesting a single carpel) (Eckardt 1937; Omori and Terabayashi 1993).

Ulmaceae is a sister group of the other Urticalean rosids (Sytsma et al. 2002), and comprises 64 species distributed in the follow seven genera: *Ampelocera, Hemiptelea, Holoptelea, Planera, Phyllostylon, Ulmus* and *Zelkova* (Neubig et al. 2012). They have flowers usually perfect, inconspicuous, with a hypanthium, a whorl of perianth, four to nine lobes of the perianth, four to nine stamens and two connate carpels (Bechtel 1921; Judd et al. 2009), forming the pseudomonomerous gynoecium (Eckardt 1937; Chernik 1981; Fukuoka 1982; Okamoto et al. 1992).

The floral morphology of the two largest groups of Rosales is distinct and are surprising the floral diversity and reduced flowers of the Urticalean rosids (Bechtel 1921; Berg 1977, 1989). In Cannabaceae and especially Ulmaceae the variation in merism of the perianth and stamens is notable. The pseudomonomerous gynoecium was reported in species of the four families of the Urticalean clade, but morphological studies are rare and very old (Payer 1857; Briosi and Tognini 1894; Bechtel 1921; Eckardt 1937), resulting in a poorly understood structure so far. A more recent study

was performed with *Humulus lupulus* (Shephard et al. 2000), a Cannabaceae species of economic value.

The secretory structures of Cannabaceae have been object of more detailed studies because of the presence of cannabinoids into secretory trichomes and laticifers of *Cannabis sativa* (Turner et al. 1980, 1981; Furr and Mahlberg 1981; Happyana et al. 2013). Although the presence of laticifers are a remarkable feature of *Cannabis* (the genus was previously inserted in Moraceae because of it - Judd 1994), they are little studied structures in the group. Even the presence of cannabinoids in the latex has not instigated researches to study laticifer morphology and latex composition in the family. Only three studies were realized with laticifers in Cannabaceae: two with *Cannabis sativa* about histochemistry (Furr and Mahlberg 1981) and ultrastructure (Mesquita and Dias 1984), and one with *Humulus lupulus* that only illustrates the presence of laticifers in the stems (Hagel et al. 2008). In Ulmaceae and in the other genera inserted recently in Cannabaceae, as *Aphananthe, Celtis, Chaetachme, Gironniera, Lozanella, Parasponia, Pteroceltis* and *Trema,* laticifers are considered absent (Sytsma et al. 2002; Judd et al. 2009).

The present study sought to analyse the floral development of eight species of Cannabaceae and one of Ulmaceae, intending to increase the knowledge of the diversity of floral morphology in Rosales and Urticalean rosids, bringing information that elucidates the floral reduction processes and the structure of the pseudomonomerous gynoecium. The floral anatomical analysis of Cannabaceae and Ulmaceae species allowed us to identify the presence of laticifers in these families. Thus, studies of morphology and distribution of the laticifers and of the latex composition were also carried out for four species of Cannabaceae and two species of Ulmaceae, bringing novelties to the genera and families. In addition, the ultrastructure and cytochemical localization (pectinase and cellulase activities) were analysed in laticifers of two species of Cannabaceae.

Table 1 Analysed species of Cannabaceae and Ulmaceae, and studies carried out with each species. Symbol: FD= Floral development (buds and anthetic flower); FM= Floral morphology (anthetic flower); V= Vascularization; L= Morphology, distribution and latex composition of the laticifers; LU= Laticifer ultrastructure; LC= Laticifer cytochemistry.

Species	FD	FM	V	L	LU	LC
Cannabaceae						
Cannabis sativa L.	X	X	X	X		
Celtis brasiliensis (Gardner) Planch.	X	X	X			
Celtis ehrembergiana (Klotzsch) Liebm.	X	X	X			
Celtis iguanaea (Jacq.) Sarg.	X	X	X			
Celtis occidentalis L.		X	X			
Celtis pubescens Spreng	X	X	X	X	X	X
Celtis sinensis Pers.		X	X			
Pteroceltis tatarinowii Maxim.				X		
Trema micrantha (L.) Blume	X	X	X	X	X	X
Ulmaceae						
Ampelocera glabra Kuhlm.	X	X	X	X		
Zelkova serrata (Thunb.) Makino				X		

Therefore, the thesis was organized in five chapters, three about floral development and two about laticifer morphology and distribution. The studies on floral development were realized in partnership with two Austrians researchers, Dr. Jürg Schönenberger and Dr. Yannick M. Staedler, from Vienna University, during a short internship abroad, and allowed the elaboration of the following chapters:

1. **"Comparative floral development reveals novel aspects of structure and diversity of Cannabaceae flowers"**. In this chapter, we compared the floral development of three species of Cannabaceae, *Cannabis sativa*, *Celtis iguanaea* and *Trema micrantha* in order to understand the origin of the floral reduction and the pathways that lead the polygamy in the group. This study will be submitted to 'American Journal of Botany'.
2. **"Ontogeny and vascularization elucidate the atypical floral structure of *Ampelocera glabra* Kuhlm., a tropical species of Ulmaceae"**. In this chapter, we analysed the floral ontogeny and vascularization of a tropical species of Ulmaceae, *Ampelocera glabra*, aiming to elucidate the atypical merism and the reduced structure of the whorls. This study is currently in press in the 'International Journal of Plant Sciences'.

3. **"Floral comparative development and morphology clarify floral reduction and indicate the occurrence of monoecy in *Celtis* (Cannabaceae)".** In this chapter, we studied the morphology of developing flowers of six species of *Celtis* (*Celtis brasiliensis, C. ehrembergiana, C. iguanaea, C. occidentalis*, *C. pubescens* and *C. sinensis*) to check the occurrence of andromonoecy and to understand the formation of such a reduced flower. This study will be submitted to 'Botanical Journal of the Linnean Society'.

The data obtained for laticifers were organized by family and resulted in two chapters:

4. **"First record of laticifers in Ulmaceae"**. In this chapter, we reported laticifers for the first time in Ulmaceae, using two species as models: a Neotropical species *Ampelocera glabra* and an Asian temperate species *Zelkova serrata*. We checked laticifer distribution, morphology and the latex composition. This study possibly will be submitted to 'Botanical Journal of the Linnean Society'.
5. **"Expanding the laticifer knowledge in Cannabaceae: distribution, morphology and latex composition"**. In this chapter the aims were to check the occurrence of laticifers and to analyse their morphology and distribution, and the main classes of compounds of the latex in three species of three different genera of Cannabaceae (*Celtis pubescens*, *Pteroceltis tatarinowii* and *Trema micrantha*). Laticifers of *Cannabis sativa* were also analysed for comparison purposes. Laticifer ultrastructure and cytochemical localization of pectinase and cellulase were also analysed in order to better understand the laticifer structure and growth. We intent to submit this study to 'Protoplama'.

References

APG IV. 2016. An update of the Angiosperm Phylogeny Group classification for the orders and families of flowering plants: APG IV. *Botanical Journal of the Linnean Society* 181: 1-20.

Ashton CH. 2001. Pharmacology and effects of *Cannabis*: a brief review. *British Journal of Psychiatry* 178: 101–106.

Bechtel AR. 1921. The floral anatomy of the Urticales. *American Journal of Botanical* 8: 386-410.

Berg CC. 1977. Urticales, their differentiation and systematic position. *Plant Systematics and Evolution* 1: 349-374.

Berg CC. 1989. Systematic and phylogeny of the Urticales. In: *Evolution, systematics, and fossil history of the Hamamelidae*. Oxford, UK: Clarendon Press, 193-219.

Briosi G, Tognini F. 1894. *Anatomia Della Canapa (Cannabis sativa* L.*)*. Milano: Istituto Botanico Della R. Universitá Di Pavia.

Chernik VV. 1981. Pseudomonemeric gynoecium of the Ulmaceae and Celtidaceae representatives. *Botanicheskii Zhurnal (Moscow & Leningrad)* 7: 958-966.

Eckardt T. 1937. Untersuchungen uber Morphologie, Entwicklungsgeschichte und systematische Bedeutung des pseudomonomeren Gynoeceums. *Nova Acta Leopold* 5: 1-112.

Fleming MP, Clarke RC. 1998. Physical evidence for the antiquity of *Cannabis sativa* L. (Cannabaceae). *Journal of the International Hemp Association* 5: 80-92.

Fukuoka N. 1982. On pseudomonomerous pistil of the Ulmaceae. *Acta Phytotax. Geobot.* 56: 84-91.

Furr M, Mahlberg PG. 1981. Histochemical analyses of laticifers and glandular trichomes in *Cannabis sativa*. *Journal of Natural Products* 44: 153–159.

Hagel JM, Yeung EC, PJ Facchini. 2008. Got milk ? The secret life of laticifers. *Trends in Plant Science*: 1360–1385.

Happyana N, Agnolet S, Muntendam R, Van Dam A, Schneider B, O Kayser. 2013. Analysis of cannabinoids in laser-microdissected trichomes of medicinal *Cannabis sativa* using LCMS and cryogenic NMR. *Phytochemistry* 87: 51-59.

Hill MN, Patel S, Campolongo P, Tasker JG, Wotjak CT, Bains JS. 2010. Functional interactions between stress and the endocannabinoid system: from synaptic signaling to behavioral output. *Journal of Neuroscience* 30: 14980–14986.

Honório KM, Arroio A, Silva ABF. 2006. Aspectos terapêuticos de compostos da planta *Cannabis sativa*. *Quimica Nova* 29: 318–325.

Judd WS, Sanders RW, Donoghue MJ. 1994. Angiosperm family pairs: preliminary phylogenetic analyses. Harvard Papers in Botany N 5:1-51.

Judd WS, CS Campbell, EA Kellogg, PF Stevens, Donoghue MJ. 2009. Sistemática vegetal. Um enfoque filogenético. Artmed, Porto Alegre, Brazil.

Measham F, Newcombe R, Parker H. 1994. The normalization of recreational drug use amongst young people in North-West England. *British Journal of Sociology* 45: 287-312.

Mesquita JF, Dias JDS. 1984. Ultrastructural and cytochemical study of the laticifers of *Cannabis sativa* L. *Bol. Soc. Brot.* 57: 337–356.

Milligan SR, Kalita JC, Heyerick A, Rong H, Cooman L, Keukeleire D. 1999. Identification of a potent phytoestrogen in hops (*Humulus lupulus* L.) and beer. *The Journal of Clinical Endocrinology & Metabolism* 83: 2249-2252.

Neubig K, Herrera F, Manchester SR, Abbott JR. 2012. Fossils, biogeography and dates in an expanded phylogeny of Ulmaceae. Botany 2012: Annual Meeting of the Botanical Society of America in Columbus, Ohio, USA.

Oginuma K, Raven PH, Tobe H. 1990. Karyomorphology and relationships of Celtidaceae and Ulmaceae (Urticales). The Bot Mag 103:113-131.

Okamoto M, Kosuge K, Fukuoka N. 1992. Pistil development and parietal placentation in the pseudomonomerous ovary of *Zelkova serrata* (Ulmaceae). *Acta Oecologica* 79: 921-927.

Omori Y, Terabayashi S. 1993. Gynoecial vascular anatomy and its systematic

implications in Celtidaceae and Ulmaceae (Urticales). J Pl Res 106:249-258.

Payer, J. B. 1857. Traité D'Organogéne Comparée de La Fleur. Paris: Librairie de Victor Masson.

Schultes R. 1976. *Hallucinogenic Plants*. Golden Press. New York. 160p.

Small E. 2017. *Cannabis: a complete guide*. Boca Raton: Taylor & Francis. 504p.

Shephard HL, Parker JS, Darby P, Ainsworth CC. 2000. Sexual development and sex chromosomes in hop. *New Phytologist* 148: 397-411.

Sytsma KJ, Morawetz J, Pires JC, Nepokroeff M, Conti E, Zjhra M, Hall JC, Chase MW. 2002. Urticalean Rosids: Circumscription, Rosid ancestry, and phylogenetics based on rbcL, trnL-F, and ndhF sequences. *Am J Bot* 89(9): 1531-1546.

The Plant List 2013. Version 1.1. Published on the Internet; http://www.theplantlist.org/ Acesso em 05 de fevereiro de 2018.

Tobe H, Takaso T. 1996. Trichome micromorphology in Celtidaceae and Ulmaceae (Urticales). Acta Phytotax. Geobot. 47: 153–168.

Turner JC, Hemphill JK, Mahlberg PG. 1980. Trichomes and Cannabinoid Content of Developing Leaves and Bracts of *Cannabis sativa* L. (Cannabaceae). *American Journal of Botany* 67: 1397-1406.

Turner JC, Hemphill JK, Mahlberg PG. 1981. Interrelationships of glandular trichomes and cannabinoid content. I: Developing pistillate bracts of *Cannabis sativa* L. (Cannabaceae). *Bulletin on Narcotics* 33: 59-69.

Ueda K, Kosuge K, Tobe H. 1997. A Molecular phylogeny of Celtidaceae and Ulmaceae (Urticales) based on rbcL nucleotide sequences. *Journal of Plant Research* 110: 171–178.

Zanoli P, Zavatti M. 2008. Pharmacognostic and pharmacological profile of *Humulus lupulus* L. Journal of Ethnopharmacology 116: 383-396.

Zavada MS, Kim M. 1996. Phylogenetic analysis of Ulmaceae. Plant Systematics and Evolution 200: 13–20.

Yang M-Q, Van Velzen R, Bakker FT, Sattarian A, Li D, Yi T. 2013. Molecular phylogenetics and character evolution of Cannabaceae. Taxon 62: 473-485.

"Caminhos não há, mas os pés na grama os inventarão"

Ferreira Gullar

CHAPTER 1: 'COMPARATIVE FLORAL DEVELOPMENT REVEALS NOVEL ASPECTS OF STRUCTURE AND DIVERSITY OF CANNABACEAE FLOWERS'

Chapter 1: Comparative floral development reveals novel aspects of structure and diversity of Cannabaceae flowers

1.1 Abstract

Cannabaceae have inconspicuous and reduced flowers that are functionally pistillate or staminate, with a single whorled perianth and a pseudomonomerous gynoecium. Our objective is to understand the developmental processes that lead to such a reduced flower morphology in *Cannabis sativa, Celtis iguanaea* and *Trema micrantha*. Floral buds in several developmental stages and anthetic flowers were processed for surface (scanning electron microscopy) and histological (microtome sections, light microscopy) examinations. In addition, we used High Resolution X-Ray Computed Tomography (HRXCT) for 3D reconstructions of vascular anatomy. The only whorl of perianth organs in Cannabaceae is homologous to the calyx of related taxa in Rosales. Petals are absent from inception in all the studied species. The dicliny is established through different ontogenetic processes: stamens and carpels may be absent from floral inception (*Cannabis sativa*), or may be present during early stages and then be aborted (*Trema micrantha*) or be aborted during later stages (*Celtis iguanaea*). Further, we confirm the bicarpellate but pseudomonomerous nature of the gynoecium, which is initiated as a single, congenitally united primordium. The unilocular ovary contains a single ovule that is formed before carpel closure. Glandular trichomes are widely distributed on the bracts, receptacle, sepals and anther connectives of the flowers. Special floral features shared by Cannabaceae species include a spiral sequence of sepal initiation, precocious ovule development, and sepals vascularized by only one bundle. Our study provides a view of floral development and structure of Cannabaceae, taking into account the recent, molecular-based phylogenetic and taxonomic circumscription of the family and related groups in the order Rosales.

Key words: anatomy, *Cannabis sativa*, *Celtis iguanaea*, floral morphology, glandular trichomes, *Trema micrantha*.

1.2 Introduction

The flowers of the popularly known family Cannabaceae are generally small and reduced, with only one whorl of perianth organs. In addition, the flowers are functionally pistillate or staminate in most species (Bechtel, 1921; Berg, 1989), not visually attractive, and generally considered to be wind pollinated (Berg, 1977). The family is relatively poor in number of species (~109) and genera (~10) (Yang et al., 2013), with hemp (*Cannabis sativa* L.) undoubtedly being the species of greatest economic interest because of its pharmacological properties (Measham et al., 1994; Fleming and Clarke, 1998; Ware and Tawfik, 2005), followed by hop (*Humulus lupulus* L.), a species used as a beer flavoring, and with sedative and antiseptic properties (Zanoli and Zavatti, 2008).

The current taxonomic circumscription of the family is largely based on molecular phylogenetic analyses (Sytsma et al., 2002; Yang et al., 2013), now including, in addition to *Cannabis* and *Humulus*, also *Aphananthe, Celtis, Chaetachme, Gironniera, Lozanella, Parasponia, Pteroceltis,* and *Trema*. These latter genera were formerly classified in the subfamily Celtidoideae of Ulmaceae (Cronquist, 1988). With the new circumscription, *Celtis* and *Trema* are the largest genera in Cannabaceae, with 73 and 12 species, respectively (Yang et al., 2013).

Current understanding of floral development and structure, especially with respect to the reduced and apparently simple floral morphology of Cannabaceae, is quite limited. Earlier studies of floral development have largely focused on widely cultivated species such as *Cannabis sativa* (Payer, 1857; Briosi and Tognini, 1894) and *Humulus lupulus* (Leins and Orth, 1979; Shephard et al., 2000). However, in spite of these early efforts, many gaps still exist in our understanding of the floral organization of this family whose flowers appear quite different from related families in the order Rosales, to which Cannabaceae belong (APG IV, 2016).

A remarkable feature of some species of Cannabaceae such as *Trema micrantha* (L.) Blume and *Cannabis sativa* is that different floral morph types (pistillate, staminate and apparently perfect flowers) occur on the same individual. Thus, these

species are considered polygamous (Torres, 1996; Yang et al., 2013). Still, an individual plant may initially produce only staminate flowers and, at the end of blossoming, it can produce pistillate flowers (Torres, 1996). In *Cannabis sativa*, this phenomenon is attributed to the production of certain phytoregulators (Heslop-Harrison, 1956; Ram and Jaiswal, 1972) or to environmental factors (Hirata, 1927; Nigam et al., 1981).

Thus, our goal was to study the floral development of three species of Cannabaceae (*Cannabis sativa* L., *Celtis iguanaea* (Jacq.) Sarg. and *Trema micrantha* (L.) Blume) in order to understand the origin of their reduced floral morphology and the developmental pathways leading to polygamy in the group. We compare our results to those reported in the literature for *Humulus lupulus* (Shephard et al., 2000) and earlier work on *Cannabis sativa* (Payer, 1857; Briosi and Tognini, 1894). Understanding the developmental pathways of Cannabaceae flowers will contribute to expanding the knowledge about the floral diversity and floral evolution of Rosales.

1.3 Materials and methods

Floral buds in different developmental stages and mature flowers of *Cannabis sativa, Celtis iguanaea* and *Trema micrantha* were obtained in the field and from herbarium specimens (Table 1). Vouchers are deposited in the SPFR herbarium (FFCLRP / USP) (Table 1).

The samples collected in the field were fixed in buffered neutral formalin (Lillie, 1965) or in Karnovsky's solution (McDowell and Trump, 1976). The herbarium samples were rehydrated in heated distilled water and then treated overnight with 2% KOH (Smith and Smith, 1942). Both types of samples were dehydrated in an ethanol series up to 70% and stored for further processing and observation by light microscopy (LM), scanning electron microscopy (SEM) and high resolution x-ray computed tomography (HRXCT).

For LM observation, samples were dehydrated up to 95% and embedded in historesin (Leica), cut into 1.5 μm thick transverse or longitudinal sections with a rotary microtome, stained with 0.05% Toluidine Blue in phosphate buffer, pH 5.8

(O'Brien et al., 1964), and finally mounted on synthetic resin. The photomicrographs were obtained with a Leica DM 5000 B photomicroscope coupled to a Leica DFC 295 digital camera.

For SEM observations, samples were dissected under a stereomicroscope, dehydrated in an ethanol series, critical point dried in a Bal Tec CPD 030, mounted on metal supports on carbon adhesive tape, and sputtered with gold in a Bal Tec SCD 050. Electron micrographs were obtained with a Zeiss EVO-50 scanning electron microscope at 20 kv.

For HRXCT, anthetic pistillate flowers were treated with a solution of 1% phosphotungstic acid in 70% ethanol for one week (Staedler et al., 2013), dehydrated in an ethanol series with 1% phosphotungstic acid (as a contrasting agent), critically point dried (Autosamdri-815), mounted on an aluminum holder with two-component epoxy glue (UHU Plus Epoxy: Binder + Hardener) and scanned. The scans were performed on a MicroXCT-200 imaging system (Zeiss Microscopy) with a L9421-02 90kV Microfocus X-ray (MFX) source (Hamamatsu Photonics, Iwata City, Japan), using the following settings: acceleration voltage, 25 kV; source current, 200 μA; exposure time, 15 s; pictures per sample, 1200; camera binning, 2; optical magnification 10 x, with pixel sizes of 4.3 μm and 1.0 μm, respectively. The total exposure time was approximately 10 hours for each sample. The software XMReconstructor 8.1.6599 (Zeiss Microscopy) was used to perform the 3D reconstruction from the scanning data. The AMIRA-based XM3DViewer 1.1.6 (Zeiss Microscopy) was used for the visualization of the scan data.

Table 1. Information on the Cannabaceae species sampled.

Species	Sample source	Voucher
Cannabis sativa	Herbarium ESA, Piracicaba, SP, Brazil.	G.M Tenório nº 5 (123034), G.A Ogasawara nº 20 (119653), O. Marilia nº 13433 (68853), J.A. Zandoval nº 102 (13268).
	Herbarium IAC, Campinas, SP, Brazil.	A.S. Lima s/nº (24827), A.P. Viégas s/nº (3881), C. Pacheco s/nº (18681).
	Herbarium RBR, Rio de Janeiro, RJ, Brazil.	RBR 4839
Celtis iguanaea	USP campus, Ribeirão Preto, SP, Brazil.	F.M. Leme nº 99 (16045) and 106 (16044).
Trema micrantha	USP campus, Ribeirão Preto, SP, Brazil.	F.M. Leme nº 94 (15957), 97 (16306) and 101 (15958).
	Base de Estudos do Pantanal, UFMS, Miranda, MS, Brazil.	F.M. Leme nº 92 (15959) and 93 (15960).

1.4 Results

Floral organization during pre-anthesis and anthesis

Cannabis sativa is a dioecious herb with either staminate (Fig. 1A-C) or pistillate (Fig. 1D, E) floral morph types. The apetalous flowers are subtended by a bract and two prophylls in staminate flowers (Fig. 1C), and a bract in pistillate flowers (Fig. 1E). The staminate flower is up to 7 mm in length and 6 mm in width, the pedicel reaches about 6.5 mm in length at anthesis (Fig. 1B). It has five free sepals and five stamens (Fig. 1C); the stamens are opposite to the sepals. Calyx aestivation is quincuncial (Fig. 1C). The stamen filament is very thin (Fig. 1B). Anthers are lanceolate, basifixed and dehiscence is latrorse. The pistillate flower can reach up to 6.6 mm in length and 0.6 mm in width. The subtending bract (Fig. 1E) completely envelopes the flower during pre-anthesis and also at anthesis (Fig. 1D, E); only the stigma is exerted at anthesis (Fig. 1D). The calyx is synsepalous, dimerous and covers approximately the lowermost third of the ovary at anthesis (Figs. 1D, E; 3H). The pistil is formed by two syncarpous carpels with a bifid stigma; the ovary is unilocular and uniovulate (Figs. 1E, 3).

Celtis iguanaea is a monoecious shrub with either functionally staminate (Fig. 1F-H) and functionally pistillate (Fig. 1I, J) floral morph types. The flowers are subtended by a bract and twoprophylls (Fig. 1H, J). They are apetalous, with five green free sepals with quincuncial aestivation (Fig. 1H, J). The functionally staminate flower

is up to 3 mm long and 5 mm wide (Fig. 1G). It has sepals with a more pronouncedly convex shape that are partly covering and protecting the stamens even at anthesis (Fig. 1F, G). It has five stamens, opposite to the sepals (Fig. 1F-H), with inflexed filaments in bud (Fig. 1F, G). The filaments straighten and elongate in the beginning of anthesis and the anthers open above the level of the sepals (Fig. 1G). Anthers are sagittate, slightly dorsifixed (filament is inserted a little above of the connective basis) and dehiscence is latrorse to slightly extrorse (Fig. 1F, G). There is a central pistillode (Fig. 1H). The functionally pistillate flower is 7 mm long and 3 mm wide (Fig. 1I). It has five free sepals that form a cup-like structure around the ovary (Fig. 1I). It has five staminodes (Fig. 1J) with short filaments and a central pistil (Fig. 1I, J) with a short style and two bifid, papillate stigmatic lobes (Fig. 1I). The pistil is formed by two carpels; the ovary is unilocular and uniovulate (Fig. 1J).

Trema micrantha is a dioecious tree with either functionally staminate (Fig. 1K-M) and pistillate (Fig. 1N, O) floral morph types. The flowers are subtended by a bract and two prophylls (Fig. 1M, O). They are apetalous, with five green, free sepals that have with quincuncial aestivation (Fig. 1M, O). The functionally staminate flower is approximately 2.5 mm long by 5.6 mm wide (Fig. 1K, L). It has five free sepals with a pronouncedly convex shape thus protecting the stamens (Fig. 1K, L). The five stamens are inflexed before anthesis, positioned opposite to the sepals (Fig. 1L, M), each of which tightly enveloped by the sepals in bud (Fig. 1K). The filaments straighten and elongate in the beginning of anthesis and the anthers open above the level of the sepals (Fig. 1L). Anthers are sagittate, slightly dorsifixed (filament is inserted a little above of the connective basis) and dehiscence is latrorse (Fig. 1K). There is a central pistillode with simple trichomes at its base (Fig. 1L, M). The pistillode is similar to a young pistil but without a stigma and an ovule (Fig. 1L, M). The pistillate flower is 4 mm long by 1.5 mm wide (Fig. 1N). It has five sepals that form a cup-like structure around the ovary (Fig. 1N), but the sepals are united only at the very base (Fig. 1O). There are five vestigial staminodes (Fig. 1O), without differentiation of anthers and

filaments, and a central pistil that has a sessile, papillate, bifid stigma (Fig. 1N). The pistil is formed by two carpels; the ovary is unilocular and uniovulate (Fig. 1O).

Floral development

Staminate flower of *Cannabis sativa* - The meristem of the flower is rounded and subtended by an abaxial bract (Fig. 2A). The floral meristem enlarges and a first sepal primordium appears on the abaxial side (Fig. 2B). The next primordia arise in a spiral sequence (but whorled phyllotaxis; divergence angles vary between about 120° and almost 180°) with distinct plastochrons between subsequent organs (Fig. 2C). The first stamen primordium arises opposite the abaxial sepal (Fig. 2C) and the other stamen primordia follow a spiral sequence while the sepals elongate (Fig. 2C-E). The central floral apex is "used up" by the stamen primordia and apparently no carpels are initiated in the center (Fig. 2E, F). Glandular trichomes concomitantly arise on the dorsal surfaces of the subtending bract (not shown) and sepals (Fig. 2E, G). Sepals and stamens are each served by a single vascular trace (Fig. 2H) and no other vascular traces (potential carpel traces) are present in the center of the floral base (Fig. 2H). Cells with oxalate druses are present in the sepals (Fig. 2G). The anthers begin to differentiate (Fig. 2F, I, J, K) and glandular trichomes arise on the dorsal (Fig. 2K) and ventral sides of the connective. Stamens complete their differentiation into a filament (Fig. 2J, K) and an anther (Fig. 2I, K). The mature anther wall has an epidermis that is colapsada during the final stages being present in some parts of the anther, a distinct endothecium layer with cell wall thickenings and mature pollen grains (Fig. 2I). In pre-anthetic stages, the filaments remain short (Fig. 2K) and to become distinctly longer only at the beginning of anthesis.

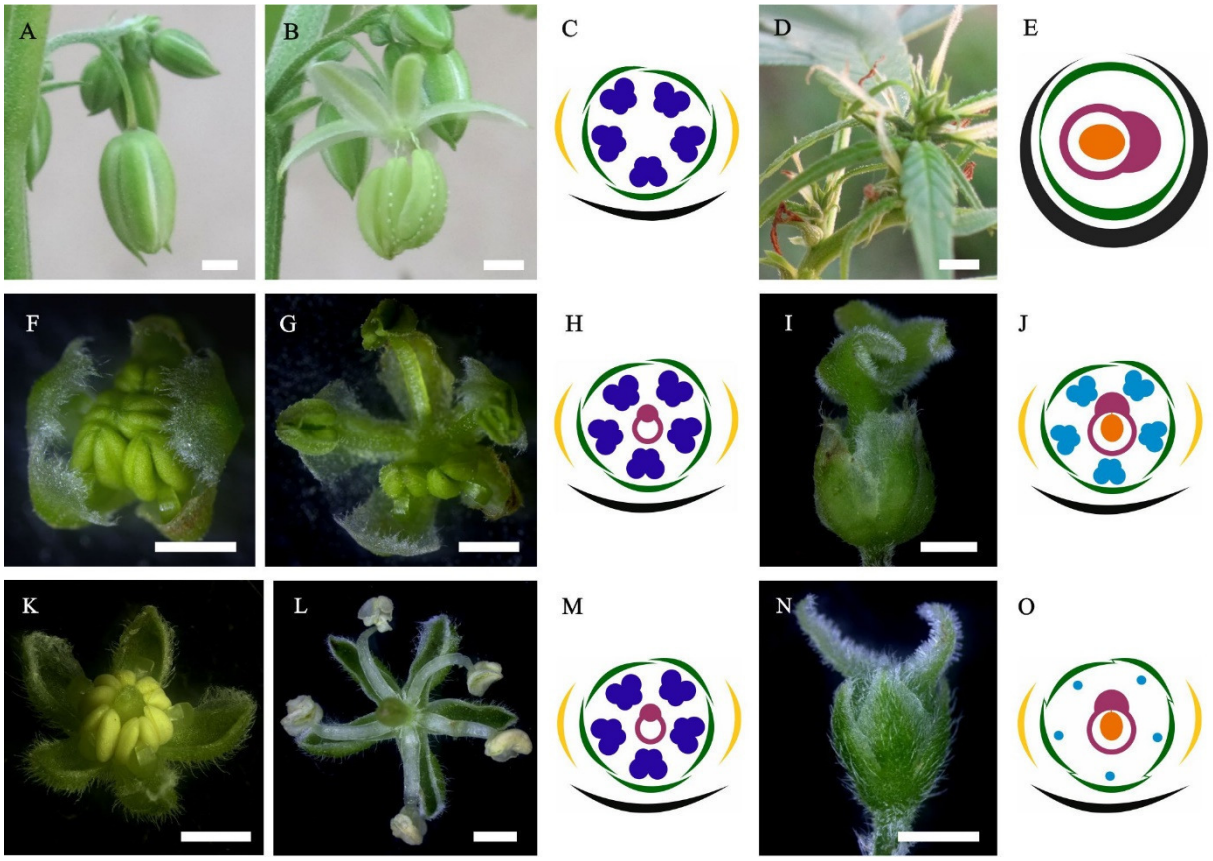

FIGURE 1 Floral organization of pre-anthetic and anthetic flowers of *Cannabis sativa* (A-E), *Celtis iguanaea* (F-J) and *Trema micrantha* (K-O). (A-B) Staminate flowers, a bud at a stage immediately prior to anthesis (A) and flowers at anthesis (B); note the pendulous stamens. (C) Diagram of a staminate flower with a subtending bract (black), two prophylls (yellow), the free sepals (green) and stamens (dark blue). (D) Pistillate flowers; some anthetic and some at a stage immediately prior to anthesis. (E) Diagram of a pistillate flower with a subtending bract (black), two united sepals (green), a syncarpous and pseudomonomerous gynoecium (purple) formed by two carpels, and a single ovule (orange). (F-G) Functionally staminate bud at a stage immediately prior to anthesis (F) and flower at anthesis (G) with two still inflexed stamens (filament bent and turgid) and three others with already dehisced anthers and straight filament. (H) Diagram of a functionally staminate flower showing a subtending bract (black), two prophylls (yellow), free sepals (green), stamens (dark blue) and a pistillode (purple). (I) Functionally pistillate bud at a stage immediately prior to anthesis. (J) Diagram of a functionally pistillate flower showing a subtending bract (black), two prophylls (yellow), free sepals (green), staminodes (light blue) and a syncarpous and pseudomonomerous gynoecium (purple) formed by two carpels, and a single ovule (orange). (K-L) Functionally staminate bud at a stage immediately prior to anthesis (K) and flower at anthesis (L) with all stamens with dehisced anther and straight filament. (M) Diagram of a functionally staminate flower showing a subtending bract (black), two prophylls (yellow), free sepals (green), stamens (dark blue) and a pistillode (purple). (N) Pistillate flower in anthesis. (O) Diagram of a pistillate flower showing a subtending bract (black), two prophylls (yellow), united sepals (green), vestigial staminodes (light blue) and a syncarpous and pseudomonomerous gynoecium (purple) formed by two carpels, and a single ovule (orange). Scale bars: (A, B) = 2 mm; (D, F-N) = 1 mm.

Pistillate flower of Cannabis sativa - The meristem of the flower is rounded and protected by an abaxial subtending bract (Fig. 3A). The bract elongates (Fig. 3B) and glandular trichomes arise on its dorsal surface (not shown). A first sepal primordium arises on the abaxial side of the floral apex, followed by a second one approximately on the adaxial side of the apex (Fig. 3B). No additional individual sepal primordia are discernible during subsequent developmental stages and the two original primordia broaden and then unite to form a ring-like structure around the floral base (Fig. 3C, F, G). On the center arises a primordium (Fig. 3B) that subsequently gives rise to two secondary carpel primordia of unequal size, which proximally are congenitally united (Fig. 3C). The carpels arises alternate with the sepals. One of the carpels elongates further early during development (carpel 1) and produces an ovule in the ventral region (Fig. 3D). The proximal, syncarpous part of the gynoecium elongates (Fig. 3E, F) and forms the ovary that later closes (Fig. 3G). The carpel tips elongate and form two distinct and unequally long stigma (Fig. 3H) that are unifacial and papillate during anthesis (Fig. 4A, C). The synsepalous calyx develops into a cup-like structure that covers the proximal part of the ovary (Fig. 3H). The ovule develops and becomes curved (Fig. 3I). At anthesis, the dorsal side of the subtending bract is covered by numerous glandular trichomes (Fig. 3J, K). The calyx epidermis is characterized by conspicuous groups of cells with thick walls (Fig. 3J, K). The mesophyll of the calyx is usually formed by two or three layers of cells (Fig. 3K), and few and small vascular bundles.

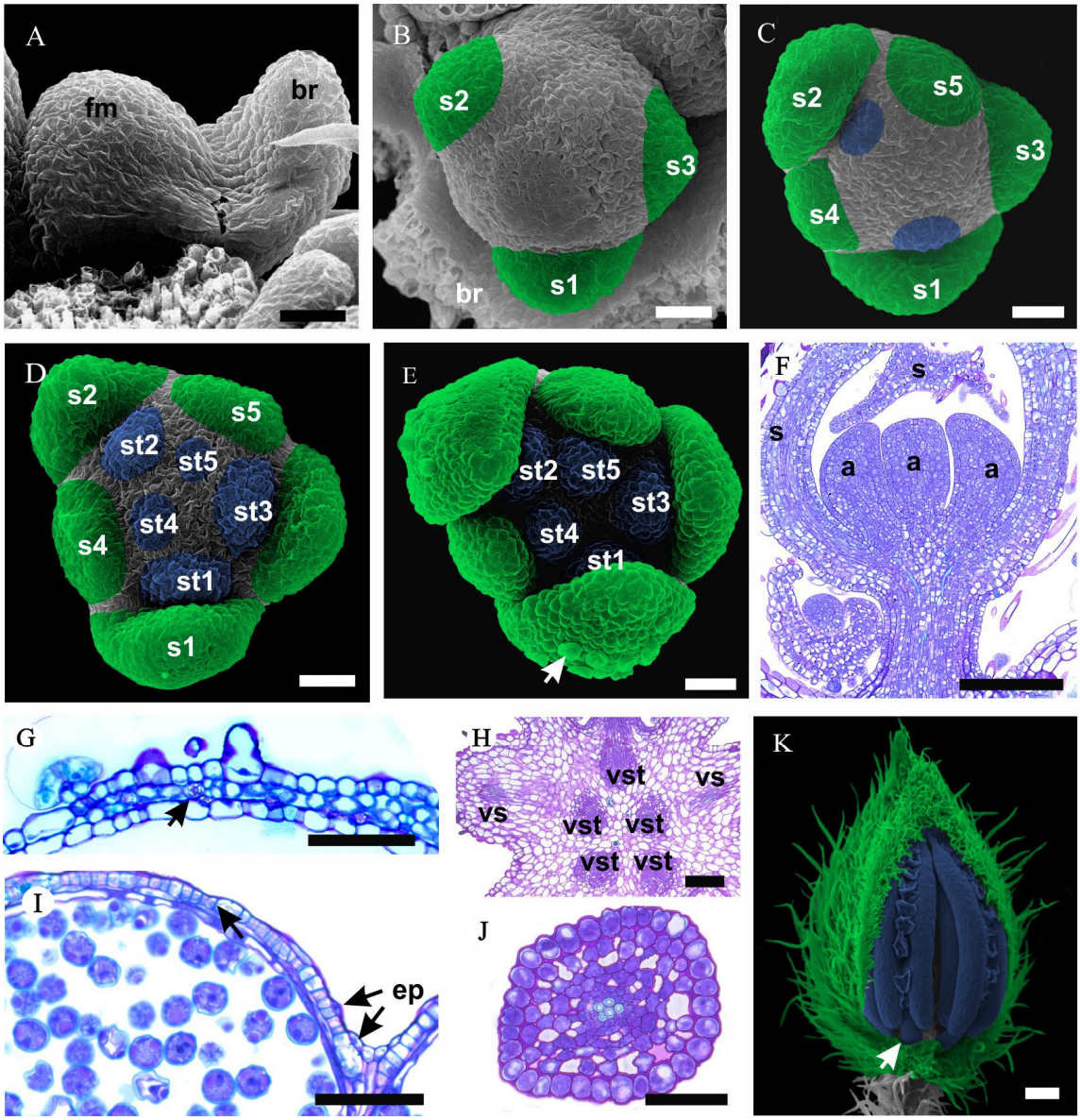

FIGURE 2 Developmental stages of staminate flowers of *Cannabis sativa* in SEM (A- E, K) and LM (F-J). (A) Lateral view of floral apex with its rounded floral meristem and an abaxial subtending bract. (B) Top view of floral apex with the first three sepal primordia clearly visible; note the size differences among the sepal primordia reflecting the spiral sequence of organ initiation. (C) Emergence of fourth and fifth sepal primordia and the almost simultaneous emergence of the first and second stamen primordium. (D) Sepal elongation and emergence of the other stamen primordia following a spiral sequence of organ initiation. (E) Sepal and stamen elongation and differentiation; note glandular trichomes on the sepals (white arrow). (F) Elongating stamens protected by the sepals (longitudinal section); note that no carpels are present. (G) Cross section of the sepal; note a glandular trichome on the epidermis and druses in the mesophyll (black arrow). (H) Cross section at the level of the floral receptacle showing the vascular traces of sepals (vs) and stamens (vst); note that no carpel vascular trace is present. (I) Mature anther in cross section showing a collapsed epidermis, a distinct endothecium layer with cell wall thickenings (black arrow), and mature pollen grains. (J) Cross section of the filament. Note the thickened cell wall. (K) Lateral view of a bud showing sepals (green), stamens (blue) with short filaments (arrow) and glandular trichomes on the anther connective. Abbreviations: a, anther; br, bract; ep, epidermis; fm, floral meristem; vs, vascular traces of sepals; vst, vascular traces of stamens; s, s1, s2, s3, s4, s5, sepals (green); st, st1, st2, st3, st4, st5, stamens (blue). Scale bars: (A-E, H) = 20 μm; (G, I) = 50 μm; (F, H, K) = 100 μm.

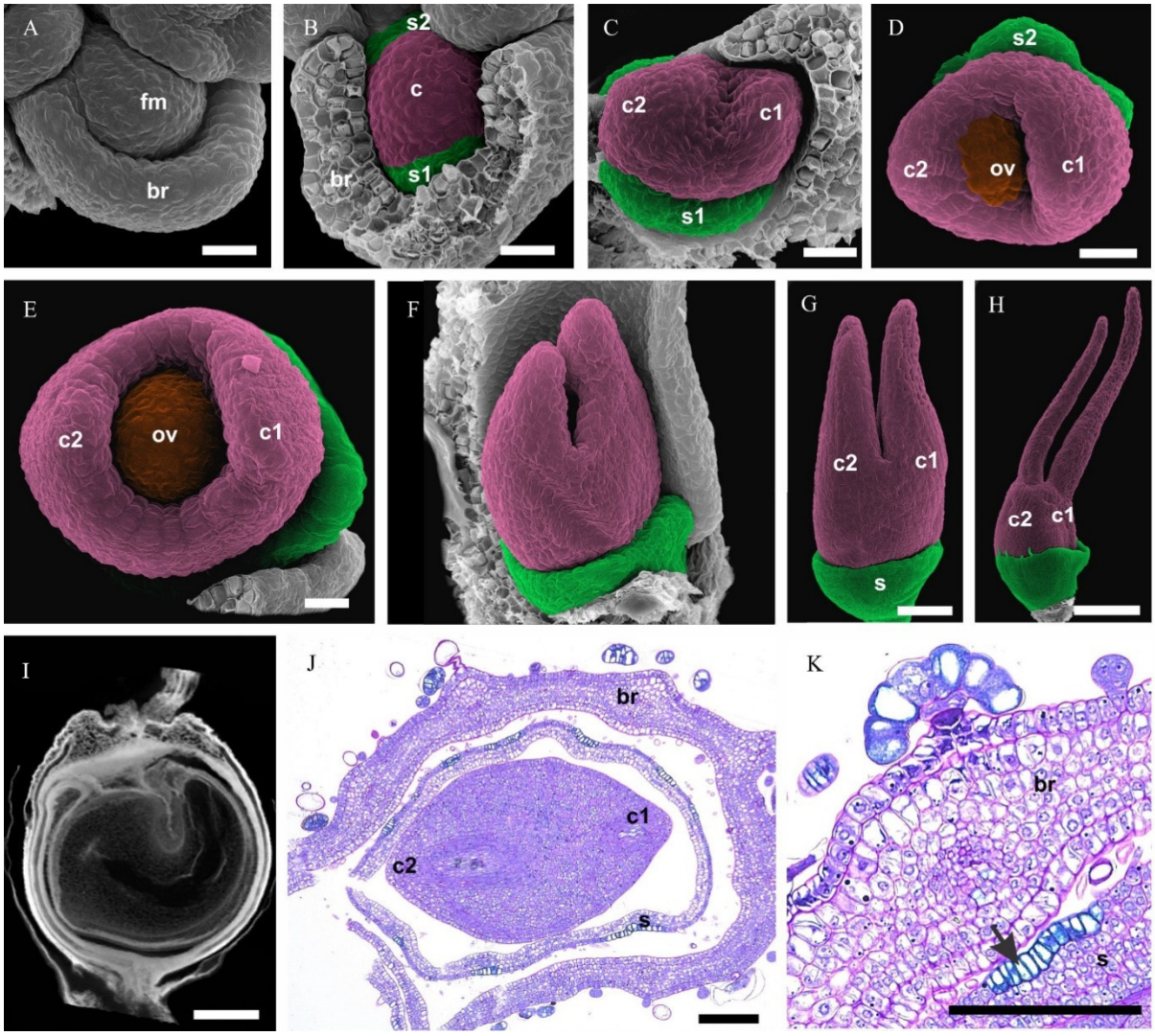

FIGURE 3 Developmental stages of pistillate flowers of *Cannabis sativa* in SEM (A-H), MicroCT 2D reconstruction (I) and LM (J-K). (A) Rounded floral meristem with a developing subtending bract. (B) Enlargement of the peripheral region of the floral meristem: the first sepal primordium appears on the abaxial side and the second one on the adaxial side (bract partly removed). Note that a primary central primordium of carpel arises. (C) The central primordium gives rise to two secondary carpel primordia of unequal size, which proximally are congenitally. (D) Top view of young gynoecium; elongation of carpels; note the onset of the ovule in the common cross zone of the two carpels; carpel 1 elongates more and forms an ovule. (E) Further carpel elongation and ovule development; note the size difference between the two carpels and that the ovule appears nearly central in the ovarian cavity. (F) Lateral view of almost closed gynoecium; note ring-like calyx with no clearly distinguishable sepals. (G) Elongation of stigmatic lobes. (H) Stigma differentiation and calyx elongation. (I) Longitudinal section of the ovary; note the pendant ovule. (J) Cross section through the basal part of the flower showing the synsepalous calyx and the bract that completely encloses the flower; note glandular trichomes on the dorsal side of the bract. (K) Details of calyx and bract; note in the calyx an epidermic region with thickened-walled cells (arrow). Abbreviations: br, bract; c, carpel, c1, carpel one, c2, carpel two (purple); fm, floral meristem; ov, ovule (orange); s, s1, s2, sepals (green). Scale bars: (A-F) = 20 μm; (G-H) = 50 μm; (I) = 250 μm; (J-K) = 100 μm.

Atypical floral morph types of <u>*Cannabis*</u> <u>*sativa*</u> - Floral morphology is structurally variable in monoecious individuals that are occasionally found (Fig. 4A-

F). Some individuals may initially produce only pistilate flowers, but later, start to produce also staminate flowers, and flowers with stamens and pistil united with each other to different degrees (Fig. 4C, D). Pistillate flowers may have three stigmatic branches (Fig. 4A) and three carpels (Fig. 4B); but all have only one developed ovule (Fig. 4B, D) irrespective of the number of carpels. Staminate flowers may have six stamens and six sepals, of which two may be united (Fig. 4E). The flowers with united carpels and stamens are also synsepalous (similar to pistillate flowers), have a uniovulate ovary, and anthers containing pollen grains (Fig. 4D).

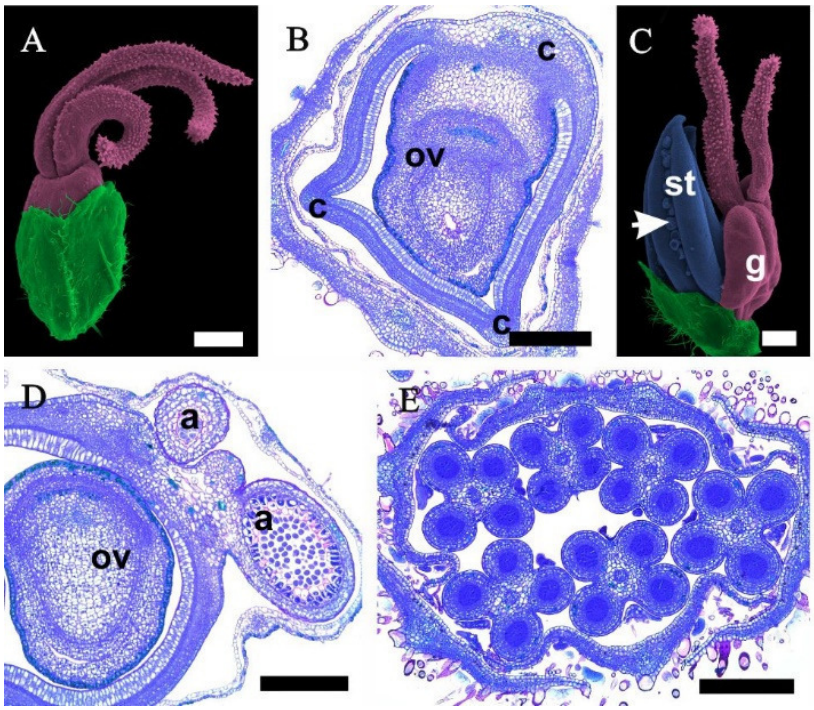

FIGURE 4 Atypical floral morph types of *Cannabis sativa* in SEM (A, C) and LM (B, D, E). (A) Anthetic pistillate flower with three stigmas. (B) Pistillate flower with ovary composed of three carpels (cross section). (C) Flower with stamens and ovary united with each other. (D) Flower with stamen and carpel united by the connective and ovary wall. (E) Staminate flower with six stamens; note also the "doubled" sepal on the upper. Abbreviations: a, anther; c, carpel; g, gynoecium (purple); ov, ovule; st, stamen (blue). Scale bars: (A) = 250 μm; (B-E) = 200 μm.

Functionally staminate flower of *Celtis* *iguanaea* - The floral meristem is rounded before the initiation of the individual floral organs and subtended by an abaxial bract and two prophylls (Fig. 5A). The floral meristem enlarges and a first sepal primordium appears on the abaxial side (Fig. 5B). The next sepal primordia arise in a spiral sequence (whorled phyllotaxis; divergence angles vary between about 120° and almost 180°) with distinct plastochrons between subsequent organs (Fig. 5B, C). The first stamen primordium emerges opposite the abaxial sepal (Fig. 5D) and the other stamen primordia follow in a spiral sequence while the sepals elongate (Fig. 5D, E). The floral apex remaining form a central primordium (Fig. 5E) that subsequently gives rise to two secondary carpel primordia of unequal size, which proximally are congenitally united (Fig. 5F, G, H). The carpels remain small and form a pistillode (Fig. 6A). Ovule formation may (Fig. 6B) or may not (Fig. 6C) occur; however, even if initiated, the ovule is aborted during further floral development. At anthesis, the sepals are free, covered by glandular trichomes, and possess oxalate druses and mucilaginous cells in the mesophyll (Fig. 6D). Each sepal is served by a single vascular bundle in the floral base (Fig. 6D). The filament has epidermal cells with thickenings on the dorsal region (Fig. 6E). The anthers have simple and short trichomes on the dorsal and ventral sides of the connective (Fig. 6A); when mature the anther wall has an epidermis that is collapsed during the final stages being present in some parts of the anther, a distinct endothecium layer with annular thickenings, and encloses viable pollen grains (Fig. 6F).

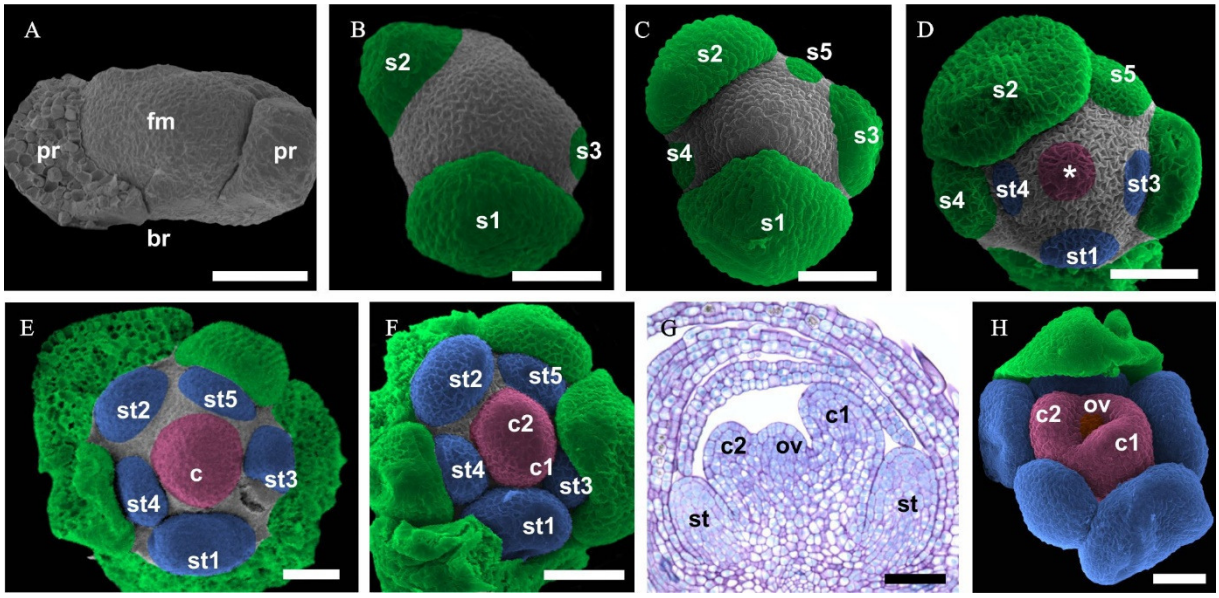

FIGURE 5 Developmental stages of flowers of *Celtis iguanaea* in SEM (A-F, H) and LM (G). (A) Rounded floral meristem with two lateral prophylls (subtending bract removed). (B) Spiral sequence of sepal formation with the first sepal in abaxial position. (C) Elongation of the three first initiated sepals and emergence of the last two; note the large size differences caused by long plastochrons between successive sepals. (D) Emergence of stamen primordia opposite to the sepals; note a central carpel primordium (*). (E) Top view of flower with stamen and carpel primordia (most sepals removed); note the spiral sequence of stamen initiation. (F) The central primordium gives rise to two secondary carpel primordia of unequal size, which proximally are congenitally. (G) Longitudinal section of floral bud, showing the single ovule that is formed by the larger carpel (1) in the cross zone between the two carpels. (H) Anther differentiation and formation of the syncarpous part of the ovary. Abbreviations: br, bract; c, carpel, c1, carpel one, c2, carpel two (purple); fm, floral meristem; ov, ovule (orange); pr, prophylls; s1, s2, s3, s4, s5, sepals (green); st, st1, st2, st3, st4, st5, stamens (blue). Scale bars: (A-H) = 50 μm.

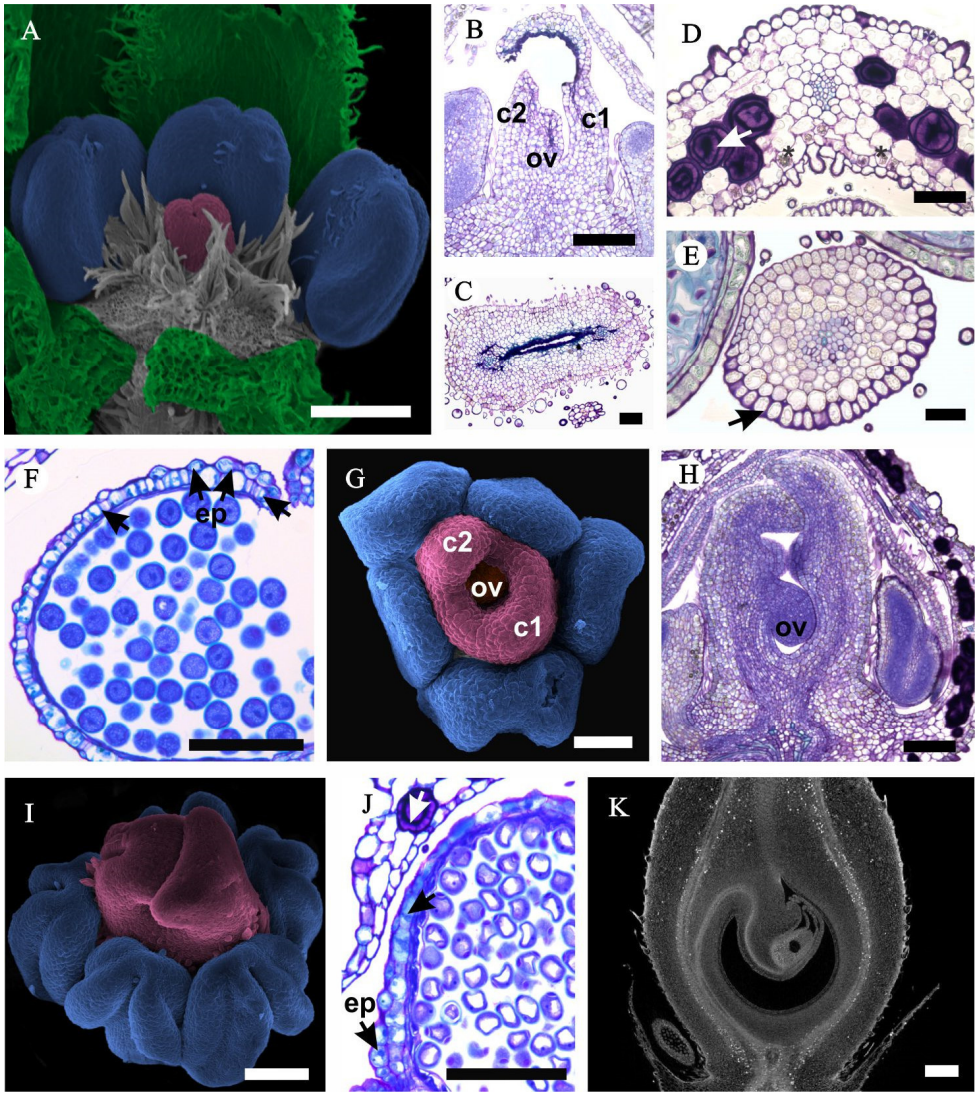

FIGURE 6 Differentiation and final developmental stages of the flowers of *Celtis iguanaea* in SEM (A, G, I), LM (B-F, H, J) and MicroCT 2D reconstructions (K). (A-F) Functionally staminate flower at a stage immediately prior to anthesis; (A) some sepals and stamens were removed; note the differentiated anthers (blue) and a central pistillode (purple). (B) Pistillode in longitudinal section formed by two carpels; note that an ovule was initiated but both the carpels and the ovule are aborted. (C) Cross section of the pistillode; note that no ovule is found. (D) Cross section of a sepal with mucilaginous cells embedded in the mesophyll (white arrow) and druses (*). (E) Cross section of the filament showing thick-walled epidermic cells (arrow) facing the abaxial side. (F) Note a mature wall anther formed by a collapsed epidermis, a distinct endothecium layer with annular cell wall thickenings (arrow). It encloses viable pollen grains (cross section). (G-K) Functionally pistillate flower. (G) Top view of a developing flower in intermediate stage with staminode differentiation, carpel elongation and ovule formation; note that carpel 1 is largest and the ovule arises near the margins in the common cross zone of the two carpels. (H) Longitudinal section of a flower with developing ovule and closed carpel. (I) Closed carpels and first stages of stigma differentiation; note the differentiated staminodes (blue). (J) Cross section of the flower showing mucilaginous cell in the sepal (white arrow). Note a mature staminodial anther formed by a collapsed epidermis, an endothecium (black arrow) lacking cell wall thickenings, and unviable, "empty", pollen grains. (K) Longitudinal section of the ovary showing a locule and a pendant ovule. Abbreviations: c1, carpel one; c2, carpel two; ep, epidermis; ov, ovule. Scale bars: (A) = 200 μm; (B-E, G) = 50 μm; (F, H, I, J) = 100 μm; (K) = 250 μm.

Functionally pistillate flower of Celtis iguanaea – The early floral development of the functionally pistillate flower is similar to that of functionally staminate flower. The differences become only evident after carpel elongation. The two carpels grow at unequal rates, with the carpel 1 soon becoming broader and longer (Fig. 6G). Carpel 1 is located on the abaxial side of the flower and produces an ovule in its ventral region (Fig. 6G, H). The proximal, syncarpous part of the gynoecium elongates (Fig. 6G) and the ovary closes (Fig. 6H, I). The carpel tips elongate and form two distinct, long styles that later subdivide forming four bifacial, stigmatic branches (Fig. 6I) with papillae on their ventral side (Fig. 1I). The style is short (Fig. 1I). The staminodes (Fig. 6I) are structurally similar to the stamens of the functionally staminate flower (compare Fig. 6A and 6I), but their pollen grains are unviable (compare Fig. 6J with 6F). No distinct endothecial cell wall thickenings are observed (Fig. 6J). At the end of development the sepals are free and possess oxalate druses and mucilaginous cells in the mesophyll (Fig. 6J). The sepals are covered by glandular trichomes arisen during the sepal elongation stage. A single vascular bundle serves the sepals in the floral base. The single ovarian locule is formed in carpel 1 (Fig. 6G, H, K). The ovule are pendant during later developmental stages (Fig. 6K).

Functionally staminate flower of Trema micrantha - The floral meristem is rounded before organ initiation, and subtended by an abaxial bract and two prophylls (Fig. 7A). The floral meristem enlarges (Fig. 7B) and a first sepal primordium appears on the abaxial side (Fig. 7C). The next sepal primordia initiate in a spiral sequence (whorled phyllotaxis; divergence angles vary between about 120° and almost 180°) with distinct plastochrons between subsequent organs (Fig. 7D). The five stamen primordia arise opposite to the sepals (Fig. 7D) following a spiral sequence while the sepals elongate (Fig. 7D, E). In the center of the flower, a primary carpel primordium appears (Fig. 7E) that later gives rise to two secondary, congenitally united carpel primordia of unequal size (Fig. 7F). One of the carpels elongates further early during development (carpel 1) and forms a cleft (Fig. 7F). The syncarpous part of the gynoecium elongates (Fig. 7G) and the ovary closes (Fig. 7H). Trichomes arise on the

receptacle between carpels and stamens during the elongation process (Fig. 7H). None of the carpels develops an ovule (Fig. 7I). At the end of development, carpels form a pistillode (Fig. 7H, I). The sepals involve the stamens and possess a distinct subepidermal layer with oxalate druses (*) and epidermis with phenolic compounds (Fig. 7J). Each sepal is served by a single vascular bundle in the floral base. The differentiated stamen has a filament with palisade-like, apparently secretory epidermal cells (Fig. 7K). The mature anthers have epidermis that is collapsed during the final stages being present in some parts of the anther, a distinct endothecium layer with wall thickenings and enclose viable pollen grains (Fig. 7J).

Pistillate flower of Trema micrantha - The floral meristem is rounded and subtended by an abaxial bract and two prophylls (Fig. 8A). The meristem becomes broad and gives rise to five sepal primordia in a spiral sequence (but whorled phyllotaxis; divergence angles vary between about 120° and almost 180°) starting at the abaxial side of the flower (Fig. 8B). Five stamen primordia arise opposite the sepals (Fig. 8C) in a spiral sequence, followed by a single primary, carpel primordium (Fig. 8C). This carpel primordium enlarges (Fig. 8D) and gives rise to two secondary, carpel primordia of unequal size that are congenitally united by the base (Fig. 8E). The carpel on the abaxial side of the flower (carpel 1), grows faster during early development and produces an ovule in its ventral region (Fig. 8F, G). The syncarpous part of the gynoecium elongates (Fig. 8F-H) and the ovary closes (Fig. 8I). The carpel tips elongate forming two distinct and unequally long styles (Fig. 8J) that are bifacial with simple unicellular trichomes on the dorsal side and papillae on the ventral side (Fig. 8J). The stamen primordia abort soon after their emergence on the floral apex and do not become differentiated into anther and filament (Fig. 8H, J). The sepals are united at the base and possess a distinct ventral, subepidermal layer with oxalate druses (arrow) and phenolic compounds, especially in the dorsal epidermis (Fig. 8K). A single vascular bundle serves each sepal in the floral base (Fig. 8K). At anthesis, the sepals are covered by glandular trichomes. The aborted stamens consist only of epidermis

and parenchyma and are not evident in at anthesis as they are covered by simple trichomes arising from the floral base (Fig. 8J).

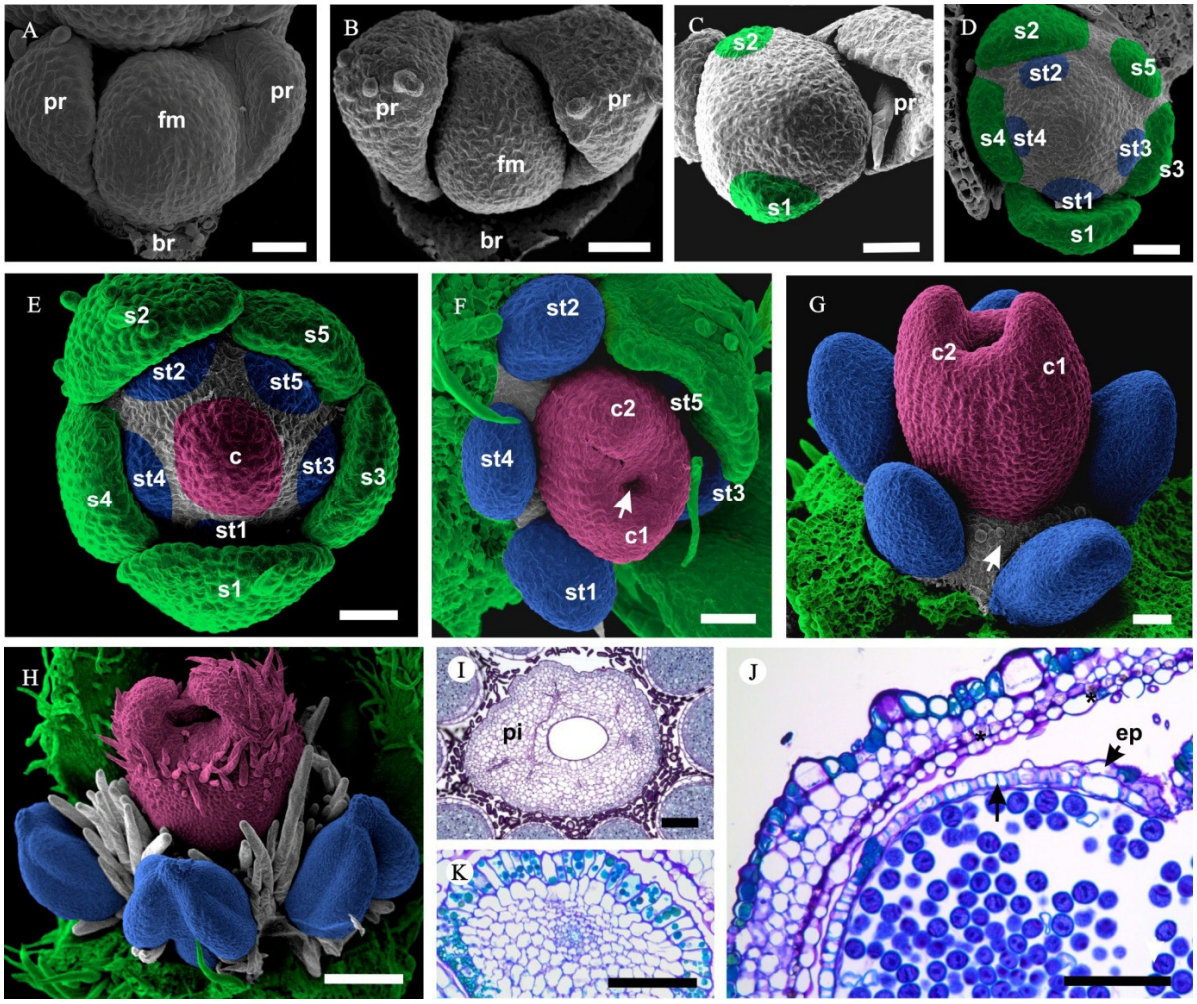

FIGURE 7 Developmental stages of functionally staminate flower of *Trema micrantha* in SEM (A-H) and LM (I, J). (A) Rounded floral meristem with two lateral prophylls (subtending bract removed). (B) Enlargement of the floral meristem. (C) Spiral sequence of sepal initiation starting with an abaxial sepal. (D) Emergence of the last sepal primordia; note that the first stamen primordia arise opposite to sepals. (E) Sepal elongation and spiral sequence of stamen initiation; note a central carpel primordium. (F) The central primordium gives rise to two secondary carpel primordia of unequal size, which proximally are congenitally; note a cleft (arrow) in the carpel 1. (G) Anther elongation and formation of the symplicate part of the ovary and trichomes begin to elongate (arrow). (H) Stage immediately prior to anthesis; note the differentiated anthers (blue), a central pistillode (purple) and glandular trichomes in the receptacle. (I) Cross section of the pistillode; note that no ovule is found. (J) Cross section of the flower showing an epidermis containing phenolic compounds and subepidermal layer with druses (*) in the sepals, anther wall with a discontinuous epidermis, a distinct endothecium layer with cell wall thickenings (arrow) and typical pollen grains. (K) Cross section of the filament; note secretory epidermal cells. Abbreviations: br, bract; c, carpel, c1, carpel one, c2, carpel two (purple); ep, epidermis; fm, floral meristem; pi, pistillode; pr, prophylls; s1, s2, s3, s4, s5, sepals (green); st1, st2, st3, st4, st5, stamens (blue). Scale bars: (A-G, I) = 25 μm; (H, J, K) = 100 μm.

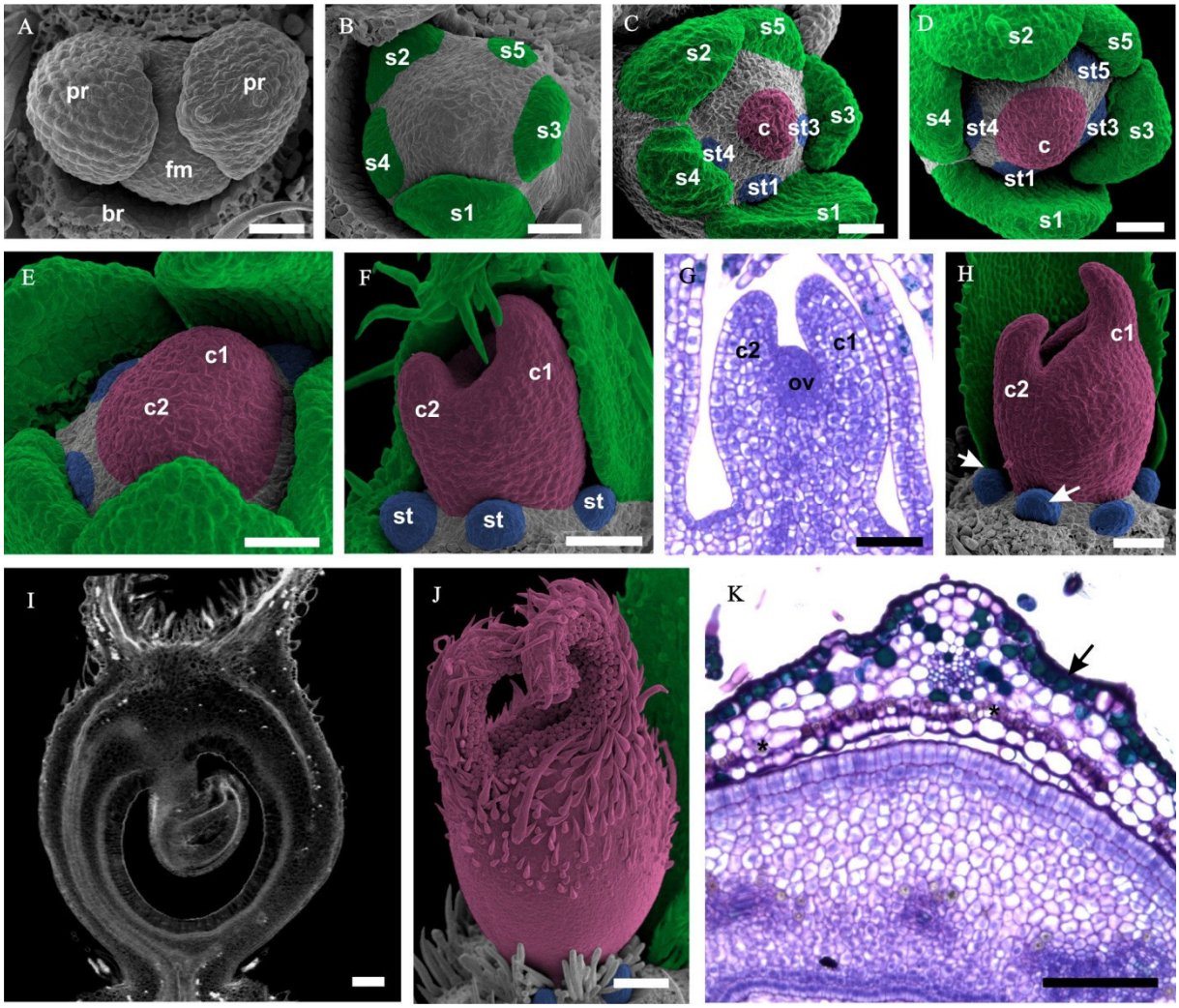

FIGURE 8 Developmental stages of pistillate flower of *Trema micrantha* in SEM (A-F, H, J), LM (G, K) and MicroCT 2D reconstructions (I). (A) Rounded floral meristem with two lateral prophylls (subtending bract removed). (B) Spiral sequence of sepal initiation starting with an abaxial sepal. (C) Sepal elongation and emergence of stamen primordia following a spiral sequence; note a central carpel primordium. (D) Sepal elongation and the emergence of last stamen primordium; note the carpel primordium becomes bulged. (E) The carpel primordium forms two primordia that remain basally united. (F) The stamen primordia stop their growing and the carpels elongate remaining a syncarpous part; note a cleft in the larger carpel (carpel 1). (G) Lateral view of the gynoecium in intermediate stage; note carpel elongation and ovule formation in a common cross zone of the two carpels (longitudinal section). (H) Flower with almost closed carpels and first stages of stigma differentiation; note the small staminodes (blue). (I) Longitudinal section of the ovary showing a locule and a pendant ovule. (J) Final stage of development of the gynoecium; note two bifacial stigmatic branches. (K) Cross section of the flower showing phenolic cells (arrow) and a subepidermal layer of druses (*) in the sepals. Abbreviations: br, bract; c, c1, c2, carpel (purple); fm, floral meristem; ov, ovule; pr, prophylls; s1, s2, s3, s4, s5, sepals (green); st, st1, st2, st3, st4, st5, vestigial staminode (blue). Scale bars: (A-F) = 25 μm; (G-I) = 50 μm; (J, K) = 100 μm.

Gynoecium vascularization

The gynoecium of *Cannabis sativa, Celtis iguanaea* and *Trema micrantha* is syncarpous, two-carpellate and the ovary contains only a single locule, with no septum formation (i.e, the ovary is symplicate throughout), and a single ovule. The vascularization of the gynoecium is described below for all species.

In *Cannabis sativa, Celtis iguanaea, Trema micrantha,* the smaller of the two carpels (labelled c2 in our figures) is vascularized by a single bundle (labelled d2) that runs in the median-dorsal plane of the carpel and extends up to the stigmatic area (Fig. 9). The larger carpel (labelled c1; i.e., the one that produces the ovule) is also served by a single vascular trace drawing in from the floral base. However, in this case, the vascular bundle divides in two in the proximal-most part of the ovary (Fig. 9A, F, K, M). One of two resulting bundles runs through the median-dorsal plane of the carpel (as in the other carpel) and extends up to the stigmatic area (labelled d1 in Fig. 9). The second bundle (labelled v1), however, runs along the ventral side of the carpel and enters into the ovule just below the apex of the ovary (Fig. 9A, E, F, J, K, O). As the smaller carpel is strongly reduced and does neither form a locule nor an ovule, the ventral bundle of carpel 1 runs in parallel with the dorsal bundle of carpel c2 up to apex of the ovary (Fig. 9A-E, K-O). Only on *Celtis iguanaea* the ventral bundle of carpel 1 runs in parallel with the dorsal bundle of carpel 2 up to half of the ovary (Fig. 9F-L) and then it begins to move away to the apex of the ovary into the ovule.

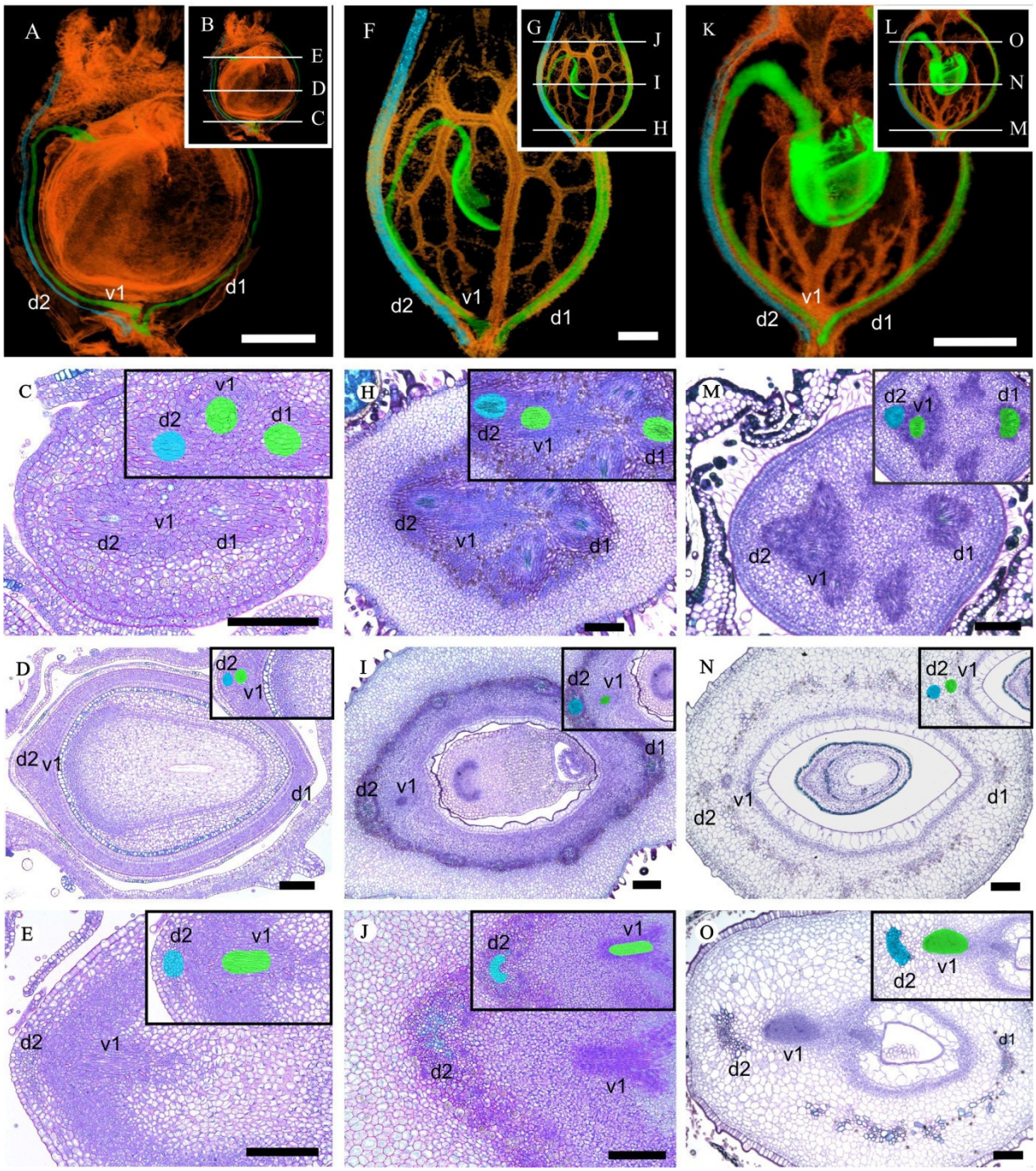

FIGURE 9 Gynoecium vasculature of of anthetic flowers of *Cannabis sativa* (A-E), *Celtis iguanaea* (F-J) and *Trema micrantha* (K-O). (A) MicroCT 3D reconstructions of the vasculature of the ovary and ovule; note the vasculature of the ovulate carpel (carpel 1 - green) and of the non-ovulate carpel (carpel 2 - blue). (B) Vasculature of the ovary with lines indicating approximate levels of cross section shown in figures C-E. (C) Cross section at the ovary base; note the details of the vasculature of carpel 1 in green with the dorsal and ventral bundles close to each other; and dorsal bundle of carpel 2 in blue opposite to dorsal bundle of carpel 1. (D) Cross section at mid-level of ovary; note the ventral bundle of carpel 1 close to dorsal bundle of carpel 2. (E) Ventral bundle curves to reach the ovule. (F) MicroCT 3D reconstructions of the vasculature of the ovary; note the vasculature of the ovulate carpel (carpel 1 - green) and of the non-ovulate carpel (carpel 2 - blue). (G) Vasculature of the ovary with lines indicating approximate levels of cross section shown in figures H-J. (H) Cross section at the ovary base; note the details of the vasculature of carpel 1 in green with ventral bundles internal to the dorsal bundle of carpel 2 in blue. (I) Cross section at mid-level of ovary; note the ventral bundle of carpel 1 close to dorsal

bundle of carpel 2. (J) Ventral bundle, distant of the dorsal bundle of the carpel 2, curves to reach the ovule. (K) MicroCT 3D reconstructions of the vasculature of the ovary and ovule; note the vasculature of the ovulate carpel (carpel 1 - green) and of the non-ovulate carpel (carpel 2 - blue). (L) Vasculature of the ovary with lines indicatingapproximate levels of cross section of M-O. (M) Cross section at the ovary base; note the details of the vasculature of carpel 1 in green with ventral bundles internal to the dorsal bundle of carpel 2 in blue. (N) Cross section at mid-level of ovary; note the ventral bundle of carpel 1 close to dorsal bundle of carpel 2. (O) Ventral bundle, distant of the dorsal bundle of the carpel 2, curves to reach the ovule. Abbreviations: d1, dorsal vascular bundle of carpel 1 (green); d2, dorsal vascular bundle of carpel 2 (blue); v1, ventral vascular bundle of carpel 1 (green). Scale bars: (A) = 250 μm; (C-E) = 100 μm; (F, H, I, J) = 100 μm; (K) 250 μm; (M, N, O) = 100 μm.

Table 2. Comparison of floral features in species of Cannabaceae, according to results from this study and data available in the literature. Symbols: + = present; - = absent; ? = data unavailable. References: 1 = Present study; 2 = Payer (1957); 3 = Dayanandam and Kaufman (1976); 4 = Oliveira and Pais (1988); 5 = Shephard et al. (2000); 6 = Sugiyama et al. (2006).

Species	Sepal number		Order of organ initiation	Sepal union		Stamen absence/abortion ♀ flower	Filament structure	Pistil absence/abortion ♂ flower	Style size	Stigma shape	Glandular trichome distribution	
	♂ flower	♀ flower		♂ flower	♀ flower						♂ flower	♀ flower
Cannabis sativa[1,2,3]	5	2	Spiral	-	+	Absence	Long and thin	Absence	-	Unifacial, two branches	Bract, sepal, anther connective, receptacle	Bract
Celtis iguanaea[1]	5	5	Spiral	-	-	Abortion (staminode)	Inflexed, with thickened epidermis	Abortion (pistillode)	+	Bifacial, four branches	Bract, sepal, receptacle	Bract, sepal, receptacle
Humulus lupulus[4,5,6]	5	Vestigial	Spiral	-	+	Absence	?	Absence	?	Unifacial, two branches	Anther connectivee	Bract
Trema micrantha[1]	5	5	Spiral	-	At the base	Abortion (rudiment)	Inflexed, with phenolic epidermis	Abortion (pistillode)	-	Bifacial, two branches	Bract, sepal, receptacle	Bract, sepal, receptacle

1.5 Discussion

The reduced flowers of Cannabaceae are the result of different developmental pathways. At anthesis, floral organs are arranged in whorls and entire whorls may be completely absent (corolla, androecium or gynoecium) or they may be initiated early during floral development and then be aborted at different stages of floral development (androecium or gynoecium).

Some unusual floral features are shared by Cannabaceae species, such as the pseudomonomerous gynoecium, the precocious ovule (sensu Endress, 2015) and sepals vascularized by only one bundle. An exception to the latter feature is present in the pistillate flowers of *Cannabis sativa* (studied here) and *Humulus lupulus* (Shephard et al., 2000) in that the calyx is two-merous, synsepalous, reduced and vascularized by few, relatively small bundles. Differences of special interest occur between species or even between floral morph types of the same species, such as the occurrence of bracts and prophylls, different degrees of sepal union, and differences in filament and style/stigma morphology (Table 2).

Developmental pathways that lead to a reduced flower in Cannabaceae

The perianth of *Cannabis sativa, Celtis iguanaea, Trema micrantha* (present study) and *Humulus lupulus* (Shephard et al., 2000) is reduced by the absence of one whorl (petals). In addition, the vascularization of the sepals appears also reduced. In accordance with recent studies dealing with floral structure in Rosales, e.g., Endress and Matthews (2006) and Endress (2010), we interpret the flowers of Cannabaceae as apetalous and, therefore, the single whorl of perianth organs as sepals. Other authors (Payer, 1857; Bechtel, 1921; Shephard et al., 2000; Basso-Alves et al., 2014) who studied urticalean species also consider that the only perianth whorl corresponds to the calyx of other representatives of Rosales with a double perianth differentiated into calyx and corolla (e.g., most Rosaceae and most Rhamnaceae). Characters supporting this interpretation of the perianth in Cannabaceae include: robustness (except for the

pistillate flower of *C. sativa*), spiral sequence of initiation, quincuncial aestivation, a broad base, and an acute apex (Endress, 1996; Soltis et al., 2005). Only the number of vascular bundles (a single one in the species studied here) that serve the organs is different from that expected for a typical eudicot sepal (three, according to Endress, 1996; Soltis et al., 2005). However, in cases of floral reduction, the vascular bundles of a given organ can be reduced to one or none (Puri, 1951), as in the studied species of Cannabaceae and also in the staminate flowers of some Moraceae species (Bechtel, 1921; Leite et al., 2018).

The morphological comparison of the developing flower among Cannabaceae species (see Table 2) demonstrates a clearer trend towards perianth reduction in the pistillate flowers of *C. sativa* (present study) and *H. lupulus* (Shephard et al., 2000): five to two sepals, thin, delicate organs, without trichomes and reduced vascular system. In these two species, the protection of the ovary is transferred to the bract. In contrast, *T. micrantha* and *C. iguanaea* flowers exhibit five, robust, vascularized (one bundle) sepals, covered with trichomes (present study), features also present in the staminate flower of *C. sativa* and *H. lupulus* (Shephard et al., 2000).

The dicliny (presence of pistillate or staminate flowers) of the studied species is achieved by two different developmental pathways in Cannabaceae. In Cannabaceae *sensu stricto*, formed by *Cannabis* and *Humulus,* carpels and stamens, respectively, are completely absent even during the earlier stages of floral development (Payer, 1857; Bechtel, 1921; Shephard et al., 2000; present study), meaning that no staminodes or pistillodes are present. In *Celtis iguanaea* and *Trema micrantha* (present study), both previously placed in the family Ulmaceae, carpels and stamens are initiated and are clearly visible during early development of all floral morph types, but further development of either carpels or stamens is stopped, respectively, in functionally staminate or pistillate flowers. There is a remarkable difference in the developmental stage when stamen abortion occurs, late in *C. iguanaea* and early in *T. micrantha*. In *C. iguanaea,* the staminodes in the pistillate flowers even produce pollen grains, which are most likely not viable, but are harvested by visiting

(non-pollinating) insects (Arruda and Sazima, 1988). In contrast, in *T. micrantha* stamen abortion occurs at the very beginning of development. Interestingly, the flowers of *C. iguanaea* were previously thought to be also functionally perfect (Berg and Dahlberg, 2001; Torres and Luca, 2005; Martins and Pirani, 2009) rather than functionally pistillate (present study), and the flowers of *T. micrantha* were not described as having aborted stamen (Torres and Luca, 2005; Pederneiras et al., 2011).

Another aspect of floral reduction is expressed in the pseudomonomerous gynoecium (*sensu* Eckardt, 1937) of Cannabaceae (Eckardt, 1937; Chernik, 1981; Shephard et al., 2000; present study) and of other urticalean rosids (e.g., *Ulmus parvifolia, Zelkova serrata,* Fukuoka, 1982; *Zelkova serrata*, Okamoto et al., 1992; *Ulmus montana, Morus alba, Dorstenia* sp., *Artocarpus* sp., *Ficus carica,* Eckardt, 1937). Our data on ontogeny and vascularization confirmes the pseudomonomery of the gynoecium in the species of Cannabaceae studied here. Their gynoecium is bicarpellate and unilocular but only one carpel produces an ovule. In all Cannabaceae species studied here, the dorsal bundle is the single vascular bundle of the reduced carpel. In contrast, the ovulate carpel has a dorsal, and a ventral bundles. Among the studied species the ventral bundle in position in relation to the ovule (to see Fig 9A, F, K).

The initiation of the unique ovule is precocious (except for *Humulus lupulus* - see Shephard et al., 2000), i.e., prior to carpel closure, a feature often present in carpels with a single ovule (Endress, 2015). In *Trema micrantha*, the major growth phase of the carpel walls is immediately followed by the appearance of the ovule, whereas in *Cannabis sativa* and *Celtis iguanaea,* the ovule appears concomitantly with the elongation of the smaller carpel (Eckardt, 1937; present study).

Floral ontogeny and polygamy in Cannabaceae

Our data shows that in *Cannabis sativa* the diclinous flowers (staminate and pistillate flowers) are determined very early during floral development (complete absence of organs). Even during the very first stages of floral development, i.e., at the stage where no organs are visible yet on the floral apex, the two floral morphs look

clearly different from each other: the floral apex of staminate flowers is relatively broad and convex (dome-shaped, Fig. 2A) whereas the apex of pistillate flowers is smaller and more or less flat (Fig. 3A). These differences in size and shape during the first stages of floral development reflect the later differences in type and especially in number of floral organs in staminate vs pistillate flowers: while mature staminate flowers consist of ten floral organs (five sepals and five stamens), pistillate flowers have only two (reduced) sepals and two carpels. Thus, in *C. sativa* (Hirata, 1927) and also in *Humulus lupulus* (Shephard et al., 2000), the changes that promote the formation of a staminate flower and a pistillate flower, respectively, occur very early during the formation of the floral meristem, before the initiation of the sepals. In *Trema micrantha*, the determination of the floral morph type occurs later, during the intermediate and final stages of floral development, as a result of organ abortion. In addition, the sepals (five) are similar in both functionally staminate and pistillate morph types. Thus, in this species, it is plausible to assume that both floral meristems could develop into a perfect flower with no organ abortion occuring.

Atypical flowers, with stamens and pistil united with each other to different degrees occasionally occur in *C. sativa* (Heslop-Harrison, 1956; present study) and *H. lupulus* (Shephard et al., 2000). We did not find any similar atypical flowers in *Trema micrantha* and in *Celtis iguanaea*. The fact is reported as response of stress factors such as high auxin-levels and carbon monoxide (Heslop-Harrison, 1956; Harrison and Heslop-Harrison, 1957; Weston 1960). Other possible explanation for such atypical flowers in *C. sativa* and *H. lupulus* but not in the latter species may perhaps be the complete absence of one of the whorls (androecium or gynoecium) in the floral morph types, which may lead to a developmental instability in the localization of the organs and also in gene expression patterns during organ development, producing flowers with united stamens and carpels. Some of the atypical floral morphologies (e.g., changes in merism) found in Cannabaceae (Heslop-Harrison and Heslop-Harrison, 1957; present study), occur also in other urticalean rosids. An example is a tricarpellate gynoecium, which is occasionally found in *Zelkova serrata* (Ulmaceae - Okamoto et al.,

1992), *Ulmus scabra* (Ulmaceae - Bechtel, 1921) and *Artocarpus* (Moraceae - Sharma, 1964).

Remarkable floral features of Cannabaceae

The morphology of the synsepalous calyx in Cannabaceae is highly variable, ranging from a vestigial calyx that starts as a united, ring-like structure during early floral development, as in *H. lupulu*s (Shephard et al., 2000), to a well-developed calyx, in which the sepals only become united at their base towards the end of floral development, as in *T. micrantha* (present study). Interestingly, synsepaly occurs only in pistillate flowers of dioecious species of Cannabaceae and seems more pronounced in species with a lower number of sepals, such as *Cannabis sativa* and *H. lupulus* (Table 2, present study, Shephard et al., 2000). The lability in merosity and shape can be caused by the lack of constraints acting on the function of the floral organ in the bud (Endress, 2008) since the flower is so reduced.

Some floral features displayed by *C. sativa, C. iguanaea, H. lupulus* and *T. micrantha*: such as partial monosymmetry (pseudomonomerous gynoecium), presence of a single ovule, wide stigmatic surface, reduced perianth, and sometimes inflexed filaments are probably associated with anemophily (Cuellar, 1967; Culley et al., 2002; Friedman and Barrett, 2009; Preston et al., 2011; Endress, 2012). Most of the characters seem to be directly related to a floral reduction, except for the stigma that deserves greater attention due to its morphological diversity in the family. It consists of two branches in *T. micrantha* (present study), two bifid branches in *C. iguanaea* (present study) and two-unifacial feathery stigmas in *C. sativa* (present study) and *H. lupulus* (Endress, 2015). The strongly increased stigmatic surface of *C. iguanaea* may be the result of selective pressures exerted by the smaller number of functionally pistillate flowers than functionally staminate ones (Arruda and Sazima, 1988) in the only monoecious species among the species studies here. These features reinforce the strongly relation between floral morphology and pollination (Ronse De Craene, 2018), in this case wind-polinattion.

Also the stamens show considerable variation in their anatomy and morphology. In *C. sativa* the filament is thin and straight while in *C. iguanaea* and *T. micrantha* they are inflexed. In *T. micrantha* the presence of a secretory epidermis together with inflexed stamens can contribute to organ protection (Fahn, 2002) as well as dehydration and anther dehiscence.

Glandular trichomes are widely distributed in the flowers of the Cannabaceae species studied (present study, see Table 2), except for *Humulus lupulus*, in which this type of trichomes is restricted to the subtending bract (Sugiyama *et al*., 2006). The glandular trichomes of *Cannabis sativa* have been exhaustively studied, so that their morphology (Hammond and Mahlberg, 1973, 1977; Dayanandan and Kaufman, 1976; Gangadhara and Inamdar, 1977), their ultrastructure (Hammond and Mahlberg, 1978), and the chemical composition of the exudate (Turner et al., 1980, 1981; Happyana et al., 2013) are well much discussed topics in the literature. Our study, surprisingly, extends their distribution to the anther connective.

Outlook

The present study clarifies the development of the flower in some Cannabaceae species. Our data contribute to the knowledge of floral construction in the group, adding new information of genera included in the latest phylogenetic analyzes (Sytsma et al., 2002; Yang et al., 2013) and allow for a broader view of patterns floral development leading to functionally staminate and pistillate flowers and general floral reduction in connection with anemophily.

The interpretation of the floral ontogeny of *Cannabis sativa, Celtis iguanaea, Humulus lupulus* and *Trema micrantha* supports the current Cannabaceae phylogeny and the close relationship between *Celtis* and *Trema*, and *Cannabis* and *Humulus*, respectively (Yang et al., 2013). *Celtis* and *Trema* share a robust calyx, diclinous flowers formed by the initiation and subsequent abortion of organs, inflexed stamens and a bifacial stigma. However, *Celtis* and *Trema* differ from each other in other aspects such as the timing of stamen abortion and the number of stigmatic branches. *Cannabis* and

Humulus, on the other hand, are more homogeneous and share diclinous flowers characterized by the complete absence from the onset of floral development, straight stamens, and a unifacial stigma. Our data help to characterize genera or subclades of Cannabaceae and contribute to a more comprehensive understanding of floral diversity and evolution in Rosales.

1.6 References

APG IV. 2016. An update of the Angiosperm Phylogeny Group classification for the orders and families of flowering plants: APG IV. *Botanical Journal of the Linnean Society* 181: 1-20.

Arruda, V.L.V., and M. Sazima. 1988. Polinização e reprodução de *Celtis iguanaea* (Jacq.) Sarg. (Ulmaceae), uma espécie anemófila. *Revista Brasileira de Botânica* 11: 113-122.

Basso-Alves, J. P., R. A. S. Pereira, Y-Q Peng, and S. P. Teixeira. 2014. Different ontogenetic processes promote dicliny in *Ficus* L. (Moraceae). *Acta Oecologica* 57: 5-16.

Bechtel, A. R. 1921. The floral anatomy of the Urticales. *American Journal of Botanical* 8: 386-410.

Berg, C. C. 1977. Urticales, their differentiation and systematic position. *Plant Systematics and Evolution* 1: 349-374.

Berg, C. C. 1989. Systematic and phylogeny of the Urticales. In: *Evolution, systematics, and fossil history of the Hamamelidae*. Oxford, UK: Clarendon Press, 193-219.

Berg, C. C., and S. V. Dahlberg. 2001. A revision of *Celtis* subg. Mertensia (Ulmaceae). *Brittonia* 53: 66-81.

Briosi, G., and F. Tognini. 1894. *Anatomia Della Canapa (Cannabis sativa* L.*)*. Milano: Istituto Botanico Della R. Universitá Di Pavia.

Chernik, V. V. 1981. Pseudomonemeric gynoecium of the Ulmaceae and Celtidaceae representatives. *Botanicheskii Zhurnal (Moscow & Leningrad)* 7: 958-966.

Cronquist, A. 1988. *The evolution and classification of flowering plants*. Bronx, NY: The New York Botanical Garden.

Cuellar, H. S. 1967. Description of a pollen release mechanism in the flower of the Mexican Hackberry Tree, *Celtis laevigata*. *Southwestern Association of Naturalists* 12: 471-474.

Culley, T. M., S. G. Weller, and A. K. Sakai. 2002. The evolution of wind pollintion in angiosperms. *Trends in Ecology and Evolution* 17: 361-369.

Dayanandan, P., and P. B. Kaufman. 1976. Trichomes of *Cannabis sativa* L. (Cannabaceae). *American Journal of Botany* 63: 578-591.

Eckardt, T. 1937. Untersuchungen uber Morphologie, Entwicklungsgeschichte und systematische Bedeutung des pseudomonomeren Gynoeceums. *Nova Acta Leopold* 5: 1-112.

Endress, P. K. 1996. Diversity and evolutionary biology of tropical flowers. New York, USA: Cambridge University Press.

Endress, P. K. 2008. The whole and the parts: relationships between floral architecture and floral organ shape, and their repercussions on the interpretation of fragmentary floral fossils. *Annals of the Missouri Botanical Garden* 95: 101-120.

Endress, P. K., and M. L. Matthews. 2006. First steps towards a floral structural characterization of the major rosid subclades. *Plant Systematics and Evolution*, 260(2-4), 223-251.

Endress, P. K. 2010. Flower structure and trends of evolution in eudicots and their major subclades. *Annals of the Missouri Botanical Garden*, 97(4), 541-583.

Endress, P. K. 2011. Evolutionary diversification of the flowers in angiosperms. *American Journal of Botany* 98: 370-396.

Endress, P. K. 2012. The immense diversity of floral monosymmetry and asymmetry across Angiosperms. *Botanical Review* 78: 345-397.

Endress, P. K. 2015. Patterns of angiospermy development before carpel sealing across living angiosperms: diversity, and morphological and systematic aspects. *Botanical Journal of the Linnean Society* 178: 556-591.

Fahn, A. 2002. Functions and location of secretory tissues in plants and their possible evolutionary trends. *Israel Journal of Plant Sciences* 50: 59-64.

Fleming, M. P., and R. C. Clarke. 1998. Physical evidence for the antiquity of *Cannabis sativa* L. (Cannabaceae). *Journal of the International Hemp Association* 5: 80-92.

Friedman, J., and S. C. H. Barrett. 2009. Wind of change: New insights on the ecology and evolution of pollination and mating in wind-pollinated plants. *Annals of Botany* 103: 1515-1527.

Fukuoka, N. 1982. On pseudomonomerous pistil of the Ulmaceae. *Acta Phytotax. Geobot.* 56: 84-91.

Gangadhara, M., and J. A. Inamdar. 1977. Trichomes and stomata, and their taxonomic significance in the Urticales. *Plant Systematics and Evolution* 127: 121-137.

Hammond, C. T., and P. G. Mahlberg. 1973. Morphology of glandular hairs of *Cannabis sativa* from scanning electron microscopy. *American Journal of Botany* 60: 524-528.

Hammond, C. T., and P. G. Mahlberg. 1977. Morphogenesis of capitate glandular hairs of *Cannabis sativa* (Cannabaceae). *American Journal of Botany* 64: 1023-1031.

Hammond, C. T., and P. G. Mahlberg. 1978. Ultrastructural development of capitate glandular hairs of *Cannabis sativa* L. (Cannabaceae). *Botanical Society of America* 65: 140-151.

Happyana, N., S. Agnolet, R. Muntendam, A. Van Dam, B. Schneider, and O. Kayser. 2013. Analysis of cannabinoids in laser-microdissected trichomes of medicinal *Cannabis sativa* using LCMS and cryogenic NMR. *Phytochemistry* 87: 51-59.

Heslop-Harrison, J. 1956. Auxin and sexuality in *Cannabis sativa*. *Physiologia Plantarum* 9: 588–597.

Heslop-Harrison, J., and Y. Heslop-Harrison. 1957. Studies on flowering-plant growth and organogenesis. I. Morphogenetic effects of 2, 3, 5-triiodobenzoic acid on *Cannabis sativa*. *Proceedings of the Royal Society of Edinburgh. Section B. Biology* 66: 409-423.

Hirata, K. 1927. Sex determination in hemp (*Cannabis sativa* L.). *Journal of Genetics* 19.1: 65–79.

Karnovsky, M. J. 1965. A formaldehyde-glutaraldehyde fixative of hight osmolality for use in electron microscopy. *Journal of Cell Biology* 27: 137-138.

Leins, P., and C. Orth. 1979. Zur Entwicklungsgeschichte mannlicher Bluten von *Humulus lupulus* (Cannabaceae). (Organogenesis in male flowers of *Humulus lupulus* (Cannabaceae)). *Bot. Jahr. Syst*, 100(3), 372-378.

Lillie, R. D. 1965. Histopathologic technic and practical histochemistry. New York: McGraw-Hill.

Martins, E. G. A., and J. R. Pirani. 2009. Flora da Serra do Cipó, Minas Gerais: Cannabaceae. *Boletim Botânico Universidade São Paulo* 27: 247-251.

Mcdowell, E. M., and B. Trump. 1976**.** Histological fixatives for diagnostic light and electron microscopy. *Archives of Pathology and Laboratory Medicine* 100: 405-414.

Measham, F., R. Newcombe, and H. Parker. 1994. The normalization of recreational drug use amongst young people in North-West England. *British Journal of Sociology* 45: 287-312.

Milligan, S. R., J. C. Kalita, A. Heyerick, H. Rong, L. de Cooman, and D. de Keukeleire. 1999. Identification of a potent phytoestrogen in hops (*Humulus lupulus* L.) and beer. *The Journal of Clinical Endocrinology & Metabolism* 83: 2249-2252.

Nigam, R. K., M. Varkey, and D. E. Reuben. 1981. Irradiation induced changes in flower formation in *Cannabis sativa* L. *Biologia Plantarum* 23: 389-392.

O'Brien, T. P., N. Feder, and M. E. McCully. 1964. Polychromatic staining of plant cell walls by toluidine blue O. *Protoplasma* 59: 368-373.

Okamoto, M., K. Kosuge, and N. Fukuoka. 1992. Pistil development and parietal placentation in the pseudomonomerous ovary of *Zelkova serrata* (Ulmaceae). *Acta Oecologica* 79: 921-927.

Oliveira, M. M., and M. S. S. Pais. 1988. Glandular trichomes of *Humulus lupulus* var. Brewer's Gold: Ontogeny and histochemical characterization of the secretion. *Nordic Journal of Botany* 8: 349-359.

Payer, J. B. 1857. Traité D'Organogéne Comparée de La Fleur. Paris: Librairie de Victor Masson.

Pederneiras, L. C., A. F. Costa, D. S. D. Araujo, and J. P. P. Carauta. 2011. Ulmaceae, Cannabaceae e Urticaceae das restingas do estado do Rio de Janeiro. *Rodriguésia* 62: 299-313.

Preston, J. C., C. C. Martinez, and L. C. Hileman. 2011. Gradual disintegration of the floral symmetry gene network is implicated in the evolution of a wind-pollination syndrome. *Proceedings of the National Academy of Sciences of the United States of America* 108: 2343-2348.

Puri, V. 1951. The role of floral anatomy in the solution of morphological problems. *The Botanical Review* XVII: 471-553.

Ram, H. Y. M., and V. S. Jaiswal. 1972. Induction of male flowers on female plants of *Cannabis sativa* by gibberellins and its inhibition by abscisic acid. *Planta (Berl.)* 105: 263-266.

Ronse Decraene, L. P., and E. F. Smets. 2001. Staminodes: Their Morphological and Evolutionary Significance. *The Botanical Review* 67: 351-402.

Ronse De Craene, L. 2018. Understanding the role of floral development in the evolution of angiosperm flowers: clarifications from a historical and physicodynamic perspective. *Journal of Plant Research* 131: 367-393.

Sharma, M. R. 1964. Morphological and anatomical investigations on *Artocarpus* Forst. *IV. The Fruit, By School of Plant Morphology, Meerut* IV: 380-393.

Schmid, R. 1976. Filament histology and anther dehiscence. *Botanical Journal of the Linnean Society* 73: 303-315.

Shephard, H. L., J. S. Parker, P. Darby, and C. C. Ainsworth. 2000. Sexual development and sex chromosomes in hop. *New Phytologist* 148: 397-411.

Smith, F. H., and E. C. Smith. 1942. Anatomy of the inferior ovary of *Darbya*. *American Journal of Botanical* 29: 464-471.

Soltis, D. E., P. S. Soltis, P. K. Endress, and M. W. Chase. 2005. Phylogeny and Evolution of Angiosperms. Sunderland, MA, USA: Sinauer Associates, Inc.

Sugiyama R, H. Oda, and F. Kurosaki. 2006. Two distinct phases of glandular trichome development in hop (*Humulus lupulus* L.). *Plant Biotechnology* 23: 493-496.

Sytsma, K. J., J. Morawetz, J. C. Pires, M. Nepokroeff, E. Conti, M. Zjhra, J. C. Hall, and M. w. Chase. 2002. Urticalean Rosids: Circumscription, Rosid ancestry, and phylogenetics based on rbcL, trnL-F, and ndhF sequences. *Acta Oecologica* 89: 1531-1546.

Torres, R. B. 1996. Biologia da reprodução *Trema micrantha*. PhD Thesis. Universidade Estadual de Campinas.

Torres, R. B., and A. Q. Luca. 2005. Ulmaceae. In: Wanderley M das GL, Shepherd G, Giulietti AM, Melhem TS, eds. Flora Fanerogâmica do Estado de São Paulo, Online. São Paulo: FAPESP: RiMa, 437.

Turner, J. C., J. K. Hemphill, P. G. Mahlberg. 1980. Trichomes and Cannabinoid Content of Developing Leaves and Bracts of *Cannabis sativa* L. (Cannabaceae). *American Journal of Botany* 67: 1397-1406.

Turner, J. C., J. K. Hemphill, and P. G. Mahlberg. 1981. Interrelationships of glandular trichomes and cannabinoid content. I: Developing pistillate bracts of *Cannabis sativa* L. (Cannabaceae). *Bulletin on Narcotics* 33: 59-69.

Ware, M. A., and V. L. Tawfik. 2005. Safety issues concerning the medical use of *Cannabis* and cannabinoids. *Pain Research and Management* 10: 31-37.

Weston EW. 1960. Changes in sex in the hop caused by plant growth substances. Nature 188: 81±82.

Yang, M-Q., R. Van Velzen, F. T. Bakker, A. Sattarian, D. Li, and T. Yi. 2013. Molecular phylogenetics and character evolution of Cannabaceae. *Taxon* 62: 473-485.

Zanoli, P., and M. Zavatti. 2008. Pharmacognostic and pharmacological profile of *Humulus lupulus* L. *Journal of Ethnopharmacology* 116: 383-396.

"Todos querem o perfume das flores, mas poucos sujam as suas mãos para cultivá-las."

Augusto Cury

CHAPTER 2: 'ONTOGENY AND VASCULARIZATION ELUCIDATE THE ATYPICAL FLORAL STRUCTURE OF AMPELOCERA GLABRA KUHLM., A TROPICAL SPECIES OF ULMACEAE'

Chapter 2: Ontogeny and vascularization elucidate the atypical floral structure of *Ampelocera glabra* Kuhlm., a tropical species of Ulmaceae

2.1 Abstract

Ampelocera glabra is an andromonoecious, wind-pollinated species of Ulmaceae, the elm family. This family comprises two clades: tropical and temperate. The species that have been morphologically studied so far all belong to the temperate clade. *A. glabra* is included in the tropical clade and is remarkable due to its atypical flower merism when compared to other Ulmaceae and to most other rosids: tetramerous calyx, polyandrous androecium, and pseudomonomerous gynoecium. Thus, our objective was to study the ontogeny and vascularization of the *A. glabra* flower to elucidate the processes involved in the atypical merism and in the reduced structure of the whorls. Additionally, the mating system of *A. glabra* was checked and its floral structure was found to be associated with anemophily, thus contributing to reproductive studies of this species under threat of extinction. Flowers and early to late floral buds were processed for surface (scanning electron microscopy) and histological investigations (light microscopy) and 3D reconstructions (X-Ray Micro Computed Tomography). *A. glabra* is actually a monoecious species with functionally staminate and functionally pistillate flowers, containing carpellodes and staminodes, respectively. The single perianth whorl is composed of sepals and there is no hypanthium. Each primordium of the sepals and stamens arises individually. A central common primordium gives rise to two carpels, but only one houses an ovule. Each carpel is vascularized by one dorsal bundle, and the carpel that bears the ovule is also vascularized by one ventral bundle. Thus, the gynoecium displays a reduction in the vascular bundle in the non-ovulate carpel. The differences in merism between the calyx and androecium are explained by the space that can support the increase in organ number. The increase in stamen number and the reduced gynoecium (pseudomonomerous) enable a high pollen:ovule ratio, an important condition for any anemophilous species.

Key words: anatomy; floral development; floral morphology; Rosales; Urticalean rosid.

2.2 Introduction

Ampelocera glabra Kuhlm is a tropical species of the elm (*Ulmus*) family, Ulmaceae. It is endemic to Brazil (Machado 2016; Pederneiras and Machado 2017) and under threat of extinction (Pederneiras et al. 2014). Together with other 11 species it composes the species-richest tropical genus of the family (The Plant List 2013).

Ulmaceae is a well-known family for its widespread ornamental and medicinal uses (Ahmed et al. 2016; Sutar et al. 2016). It comprises 64 species distributed into seven genera (Neubig et al. 2012; The Plant List 2013). Phylogenetic studies have shown that the generic relationships form two main clades, one with tropical genera (*Ampelocera, Holoptelea, Phyllostylon*) and the other with the North Temperate genera (*Hemiptelea, Planera, Ulmus,* and *Zelkova*) (Neubig et al. 2012). This family, together with Cannabaceae, Moraceae, and Urticaceae, forms the urticalean rosid clade (Sytsma et al. 2002; Zhang et al. 2011), which belongs to the order Rosales (APG IV 2016). Members of Rosales are morphologically diverse (see Baas et al. 2000; Judd et al. 2009), but the urticalean rosids have several synapomorphies, such as the presence of globular cystoliths, inconspicuous flowers, two carpels forming a unilocular or bilocular and uniovulate ovary, and porate pollen (Judd et al. 2009).

The members of Ulmaceae exhibit a variety of breeding systems: monoecy, andromonoecy, hermaphroditism or polygamy (definitions according to Richards 1997) and of floral morph types: staminate, pistillate and/or perfect flowers (Bechtel 1921; Berg 1977, 1989). Similar to other urticalean rosids, their flowers have only one whorl of perianth organs, cited as perianth lobes (Bechtel 1921), sepals (Todzia 1989) or tepals (Pederneiras 2011), and a pseudomonomerous gynoecium (apparently unicarpellate but formed by two or more carpels) (Berg 1977, 1989; Fukuoka 1982; Todzia 1989, 1992; Okamoto *et al.* 1992). Taken together, these characteristics point to a pervasive reduction at different levels of floral structure. However, in contrast to other members of the urticalean clade, the flower of Ulmaceae species seems to have a hypanthium (Sytsma et al. 2002; Judd et al. 2009) as observed in Barbeyaceae,

Dirachmaceae, Elaeagnaceae, Rhamancaeae and Rosaceae, the other five families of Rosales. In addition, some species of Ulmaceae have perfect flowers and a polyandrous androecium composed of four to 10 (Berg 1989; Todzia 1992) or up to 16 stamens (Todzia 1989). In *Ulmus* (Bechtel 1921) and *Phyllostylon* (Todzia 1992), unlike *Ampelocera* (Todzia 1989), the sepal number is similar to the stamen number. The high variation in the stamen number has not been investigated in Ulmaceae.

The floral ontogeny of Ulmaceae is generally poorly known. Nonetheless, the early, classic study by Bechtel (1921) is notable for the quality and amount of information for *Ulmus* species {*U. americana*, *U. rubra* (*syn. U. fulva*), *U. thomassi* (*syn. U. racemosa*), *U. glabra* (*syn. U. campestris* and *U. scabra*)} and for the discussion of floral reduction in the family and other urticalean rosids. The following floral characteristics of this plant group have been studied: vascularization of the pseudomonomerous gynoecium in *Ulmus glabra* (*syn. U. montana*) (Eckardt 1937; Chernik 1981), *Hemiptelea davidii* and *Zelkova carpinifolia* (Chernik 1981); placentation in *Ulmus parvifolia* and *Zelkova serrata* (Fukuoka 1982); and gynoecium development in *Zelkova serrata* (Okamoto et al. 1992). Most of the studies have focused on the gynoecium structure; thus, the variation of merism in Ulmaceae remains poorly understood. Also, the polyandry of the flowers has received little if any attention. The species of Ulmaceae that have been morphologically studied so far all belong to the temperate clade.

The present study focused on *Ampelocera glabra,* a wind-pollinated species, described as andromonoecious (Todzia 1989; Pederneiras and Machado 2017) and a representative of the tropical clade of Ulmaceae. It is a remarkable species due to its atypical flower merism when compared to other Ulmaceae and to most other rosids: tetramerous calyx, polyandrous androecium (8-16 stamens), and pseudomonomerous gynoecium (two carpels) (Todzia 1989). Thus, the objective of the present investigation was to study the ontogeny and vascularization of the flowers to elucidate the processes involved in the atypical merism, the reduced structure of the whorls and the nature of the single perianth whorl. In addition, we checked the occurrence of andromonoecy, of a hypanthium, and identified floral features associated with anemophily in this

species. The information about the floral structure is considered from a broad comparative perspective for Ulmaceae and urticalean rosids.

2.3 Materials and methods

Buds in several developmental stages and anthetic flowers of *Ampelocera glabra* were collected in the Reserva Particular do Patrimônio Natural (RPPN), Serra do Teimoso, Jussari, BA, Brazil. Voucher specimens were deposited in the SPFR herbarium (FFCLRP/USP), under the following accessions: Leme F.M. nº 102 and Leme F.M. nº 112.

Samples were fixed in buffered formalin (Lillie 1965) or in Karnovsky's solution (Mcdowell and Trump 1976) and dehydrated in an ethanol series up to 100% for further processing and observation under light microscopy (LM), scanning electron microscopy (SEM) and high resolution computed x-ray tomography (microCT).

For the anatomical study (LM), samples were embedded in histological resin (Leica) and sectioned in both transverse and longitudinal planes (1-3 μm thick) using a rotary microtome (Leica RM 2245). Serial sections were stained with 0.05% toluidine blue in phosphate buffer, pH 5.8 (O'Brien et al. 1964), mounted on a slide using water, and observed under a light microscope. Photomicrographs were obtained with a Leica DM 5000 B light microscope coupled to a Leica DFC 295 digital camera.

For SEM analysis, samples were critical point dried in a Bal Tec CPD 030 apparatus, mounted on metal supports with carbon adhesive tape, and coated with gold for 360 s using a Bal Tec SCD 050 sputter coater. Electron micrographs were obtained with a Zeiss EVO-50 scanning electron microscope at 15 kv.

For micro-CT, anthetic flowers were treated with a solution of 1% phosphotungstic acid in 70% ethanol for one week (Staedler et al. 2013), dehydrated in an ethanol series with 1% phosphotungstic acid, critical point dried (Autosamdri-815), mounted on an aluminum holder with two-component epoxy glue (UHU Plus Epoxy: Binder + Hardener) and scanned. The scans were performed on a MicroXCT-200

imaging system (Xradia, Pleasanton, CA, USA) with a L9421-02 90kV Microfocus X-ray (MFX) source (Hamamatsu Photonics, Iwata City, Japan) using the following settings: acceleration voltage, 23 kV; source current, 173 μA; exposure time, 23 s; pictures per sample, 1200; camera binning, 1; optical magnification, 1 x and 4 x, with pixel sizes of 7.7 μm and 1.5 μm, respectively. The total exposure time was approximately 10 hours for each sample. The XMReconstructor 8.1.6599 software (XRadia Inc.) was used to perform the 3D reconstruction from the scanning data. The AMIRA-based XM3DViewer 1.1.6 (XRadia) was used for the visualization of the scan data.

2.4 Results

Floral organization

Ampelocera glabra is a monoecious tree (Figs. 1, 2) with inflorescences of the dichasium type (Fig. 2D). The dichasium is usually formed by three flowers of the same morph type (Figs. 1A, 2A, D).

Flowers are functionally staminate (3.5 mm long and 2.75 mm wide - Fig. 1A-D) or functionally pistillate (structurally perfect) (3.5 mm long and 2.75 mm wide - Fig. 2A-C), with a single whorl of perianth interpreted as sepals, 11 to 13 (rarely 14) stamens or staminodes and two carpels or carpellodes. The calyx of both morph types has four green imbricate and united sepals forming a cup (Figs. 1A-D, 2C). In the functionally staminate flowers, stamens have straight, green filaments connected at the base of the anther; the anthers are rimose, latrorse and white, and have a conspicuous apical protrusion (Fig. 1B); the pistillode is similar to a reduced pistil (Fig. 1C, D). In the functionally pistillate flowers, staminodes have short filaments thickened at the base, and the pistil has a bifid stigma (Fig. 2A) and an uniloculate, uniovulate ovary (Fig. 2B, C).

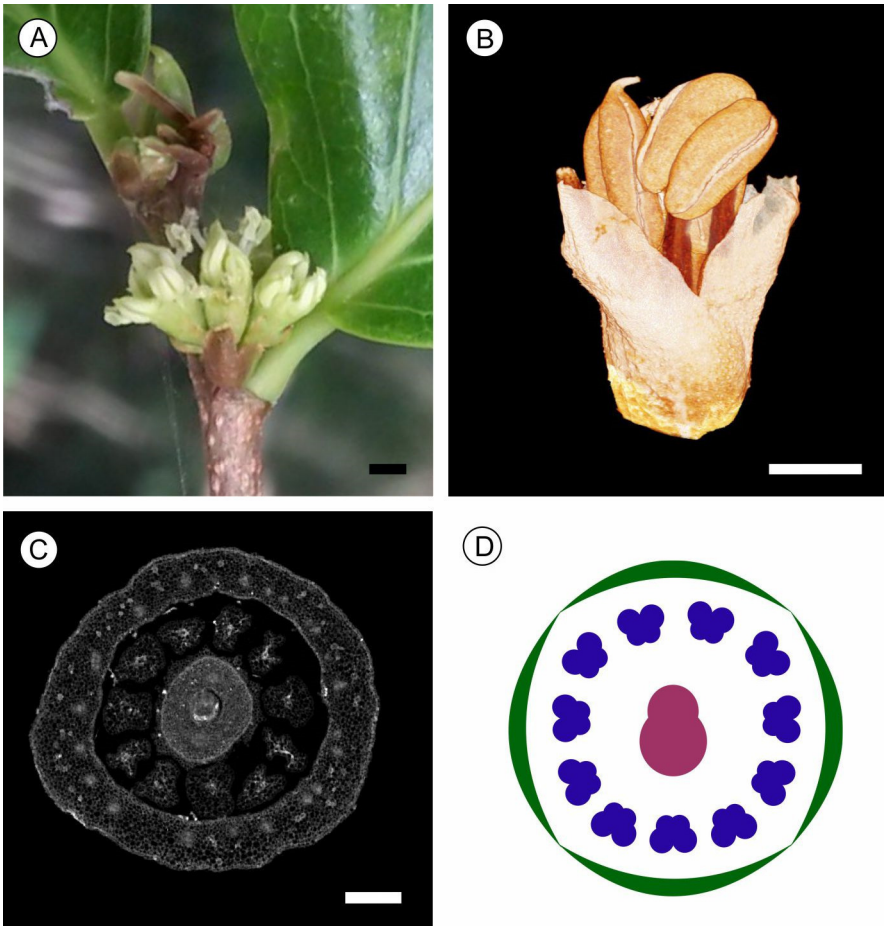

Fig. 1 Inflorescence and functionally staminate flower of *Ampelocera glabra*. A, Determinate inflorescence in a leaf axil with an evident bract and only three anthetic flowers. B, MicroCT 3D reconstruction of the flower; note the connective protrusion visible in one of the anthers. Two anthers are visible with longitudinal dehiscence; other anthers fell but the filaments are present although covered with sepals (see C). C, Micro CT 2D reconstruction in cross section; note the united sepals, the filament number (11) and the pistillode at the center. D, Floral diagram with four united sepals (green), 11 stamens (dark blue), and a central pistillode (purple) formed by two carpellodes. Scale bars: A-B = 1 mm, C = 250 μm.

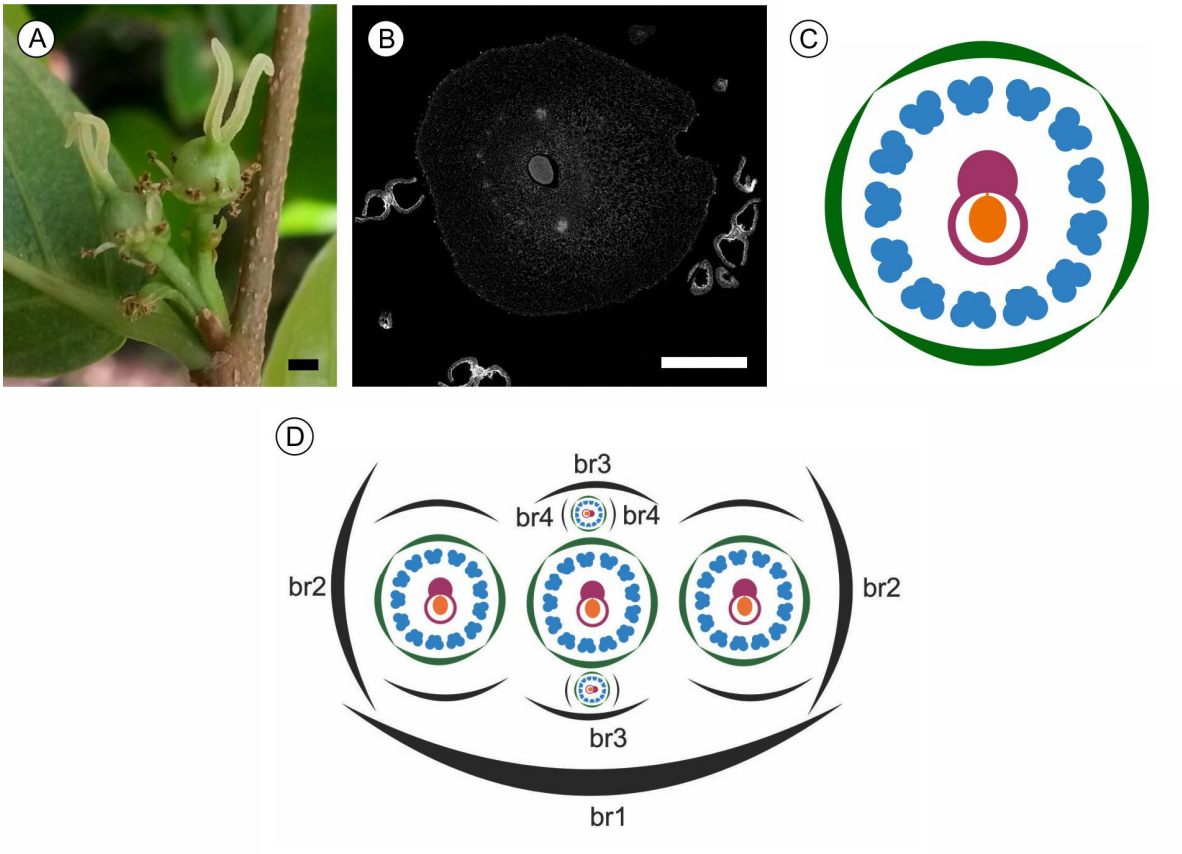

Fig. 2 Inflorescence and functionally pistillate flower of *Ampelocera glabra*. A, Determinate inflorescence in a leaf axil with a bract at the base and only two anthetic flowers. There are usually three, but here one did not develop. B, MicroCT 2D reconstruction in cross section; note the large pistil with one ovule. C, Floral diagram with four united sepals (green), 13 staminodes (light blue), and a pistil formed by two carpels (purple) with an ovule (orange). D, Inflorescence diagram with bracts of first (br1), second (br2), third (br3) and fourth (br4) orders. Scale bars: A-B = 1 mm.

Floral development

The inflorescence meristems of functionally staminate and functionally pistillate flowers (Fig. 3A) are subtended by an abaxial bract of first order and two lateral bracts of second order (Figs. 2D, 3B).

Each floral meristem is subtended by two opposite bracts of third order (Figs. 2D, 3B, C). These third-order bracts are arranged in parallel in the three floral meristems (Figs. 2D, 3A, B) and sometimes protect a new floral meristem (Fig. 2D, arrow - Fig. 3C), which is usually aborted. During development of the inflorescence only the three central floral meristems develop.

The floral meristem is rounded before the initiation of the floral organs (Fig. 3A, B). The meristem then enlarges (Fig. 3B), and the first sepal primordium emerges

on the abaxial side, followed by the second primordium, opposite to the first (Fig. 3B, D). Soon thereafter the third and then the fourth sepal primordia emerge in opposite and in lateral positions (Fig. 3C).

The sepal primordia elongate, and the first two or three stamen primordia arise alternate with the sepals (Fig. 3E-G). Other stamen primordia arise on the side of the first stamens (Fig. 3E, F), apparently opposite to each other. Concomitantly, a central carpel primordium arises (Fig. 3E-G). The stamen primordia continue arising in an irregular pattern, completing the four alternisepalous stamens and others in different positions (Fig. 3G-J), while the carpel primordium enlarges (Figs. 3J, 4A, 5A). The stamens initiated occupy all the space between the calyx and the pistil (Figs. 4A, 5A). Then, the carpel primordium divides, partially forming two carpel primordia congenitally united (Figs. 4A, B, 5B), opposite to each other (abaxial and adaxial) (Figs. 4A, B, 5B) which elongate together with the first formed stamen primordium (Figs. 4B, 5B). In the subsequent stages, one carpel forms a locule (carpel 1 = the largest carpel) (Figs. 4B, 5B), while the other remains small (carpel 2). The carpels elongate from the apex and form two stigmatic branches (Figs. 4C, H, 5C). The sepals, which initiated as individual primordia, start to elongate united, forming a synsepalous calyx. The sepals have mucilaginous idioblasts embedded in the mesophyll (Figs. 4E-G, 5D).

The initial developmental stages of both floral morph types, functionally staminate and functionally pistillate, are similar. The main differences between the morph types are the presence of a pistillode or a pistil, the presence or absence of a functional endothecium in the anther wall, and the presence or absence of viable pollen grains (Fig. 4A).

In the functionally staminate developing flower, the anthers differentiate concomitant to the carpellode elongation (Fig. 4C). The anthers finish differentiation (Fig. 4D), the filaments elongate (Fig. 4E), and the stamens are enclosed by the synsepalous calyx, whose sepals elongate at the same time (Figs. 1C, 4E, F). The emerged carpellodes do not develop further, remaining as a reduced gynoecium (Fig. 4E, H). The single ovule may be initiated in carpel 1 (abaxial) (Fig. 4H) or be absent. At

the end of development, the filaments are straight (Fig. 4H), and the anthers have a distinct endothecium layer with annular thickenings in the protuberant part of the microsporangia (Fig. 4I-J). Bicellular pollen grains are observed at this stage (Fig. 4I-J).

In the functionally pistillate flower, carpel 1 forms a cleft and initiates a single ovule; carpel 2 has short margins and does not form a cleft or an ovule. The carpels unite by their margins and elongate from the apex. The margins of carpel 1 are larger than the margins of carpel 2. Carpel 1 composes most of the ovary and one stigmatic branch, whereas carpel 2 forms only a column that makes up a part of the ovary and the other stigmatic branch. The two stigmatic branches remain near to each other until the cleft closes; there is no style (Fig. 5C). The staminodes have short or long filaments (Fig. 5D) and are randomly positioned. The anthers contain fewer pollen grains (Fig. 5E), some of which are atypical (Fig. 5F). No distinct endothecial cell wall thickenings are present in the anther wall (Fig. 5E). At the end of development, the ovary is unilocular and houses a single antitropous ovule (Fig. 5G) with two integuments of the same thickness (Fig. 5H). The ovary is covered with many secretory trichomes (Fig. 6A) which consist of a thin stalk and a multicellular head (Fig. 6A, detail). The two stigmatic branches are feathery, of equal size and bifacial (Fig. 6B). The inner face of the stigmatic branches is papillose (Fig. 6C) and reaches the ovary region (Fig. 6D). Both stigmatic branches show germinating pollen grains, characterized as both receptive and functional (Fig. 6B, E, F).

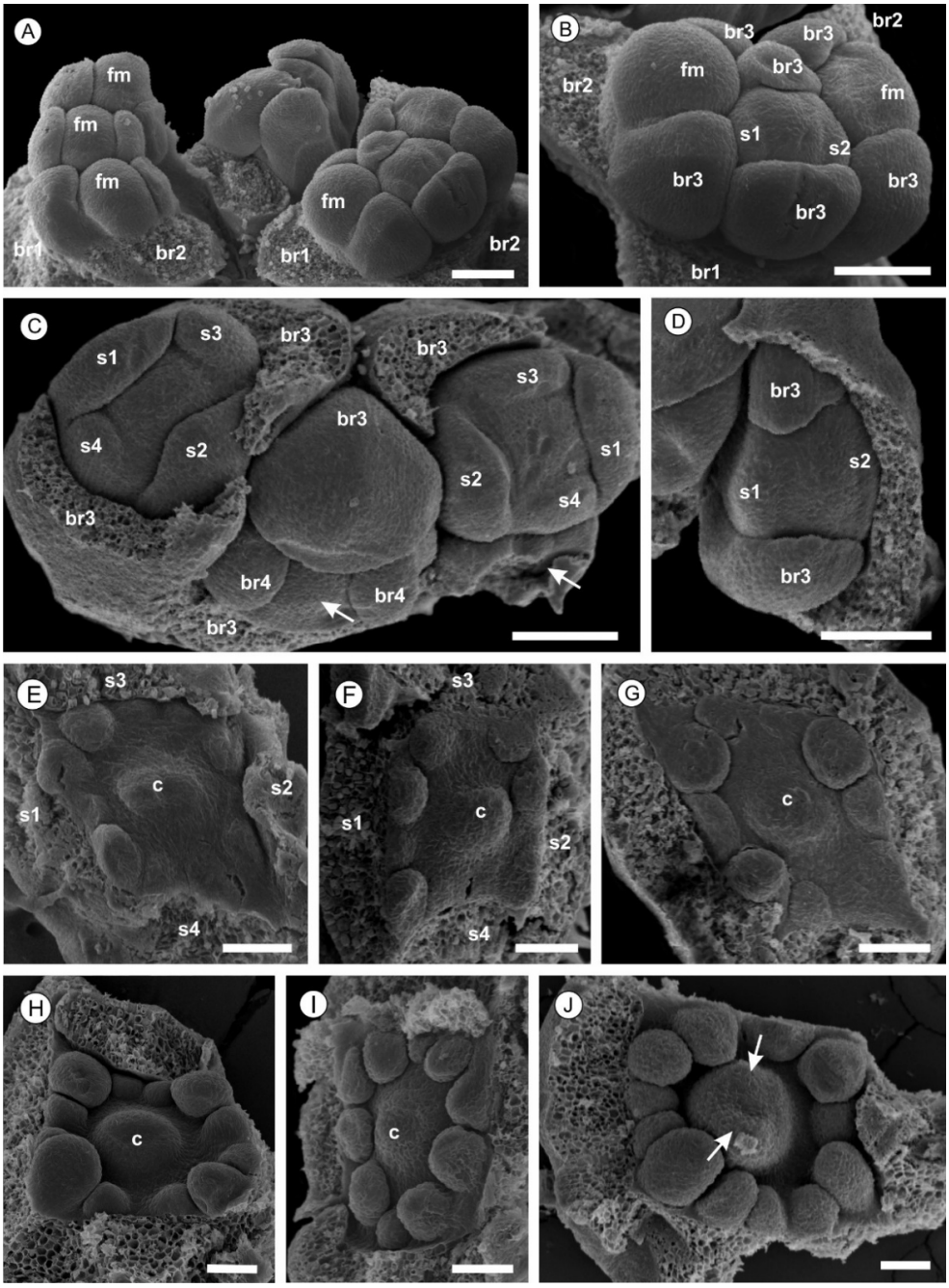

Fig. 3 Floral ontogeny of functionally staminate and pistillate flowers of *Ampelocera glabra*. A-G, SEM. H-J, LM. A-B, The inflorescence is subtended by one abaxial bract of first order and two lateral bracts of second order (removed) that cover three floral meristems. Observe the rounded floral meristems, each with two third-order bracts on the same plane. B, Enlargement of the floral meristem showing the first two sepal primordia on opposite sides of the floral apex in the inflorescence center. C, Bracts of third order removed to show the third and fourth sepal primordia alternating with the first two. Developing inflorescence with two small floral meristems with bracts of fourth order (arrows) perpendicular to the central floral meristem. D, Detail showing the first two sepal primordia on opposite sides of the floral apex. E-G, Sepals removed showing stamen primordia (arrow) and a central carpel primordium. Note that the first three stamens are alternate to the sepals and no stamens are found in the space between two sepals (s2 and s4) in the lower right. H-I, Stamens in irregular initiation totally occupy the available space. J, Final stage of initiation of stamens and elongation of the first stamens formed. Note the stamens occupying the entire space between sepals and gynoecium; division of the carpel primordium into two carpel primordia (arrow). Abbreviations: fm, floral meristem; br1, first order bract; br2, second order bracts; br3, third order bracts; br4, fourth order bracts; c, carpel primordium; s1, s2, s3, s4, sepal; st, stamen. Scale bars: A, B, C, D = 100 μm; E, F, G, H, I, J = 50 μm.

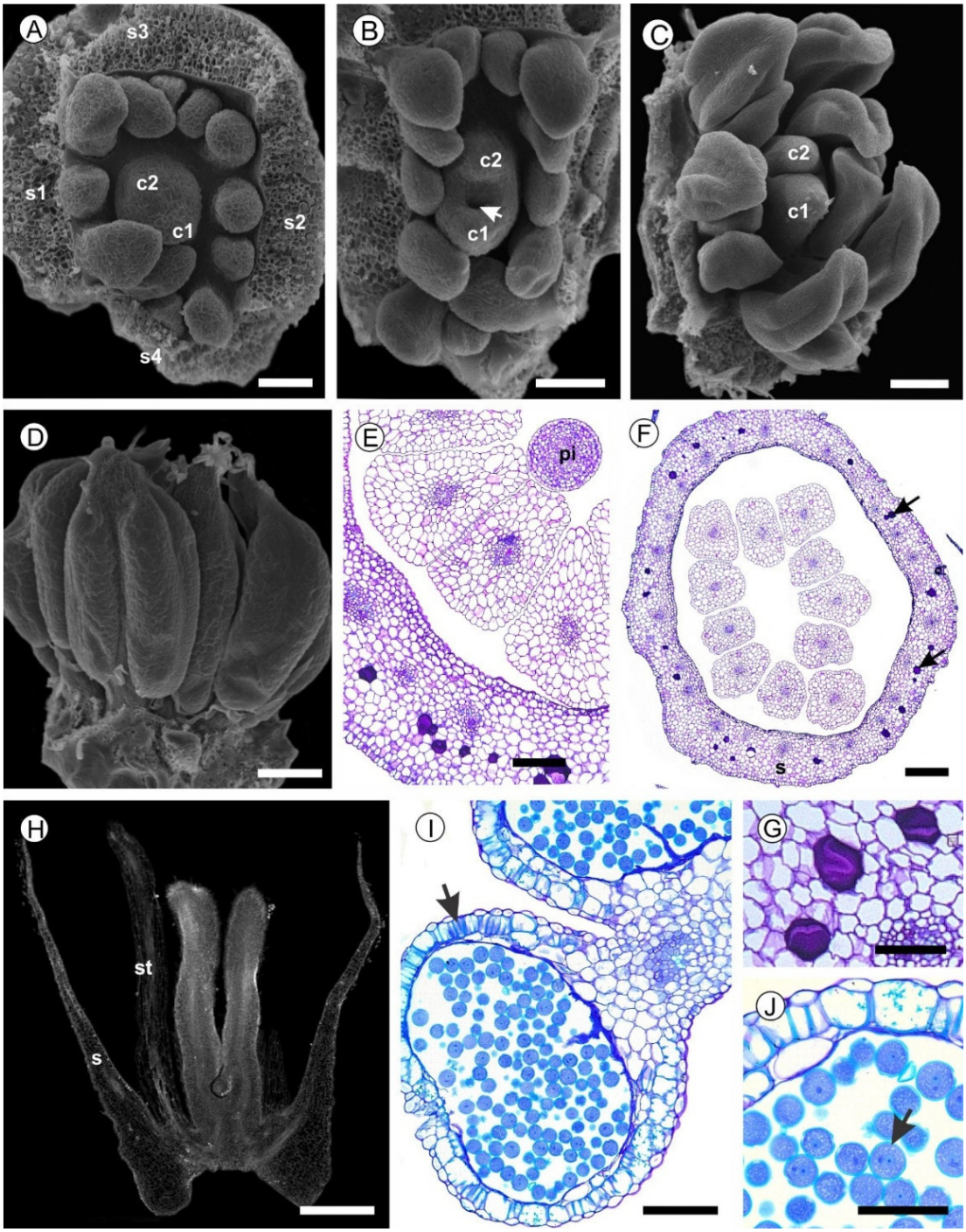

Fig. 4 Floral ontogeny of a functionally staminate flower of *Ampelocera glabra*. A-D, SEM; E-G, I-J, LM; H, MicroCT 3D reconstructions. A, Floral bud (sepals removed) with 12 stamens in different developmental stages and the division of the carpel primordium into two carpel primordia in the center. B, Floral bud (sepals removed) with 13 stamens in elongation and two united carpels in the center. Note that the carpel positioned in the lower part of the image is larger and already shows a differentiating locule (arrow). C, Differentiation of the anthers and elongation of the carpels. D, Stamens with differentiated anthers and short filaments. E, Mature flower in cross section (close to the floral base). Note the sepal with mucilaginous cells, the filaments and a central pistillode. F, Mature flower in cross section (median region of the flower). Note the synsepalous calyx with mucilaginous cells (arrow). G, Detail of the mucilaginous cells of the calyx stained with toluidine blue with a thickened mucilaginous inner cell wall. H, Note the straight filament and an ovule primordium in the pistillode (longitudinal section). I, Anther with pollen grains and distinct endothecium cells (arrow). J, Bicellular pollen grains. Abbreviations: c1, c2, carpels; pi, pistillode; s1, s2, s3, s4, sepal; st, stamen. Scale bars: A = 50 μm; B, C, D, E, F = 100 μm; G = 50 μm; H = 500 μm; I = 100 μm; J = 50 μm.

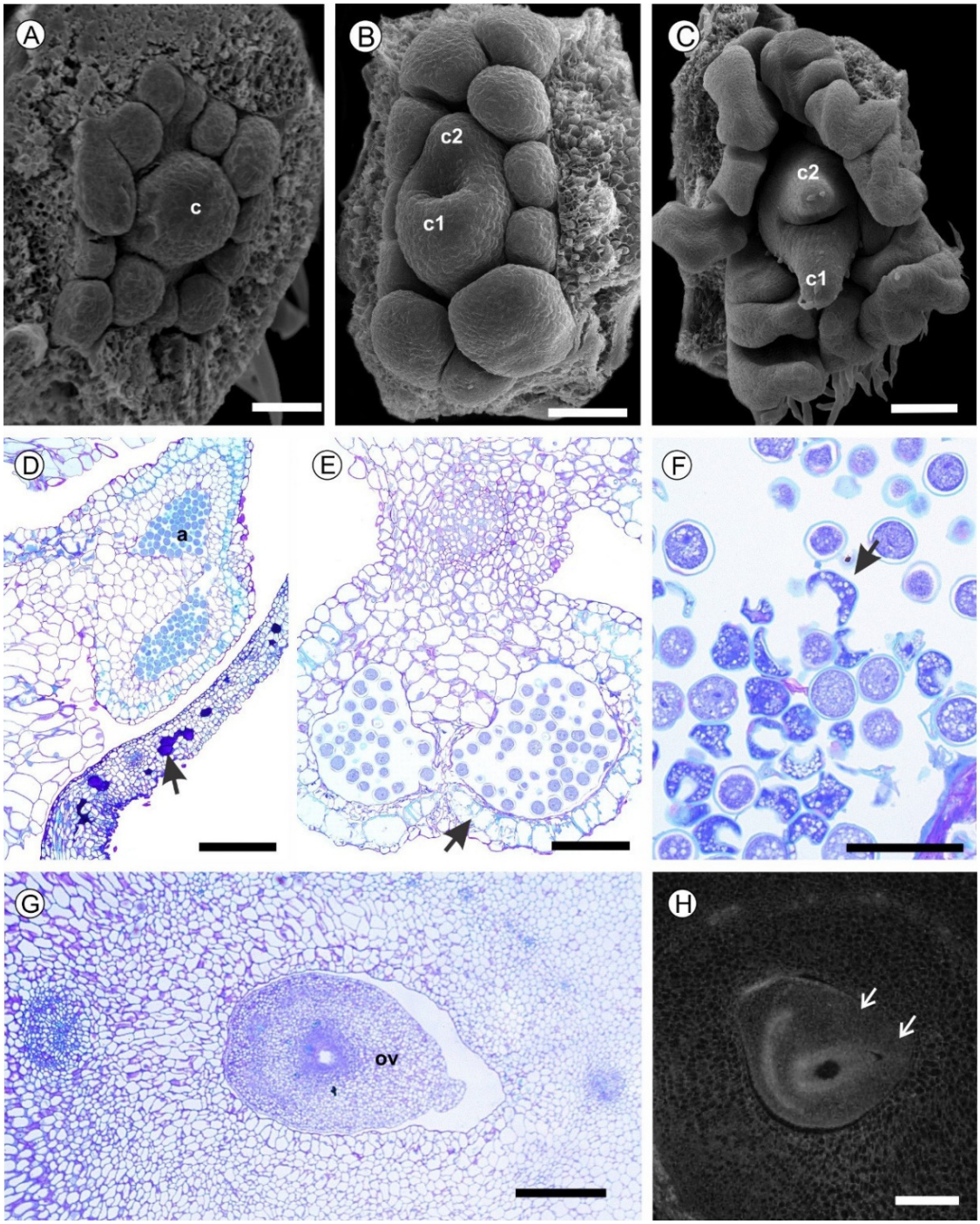

Fig. 5 Floral ontogeny of a pistillate flower of *Ampelocera glabra*. A-C, SEM; D-G, LM; H, MicroCT 3D reconstructions. A, Floral bud (sepals removed) with 13 staminodes initiated and one broad carpel primordium in the center. B, Floral bud (sepals removed) with 11 staminodes in different developmental stages and two united carpels in the center. Note that the carpel positioned in lower part of the image is larger. C, Differentiation of the anthers and elongation of the carpels. D, Mature flower in longitudinal section showing the sepal and staminode. Note the mucilaginous idioblasts in the sepal and one short filament. E, Cross section of the staminode anther. Note two small sporangia with few pollen grains and the endothecium with no distinct cell wall thickenings. F, Atypical pollen grains in the staminode. G, Cross section of the ovary and a central ovule. H, Longitudinal section of the ovary showing the pendule ovule positioned in the apex locule. Note the presence of two integuments (arrow). Abbreviations: a, anther; c, carpel primordium; c1, c2, carpel; ov, ovule. Scale bars: A = 50 μm; B, C = 100 μm; D, E = 250 μm; F = 200; G = 100 μm; H = 25 μm.

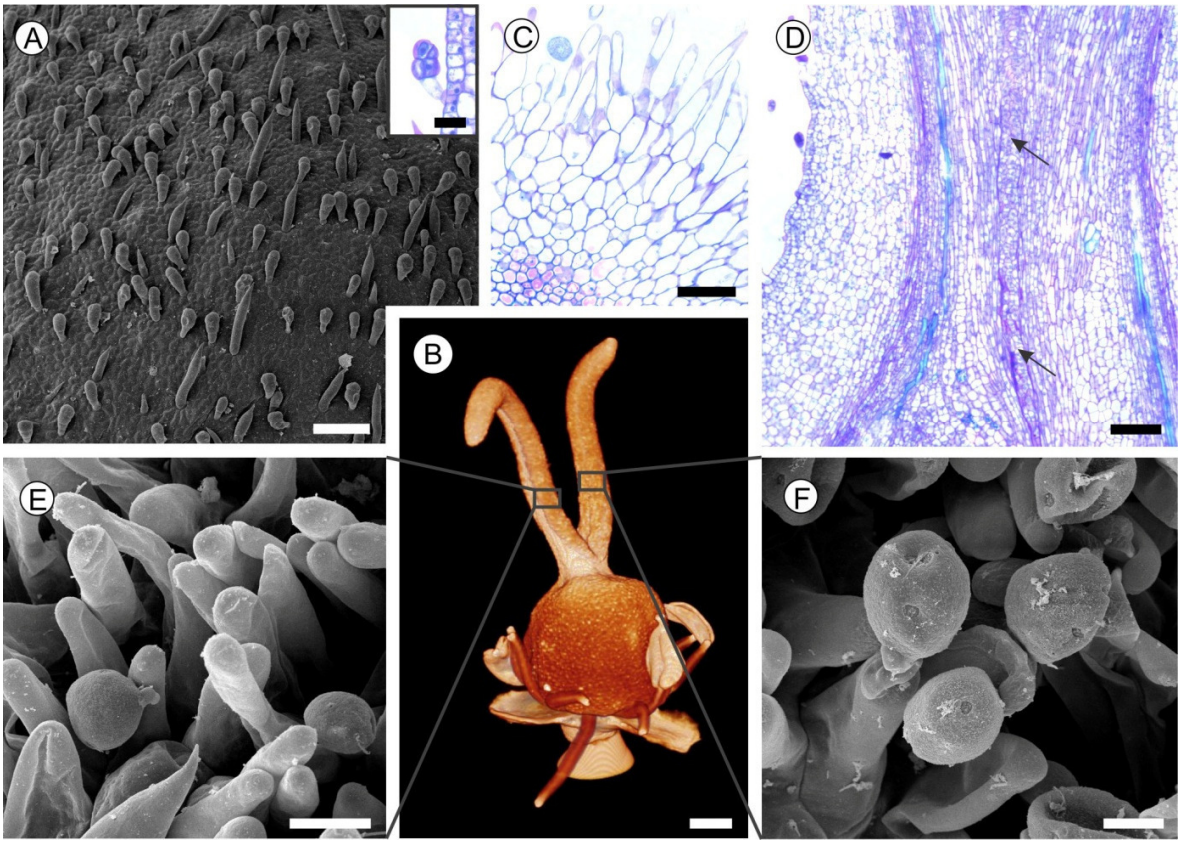

Fig. 6 Details of the ovary and stigma of *Ampelocera glabra.* A, E, F, SEM; detail A, C, D, LM; B, MicroCT 3D reconstructions. A, Ovary surface with many secretory trichomes and a detail of the trichome anatomy in the corner. B, Functionally pistillate flower with two stigmatic branches. Note the bifacial stigma. C, Papillose stigma with germinating pollen grains. Note the large nuclei of the papillose cells. D, Ovary apex. Note the union of the stigmatic branches by papillae and secretory trichomes. E, Germinating pollen grains on the stigmatic branch on the left of figure B. F, Germinating pollen grains on the stigmatic branch on the right of figure B. Scale bars: A = 100 μm, detail = 25 μm; B = 1 mm; C = 50 μm; D = 100 μm; E = 20 μm; F = 10 μm.

Floral vascularization

The single whorled perianth of both functionally staminate and pistillate flowers is vascularized by 15 bundles (Fig. 7A-D). Each sepal is served by three or sometimes four vascular traces. Occasionally, two neighboring sepals share a synlateral vascular trace that forms two bundles. Each stamen/staminode has only one vascular bundle (Fig. 7C).

Each carpel is vascularized by one dorsal bundle, and carpel 1 (the larger carpel) is also vascularized by one ventral bundle (Fig. 8A-H). The dorsal bundles are opposite to each other and extend up into the stigma lobes (Fig. 8A, B); one belongs to carpel 1 (in green – Fig. 8B), and the other belongs to carpel 2 (in blue - Fig. 8B). The ventral bundle of carpel 1 is united to the dorsal bundle of carpel 2 (blue) (Fig. 8B-H),

but it is difficult to demonstrate the individuality of the vascular unit. Close to the locule apex, the ventral bundle of carpel 1 veers off to vascularize the ovule (in green - Fig. 8B, G, H).

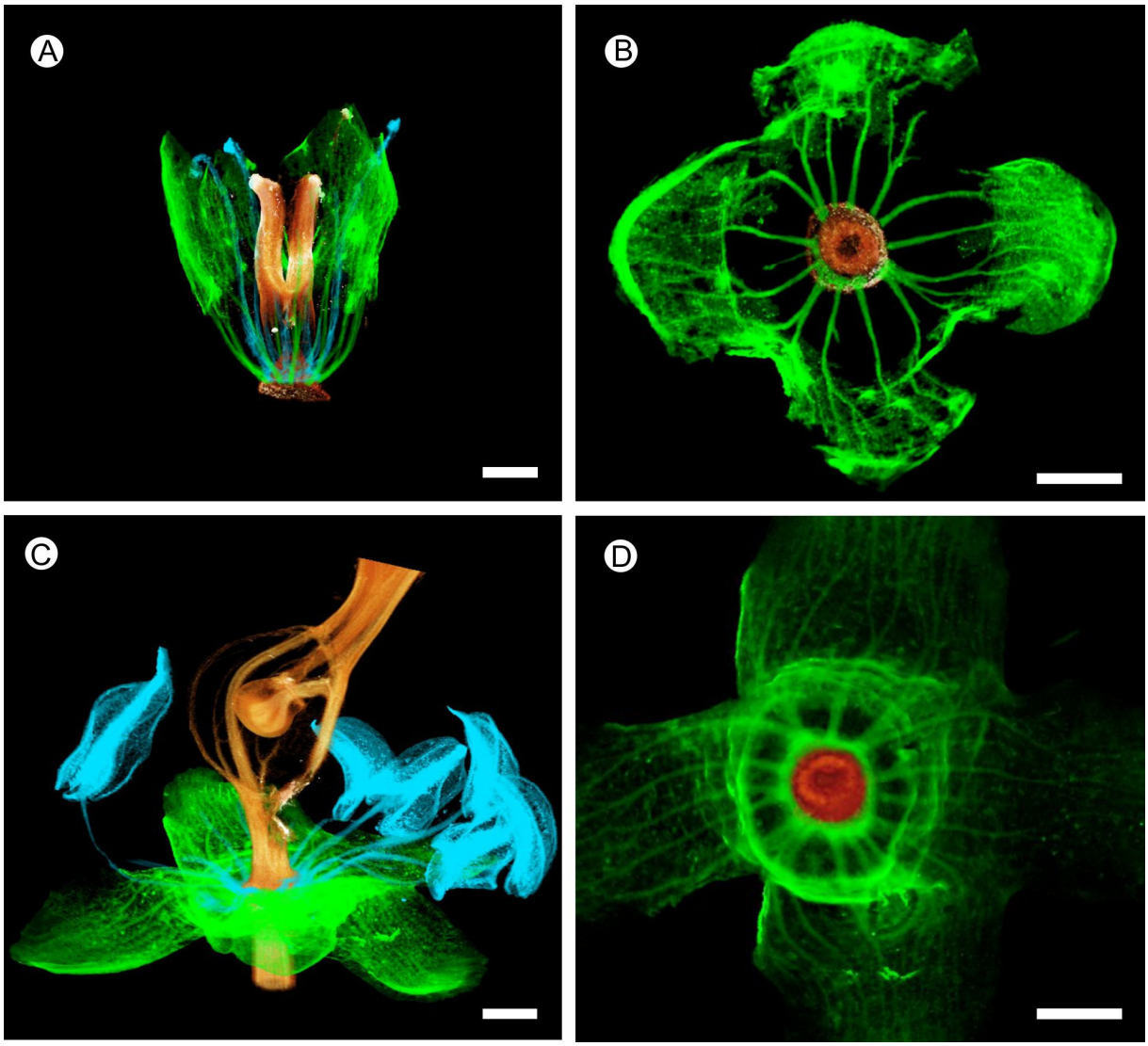

Fig. 7 Floral vasculature of functionally staminate and pistillate flowers of *Ampelocera glabra*. MicroCT 3D reconstructions. A-B, Functionally staminate flower. Floral vasculature of sepals (green), stamens (blue) and pistillode (orange). Note the synsepalous calyx and the fact that two neighboring sepals share a synlateral vascular strand that forms two strands. C-D, Functionally pistillate flower. Note the difference in size between the floral morph types and their organs. Floral vasculature of sepals (green), stamens (blue) and pistil (orange). Note the synsepalous calyx and the fact that two neighboring sepals share a synlateral vascular strand that forms two strands. Scale bars: A, B, C, D = 500 μm.

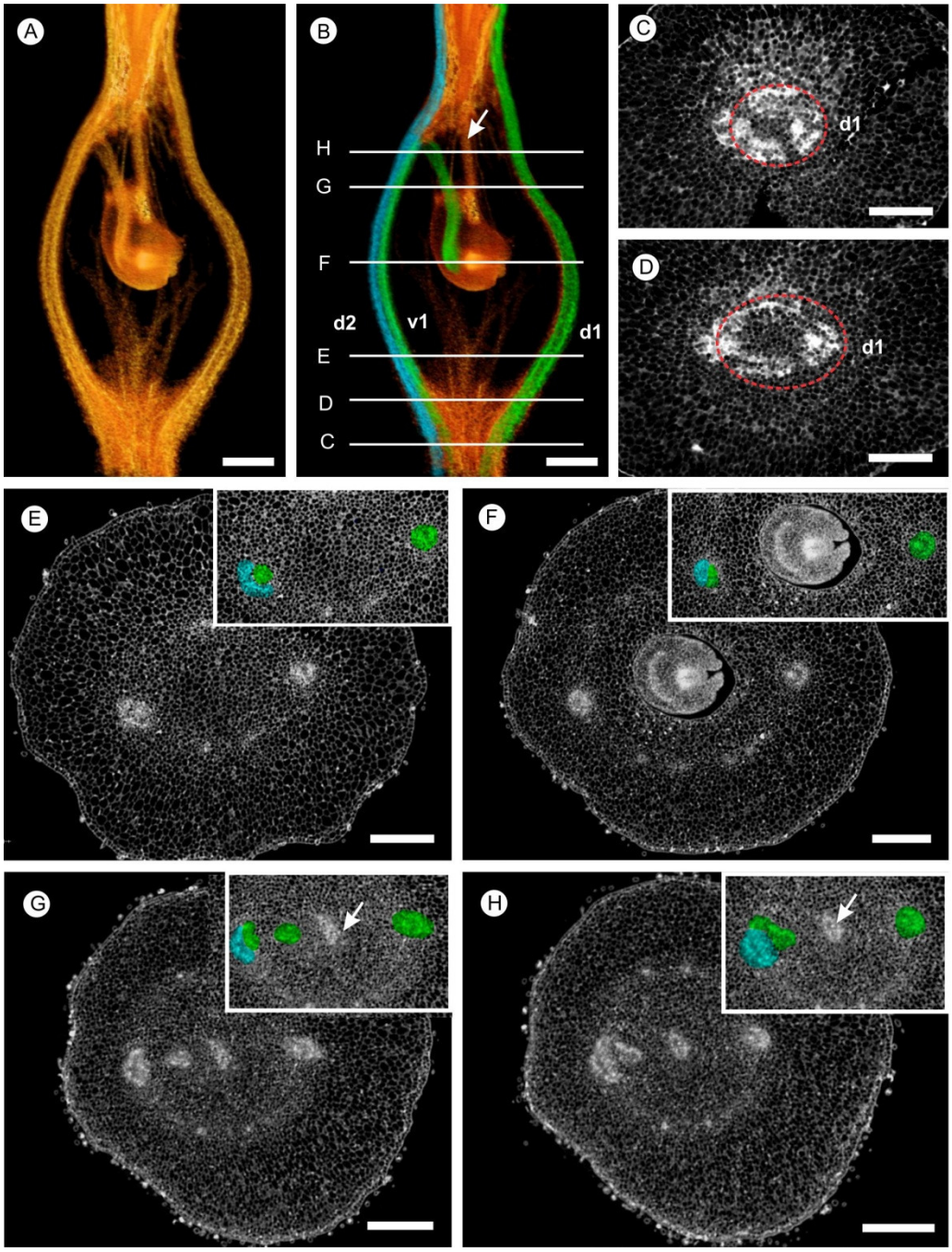

Fig. 8 Ovary vasculature of the functionally pistillate flower of *Ampelocera glabra*. A-B, MicroCT 3D reconstructions; C-H, MicroCT 2D reconstructions. A, Vasculature of the ovary and ovule. B, Vasculature of the ovulate carpel (carpel 1 - green) and of the non-ovulate carpel (carpel 2 - blue); lines indicate approximate levels of cross section shown in figures C-H. Note the transmitting tissue (arrow) above the ovule. C-D, Vasculature of carpels 1 and 2 at the ovarian base; the red circle indicates vascular bundles of carpel 1, and vascular bundle of carpel 2 is external (arrow). E-F, Cross section of the ovary showing the dorsal bundle of carpel 2 (blue), dorsal bundle of carpel 1 (green) and ventral bundle of carpel 1 (green). Note the ventral bundle of carpel 1 (green) united to the dorsal bundle of carpel 2 (blue). G-H, Path of the vascular ventral bundle that separates the dorsal bundle reaching the ovule. Note the transmitting tissue in the center (arrow). Abbreviations: d1, dorsal bundle of carpel 1; d2, dorsal bundle of carpel 2; v1, ventral bundle of carpel 1 (v1). Scale bars: A-B = 500 μm; C, D, E, F, G, H = 250 μm.

2.5 Discussion

The discussion is structured based on the three types of floral organs found in *Ampelocera glabra* (sepals, stamens and carpel), on its breeding system and its floral structure, with comparisons to other Ulmaceae, other Urticalean rosids and other Rosales.

Perianth

The unusual structure of the one-whorled perianth of *Ampelocera glabra* is the result of the absence of the corolla (Bechtel 1921; Berg 1977), a common feature in Ulmaceae and in other urticalean families (Bechtel 1921; Chernik 1975; Berg 1977, 1989). In *A. glabra* the single perianth whorl was also interpreted as a calyx due to some morphological evidence such as robustness, wide base and acute apex, helical order of primordium initiation and three or more vascular bundles in each organ. The presence of alternisepalous stamens is an unusual condition to consider the present whorl as a calyx, because usually the outermost staminal whorl is opposite to sepals (Soltis et al. 2005), as is the case for other urticalean rosids (Sattler 1973; Okamoto et al. 1992; Leite et al. 2018). It is noteworthy that alternisepalous stamens have been previously recorded in other families of Rosales that have small petals (e.g., Rhamnaceae, Medan and Hilger 1992; Dirachmaceae, Ronse De Craene and Miller 2004).

The merism of the calyx is stable in *A. glabra* as well as in other *Ampelocera* species (Tab. 1). However, calyx merism varies widely in other members of Ulmaceae, from 4 to 9 (see Tab. 1 and references therein). Species of *Ulmus, Phyllostyllon* and *Zelkova* may have a pentamerous calyx (Tab. 1), but merism is variable among species and even within species (see Tab. 1). The flower of other urticalean rosids is also apetalous and the calyx displays a wide variation of merism, from 2-5-merous calyx in Cannabaceae (Payer 1857; Shephard et al. 2000) to the complete absence of a calyx in some Moraceae (Leite et al. 2018) and Urticaceae (Berg 1989). Given that a pentamerous calyx is a characteristic of the Rosales and even of rosids (Berg 1989; Endress 2010), the

tetramerous calyx in *Ampelocera* can be explained by the loss of an organ from a pentamerous whorl (Endress 2011; Ronse De Craene 2016).

Stable merism and synsepaly are features of *Ampelocera glabra.* Synsepaly also occurs in *Ulmus* but the cup is formed by the calyx and the bases of the stamens (Bechtel 1921). This structure was considered to be a hypanthium and a synapomorphy in Ulmaceae (Judd et al. 2009). Other urticalean rosids have a completely united calyx or a basally united calyx (some also have free sepals, Tab. 1). In Rhamnaceae and all Rosaceae, there is a hypanthium, which comprises the calyx, corolla, androecium and gynoecium (Fahn 1990; Medan and Aagesen 1995; Evans and Dickinson 2005). Thus, the cup calyx formed by congenital union of sepals found in *A. glabra* was misinterpreted as a hypanthium such as described for some species of Ulmaceae, Rhmanaceae and Rosaceae (Sytsma et al. 2002; Judd et al. 2009), indicating the need for a revision of this synapomorphy for the family. The synorganization among whorls or organs occurs at different levels in Rosales (among organs of the same whorl, between two whorls or among all the whorls of the flower), with a tendency to free whorls and organs in urticalean rosids (see Tab. 1; Medan and Aagesen 1995; Evans and Dickinson 1996, 1999, 2005).

Androecium

Ampelocera glabra has a flower with a number of stamens three to four times greater than the number of sepals, as is also the case for many other rosids (Evans and Dickinson 1999, 2005). However, in other Ulmaceae and urticalean rosids the number of stamens is equal to or less than the number of sepals (to see Tab. 1). Stamens alternating with the sepals are also an exclusive feature of *A. glabra* (present study) within the urticalean rosids, which so far has not been recorded for other urticalean species. It should be emphasized that in this species the stamens arise sequentially from individual primordia (primary polyandry) with short plastochrones. Thus, the polyandry fits the irregular (chaotic) pattern (see Endress 1996) and may be

responsible for the atypical position of the stamens that arise quickly and close to each other, displacing the four stamens that were initially alternating with the sepals.

The androecium merism and the ontogeny described for *A. glabra* differ from other Ulmaceae species and other urticalean rosids (see Table 1). *Phyllostylon* is a genus of Ulmaceae that illustrates a case in which the sepal number is equal to the stamen number; other genera such as *Ulmus* and *Zelkova* have flowers with five up to eight and five up to seven stamens, respectively. In Moraceae, an urticalean rosid family, some genera such as *Artocarpus, Brosimum, Castilla* and *Clarisia* have only one or three stamens. Nevertheless, the large stamen number and irregular pattern of initiation are common conditions in some rosids (Endress 2011), in many Rosaceae studied so far (Lindenhofer and Weber 2000; Judd et al. 2009) and in *Barbeya oleoides* (Barbeyaceae, Friis 1993). Likewise, the alternisepalous stamens are commonly found in Elaeagnaceae (Bartish and Swenson 2004), Dirachmaceae (Ronse De Craene and Miller 2004) and Rhamnaceae (Beille 1902; Medan and Hilger 1992).

The irregular increase or decrease in the number of organs may be related to a reduction in size and/or loss of function of that organ (e.g. *Bauhinia galpinii*, Fabaceae: the flower has only three well developed stamens, while the other seven are modified as staminodes without anthers - Endress 1996, 2008), or may be due to the loss of floral whorls (e.g. Caryophyllales: apetalous flower with a single whorled sepalar perianth in general - Ronse De Craene 2013, 2016). In *A. glabra* it seems to be related to the reduction (1) of number of whorls of the perianth (only one whorl), (2) to the number of organs in a whorl (tetramery), and (3) to the number of functional carpels in the gynoecium (reduction to only one functional carpel - pseudomonomerous); all of them later increasing the available space, leading to the appearance of more, irregularly placed organs, such as stamens. Hence, the increase in the number of stamens also probably increases the number of pollen grains and, added to the presence of a wide stigmatic area, is a feature that may render pollination more efficient, a remarkable feature of wind-pollinated species (Friedman and Barrett 2009). Indeed, abiotic pollination is not as specific as biotic pollination because the

pollen can fall on all the floral organs. These factors can favor an increase in the pollen/ovule ratio, providing conditions that increase the probability of fertilization. A high pollen/ovule ratio is also a common condition in wind-pollinated species (Cruden 2000; Culley et al. 2002; Friedman and Barrett 2009), including some Ulmaceae such as *Ulmus* (Elias 1970) and other urticalean rosids such as *Artocarpus*, *Brosimum* (Moraceae - Barth 1975), *Pourouma*, *Fleurya*, *Pilea* (Urticaceae - Barth 1975), *Cannabis, Celtis*, *Humulus* and *Trema* (Cannabaceae - Barth 1975; Miller 1970; Arruda and Sazima 1988).

Gynoecium

Our study of floral vasculature and ontogeny confirmed the presence of a bicarpellate, unilocular and uniovulate ovary in *Ampelocera glabra,* a condition known as pseudomonomerous gynoecium and shared with other Ulmaceae and urticalean rosids (Eckardt 1937; Chernik 1981; Fukuoka 1982; Berg 1989; Okamoto et al. 1992; Omori and Terabayashi 1993).

Ampelocera glabra and *Zelkova serrata* display an ovary with only one ventral bundle, which is united to the dorsal bundle of the reduced carpel (see Fig. 8A-H; Okamoto et al. 1992; present study). Other Ulmaceae species possess two to four ventral bundles distinctly separated from the dorsal bundle in the ovary and in the stigmatic region (*Ulmus, Holoptelea, Phyllostylon* and *Hemiptelea;* Bechtel 1921; Eckardt 1937; Chernik 1981; Omori and Terabayashi 1993) or only in the stigmatic region (*Planera* and *Zelkova carpinifolia*; Chernik 1981; Omori and Terabayashi 1993). Thus, *Ampelocera* has the most reduced gynoecium vasculature among the Ulmaceae studied thus far.

In urticalean rosids, the structure of the pseudomonomerous gynoecium has received different interpretations, mainly related to the degree of carpel reduction. Eckardt (1937) reported that the reduced carpel is composed of only one dorsal bundle (*Artocarpus altilis* (*syn. A. incisa*), *A. integra, Dorstenia psilurus, Ficus carica, F. hirta* and *Morus alba* – Moraceae; *Cannabis sativa* and *Celtis tournefortii* – Cannabaceae; *Boehmeria biloba* - Urticaceae) or rarely one dorsal and one ventral bundle (*Artocarpus altissima* –

Moraceae). Omori and Terabayashi (1993), on the other hand, reported one dorsal and one or two ventral bundles of the reduced carpel in *Holoptelea, Phyllostylon* and *Ulmus.* Our data support the interpretation of Eckardt (1937) that the reduced carpel has only the dorsal vascular bundle.

Breeding system

Our data showed that *Ampelocera glabra* is a monoecious species. Previous studies have described perfect flowers in addition to staminate flowers (Todzia 1989; Pederneiras and Machado 2017), but our study clearly shows that perfect flowers act as functionally pistillate. The (functionally) staminate flowers have a pistillode instead of a pistil with a developed but non-functional ovule. The functionally pistillate flowers have non-functional anthers because the endothecium lacks cell wall thickenings and the anthers produce atypical pollen grains. Thus, *A. glabra* is not an andomonoecious species as previously reported.

Ulmaceae displays genera with different breeding systems (see Table 1) such as hermaphroditism (perfect flowers on one individual, e.g. *Ulmus*), polygamy (perfect, pistillate and staminate flowers in the same individual, e.g. *Zelkova* and *Planera*), andromonoecy (perfect, staminate flowers on the same individual, e.g. *Phyllostylon*), and monoecy (pistillate and staminate flowers in the same individual, e.g. *Ampelocera glabra*). Among the other urticalean rosids only a few species are andromonoecious, such as *Achudemia* and *Parietaria* (Urticaceae - Berg 1989). Although the flowers of *Celtis iguanaea* (Cannabaceae), and *A. glabra* have been previously described as perfect and staminate (Arruda and Sazima 1988; Todzia 1989; Torres and Luca 2005; Pederneiras and Machado 2017), they are actually functionally pistillate and functionally staminate (F.M. Leme, unpublished data; present study). These reports deserve further scrutiny, especially in terms of histology, because anthers, pollen grains, carpels and ovules can display atypical structure even late during floral development. In this case, the flowers are characterized as diclinous. Dicliny in these

species is thus the result of structural modifications in the final stages of development. Early or late abortions are found in the floral development stages of urticalean rosids (Tab. 1), and absence from inception may also occur (Payer 1857; Shephard et al. 2000; Basso-Alves et al. 2014; Leite et al. 2018). Therefore, the main processes of floral reduction are absence or abortion in the urticalean rosids, while only late abortion is present in Ulmaceae. Perfect flowers occur in some species of Ulmaceae; however, they are more commonly found in Rhamnaceae, Rosaceae and Dirachmaceae (Medan and Aagesen 1995; Evans and Dickinson 1999, 2005; Ronse De Craene and Miller 2004).

Floral structure

The flowers of *Ampelocera glabra* are reduced in number of whorls per flower and number of organs per whorl compared to other Ulmaceae (e.g. *Holoptelea, Phyllostylon*, *Planera, Ulmus* and *Zelkova* – see Table 1) and to the ancestral condition of rosids (likely pentamerous flowers with two perianth whorls) (Endress and Matthews 2006; Endress 2011; Ronse De Craene and Brockington 2013). The perianth is characterized by absence of petals, typical of the urticalean rosids (Bechtel 1921; Berg 1977; Endress and Matthews 2006).

In Rosales, apetaly has been recorded for almost all nine families and, except for Dirachmaceae (Endress and Matthews 2006), is considered to be a tendency in the nitrogen-fixing clade (rosids) (Matthews and Endress 2006), and is possibly stable in urticalean rosids. In the tropical clade of Ulmaceae, calyx merism (4) is fixed in almost all species of *Ampelocera* and *Holoptelea*, and only *Phyllostylon* has five sepals. However, calyx merism seems to be unstable in the species of the temperate clade of Ulmaceae (4-5 *Hemiptelea*, 5-9 *Ulmus*, 5-7 *Zelkova*), with only *Planera* having a fixed number (5) (see Table 1). Therefore, the calyx of an Ulmaceae flower seems to be characterized by five sepals, suggesting the loss of one sepal in *A. glabra* and perhaps in most of the species of the tropical clade. Merism is also unstable in other urticalean rosids (see Table 1). Indeed, merism lability attests to floral reduction (Ronse De

Craene 2016). The apetaly and loss of one sepal from inception appear to affect the vasculature of the sepals: each sepal possesses more than three strands, an unusual characteristic for sepals. It is likely that the bundle that would vascularize a fifth sepal remains in the total composition of the calyx vasculature.

The polyandry of *A. glabra* flowers is also found in *Holoptelea* species (8-12 stamens, Todzia 1993), but not in *Phyllostylon* species (5 stamens, Todzia 1993; Pederneiras et al. 2011), other groups of the tropical clade of Ulmaceae. Such atypical androecium merism is likely a result of the loss and reduction of number of organs, such as apetaly and pseudomonomerous gynoecium. It is also much different from the ancestral condition of urticalean rosids (4-5 stamens, Berg 1989). It is noteworthy that the putative Rosales ancestor had two whorls of stamens and some of Rosales families have a higher androecium merism, such as 6-12 in Dirachmaceae (Ronse De Craene and Miller 2004), 6-12 in Barbeyaceae (Friis 1993), 4-8 in Elaeagnaceae (Bartish and Swenson 2004), and 10-60 in Rosaceae (Evans and Dickinson 1996, 1999, 2005). This lability in Ulmaceae, and likely in other cited families, may have resulted from floral reduction (apetaly and pseudomonomerous gynoecium) together with the pressure for a high production of pollen, a condition commonly found in anemophilous species.

The pseudomonomerous gynoecium found in *Ampelocera glabra* has a similar structure to that described by Eckardt (1937) for most of the urticalean rosids. The reduced carpels possess only one dorsal bundle. However, for some Ulmaceae species the reduced carpel can also be composed of two ventral bundles, as is the case for *Ulmus americana* (Bechtel 1921) and *U. glabra* (*syn. U. montana*) (Eckardt 1937). Therefore, the presence of one ventral bundle may represent a recent character state in Ulmaceae, such as the presence of one-bundle stigma in some urticalean rosids (Cannabaceae, Omori and Terabayashi 1993; Moraceae, Eckardt 197) and in *Ampelocera* within Ulmaceae (Omori and Terabayashi 1993). The evolution of the pseudomonomerous gynoecium in Ulmaceae seems to have occurred independently in each genus, because the temperate and tropical clades do not have a vascularization pattern (Okamoto et al. 1992; Omori and Terabayashi 1993; present study). Our

vascularization and ontogeny data confirm a tendency towards the reduction of a bicarpellate to unicarpellate gynoecium in Ulmaceae and urticalean rosids (Bechtel 1921). Thus, it is striking that both stigmatic branches are functional, a condition that seems to increase the probability of fertilization of the embryo sac.

In conclusion, the reduced flowers of Ulmaceae are apetalous, and the petals are absent from the inception; carpellodes and staminodes arise by abortion of carpels and stamens later during floral development. Thus the single whorl of the perianth is sepalar and there is no hypanthium. The atypical merism (increase or decrease of organs numbers) is a result of the space left by reduction of the whorls and/or of organs, and thus favors wind pollination in *Ampelocera glabra*. The flowers of the species of the tropical clade of Ulmaceae have acquired features more recently than temperate ones, such as monoecy, diclinous flowers, tetramerous calyx, polyandry, and a suppressed carpel with fewer vascular bundles. There is a remarkable impact of wind pollination on the evolution of the floral morph types in *A. glabra,* a tropical member of Ulmaceae. Thus, expanding the study of the flower ontogeny to the tropical species is an extremely important step to better understand the floral evolutionary processes of Ulmaceae and other urticalean rosids.

Table 1 Comparative floral data of Urticalean species based on a literature search. Symbols: (-) character absent/not applicable; (?) character not observed.

Family	Species	Floral types	Merism sepals	Synsepaly	No. of stamens/staminodes	Gynoecium structure	Reference
Ulmaceae	*Ampelocera albertiae*	Perfect	4	United at the base	8 (-12) stamens	-	Todzia 1989
		Staminate	4	United at the base	4-8 stamens	Pistillode	
	Ampelocera cubensis	Perfect	4-5	United at the base	12-16 stamens	-	Todzia 1989
	Ampelocera edentula	Perfect	4	United in lower half	(6-)8 stamens	?	Todzia 1989
		Staminate	4	United in lower half	(6-)8 stamens	Pistillode	
	Ampelocera glabra	Perfect	4	United at the base	16 stamens	-	Todzia 1989
		Staminate	4	United at the base	12-14 stamens	Rudimentary pistil	Todzia 1989
		Functionally pistillate	4	United in lower half	11-13 (14) staminodes	2 carpels	Present study
		Functionally staminate	4	United in lower half	11-13 stamens	Pistillode	Present study
	Ampelocera hottlei	Perfect	5	United at the base	16 stamens	-	Todzia 1989
		Staminate	5	United at the base	8 stamens	?	
	Ampelocera longissima	Perfect	4	United in lower half	8-10 stamens	?	Todzia 1989
		Staminate	4	United in lower half	8-10 stamens	Pistillode	
	Ampelocera macrocarpa	Perfect	4-5	United at the base	8 stamens	?	Todzia 1989
		Staminate	4-5	United at the base	4-6 stamens	Pistillode	
	Ampelocera ruizii	Perfect	4	United at the base	16 stamens	?	Todzia 1989
		Staminate	?	?	?	?	
	Holoptelea integrifolia	Perfect	4	?	8-12 stamens	?	Todzia 1993
		Staminate	4	?	8-12 stamens		
	Planera	Perfect	5	United in higher half	4-5 stamens		Browne 1846
		Pistillate	5	United in higher half	-	?	
		Staminate	5	United in higher half	4-5 stamens		
	Phyllostylon brasiliense	Perfect	5	?	5 stamens	?	Todzia 1992
		Staminate	5	?	5 stamens	Absent	
	Phyllostylon rhamnoides	Perfect	5 -6	?	5 stamens	?	Todzia 1992
		Staminate	5 -6	?	5 stamens	Present or absent	

	Ulmus americana	Perfect	8	United in higher half	8 stamens	-	Bechtel 1921
	Ulmus fulva	Perfect	7 or 6 (9 to 5)	United in higher half	7 or 6 (9 to 5) stamens	-	Bechtel 1921
	Ulmus racemosa	Perfect	8 to 5	United in higher half	8 to 5 stamens	-	Bechtel 1921
	Ulmus campestris	Perfect	5 to 3	United in higher half	5 to 3 stamens	-	Bechtel 1921
	Ulmus scabra	Perfect	6 (5)	United in higher half	6 (5) stamens	-	Bechtel 1921
	Zelkova serrata	Perfect	5 to 7	United in higher half	5 to 7 stamens	2 carpels	Okamoto et al. 1992
		Pistillate	5 to 7	United in higher half	5 to 7 staminodes		
		Staminate	5 to 7	United in higher half	5 to 7 stamens	Rudimentary pistil	
Cannabaceae	*Cannabis sativa*	Pistillate	2	United completely	-	2 carpels	F. M. Leme unpublished data; Payer 1857; Briosi and Tognini 1894
		Staminate	5	Free	5 stamens	-	
	Celtis iguanaea	Perfect	5	-	5 stamens	?	Torres and Luca 2005
		Pistillate	5	Free	5 staminodes	2 carpels	F. M. Leme unpublished data
		Staminate	5	Free	5 stamens	Pistillode	F. M. Leme unpublished data; Torres and Luca 2005
	Humulus lupulus	Pistillate	2	United completely	-	2	Shephard et al. 2000
		Staminate	*5*	Free	5 stamens	-	
	Trema micrantha	Pistillate	5	United at the base	5 staminodes	2 carpels	F. M. Leme unpublished data
		Staminate	5	Free	5 stamens	Pistillode	
Urticaceae	*Laportea aestuans*	Pistillate	4 - 5	United at the base	?	?	G. D. Pedersoli unpublished data
		Staminate	4 - 5	United at the base	4-5 stamens	Pistillode	
	Laportea canadensis	Pistillate	4	?	-	?	Sattler 1973
		Staminate	5	?	5 stamens	Pistillode	
	Myriocarpa stipitata	Pistillate	2	Free	-	?	G. D. Pedersoli unpublished data
		Staminate	4	Free	4 stamens	Pistillode	
	Pilea cadierei	Pistillate	4	United at the base	4 rudimentary	?	G. D. Pedersoli unpublished data
		Staminate	4	United at the base	4 stamens	Pistillode	
	Urera bacifera	Pistillate	4	United at the base	?	?	G. D. Pedersoli unpublished data
		Staminate	5	United at the base	5 stamens	Pistillode	
Moraceae	*Artocarpus heterophyllus*	Pistillate	2	United completely	?	?	Moncur 1985
		Staminate	2	Free	1 stamen	?	
		Pistillate	0	-	-	2 carpels	Leite et al. 2018

Brosimum gaudichaudii	Staminate	0	-	1 stamen	Rudimentary carpel	
Castilla elastica	Pistillate	5	United completely	0-2 stamens	2 carpels	Leite et al. 2018
	Staminate	0	-	3 stamens	?	
Clarisia ilicifolia	Pistillate	2	United completely	-	2 carpels	Leite et al. 2018
	Staminate	2	United at the base	1 stamen	?	
Maclura tinctoria	Pistillate	4-5	United at the base	-	2 carpels	Leite et al. 2018
	Staminate	5	United at the base	5 stamens	?	
Maclura pomifera	Pistillate	4	?	-	2 carpels	Maier et al. 1997
	Staminate	4	?	4 stamens	-	
Morus alba	Pistillate	4-5	?	?	2 carpels	Bechtel 1921
	Staminate	4-5	?	4-5 stamens	Pistillode	
Morus nigra	Pistillate	4	United at the base	-	2 carpels	Leite et al. 2018
	Staminate	4	United at the base	4 stamens	Pistillode	
Morus rubra	Pistillate	4	?	-	?	Maier et al. 1997
	Staminate	4	?	4 stamens	Vestigial gynoecium	
Ficus citrifolia	Pistillate	3	United or free	-	?	Basso-Alves et al. 2014
	Staminate	2	United at the base	1 stamen	-	
Ficus religiosa	Pistillate	4-5	Free	-	?	Basso-Alves et al. 2014
	Staminate	3	Free	1 stamen	-	
Ficus racemosa	Pistillate	3-4	United at the base	-	?	Basso-Alves et al. 2014
	Staminate	4	United at the base	2 stamens	-	
Ficus hispida	Pistillate	3	United completely	-	?	Basso-Alves et al. 2014
	Staminate	4	United completely	1 stamen	Pistillode	

2.6 References

Ahmed I, M Arsiwala, C Singh, M Adlakha 2016 *Holoptelea integrifolia* Roxb-Birds eye view. Int Ayurvedic Med J. Online Available from: http://www.iamj.in/posts/images/upload/2568_2572.pdf. Accessed 5 March 2017.

APG IV 2016 An update of the Angiosperm Phylogeny Group classification for the orders and families of flowering plants: APG IV. Bot J Linn Soc 181:1-20.

Arruda VLV, M Sazima 1988 Polinização e reprodução de *Celtis iguanaea* (Jacq.) Sarg. (Ulmaceae), uma espécie anemófila. Braz J Bot 11:113-122.

Baas P, E Wheeler, M Chase 2000 Dicotyledonous wood anatomy and the APG system of angiosperm classification. Bot J Linn Soc 134:3-17.

Bartish IV, U Swenson 2004 Elaeagnaceae. Pages 131-132 in K Kubitzki ed. The Families and Genera of Vascular Plants – VI. Flowering Plants - Dicotyledons. Springer, Hamburg, Germany.

Barth OM, EG Macieira, S Côrte-Real 1975 Morfologia do pólen anemófilo e alergisante no Brasil: Casuarinaceae, Salicaceae, Moraceae, Ulmaceae e Urticaceae (I). Mem Inst Oswaldo Cruz 73:141-150.

Basso-Alves JP, RAS Pereira, Y-Q Peng, SP Teixeira 2014 Different ontogenetic processes promote dicliny in *Ficus* L. (Moraceae). Acta Oecol 57:5-16.

Bechtel AR 1921 The floral anatomy of the Urticales. Am J Bot 8:386-410.

Beille L 1902 Recherches sur le développement floral des Disciflores. Bordeaux: Durand.

Berg CC 1977 Urticales, their differentiation and systematic position. Pl Syst Evol 1:349-374.

Berg CC 1989 Systematic and phylogeny of the Urticales. Pages 193-219 in PR Crane, S Blackmore, eds. Evolution, Systematics, and Fossil History of the Hamamelidae. Clarendon Press, Oxford, UK.

Briosi G, F Tognini 1894 Anatomia Della Canapa (*Cannabis sativa* L.). Milano: Istituto Botanico Della R. Universitá Dii Pavia.

Browne DJ 1846 Trees of America. Harper & Brothers, New York, USA.

Chernik VV 1975 Arrangement and reduction of perianth and androecium parts in representatives of Ulmaceae Mirbel. and Celtidadeae Link. Bot Zh 11:1561-1573.

Chernik VV 1981 Pseudomonemeric gynoecium of the Ulmaceae and Celtidaceae representatives. Bot Zh 7:958-966.

Cruden RW 2000 Pollen grains: why so many? Pl Syst Evol 222:143-165.

Culley TM, SG Weller, AK Sakai 2002 The evolution of wind pollination in angiosperms. Tr Ecol Evol 17:361-369.

Eckardt T 1937 Untersuchungen über Morphologie, Entwicklungsgeschichte und systematische Bedeutung des pseudomonomeren Gynoeceums. Nova Acta Leopold 5:1-112.

Elias TS 1970 The genera of Ulmaceae in the southeastern United States. J Arnold Arbor 51:18-40.

Endress PK 1996 Diversity and evolutionary biology of tropical flowers. Cambridge University Press New York, USA

Endress PK 2008 The whole and the parts: relationships between floral architecture and floral organ shape, and their repercussions on the interpretation of fragmentary floral fossils. Ann Miss Bot Gard 95:101-120.

Endress PK 2010 Flower structure and trends of evolution in eudicots and their major subclades. Ann Miss Bot Gard 97:541-583.

Endress PK 2011 Evolutionary diversification of the flowers in angiosperms. Am J Bot 98:370-396.

Endress PK, ML Matthews 2006 First steps towards a floral structural characterization of the major rosid subclades. Pl Syst Evol 260:223-251.

Evans RC, TA Dickinson 1996 North American black-fruited hawthorns. II. Floral development of morph types in *Crataegus* section *Douglasii* (Rosaceae: Maloideae). Am J Bot 83:961-978.

Evans RC, TA Dickinson 1999 Floral ontogeny and morphology in subfamily Amygdaloideae T. & G. (Rosaceae). Int J Pl Sci 160:955-979.

Evans RC, TA Dickinson 2005 Floral ontogeny and morphology in Gillenia ("Spiraeoideae") and subfamily Maloideae C. Weber (Rosaceae). Int J Pl Sci 166:427-447.

Fahn A 1990 Plant Anatomy. Butterworth-Heinemann, London, UK

Friedman J, SCH Barrett 2009 Wind of change: new insights on the ecology and evolution of pollination and mating in wind-pollinated plants. Ann Bot 103:1515-1527.

Friis I 1993 Barbeyaceae. Pages 141-143 in K Kubitzki, JG Rohwer, V Bittrich, eds. The Families and Genera of Vascular Plants - II. Flowering Plants - Dicotyledons. Springer-Verlag, Berlin, Germany.

Fukuoka N 1982 On pseudomonomerous pistil of the Ulmaceae. Acta Phytotax Geobot 56:84-91.

Judd WS, CS Campbell, EA Kellogg, PF Stevens, MJ Donoghue 2009 Sistemática vegetal. Um enfoque filogenético. Artmed, Porto Alegre, Brazil.

Leite VG, VF Mansano, SP Teixeira 2018 Floral development of Moraceae species with emphasis on the perianth and androecium. Flora 240:116–132.

Lillie RD 1965 Histopathologic Technic and Practical histochemistry. McGraw-Hill, New York, USA.

Lindenhofer A, A Weber 2000 Diversification of the Androecium within Rosaceae. Linzer Biol Beitr 32:670-671.

Machado AFP 2016 Ulmaceae in Flora do Brasil 2020 em construção. http://floradobrasil.jbrj.gov.br/reflora/floradobrasil/FB21357. Accessed 12 May 2017.

Maier CG-A, KD Chapman, DW Smith 1997 Phytoestrogens and floral development in dioecious *Maclura pomifera* (Raf.) Schneid. and *Morus rubra* L. (Moraceae). Plant Sci 130:27-40.

Matthews ML, PK Endress 2006 Floral structure and systematics in four orders of rosids, including a broad survey of floral mucilage cells. Pl Syst Evol 260:199-221.

Mcdowell EM, B Trump 1976 Histological fixatives for diagnostic light and electron microscopy. Arch Pathol Lab Med 100:405-414.

Medan D, L Aagesen 1995 Comparative flower and fruit structure in the Colletieae (Rhamnaceae). Bot Jahrb Syst 117:531-564.

Medan D, HH Hilger 1992 Comparative flower and fruit morphogenesis in *Colubrina* (Rhamnaceae) with special reference to *C. asiatica*. Am J Bot 79:809-819.

Miller NG 1970 The genera of Cannabaceae in the southeastern United States. J Arnold Arbor 51(2):185-203.

Moncur MW 1985 Floral ontogeny of the jackfruit, *Artocarpus heterophyllus* Lam. (Moraceae). Austr J Bot 33:585–593.

Neubig K, F Herrera, SR Manchester, JR Abbott 2012 Fossils, biogeography and dates in an expanded phylogeny of Ulmaceae. Botany 2012: Annual Meeting of the Botanical Society of America in Columbus, Ohio, USA

O'Brien TP, N Feder, ME McCully 1964 Polychromatic staining of plant cell walls by toluidine blue O. Protoplasma 59:368-373.

Okamoto M, K Kosuge, N Fukuoka 1992 Pistil development and parietal placentation in the pseudomonomerous ovary of *Zelkova serrata* (Ulmaceae). Acta Oecol 79:921-927.

Omori Y, S Terabayashi 1993 Gynoecial vascular anatomy and its systematic implications in Celtidaceae and Ulmaceae (Urticales). J Pl Res 106:249-258.

Payer JB 1857 Traité D'Organogéne Comparée de La Fleur. Paris: Librairie de Victor Masson

Pederneiras LC, AF Costa, DSD Araujo, JPP Carauta 2011 Ulmaceae, Cannabaceae e Urticaceae das restingas do estado do Rio de Janeiro. Rodriguésia 62:299-213.

Pederneiras LC, AF Costa, JPP Carauta, S Romaniuc-Neto 2014 Avaliação do risco de extinção das Urticineae das restingas do estado do Rio de Janeiro. Rodriguésia 65:261-273.

Pederneiras LC, AFP Machado 2017 Flora do estado do Rio de Janeiro: Ulmaceae. Rodriguésia 68(2):541-543.

Richards AJ 1997 Plant Breeding Systems. Second edition. Chapman & Hall, London, UK

Ronse De Craene LP 2013 Reevaluation of the perianth and androecium in Caryophyllales: implications for flower evolution. Plant Syst Evol 299:1599-1636.

Ronse De Craene LP 2016 Meristic changes in flowering plants: How flowers play with numbers. Flora 221:22-37.

Ronse De Craene LP, SF Brockington 2013 Origin and evolution of petals in angiosperms. Pl Ecol Evol 146:5-25.

Ronse De Craene LP, AG Miller 2004 Floral development and anatomy of *Dirachma socotrana*, (Dirachmaceae): a controversial member of the Rosales. Pl Syst Evol 249:111-127.

Sattler R 1973 Organogenesis of flowers: a photographic text-atlas. Toronto: University of Toronto Press.

Shephard HL, JS Parker, P Darby, CC Ainsworth 2000 Sexual development and sex chromosomes in hop. New Phytol 148:397-411.

Soltis DE, PS Soltis, PK Endress, MW Chase 2005 Phylogeny and Evolution of Angiosperms. Sinauer, Sunderland, USA.

Staedler YM, D Masson, J Schönenberger 2013 Plant Tissues in 3D via X-Ray Tomography: Simple Contrasting Methods Allow High Resolution Imaging. Plos One 8.

Sutar RC, SS Gangwar, RN Thakur, R Sharma, SP Krishnan 2016 HPTLC finger printing analysis of the tannins from *Holoptelea integrifolia* (Roxb.) Planch Leaves. J Pharmaco Phytoch 5:199-204.

Sytsma KJ, J Morawetz, JC Pires, M Nepokroeff, E Conti, M Zjhra, JC Hall, MW Chase 2002 Urticalean rosids: Circumscription, rosid ancestry, and phylogenetics based on rbcL, trnL-F, and ndhF sequences. Acta Oecol 89:1531-1546.

The Plant List 2013 Version 1.1. Published on the Internet; http://www.theplantlist.org/ Accessed 22 November 2017.

Todzia CA 1989 A revision of *Ampelocera* (Ulmaceae). Ann Miss Bot Gard 76:1087-1102.

Todzia CA 1992 A reevaluation of the genus *Phyllostylon* (Ulmaceae). SIDA 15:263-270.

Todzia CA 1993 Ulmaceae. Pages 603-613 in K Kubitzki, JG Rohwer, V Bittrich, eds. The Families and Genera of Vascular Plants - II. Flowering Plants - Dicotyledons. Springer-Verlag, Berlin, Germany.

Torres RB, AQ Luca 2005 Ulmaceae. Pages 361-369 in M das GL Wanderley, G Shepherd, AM Giulietti, TS Melhem, eds. Flora Fanerogâmica do Estado de São Paulo, Online. RiMa, São Paulo, Brazil.

Zhang S, DE Soltis, Y Yang, D Li, T Yi 2011 Multi-gene analysis provides a well-supported phylogeny of Rosales. Mol Phyl Evol 60:21-28.

"Há pessoas que choram por saber que as rosas têm espinho. Há outras que sorriem por saber que os espinhos têm rosas!"

Machado de Assis

CHAPTER 3: 'FLORAL COMPARATIVE DEVELOPMENT AND MORPHOLOGY CLARIFY FLORAL REDUCTION AND INDICATE THE OCCURRENCE OF MONOECY IN *CELTIS* (CANNABACEAE)'

Chapter 3: Floral comparative development and morphology clarify floral reduction and indicate the occurrence of monoecy in *Celtis* (Cannabaceae)

3.1 Abstract

Celtis is the species-richest genus of Cannabaceae, an economically important family because of the medicinal and recreational uses of *Cannabis sativa* and *Humulus lupulus*. *Celtis* is the single andromonoecious genus of the family, and its flowers are reduced, with a whorl of perianth, staminate or perfect and pseudomonomerous gynoecium. The genus is monophyletic, formed by Asian, African, and South American species included in clades of weak support or unresolved polytomies. Thus, the objectives of the present investigation were to study the morphology of developing flowers of *Celtis* to check the occurrence of andromonoecy and to understand the formation of such a reduced flower. We also intended to provide floral features to help characterize the clades that emerged in *Celtis* in the last phylogeny. Flowers and early to late floral buds of *Celtis brasiliensis, C. ehrembergiana, C. iguanaea* and *C. pubescens* were processed for surface analyses (scanning electron microscopy) and developed flowers these species and of *C. occidentalis* and *C. sinensis* were also investigated histologically (light microscopy), with 2D and 3D reconstructions being performed (High Resolution X-Ray Computed Tomography). The *Celtis* species analysed are actually monoecious. The single perianth whorl is composed of sepals with labile merism (4 or 6) in the Asian species. The diclinous flowers are formed by abortion of carpels and stamens. The aborted carpels form the pistillode that may act in the wind-pollinated mechanism. The staminodes have no typical endothecium and no viable pollen grains. The gynoecium is composed of two carpels, but only one houses an ovule and the other has a reduced vasculature, has only one dorsal bundle, and no ovule. Floral features may support the *Celtis* clades, such as number of sepals and stamens, number of stigmatic branches and occurrence and distribution of secretory structures. In conclusion, *Celtis* species are monoecious with late abortion of stamens in the pistillate flower, which is structurally perfect but functionally pistillate. Floral anatomical features are extremely important in the studies of the breeding systems, and systematics of *Celtis* species and clades.

Key words: Anatomy, andromonoecious, ontogeny, pseudomonomerous gynoecium, urticalean.

3.2 Introduction

Celtis is a monophyletic genus and the species-richest in the Cannabaceae family (Sattarian, 2006; Yang *et al.,* 2013), an economically important family popularly known since prehistory (Fleming & Clarke, 1998) because of the medicinal and recreational uses of marijuana (*Cannabis sativa*) and hops (*Humulus lupulus*) (Milligan *et al*., 1999; Ashton, 2001; Zanoli & Zavatti, 2008).

The inclusion of *Celtis* in Cannabaceae occurred from the beginning of the last decade (Sytsma *et al.,* 2002) when, together with other genera of Celtidoideae (*Gironniera, Parasponia, Pteroceltis, Trema, Lozanella, Chaetachme* and *Aphananthe*), it was removed from Ulmaceae (Ueda *et al*., 1997; Wiegrefe *et al*., 1998; Song *et al*., 2001; Sytsma et al. 2002). *Celtis* comprises 73 species widely distributed in tropical areas and some in temperate regions (Yang *et al.,* 2013) which represent more than 50% of Cannabaceae species. The most recent phylogenetic analysis has shown the emergence of some *Celtis* clades, one involving South American species and other with African and Asian species (Sattarian, 2006; Yang *et al.,* 2013).

Celtis is the only Cannabaceae genus whose species are classified as andromonoecious (Berg & Dahlberg, 2001; Torres and Luca 2005; Sattarian 2006) (= presence of staminate and perfect flowers in the same individual, Richards, 1997). However, the andromonoecy of this group has been questioned, since some authors have reported that perfect flowers can have non-opening anthers inserted in short filaments, thus acting as pistillate flowers (Arruda & Sazima, 1988; Berg & Dahlberg, 2001). Indeed, the breeding system of Cannabaceae is inconclusive since monoecious, dioecious, andromonoecious, and polygamous species have been reported for this family (Yang *et al.,* 2013).

Another intriguing feature of *Celtis* species is the occurrence of very reduced inconspicuous flowers, characterized as monoclinous, with only one perianth whorl (Bechtel, 1921; Arruda & Sazima, 1988; Berg & Dahlberg, 2001) and a pseudomonomerous gynoecium (= bicarpellate gynoecium with a single ovule -

Payer, 1857; Bechtel, 1921; Eckardt, 1937; Chernik, 1981; Fukuoka, 1982; Weberling, 1989; Omori & Terabayashi, 1993). In addition, these flowers can display a variable merism, with 4-5 (6) perianth organs (Bechtel, 1921; Sattarian, 2006) and 4-5 (6) inflexed stamens (Bechtel, 1921; Torres & Luca, 2005; Sattarian, 2006).

No studies about floral development and anatomy were found for *Celtis* species, a fact that makes it difficult to understand the origin of their reduced flowers and even to attest the occurrence of andromonoecy in this group. The excellent and early studies of Becthel (1921) and Eckardt (1937) cannot be neglected because they presented very good descriptions of the flower structure of *C. occidentalis* L. (Becthel, 1921) and of the pseudomonomerous gynoecium of *C. tournefortii* Lam. (Eckardt, 1937).

Thus, our objective was to study the morphology of developing flowers of different lineages of *Celtis* (*Celtis brasiliensis* (Gardner) Planch., *C. ehrembergiana* (Klotzsch) Liebm., *C. iguanaea* (Jacq.) Sarg., and *C. pubescens* Spreng.) to check the occurrence of andromonoecy and to understand the formation of such a reduced flower. In addition, the developed flowers of *C. occidentalis* L. and *C. sinensis* Pers. were analysed for comparison purposes. We also intend to provide floral features to help characterize the clades that emerged in *Celtis* in recent phylogenies (see Sattarian, 2006; Yang *et al*., 2013).

3.3 Materials and methods

Flowering branches of the six species of *Celtis* were collected, herborized and deposited in the SPFR herbarium (FFCLRP/USP), CTES herbarium (Instituto de Botánica del Nordeste, Província de Corrientes, Argentina), or CGMS herbarium (Universidade Federal de Mato Grosso do Sul, Campo Grande, MS, Brazil) (Table 1).

Floral buds from early to late developmental stages and mature flowers were fixed in buffered formalin (Lillie, 1965) or in Karnovsky solution (Mcdowell & Trump, 1976) for 24 h, dehydrated in an ethanol series up to 70% and stored in it. The samples were then processed for surface (scanning electron microscopy - SEM) and

anatomical analyses (light microscopy - LM) and high resolution x-ray computed tomography (HRXCT).

For the surface analyses (SEM), the samples were dissected, dehydrated with up to absolute ethanol, dried in a Bal Tec CPD 030 apparatus, mounted on metal supports on carbon adhesive tape, coated with gold for 360 s using a Bal Tec SCD 050 sputter coater, and observed with a Zeiss EVO-50 scanning electron microscope at 15 kv.

For the anatomical analyses (LM), the samples were gradually dehydrated in an ethanol series, embedded in histological resin (Leica) and cut with a rotary microtome. Transverse and longitudinal sections (1 - 3 μm thick) were stained with 0.05% toluidine blue in phosphate buffer, pH 5.8 (O'Brien *et al.,* 1964), mounted in water, and observed with a light microscope. Photomicrographs were obtained using a Leica DM 5000 B light microscope coupled to a Leica DFC 295 digital camera.

For high resolution x-ray computed tomography (HRXCT), anthetic pistillate flowers were treated with a solution of 1% phosphotungstic acid in 70% ethanol for 1 week (Staedler *et al.*, 2013), dehydrated in an ethanol series with 1% phosphotungstic acid, critical point dried (Autosamdri-815), mounted on an aluminum holder with two-component epoxy glue (UHU Plus Epoxy: Binder + Hardener), and scanned. The scans were performed on a MicroXCT-200 imaging system (Zeiss Microscopy) with an L9421-02 90kV Microfocus X-ray (MFX) source (Hamamatsu Photonics, Iwata City, Japan), using the following settings: acceleration voltage, 23 kV; source current, 173 μA; exposure time, 23 s; pictures per sample, 1200; camera binning, 1; optical magnification, 1 x and 4 x, with pixel sizes of 7.7 μm and 1.5 μm, respectively. The total exposure time was approximately 10 hours for each sample. The XMReconstructor 8.1.6599 software (Zeiss Microscopy) was used to perform the 3D reconstruction from the scanning data. The AMIRA-based XM3DViewer 1.1.6 (Zeiss Microscopy) was used for the visualization of the scan data.

Table 1. Information about the *Celtis* species sampled.

Species	Clade	Sample	Voucher
C. brasiliensis	South American	Mata Ciliar do Rio Pardo, Ribeirão Preto, SP, Brazil.	F.M. Leme et al. nº 116 and 117 (SPFR)
C. ehrenbergiana	South American	Reserva de Tres Cerros, La Cruz, Província de Corrientes, Argentina.	W.A. Medina 948 (CTES)
C. iguanaea	South American	Campus da USP de Ribeirão Preto, SP, Brazil.	F.M. Leme nº 99 and 106 (SPFR)
C. occidentalis	Asian	Botanical Garden, Vienna, Áustria	FM. Leme nº 127 and 129 (CGMS)
C. pubescens	South American	Campus da USP de Ribeirão Preto, SP, Brazil.	F.M. Leme nº 98, 107, 108 and 110 (SPFR)
C. sinensis	Asian	Jardim Botânico de Buenos Aires, Argentina.	F.M. Leme nº 113 (SPFR)

3.4 Results

Floral structure

Celtis brasiliensis, *C. ehrenbergiana*, *C. iguanaea*, *C. occidentalis*, *C. pubescens*, and *C. sinensis* are monoecious trees or shrubs, with staminate and functionally pistillate flowers (Fig. 1A-L). No functionally perfect flowers were found.

The inflorescence of most species is composed of many staminate flowers and few pistillate flowers, while that of *C. occidentalis* has many pistillate flowers.

The staminate and pistillate flowers have one whorl of the perianth (Fig. 1B-L) formed by five green sepals in *C. brasiliensis*, *C. iguanaea*, *C. pubescens* (Fig. 1B, F, J), five or rarely four sepals in *C. ehrenbergiana* (Fig. 1C, D), four to six sepals in *C. occidentalis* (Fig. 1G, H), and four to five sepals in *C. sinensis* (Fig. 1K-L). All species showed quincuncial imbricate sepals.

The staminate flowers (Fig. 1B, D, F, H, J, L) are up to 3 mm long and approximately 5 mm wide. The androecium of *C. brasiliensis*, *C. iguanaea* and *C. pubescens* is formed by five antesepalous stamens (Fig. 1B, F, J), five or rarely four stamens in *C. ehrenbergiana* (Fig. 1C, D), four to six (most frequent) stamens in *C. occidentalis* (Fig. 1H), and four stamens in *C. sinensis* (Fig. 1L). The stamens are inflexed during the pre-anthetic phase (Fig. 1F, L), and the anthers are latrorse and greenish (Fig. 1D, I). Pistillodes were evident only in *C. brasiliensis* (Fig. 1B) and *C. sinensis* (Fig. 1L).

The pistillate flowers are up to 7 mm long and 3 mm wide. The gynoecium has a superior ovary, a short style, and two papillose stigmatic branches that are undivided in *C. occidentalis* (Fig. 1G) and *C. sinensis* (Fig. 1K); in the other species each stigmatic branch forms two branches, for a total of four stigmatic branches (Fig. 1A, C, E, I). The ovary is unilocular with one apical ovule. There are four to six staminodes according to the species analysed (see previous description of staminate flowers), sometimes with a short filament.

Floral development

The floral meristem of *Celtis brasiliensis, C. iguanaea, C. pubescens* and *C. ehrenbergiana* is rounded and subtended by an abaxial bract and two prophylls (Fig. 2A-D). Five sepal primordia arise in a spiral sequence (whorled phyllotaxis; divergence angles vary between about 120° and almost 180°) from the abaxial side, with distinct plastochrons (Fig. 2E-H).

Five stamen primordia arise in spiral order opposite to the sepals (Fig. 2I, J), followed by the carpel emergence as a single central primordium (Fig. 2J-L). The central primordium subsequently gives rise to two secondary carpel primordia of unequal size, which proximally are congenitally united (Fig. 3A-C). Then, each carpel primordium becomes bulged (Fig. 3A-D).

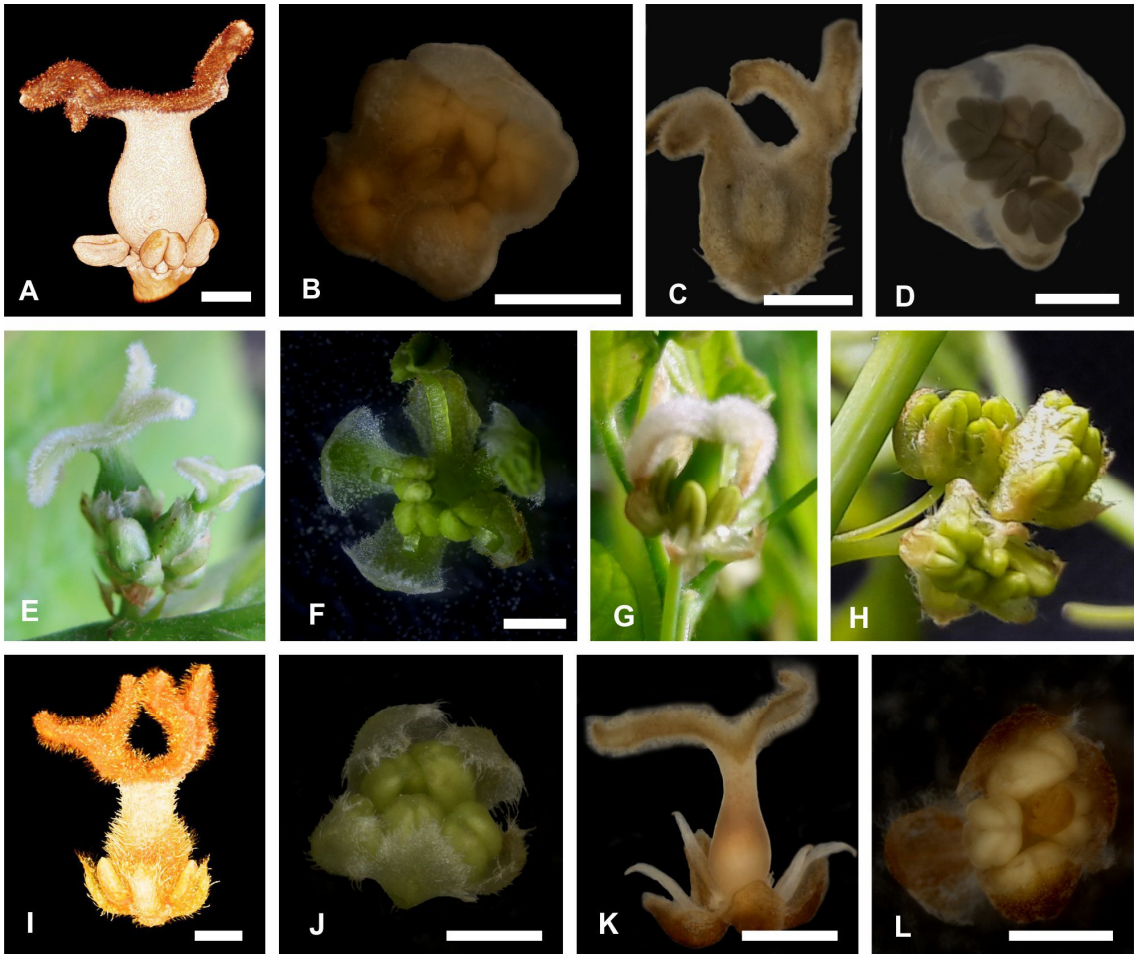

Figure 1. Flowers of *Celtis* in HRXCT 3D reconstructions (A, I), or in photo-stereomicroscopy (B, C, D, F, J, K, L), or in a Light photograph (E, G, H). A-B, *Celtis brasiliensis*, staminodes (sepals removed) and gynoecium of the pistillate flower (A) and staminate flower with sepals, stamens and an evident pistillode (B). C-D, *C. ehrenbergiana,* pistillate flowers with four stigmatic branches (C) and staminate flower with sepal and stamens and a non-evident pistillode (D). E-F, *C. iguanaea,* inflorescence of the pistillate flower with four stigmatic branches but only three evident (E) and staminate flowers with five sepals and five stamens, three inflexed filaments and two distended filaments (F). G-H, *C. occidentalis,* pistillate flowers with sepals, staminodes and gynoecium with two stigmatic branches (G) and staminate flowers with six evident stamens (H). I-J, *C. pubescens,* pistillate flowers with sepals, staminodes and gynoecium with four stigmatic branches (I) and staminate flowers with five sepals and five stamens and a non-evident pistillode. (J). K-L, *C. sinensis,* pistillate flower, stamens without anthers and pistil with two stigmatic branches. L, staminate flower with four sepals, four stamens and an evident pistillode. Scale bars: 1 mm.

In the pistillate flower the carpel primordia elongate from the apex. One of the carpels elongates further early during development (carpel 1) and produces a cleft (Fig. 3A, B, C, D) and an ovule in the ventral region (Fig. 3B, C, E-F). The smaller carpel (carpel 2) forms a small cleft (Fig. 3G, asterisk) and no ovule. The syncarpous region elongates (Fig. 3E, F, G), as also does the apex of each carpel that forms two distinct

unequal stigmas (Fig. 3E, G, H). Each stigma divides into two branches (Fig. 3H) which result in four stigmatic branches. The region below each stigmatic branch elongates and forms a short style that maintains the stigmatic branches almost united, so that the carpels close (Fig. 3H, I). The stamen primordia originate staminodes with typical anther and filament (Fig. 4A-F), but no anther wall thickenings were observed (Fig. 4A-D). The anthers house atypical pollen grains (Fig. 4C, D) or are empty (Fig. 4A). The anthers of *C. occidentalis* have an appendix at the base (Fig. 4F). The gynoecium consists of an ovary with a hick mesophyll, short style and papillose stigma (Fig. 4G-K).

In the staminate flower, each stamen primordium elongates and differentiates into anther and filament (Fig. 5A, B) and the emerged carpel primordia elongate and originate a pistillode that varies in size among the species (Fig. 5A-D). At the end of floral development, the anther has a distinct endothecium layer with cell wall thickenings (Fig. 5E-J). In *C. occidentalis* the anthers have an appendix at their bases (Fig. 4F). The pistillode can contain an ovule or not (Fig. 5C, D). If the ovule arises it does not develop. In *C. occidentalis,* sometimes two sepals united in the developed flower were observed.

The ovule curvature found was of two types: anatropous ovule and hemitropous ovule. The anatropous ovule occurs in *C. brasiliensis*, *C. iguanaea* and *C. pubescens* (Fig. 6A-C); in these species, the nucellus is straight and the micropyle is directed backwards towards the base of the funiculus. The hemitropous ovule occurs in *C. occidentalis*, *C. ehrenbergiana* and *C. sinensis* (Fig. 6C-F); in these species, the nucellus and micropyle are weakly curved, but not so much as in the anatropous ovule.

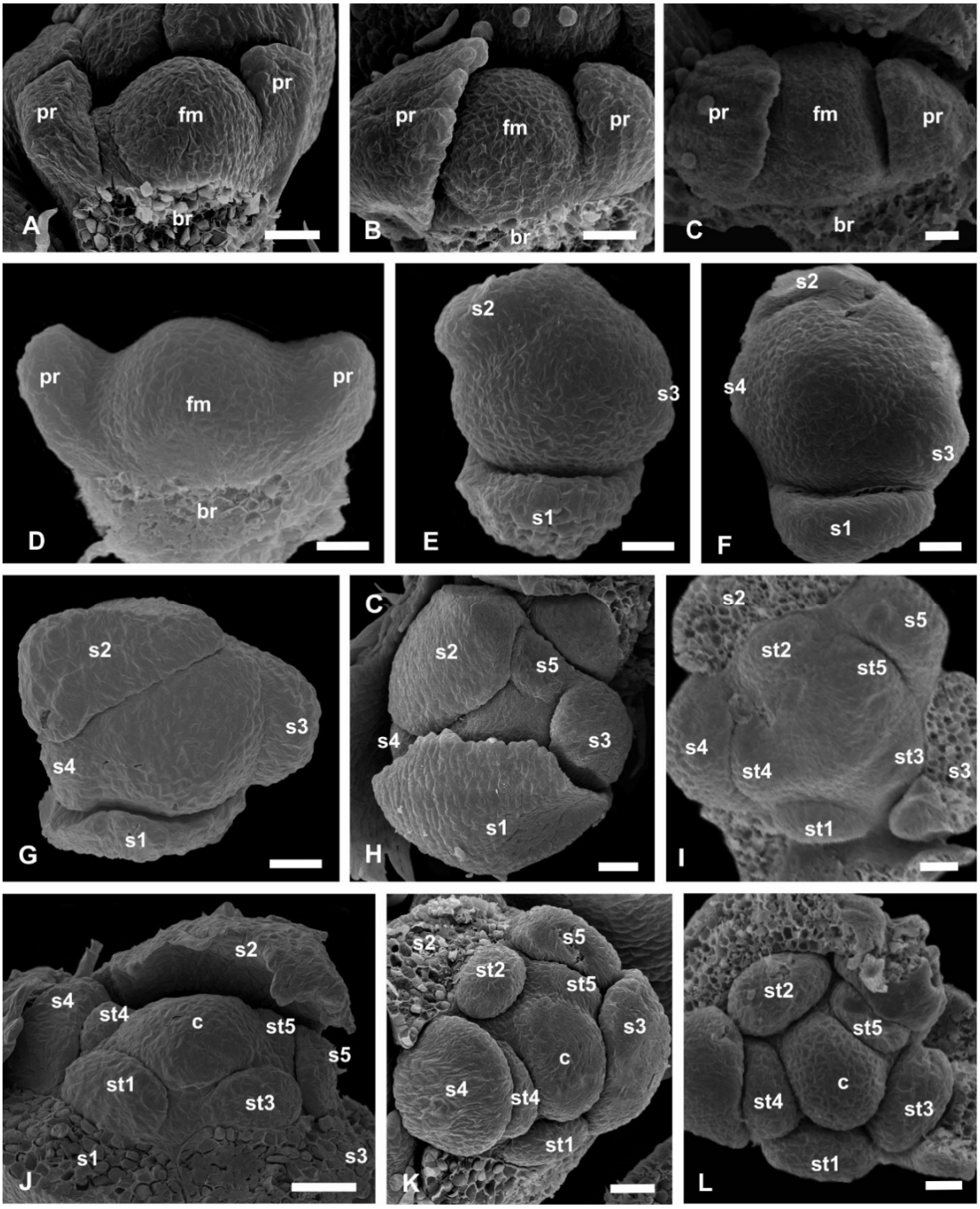

Figure 2. Early floral development of *Celtis brasiliensis* (A, H, K), *C. ehrenbergiana* (B, F), *C. iguanaea.* (C, I, L) and *C. pubescens* (D, E, G, J) (SEM). A-D, Rounded floral meristems with an abaxial bract (removed) and two prophylls. E-H, emergence of sepal primordia in a spiral sequence; note the great size differences caused by long plastochrons between successive sepals. I, emergence of stamen primordia in a spiral sequence; note that they are opposite to the sepals (sepals removed). J-L, elongation of the stamens and emergence of one central carpel primordium that becomes bulged. Abbreviations: br, bract; fm, floral meristem; pr, prophylls; s, s1, s2, s3, s4, s5, sepals; st, st1, st2, st3, st4, st5, stamens; c, carpel. Scale bars: A-C, H-L, 25 μm; D-G, 20 μm.

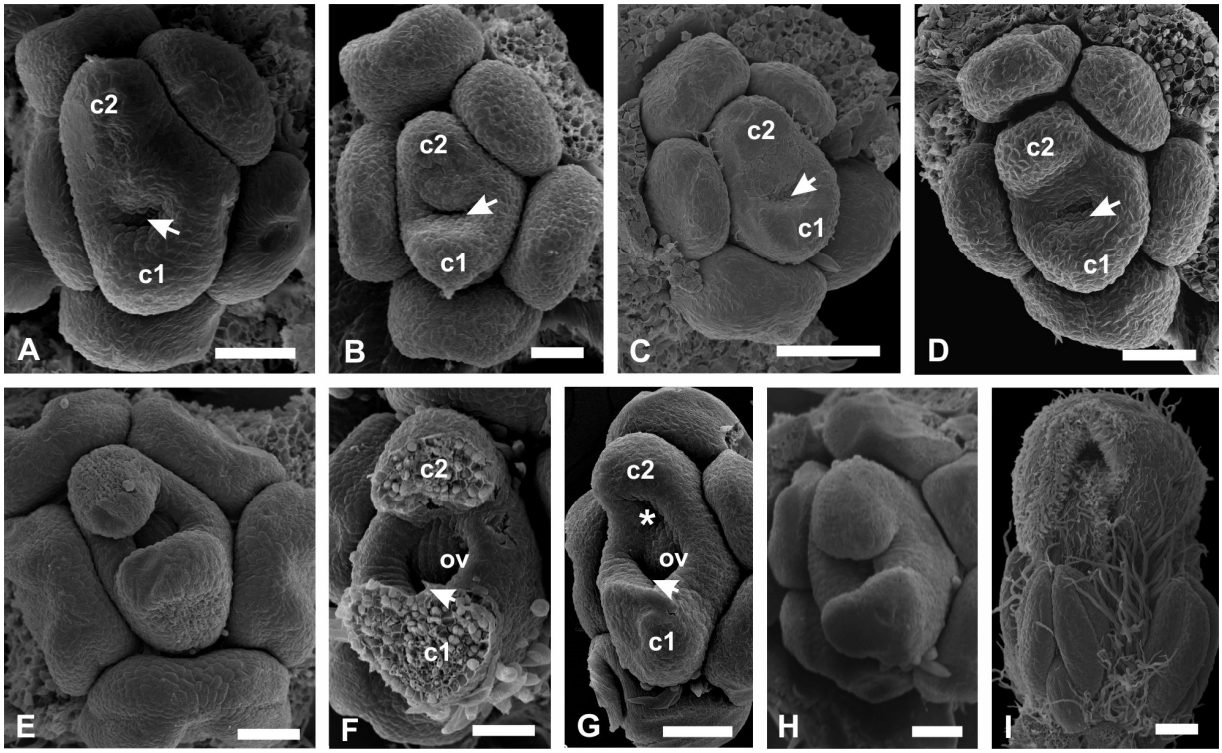

Figure 3. Development of a pistillate flower of *Celtis ehrenbergiana* (A, G, I), *C. pubescens* (B, F), *C. iguanaea.* (C, H) and *C. brasiliensis* (D, E) (SEM). A-D, elongation of staminodes; the central carpel primordium subsequently gives rise to two secondary carpel primordia of unequal size, which proximally are congenitally united; note the cleft (arrow) in the larger carpel (c1) (sepals removed). E-G, elongation of the carpels from the apex and emergence of an ovule in the locule of carpel 1; note a small cleft in the carpel 2 in G (asterisk) and that this carpel has no ovule. H, formation of two stigmatic branches, which divide and form four branches. I, developed staminodes and papillose stigmatic branches. Abbreviations: c1, c2, carpel; ov, ovule. Scale bars: A-H, 50 μm; I, 1 mm.

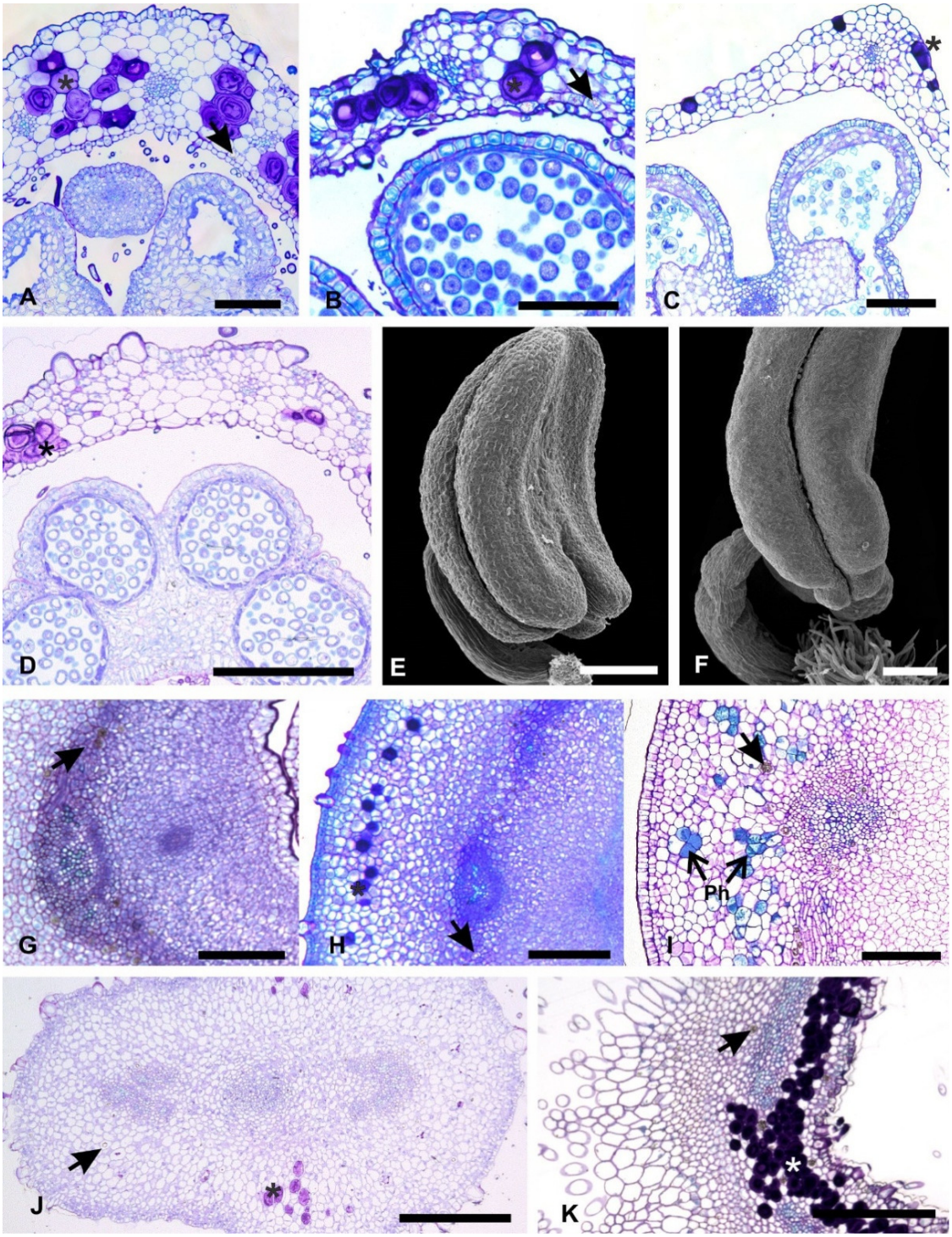

Figure 4. Comparative morphology of a mature pistillate flower of *Celtis.* A-D, G-K, (LM); E-F, (SEM). *C. ehrenbergiana* (A, J), *C. iguanaea.* (B, G, K), *C. occidentalis* (C, F), *C. pubescens* (D), *C. brasiliensis* (E, H) and *C. sinensis* (I). A-D, mucilaginous cells (asterisk) in the mesophyll (A-B, D) and in the epidermis (C) of sepals; anthers without pollen grains (A) or with atypical pollen grains without cellular division (B) or content (D). E, sagittate anthers with a rounded base. F, anthers with appendices in the base. G-I, ovarian mesophyll containing cells with druses (arrow), mucilage (asterisk) and phenolic compounds (Ph). J-K, style and stigma containing cells with mucilage and druses. Scale bars: A-B, G-I, 100 μm; C-D, J-K, 200 μm; E-F, 250 μm.

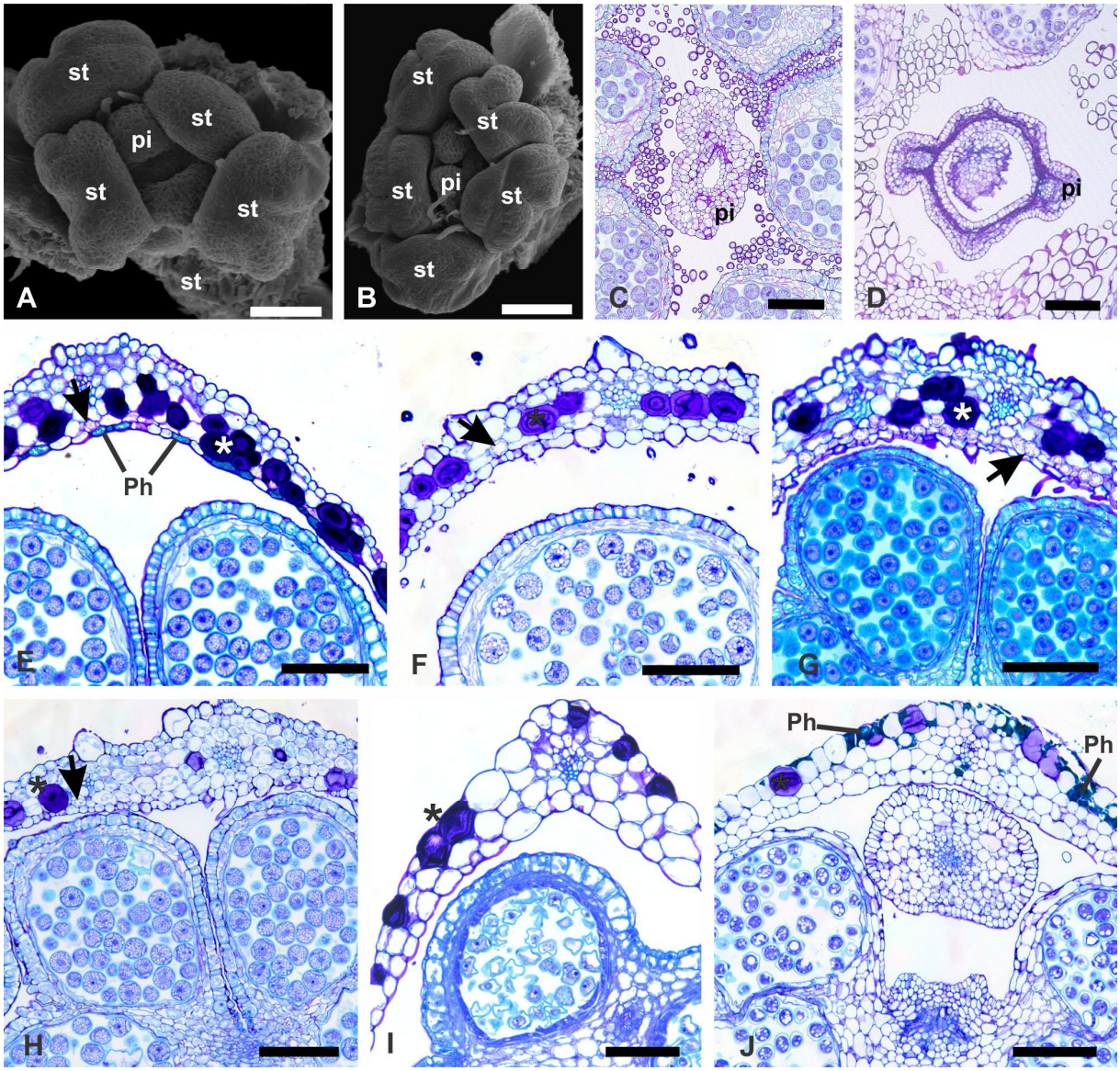

Figure 5. Development and anatomy of staminate flower of *Celtis* species. A-B (SEM); C-J, (LM). *C. pubescens* (A, C, H), *C. ehrenbergiana* (B, F), C. sinensis (D, J), *C. brasiliensis* (E), *C. iguanaea.* (G) and *C. occidentalis* (I). A, anthers in differentiation and elongating carpels (sepals removed). B, differentiated anthers and carpel abortion forming a pistillode. C, pistillode without an ovule. D, pistillode with an aborted ovule. E, Sepal containing phenolic compounds (Ph) in the epidermis, and idioblasts containing druses (arrow) and mucilage (asterisk) in the mesophyll. The anther has a distinct endothecium layer with a thickening cell wall. F-H, Mesophyll of the sepal with idioblasts containing druses (arrow) and mucilage (asterisk). The anther has a distinct endothecium layer with a thickening cell wall. I, Epidermis of the sepal with idioblasts containing mucilage (asterisk). J, Epidermis of the sepal with idioblasts containing mucilage (asterisk) and phenolic compounds (Ph). Abbreviations: st, stamens; pi, pistillode; Ph, phenolic compounds. Scale bars: A, 50 μm, B-J, 100 μm.

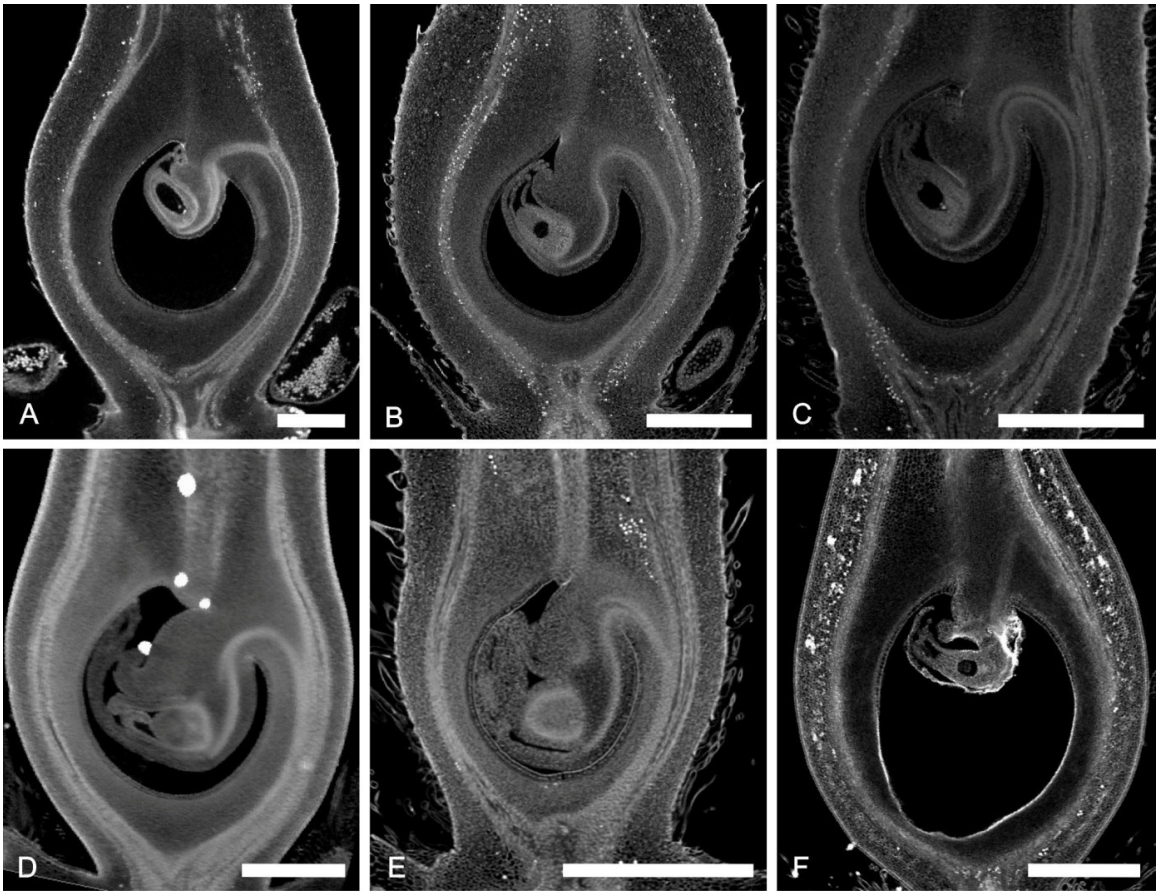

Figure 6. Types of ovule in *Celtis* species according to the curvature (HRXCT, 2D reconstructions in longitudinal sections). A-C, anatropous ovule of *C. brasiliensis* (A), *C. iguanaea* (B) and *C. pubescens* (C). D-F, hemitropous ovule of *C. occidentalis* (D), *C. ehrenbergiana* (E) and *C. sinensis* (F). Scale bars: A-F, 500 μm.

Gynoecium vascularization

The gynoecium of the six *Celtis* species has carpels that are vascularized in two different ways. Carpel 1 (the larger carpel) is vascularized by two bundles, a dorsal one and a ventral one, which enter from the basal-most part of the ovary (Fig. 7A-F). The dorsal bundle (labeled d1) runs in the median-dorsal plane of the carpel and extends up to the stigmatic area (Fig. 7A-F). The ventral bundle (labeled v1) runs along the ventral side of the carpel and enters into the ovule just below the apex of the ovary locule (Fig. 7A-F). Carpel 2 is vascularized only by one dorsal bundle (labeled d2) that runs in the median-dorsal plane of the carpel, opposite to the dorsal bundle of carpel 1, and extends up to the stigmatic area (Fig. 7A-F).

In most species the ventral bundle of carpel 1 runs in parallel to the dorsal bundle of carpel 2 (Figs. 7A-E; 8A-I; 9A-F). Nevertheless, these vascular bundles are

distinct and separated (Figs. 7A-E; 8A-I; 9A-F). In *C. sinensis,* the dorsal bundle of carpel 2 and the ventral bundle of carpel 1 are indistinct and united, forming a single dorsal-ventral bundle (labelled dvb) (Figs. 7F; 9G, H). Each species exhibits a different format for the curvature of the ventral bundle (carpel 1) running to the ovule (to see Fig. 7A-F).

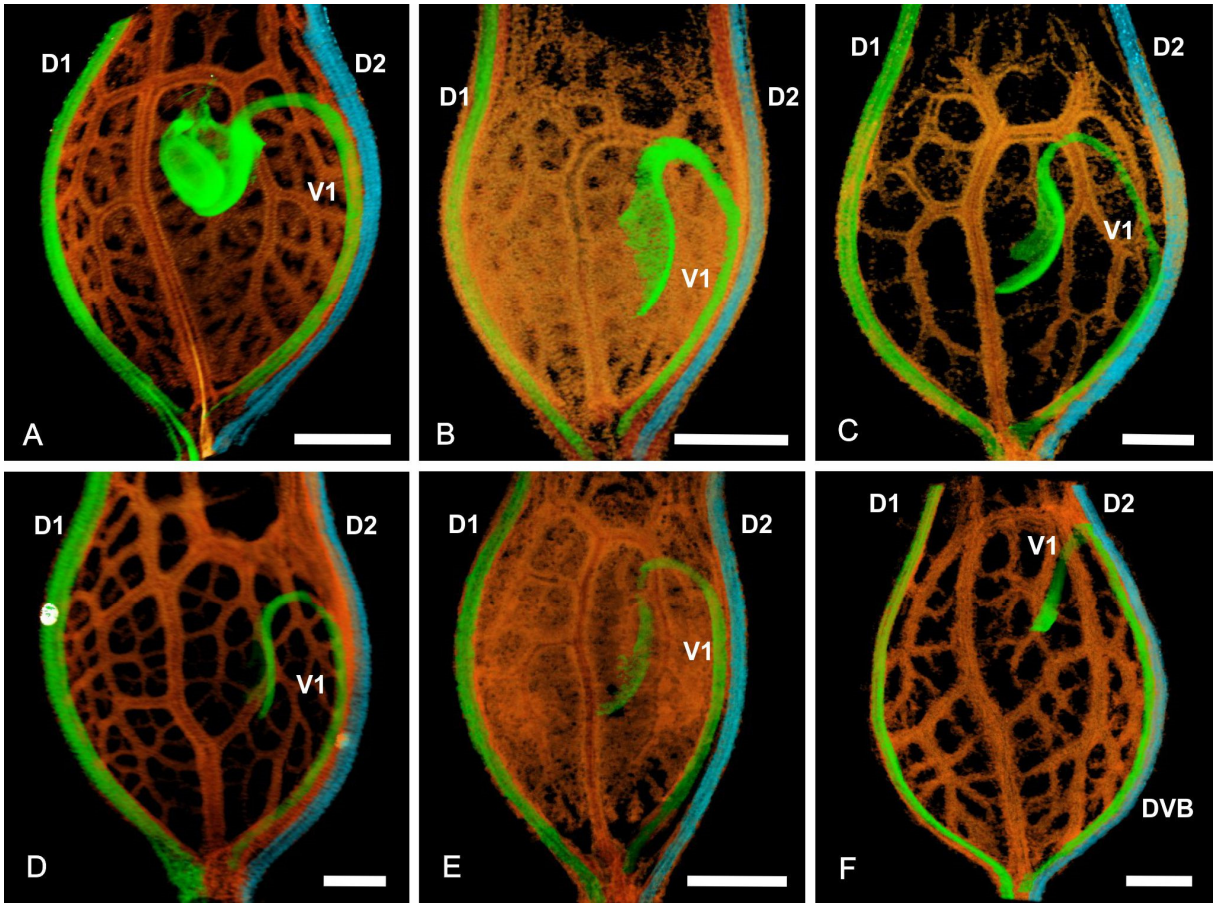

Figure 7. Gynoecium vasculature in the pistillate flower of the *Celtis* species studied (HRXCT 3D reconstructions). *C. brasiliensis* (A), *C. ehrenbergiana* (B), *C. iguanaea.* (C), *C. occidentalis* (D), *C. pubescens* (E) and *C. sinensis* (F). Note the different curvature of the ventral bundle towards the ovule and different degrees of proximity between the ventral bundle (V1) of carpel 1 and the dorsal bundle (D2) of carpel 2. The larger carpel (carpel 1, green) is vascularized by one dorsal bundle (D1) that extends up the stigma and by one ventral bundle (V1) that veers off to serve the ovule. The smaller carpel (carpel 2, blue) is vascularized by one dorsal bundle (D2) that extends up the stigma. F, Ventral bundle of carpel 1 and dorsal bundle of carpel 2 indistinct and united, forming one single dorsal-ventral bundle (DVB). Scale bars: 250 μm.

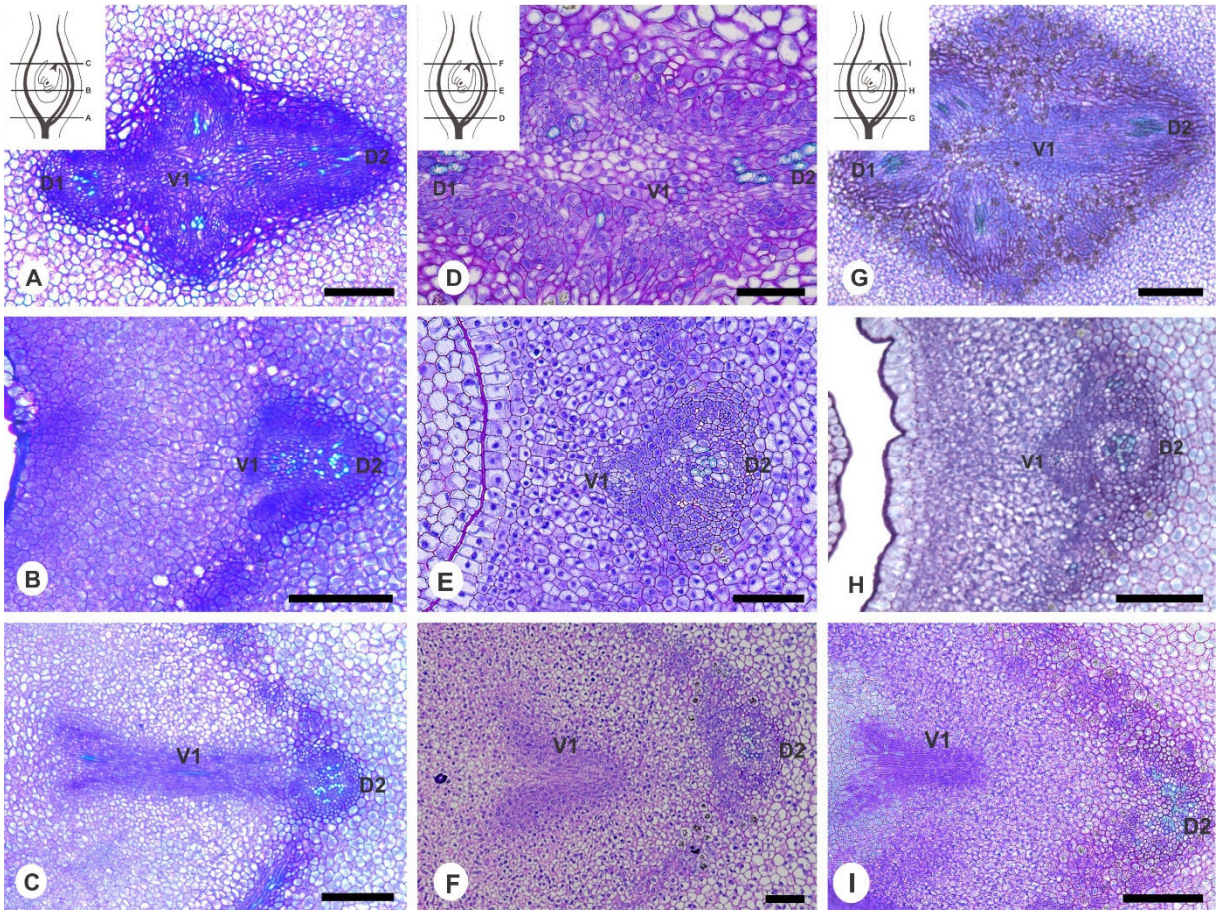

Figure 8. Gynoecium vasculature in the pistillate flower of the *Celtis* species studied (histological analyses). *C. brasiliensis* (A-C), *C. ehrenbergiana* (D-F) and *C. iguanaea.* (G-I). A, D, G, cross-section at the ovary base showing the ventral bundle (V1) running close to the dorsal bundle (D1) in carpel 1; and the dorsal bundle (D2) of carpel 2 running opposite to the dorsal bundle (D1) of carpel 1. B, E, H, cross-section of the ovary mid-part showing the ventral bundle (V1) of carpel 1 running close to the dorsal bundle (D2) of carpel 2. C, F, I, cross-section of the ovary-locule apex showing the ventral bundle (V1) curving to serve the ovule. Lines in black and white indicate the ovary vasculature at the same levels of the cross-sections shown in the figures of the plate. Abbreviations: D1, dorsal vascular bundle of carpel 1; D2, dorsal vascular bundle of carpel 2; V1, ventral vascular bundle of carpel 1. Scale bars: A-C, G- I, 100 μm; D- F, 50 μm.

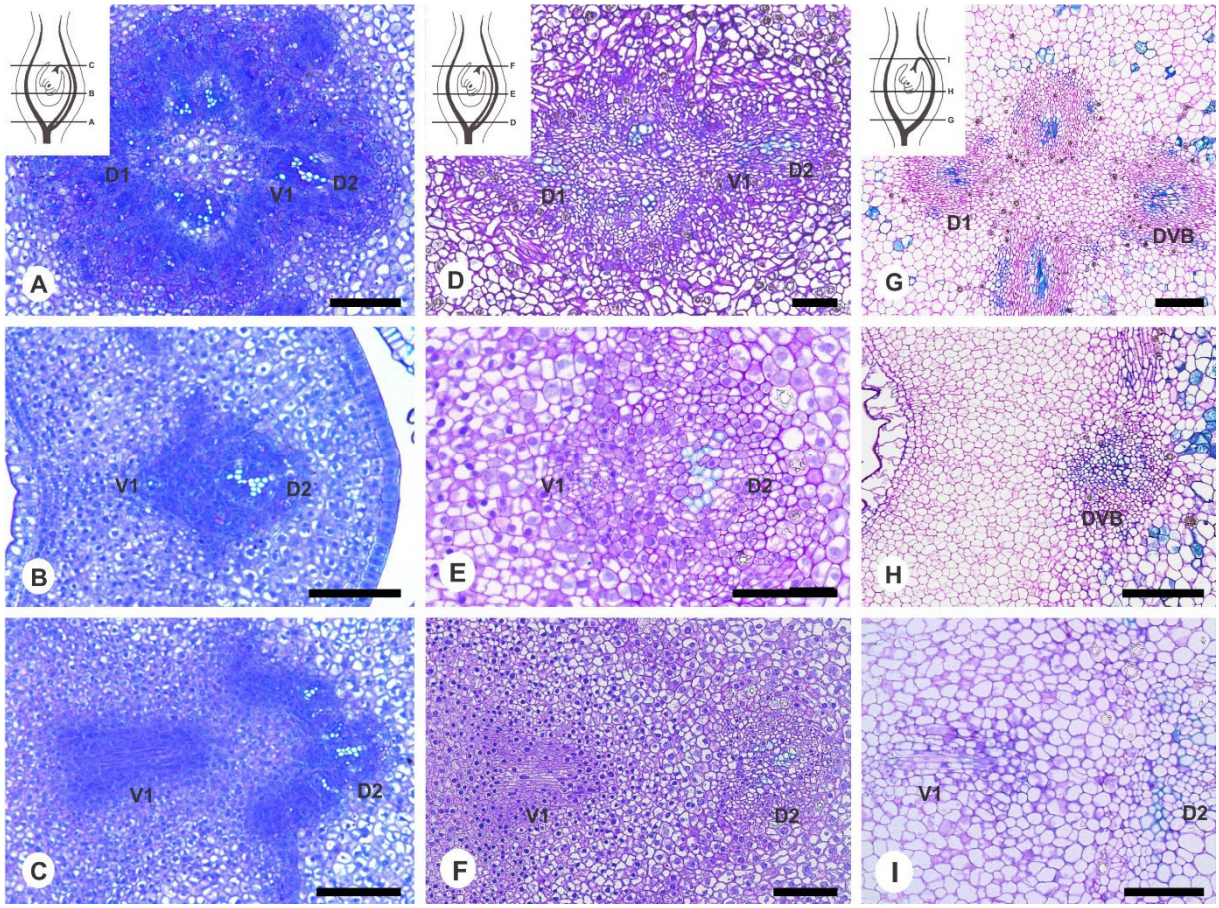

Figure 9. Gynoecium vasculature in the pistillate flower of the *Celtis* species studied (histological analyses). *C. occidentalis* (A-C), *C. pubescens* (D-F) and *C. sinensis* (G-I). A, D, cross-section at the ovary base showing the ventral bundle (V1) and the dorsal bundle (D1) of carpel 1; and dorsal bundle (D2) of carpel 2 running opposite to the dorsal bundle (D1) of carpel 1. G, cross-section of the ovary base showing the ventral bundle of carpel 1 and the dorsal bundle of carpel 2 indistinct and united, forming one single dorsal-ventral bundle (DVB). B, E, cross-section of the ovary mid-part showing the ventral bundle (V1) of carpel 1 running close to the dorsal bundle (D2) of carpel 2. H, cross-section of the ovary mid-part showing the ventral bundle of carpel 1 and the dorsal bundle of carpel 2 indistinct and united, forming one single dorsal-ventral bundle (DVB). C, F, I, cross section of the ovary-locule apex showing the ventral bundle (V1) curving to serve the ovule. Lines in black and white indicate the ovary vasculature at the same levels of the cross-sections shown in the figures of the plate. Abbreviations: D1, dorsal vascular bundle of carpel 1; D2, dorsal vascular bundle of carpel 2; V1, ventral vascular bundle of carpel 1; BDV, dorsal-ventral vascular bundle. Scale bars: A-C, G-H, 100 μm; D-F, I, 50 μm.

Floral secretory structures

Three types of secretory structures were found in the flower: mucilaginous idioblasts (Figs. 4A-D, H, J, K; 5E-J), phenolic idioblasts (Fig. 4I; 5E, J), and secretory trichomes (Fig. 10).

Mucilaginous idioblasts were found in the sepal of all species (Figs. 4A-D; 5E-J), with different distribution in the tissues among the species. *C. brasiliensis*, *C.*

ehrenbergiana, C. iguanaea and *C. pubescens* have mucilaginous idioblasts in the mesophyll (Figs. 4A, B, D; 5E-H), while *C. occidentalis* and *C. sinensis* have mucilaginous idioblasts in the epidermis (Figs. 4C; 5I, J). They were also found in the mesophyll of the ovary of *C. brasiliensis* (Fig. 4H), and in whole style and stigma of all analysed species (Fig. 4J, K) (Table 2).

Phenolic idioblasts were found in the sepals of two species, in the epidermis of *C. brasiliensis* (Fig. 5E) and in the epidermis and mesophyll of *C. sinensis* (Fig. 5J). In *C. sinensis*, phenolic idioblasts were also found in the mesophyll of the ovary (Fig. 4I).

Secretory trichomes are widely distributed on the sepals and gynoecium (see Table 3; Fig. 10) and are structurally similar among the species (Fig. 10). All species exhibit secretory trichomes on the sepals (Fig. 10A-G) and only some species have no trichomes on the margin (e.g. *C. pubescens*, Fig. 10H) or on the adaxial side (e.g. *C. sinensis* and *C. ehrenbergiana*). In the stamens, staminodes and pistillode, no secretory trichomes were found. On the ovary, they are absent only in *C. sinensis* and *C. occidentalis* (Fig. 10L, N). They can have a unicellular head and a uniseriate stalk (Fig. 10O) or a multicellular head and a uniseriate stalk (Fig. 10P). In addition, tector trichomes were found in almost all floral organs of all species studied, with the exception of *C. occidentalis* (Fig. 10L).

Floral Crystal

Druses were found in all species analysed. They occur in the mesophyll of the sepals (Figs. 4A-B, 5E-G), in the cortex of the filament, and close to the vascular bundles in the ovary (Fig. 4G-I), style (Fig. 4J) and stigma (Fig. 4K). They were only absent in the sepals of *C. sinensis* and in the sepals and filament of *C. occidentalis*.

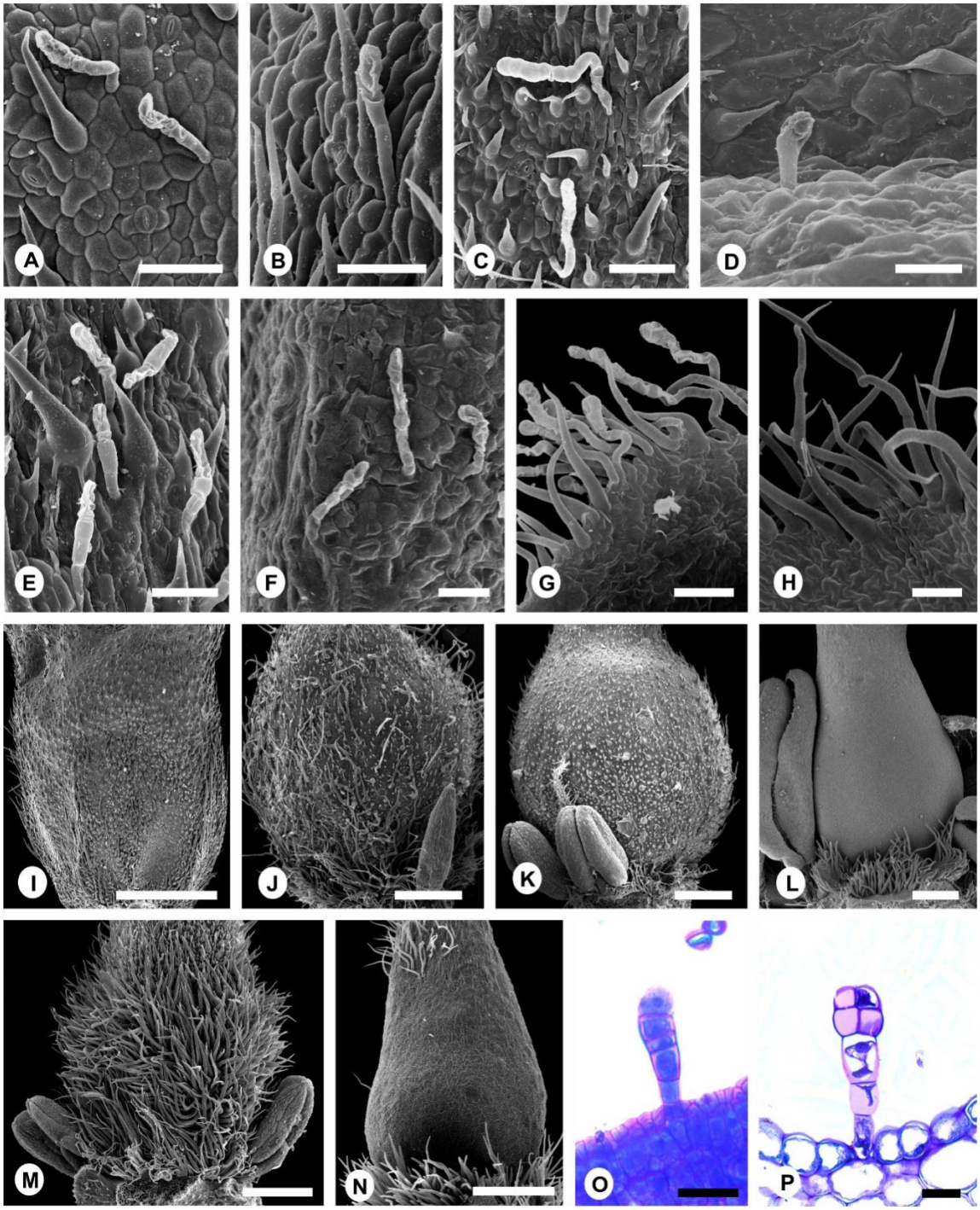

Figure 10. Distribution of tector and secretory trichomes in the floral organs of *Celtis*. A-N, (MEV); O-P (ML). (A, I, O) *C. brasiliensis.* (B, J) *C. ehrenbergiana*. (C, G, K) *C. iguanaea.* (D, L, P) *C. occidentalis.* (E, H, M) *C. pubescens.* (F, N) *C. sinensis*. A-F, Abaxial side of the sepals covered with secretory and tector trichomes. G-H, Detail of the sepal margin with secretory trichomes (G) and tector trichomes (H). I, ovary surface with short tector trichomes. J, ovary surface with short and long tector trichomes. K, ovary surface with short tector trichomes of wide base. L, ovary surface without trichomes. M, ovary surface with high density of tector trichomes. N, ovary surface without trichomes and few tector trichomes in the style. O, detail of a secretory trichome with a unicellular head. P, detail of a secretory trichome with a pluricellular head. Scale bars: A-H, 50 μm; I-N, 500 μm; O-P, 25 μm.

Table 2. Comparative floral features of the *Celtis* species studied. Symbols: (Ep) epidermis; (Me) mesophyll; (Ov) ovary; (Sep) sepal; (St) stamen; (-) absent; (+) present.

Species	Floral organization				Occurrence of mucilaginous idioblasts			Occurrence of druses				Occurrence of phenolic idioblasts			
	Sepal number	Stamen number	Carpel number	Number of stigmatic branches	Sep	Ov	Style/ Stigma	Sep	St	Ov	Style/ Stigma	Sep	St	Ov	Style/ Stigma
C. brasiliensis	5	5	2	4	+	+	+	+	+	+	+	+	-	-	+
C. ehrenbergiana	5(4)	5(4)	2	4	+	-	+	+	+	+	+	-	-	-	-
C. iguanaea	5	5	2	4	+	-	+	+	+	+	+	-	-	-	-
C. occidentalis	6-4(5)	6-4(5)	2	2	+	-	+	-	-	+	+	-	-	-	-
C. pubescens	5	5	2	4	+	-	+	+	+	+	+	-	-	-	-
C. sinensis	4	4	2	2	+	-	+	-	+	+	+	+	+	+	+

Table 3. Comparative trichome distribution in the floral organs of the *Celtis* species studied. Symbols: (TT) tector trichome; (ST) secretor trichome; (-) absent; (+) present.

Floral organ	Pistillate flower										Staminate flower									
	Sepal/Ada		Sepal/Aba		Sepal/ Margin		Staminode		Gynoecium		Sepal/Ada		Sepal/Aba		Sepal/ Margin		Stamen		Pistillode	
	TS	ST	TT	ST	TT	ST	TT	ST	TT	ST	TT	ST	TT	ST	TT	ST	TT	ST	TT	ST
C. brasiliensis	+	+	+	+	+	+	-	-	+	+	+	-	+	-	+	+	-	-	-	-
C. ehrenbergiana	+	-	+	+	+	-	+	-	+	+	+	-	+	+	+	-	+	-	-	-
C. iguanaea	+	+	+	+	+	+	+	-	+	+	+	+	+	+	+	+	+	-	-	-
C. occidentalis	+	-	+	+	+	-	-	-	-	-	+	-	+	-	+	-	-	-	+	-
C. pubescens	+	+	+	+	+	+	+	-	+	+	+	+	+	+	+	+	+	-	+	-
C. sinensis	-	-	+	+	+	-	+	-	-	-	-	-	-	+	+	-	+	-	-	-

3.5 Discussion

Although the studied species of *Celtis* have been previously described as andromonoecious (Berg & Dahlberg, 2001; Torres & Luca, 2005; Sattarian, 2006), our data showed that they are all monoecious because they exhibit two floral morph types, pistillate and staminate. The perfect flower described before actually acts as a functionally pistillate flower because its stamens do not produce dehiscing anthers or viable pollen grains and are, thus, staminodes. Such anthers are not dehiscent because a typical endothecium is lacking, and wall thickenings were not found. The endothecium is the anther wall layer that promotes anther dehiscence by dehydration; it loses water in the region along which anthers dehisce where there are thin-walled cells and therefore the endothecium shrinks in a manner that results in the opening of the anthers. This mechanism does not occur without a typical endothecium.

The reduced flower of the studied species of *Celtis* results from three different processes: 1) absence of one perianth whorl from inception, forming apetalous flowers; 2) abortion of stamens or carpels resulting in diclinous flowers, and 3) abortion of part of one of the two carpels emerged constituting a pseudomonomerous gynoecium.

Apetalous flower

The absence of petals in the flower of *Celtis* is observed even early during floral development. The perianth has been classified as sepalar based on recent studies with close families (Moraceae – Leite *et al.*, 2018; Ulmaceae – Leme *et al*., 2018) showing that apetaly is a recurrent feature in the order Rosales (Endress & Matthews, 2006; Endress, 2010). In these groups, apetaly seems to be directly related to wind pollination (Culley *et al.*, 2002; Matthews & Endress, 2006; Friedman & Barrett, 2009).

The floral reduction in *Celtis* also reaches the calyx and androecium merism that ranges from 4 to 6 organs (*C. sinensis*, *C. ehrenbergiana* and *C. occidentalis*). A pentamerous or tetramerous flower is usual in Cannabaceae (Bechtel, 1921; Berg & Dahlberg, 2001; Sattarian, 2006), although in *Cannabis sativa* (Payer, 1857b; Briosi &

Tognini, 1894; F.M. Leme, unpublished data) and *Humulus lupulus* (Shephard *et al.*, 2000) the pistillate flowers are dimerous. The occurrence of six sepals in *Celtis occidentalis*, besides being atypical, reflects the merism lability of the group. It can be promoted by the union of two adjacent organs (e.g. *Celtis occidentalis*) or by the organ suppression from the inception (e.g. *Celtis sinensis*, *C. ehrenbergiana*) and be related to the loss or gain of one organ in pentamerous flowers, typical of the Rosids (see Endress, 2011).

Diclinous flower

The non-functioning carpels and stamens of staminate and pistillate flowers of the *Celtis* species studied are the result of abortion during the intermediate and final developmental stages, respectively. Carpel abortion can also occur early during floral development, even before the ovule arises, thus resulting in a small-sized carpel rudiment, as found in some flowers of *Celtis pubescens.* In other Cannabaceae, diclinous flowers can also result from the absence of stamen/carpel from inception, as in *Cannabis sativa* (Payer, 1857; F.M. Leme, unpublished data) and *Humulus lupulus* (Shephard *et al.*, 2000). Both processes, absence since inception (Granville, 1971; Sattler, 1973; Maier *et al.*, 1997; Basso-Alves *et al.*, 2014) and abortion (Payer, 1857; Okamoto *et al*., 1992; Basso-Alves *et al*., 2014; Leite *et al.* 2018, Leme *et al*. 'in press'), are extensively found in the Urticalen rosid clade that comprises, in addition to Cannabaceae, Moraceae, Ulmaceae and Urticaceae (Sytsma *et al*., 2002) (see table 4). Therefore, abortion and absence from inception are processes that can occur in the same family, genera or species (different morph types), showing lability in the formation of diclinous flowers among urticalean rosids that provides sources of floral diversification in the group (see Endress, 2011).

The functions of the pistillode and staminodes in staminate and pistillate flowers are still poorly known in Urticalean rosid species. Only for Urticaceae species the pistillode has been reported as a supporting feature in the mechanism of explosive pollen release together with sepals and inflexed stamens. Anatomical findings such as

pistillode aerenchyma and mucilaginous cells helped to elucidate the pollen release mechanism. The pistillode aerenchyma accumulates air and after pressed by the filament elongation liberates the anther that contains pollen agglutinated by the mucilage produced in the epidermis (Pedersoli & Teixeira, 2016). For *Celtis* species the pistillode is much variable in size, but this explanation can be also plausible, mainly for *C. iguanaea, C. brasiliensis* and *C. sinensis* with an evident pistillode and inflexed stamens (present study).

Pseudomonomerous gynoecium

A pseudomonomerous gynoecium is found in the *Celtis* species studied (Eckardt, 1937; present study), in other Cannabaceae species (Leme *et al*. unpublished data), and in other Urticalean rosids (Eckardt, 1937; Weberling, 1989), evidenced by the emergence of two carpel primordia and/or by gynoecium vascularization by two dorsal bundles. This condition causes the flower to be monosymmetrical in the Urticalean rosids, and is sometimes confused with monomery (see Endress, 2012). Although the occurrence of a pseudomonomerous gynoecium is widely found among Urticalean rosids, the developmental pathways, the carpel number (Leite, unpublished data) and the route and number of vascular bundles can vary among species (Eckardt, 1937; Chernik, 1981; Omori & Terabayashi, 1993).

The gynoecium vascularization in the urticalean rosids is highly variable. The gynoecium can be vascularized by two dorsal and four ventral bundles as in Ulmaceae (Bechtel, 1921; Eckardt, 1937; Omori & Terabayashi, 1993), by two dorsal bundles and a ventral one as in Cannabaceae (present study), and by only one dorsal and one ventral bundle as in Urticaceae (Pedersoli, unpublished data). Interestingly, the carpel reduction in the pseudomonomerous gynoecium can provoke union or disappearance of the ventral bundles (Wilson & Just, 1939). Thus, some researchers have interpreted the single ventral bundle as a result of the union of each ventral bundle of both carpels (Singh & Dublish, 1974; Tobe, 2012). The disappearance of the ventral bundles (suppressed carpel) or their union with the dorsal bundle are also

plausible hypotheses. This reasoning agrees with the reduction of bundle number in sepals (only one vascular bundle – present study, Wilson & Just, 1939). Our data showed that the smaller carpel (carpel 2) consists of only one column with one dorsal vascular bundle, indicating that only the larger carpel (carpel 1) participates in the formation of the locule and placenta, as also observed for *Celtis occidentalis* (Bechtel, 1921).

Supporting floral features for the emerged clades of Celtis

Some emerged clades of *Celtis* have been detected in a recent phylogeny of the genus (Sattarian, 2006) and of the family (Yang *et al.*, 2013): a clade comprises South American species and is clearly monophyletic and the other two comprise Asian and African species whose relationships continue to be unresolved by molecular data (Sattarian, 2006). *Celtis occidentalis* and *C. sinensis* belong to the Asian clade and the other species studied belong to the South American clade.

Although the six *Celtis* species studied are similar in floral organization, we found some differences regarding ontogeny and calyx and androecium merism (see tables 2 and 3). These floral features can help with the characterization of each emerged clade of *Celtis.*

The South American clade is supported by the following floral features: five sepals and stamens, four stigmatic branches, mucilaginous cells and druses in the mesophyll of the sepals, and a higher occurrence of secretory trichomes. The Asian clade is supported by the following floral features: four or six sepals and stamens, two stigmatic branches, mucilaginous cells in the epidermis of the sepals, absence of druses in the sepals, and absence of trichomes in the ovary.

Each species of *Celtis* analysed exhibits specific features within the clades. In the South American clade, *C. brasiliensis* is a single species characterized by the presence of phenolic compounds, *C. ehrenbergiana* has a hemitropous ovule, while *C. iguanaea* and *C. pubescens* are distinguished by difference in the density of trichomes on the ovary surface (Fig. 6K, M) and by the different position of the ventral bundle

serving the ovule (Fig. 7C, E). In the Asian clade, *C. sinensis* has phenolic compounds while in *C. occidentalis* the phenolic compounds are absent, and the two species differ in the vascularization of the gynoecium (Fig. 7D-F).

3.6 Conclusion

The breeding system of *Celtis* is monoecy with two floral morph types, pistillate and staminate flowers in the same individual. Flowers classified as perfect are actually structurally perfect but functionally pistillate, the staminodes have no pollen or have atypical pollen grains and the anther wall lacks a typical endothecium. The reduced flowers of *Celtis* are apetalous and diclinous, the petals are absent from inception and carpels and stamens are aborted during floral development. The pseudomonomerous gynoecium is formed by abortion of one of the carpels. The reduced carpel exhibits reduced vascularization and does not form an ovule. The floral features are important for the characterization of the clades and species of *Celtis.* Thus, more studies with Asian and African species would be important for the systematics of the group.

Table 4. Absence of carpel/stamen from inception (I) or by abortion (A) in species of the Urticalean rosid clade studied so far, classified according to sexual expression (Ad = androdioecious, Am = andromonoecious, D = dioecious, G = gynodioecious, M = monoecious). Empty cells mean no data available in the literature.

Family	Species	Sexual system	Pistillate flower	Staminate flower	References
Cannabaceae	*Cannabis sativa* L.	D	I	I	Payer (1957)
	Celtis brasiliensis (Gardner) Planch.	M	A	A	This study
	Celtis ehrenbergiana (Klotzsch) Liebm.	M	A	A	This study
	Celtis iguanaea (Jacq.) Sarg	M	A	A	This study
	Celtis occidentalis L.	M	A	A	This study
	Celtis pubescens Spreng.	M	A	A	This study
	Celtis sinensis Pers.	M	A	A	This study
	Humulus lupulus L.	D	I	I	Shephard et al. 2000
	Trema micrantha (L.) Blume	D	A	A	F.M. Leme, unpublished data
Moraceae	*Artocarpus heterophyllus* Lam.	M	I	I	Moncur 1985
	Clarisia ilicifolia (Spreng.) Lanj. & Rossberg	D	I	I	Leite et al. 2018
	Castilla elastica Sessé	Ad	I, A	I	Leite et al. 2018
	Broussonetia papyrifera (L.) L'Hér. ex Vent.	D	I		Baillon 1861
	Brosimum gaudichaudii Trécul	M	I	A	Leite et al. 2018
	Dorstenia astyanactis Aké Assi	M	I	A	Granville 1971
	Dorstenia contrajerva L.	M	I	A	Granville 1971
	Dorstenia embergeri Mangenot	M	I	A	Granville 1971
	Dorstenia volkensii Engl.	M	I	A	Granville 1971
	Ficus citrifolia Mill.	M	I	I	Basso-Alves et al. 2014
	Ficus carica L.	G	I	A	Condit 1932; Beck and Lord 1988
	Ficus asperifolia Miq.	G	I	A	Verkerke 1987
	Ficus hispida L.	G	I	A	Basso-Alves et al. 2014
	Ficus racemosa L.	M	I	I	Basso-Alves et al. 2014
	Ficus sycomorus L.	M	I	A	Galil et al., 1970
	Ficus sur Forssk.	M	I	I	Verkerke 1988
	Ficus religiosa L.	M	I	I	Johri and Konar 1956, Basso-Alves et al. 2014
	Maclura pomifera (Raf.) C.K. Schneid.	D	I	I	Bechtel 1921, Maier et al., 1997
	Maclura. tinctoria (L.) D.Don	D	I	A	Leite et al. 2018
	Morus alba L.	D	I	A	Bechtel 1921
	Morus nigra L.	D	I	A	Baillon 1861, Leite et al. 2018
	Morus rubra L.	D	I	A	Maier et al., 1997
Ulmaceae	*Ampelocera albertiae* Todzia	Am		A	Todzia 1989
	Ampelocera glabra Kuhlm.	M	A	A	Leme et al. 2018
	Phyllostylon brasiliense Capan. ex Benth. & Hook. f.	Am		A	Todzia 1992
Urticaceae	*Laportea Canadensis* (L.) Wedd.	D		A	Sattler 1973

3.7 References

Arruda VLV, Sazima M. **1988**. Polinização e reprodução de *Celtis iguanaea* (Jacq.) Sarg. (Ulmaceae), uma espécie anemófila. *Revista Brasileira de Botânica* **11**: 113–122.

Ashton CH. **2001**. Pharmacology and effects of *Cannabis*: a brief review. *British Journal of Psychiatry* **178**: 101–106.

Baillon, H., 1861. Mémoire sur le développement du fruit des Morées. *Adansonia* **1**, 214-231.

Basso-Alves JP, Pereira RAS, Peng Y-Q, Teixeira SP. **2014**. Different ontogenetic processes promote dicliny in *Ficus* L. (Moraceae). *Acta Oecologica* **57**: 5–16.

Bechtel AR. **1921**. The floral anatomy of the Urticales. *American Journal of Botanical* **8**: 386–410.

Beck N, Lord E. 1988. Breeding system in Ficus carica, the common fig. I. Floral diversity. *Am. J. Bot.* **75**: 1904-1912.

Berg CC, Dahlberg S V. 2001. A revision of *Celtis* subg. Mertensia (Ulmaceae). *Brittonia* **53**: 66–81.

Briosi G, Tognini F. **1894**. *Anatomia Della Canapa (Cannabis sativa L.)*. Milano: Istituto Botanico Della R. Universitá Dii Pavia.

Chernik V V. 1981. Pseudomonemeric gynoecium of the Ulmaceae and Celtidaceae representatives. *Botanicheskii Zhurnal (Moscow & Leningrad)* **7**: 958–966.

Condit, I.J., 1932. The structure and development of flowers in *Ficus carica* L. *Hilgardia* **6**, 443-481.

Culley TM, Weller SG, Sakai AK. **2002**. The evolution of wind pollintion in angiosperms. *Trends in Ecology and Evolution* **17**: 361–369.

Eckardt T. **1937**. Untersuchungen uber Morphologie, Entwicklungsgeschichte und systematische Bedeutung des pseudomonomeren Gynoeceums. *Nova Acta Leopold* **5**: 1–112.

Endress PK. **2010**. Flower structure and trends of evolution in Eudicots and their major subclades. *Annals of the Missouri Botanical Garden* **97**: 541–583.

Endress PK. **2011**. Evolutionary diversification of the flowers in angiosperms. *American Journal of Botany* **98**: 370–396.

Endress PK. **2012**. The immense diversity of floral monosymmetry and asymmetry across Angiosperms. *Botanical Review* **78**: 345–397.

Endress PK, Matthews ML. **2006**. First steps towards a floral structural characterization of the major rosid subclades. *Plant Systematics and Evolution* **260**: 223–251.

Fleming MP, Clarke RC. **1998**. Physical evidence for the antiquity of Cannabis sativa L. (Cannabaceae). *Journal of the International Hemp Association* **5**: 80–92.

Friedman J, Barrett SCH. **2009**. Wind of change: New insights on the ecology and evolution of pollination and mating in wind-pollinated plants. *Annals of Botany* **103**: 1515–1527.

Fukuoka N. **1982**. On pseudomonomerous pistil of the Ulmaceae. *Acta Phytotax. Geobot.* **56**: 84–91.

Granville de J.-J. 1971. Notes sur la biologie florale de quelques espèces du genre Dorstenia (Moracées). *Cah. Orstom (Sci. Biol.)* **15**, 61-97.

Johri, B.M., Konar, R.N., 1956. The floral morphology and embryology of Ficus religiosa Linn. *Phytomorphology* **6**, 97-100.

Leite VG, Mansano VF, Teixeira SP. **2018**. Floral development of Moraceae species with emphasis on the perianth and androecium. *Flora* **240**: 116–132.

Leme FM, Staedler YM, Schönenberger J, Teixeira SP. 2018. Ontogeny and vascularization elucidate the atypical floral structure of *Ampelocera glabra*, a tropical species of Ulmaceae. Int. J. Plant Sci. 179(6). Doi: 10.1086/697899.

Lillie RD. **1965**. *Histopathologic technic and practical histochemistry*. New York: McGraw-Hill Book Company.

Maier CG-A, Chapman KD, Smith DW. 1997. Phytoestrogens and floral development in dioecious *Maclura pomifera* (Raf.) Schneid. and *Morus rubra* L. (Moraceae). **Plant Sci 130**: 27-40.

Matthews ML, Endress PK. **2006**. Floral structure and systematics in four orders of

rosids, including a broad survey of floral mucilage cells. *Plant Systematics and Evolution* **260**: 199–221.

Mcdowell EM, Trump B. **1976**. Histological fixatives for diagnostic light and electron microscopy. *Archives of Pathology and Laboratory Medicine* **100**: 405–414.

Milligan SR, Kalita JC, Heyerick A, Rong H, Cooman L de, Keukeleire D de. **1999**. Identification of a potent phytoestrogen in hops (*Humulus lupulus* L.) and beer. *The Journal of Clinical Endocrinology & Metabolism* **83**: 2249–2252.

Moncur MW. 1985. Floral ontogeny of the jackfruit, *Artocarpus heterophyllus* Lam. (Moraceae). *Austr J Bot* **33**: 585–593.

O'Brien TP, Feder N, McCully ME. **1964**. Polychromatic staining of plant cell walls by toluidine blue O. *Protoplasma* **59**: 368–373.

Okamoto M, Kosuge K, Fukuoka N. **1992**. Pistil development and parietal placentation in the pseudomonomerous ovary of *Zelkova serrata* (Ulmaceae). *Acta Oecologica* **79**: 921–927.

Omori Y, Terabayashi S. **1993**. Gynoecial vascular anatomy and its systematic implications in Celtidaceae and Ulmaceae (Urticales). *Journal of Plant Research* **106**: 249–258.

Payer JB. **1857**. *Traité D'Organogéne Comparée de La Fleur*. Paris: Librairie de Victor Masson.

Pedersoli GD, Teixeira SP. **2016**. Light and electron microscopy analyses elucidate the structure and function of the pistillode in Urticaceae species In: *European Microscopy Congress 2016: Proceedings, 1*. Lyon, 262–263.

Richards AJ. **1997**. *Plant breeding systems*. London: Chapman & Hall.

Sattler R. 1973. Organogenesis of flowers: a photographic text-atlas. Toronto: University of Toronto Press.

Sattarian A. **2006**. *Contribution to the biosystematics of Celtis L. (Celtidaceae) with special emphasis on the African species*. PhD thesis Wageningen University, Wagwningen.

Shephard HL, Parker JS, Darby P, Ainsworth CC. **2000**. Sexual development and sex chromosomes in hop. *New Phytologist* **148**: 397–411.

Singh V, Dublish PK. **1974**. Floral anatomy *Broussonetia papyrifera* Vent. (Moraceae) with special reference to its gynoecium. *Current Science* **43**: 562–563.

Song B-H, Wang X-Q, Li F-Z, Hong D-Y. **2001**. Further evidence for paraphyly of the Celtidaceae from the chloroplast gene mat K. *Plant Systematics and Evolution* **228**: 107–115.

Staedler YM, Masson D, Schönenberger J. **2013**. Plant tissues in 3D via X-Ray tomography: Simple contrasting methods allow high resolution imaging. *PLOS ONE* **8 (9)** 1-9.

Sytsma KJ, Morawetz J, Pires JC, *et al.* 2002. Urticalean Rosids: Circumscription, Rosid ancestry, and phylogenetics based on rbcL, trnL-F, and ndhF sequences. *Am J Bot* **89(9)**: 1531–1546.

Tobe H. **2012**. Floral structure of *Cardiopteris* (Cardiopteridaceae) with special emphasis on the gynoecium: Systematic and evolutionary implications. *Journal of Plant Research* **125**: 361–369.

Todzia CA. 1989. A revision of *Ampelocera* (Ulmaceae). Ann Miss Bot Gard **76**: 1087-1102.

Todzia CA. 1992. A reevaluation of the genus *Phyllostylon* (Ulmaceae). SIDA **15**: 263-270.

Torres RB, Luca AQ. **2005**. Ulmaceae. In: Wanderley M das GL, Shepherd G, Giulietti AM, Melhem TS, eds. *Flora Fanerogâmica do Estado de São Paulo, Online*. São Paulo: FAPESP: RiMa, 437.

Ueda K, Kosuge K, Tobe H. **1997**. A Molecular phylogeny of Celtidaceae and Ulmaceae (Urticales) based on rbcL nucleotide sequences. *Journal of Plant Research* **110**: 171–178.

Verkerke W. 1987. Syconial anatomy of Ficus asperifolia (Moraceae), a gynodioecious tropical fig. Proc. K. Ned. Akad. Wet. C 90, 461-492.

Verkerke W. 1988. Flower development in Ficus sur Forsskal (Moraceae). Proc. K. Ned. Akad. Wet. C 91, 175-195.

Weberling F. **1989**. Morphology of Flowers and inflorescences. Cambridge University

Press, Cambridge, 349.

Wiegrefe SJ, Sytsma KJ, Guries RP. **1998**. The Ulmaceae, one family or two? Evidence from chloroplast DNA restriction site mapping. *Plant Systematics and Evolution* **210**: 249–270.

Wilson CL, Just T. **1939**. The morphology of the flower. *The Botanical Review* **V**: 1339–1344.

Yang M-Q, Velzen R Van, Bakker FT, Sattarian A, Li D, Yi T. **2013**. Molecular phylogenetics and character evolution of Cannabaceae. *Taxon* **62**: 473–485.

Zanoli P, Zavatti M. **2008**. Pharmacognostic and pharmacological profile of *Humulus lupulus* L. *Journal of Ethnopharmacology* **116**: 383–396.

"Sempre fica um pouco de perfume nas mãos
que entregam flores..."

(Provérbio chinês)

CHAPTER 4: 'FIRST RECORD OF LATICIFERS IN ULMACEAE'

Chapter 4: First record of laticifers in Ulmaceae

4.1 Abstract

Laticifers have not been reported for the Ulmaceae family although they have been observed in closely related families of the Urticalean clade (Moraceae, Urticaceae and Cannabaceae). In these families, laticifer structure and distribution as well as the latex composition are poorly known. Thus, the objectives of this study were to carefully check the occurrence of laticifers and to analyse the origin, morphology and the secretion composition of laticifers in the aerial parts of two species of Ulmaceae, *Ampelocera glabra* (tropical species) and *Zelkova serrata* (temperate species). Floral and shoot apices, flowers and stem branches were processed for anatomical studies. The latex composition was histochemically analised in the stem. Laticifers were found in both species, distributed along the stem, leaves, and in almost all floral parts (pedicel, sepals, filament, ovary and stigma), being absent only in the anthers. They are of the articulated type, with thick walls composed of hemicellulose and pectin. The latex contains polysaccharides, proteins, lipids and large starch grains. The articulated type found here in Ulmaceae is by first time described for urticalean rosids species. Thus, the presence of laticifers may be of taxonomic importance for the Ulmaceae and for Urticalean rosids. The presence of laticifers in floral organs seems to play defense role, minimizing the attack of galler animals. The rare occurrence of laticifers in the stigma opens new possibilities regarding the functions of these structures in the flowers. It is noteworthy that this is the first report of laticifers for Ulmaceae.

Key words: *Ampelocera glabra*, anatomy, cell wall, flowers, latex, Urticalean rosids, *Zelkova serrata*.

4.2 Introduction

Laticifer is a specialized cell or a serie of cells containing a suspension, or in some cases an emulsion, of many small particles in a liquid with a different refractive index termed latex (Fahn, 1979, 1990). The laticifer can be non-articulated (when it develops from a single cell which greatly elongates with the growth of the plant) or articulated (when it is formed from series of cells). The non-articulated type can also be classified as branched or unbranched and the articulated type can be anastomosing or non-anastomosing (Fahn, 1979). In addition, the composition of the latex is highly variable among families and species. Some of the substances generally found are rubber, resins, essential oils, proteins, carbohydrates, alkaloids, and cannabinoids among others (Metalfe, 1967; Fahn, 1990; Evert, 2006).

Laticifers have been found in approximately 36 families of Angiosperms (Lewinsohn 1991, Judd *et al*., 2009). Ulmaceae is the only family of the Urticalean rosids, a clade formed by Cannabaceae, Moraceae, Ulmaceae and Urticaceae within the order Rosales (APG IV, 2016), for which there were no reports of laticifers (see Sytsma *et al*., 2002; Judd *et al*., 2009). This family comprises 64 species distributed in seven genera that emerge in two clades in the last phylogeny, one with Tropical genera (*Ampelocera, Holoptelea, Phyllostylon*) and other with the North Temperate genera (*Hemiptelea, Planera, Ulmus, and Zelkova*) (Neubig *et al*., 2012).

In the Urticalean rosids, the latex appearance and the type of laticifers are quite variable. In Moraceae the latex is clear or milky and the laticifers are non-articulated branched (Fahn, 1979; Evert, 2006; Marinho *et al*., 2018); in Urticaceae species the latex is clear (Evert, 2006) and the laticifers are non-articulated unbranched (Meeuse, 1942; Fahn, 1979; Evert, 2006); in Cannabaceae the latex is yellow-brown or clear (Mahlberg, 1993; Evert, 2006) and the laticifers are non-articulated unbranched (Meeuse, 1942; Mesquita & Dias, 1984; Hagel *et al*., 2008). Thus, the absence of laticifers in Ulmaceae is totally unexpected.

Studies on the distribution of laticifers along the plant body of the Urticalean rosids are rarely found in the literature. The few studies are focused on a detailed description of laticifers (Guérin, 1923; Metcalfe, 1966; Mesquita & Dias, 1984; Hagel *et al.,* 2008) or on the latex composition (Furr & Mahlberg, 1981) in a particular plant organ. Only recent studies have described laticifers in organs related to plant reproduction (Souza *et al.,* 2015; Marinho *et al.* 2018). Thus, the role played by laticifers in the flowers is poorly known. Authors in general suggest they act in plant protection against herbivores (Fahn, 1979; Evert, 2006; Souza *et al.,* 2015). Nevertheless, recent studies with *Ficus* (Moraceae) indicate another important role of laticifers in the fig-fig wasp mutualism, helping the promotion of fig tree pollination (Marinho *et al.,* 2018). Certainly, studying the laticifer distribution, especially in floral organs, can bring new insights into ecological functions of such interesting secretory structure.

Thus, this study brings new information about the occurrence of laticifer in Ulmaceae by checking its distribution in the stem, leaf and floral organs, and describing its morphology and the latex composition in two monoecious species of Ulmaceae, the Neotropical *Ampelocera glabra* Kuhlm. and the Asian Temperate *Zelkova serrata* (Thunb.) Makino. Sampling these species allows us to infer the occurrence of laticifers in both clades of the family (see Neubig *et al.,* 2012).

4.3 Materials and methods

Ampelocera glabra and *Zelkova serrata* are tree species of Ulmaceae with distinct geographical distribution, the first in Tropical America and the last in Temperate Asia. *Ampelocera glabra* specimens were collected in the Reserva Particular do Patrimônio Natural (RPPN), Serra do Teimoso, Jussari, BA, Brazil, and *Zelkova serrata* specimens were collected in the Botanical Garden, University of Vienna, Vienna, Austria. Voucher specimens were deposited in the SPFR herbarium (FFCLRP / USP), under the following accessions: F.M. Leme nº 102 and 112; and in the CGMS herbarium (INBIO/UFMS), under the following accessions: F. M. Leme nº 124.

Samples of flowers, stems and leaves of both species were collected; for *Ampelocera glabra* floral and shoot apices were also collected. The samples were fixed in buffered formalin (Lillie, 1965) or in formalin – acetic acid – ethanol (FAA 70%) for 48 h (Johansen, 1940), dehydrated in an ethanolic series, embedded in histological resin (Historesin - Leica), and sectioned on transverse and longitudinal planes (5 μm) using a rotary microtome (Leica RM 2245). The serial sections were stained with 0.1% Toluidine blue in phosphate buffer, pH 6.8 (O'Brien *et al.,* 1964), mounted under a coverslip using water, and observed under a light microscope in order to analyse the laticifer structure and distribution.

The latex composition was studied using histochemical tests performed on embedded samples sectioned using a microtome and on alcohol-stored samples free-hand sectioned. Sections from embedded samples were stained with Toluidine blue for the detection of phenolic compounds (O'Brien *et al.* 1964), with period acid and Schiff (PAS) for neutral polysaccharides (Jensen 1962), with Ruthenium red for pectins (Johansen 1940), and with Xylidine Ponceau for proteins (Vidal 1970). Alcohol-stored samples of stems and leaves were free-hand sectioned and stained with Sudan III for total lipids (Pearse 1985), with Lugol for starch (Johansen 1940), and with ferric chloride for phenolic compounds (Johansen 1940). Astra blue and safranin were used for the identification of lignified cell walls (Bukatsch 1972 apud Kraus and Arduin 1997). Photomicrographs were obtained with a Leica DM 5000 B light microscope coupled to a Leica DFC 295 digital camera.

4.4 Results

Distribution

Laticifers are widely found in the plant body of *Ampelocera glabra* and *Zelkova serrata* (Table 1, Figs. 1, 2, 3 and 4). They are arranged in a set of five or more laticifers, external and in parallel to the vascular bundles (Fig. 1). In general, they are straight with slight curves in leaves and ovary (Figs. 3, 4). In the stem, laticifers are

found externally to the vascular bundles between the cortical parenchyma and phloem, and were absent in the pith (Figs. 1A-D). In leaves, laticifers occur in the midrib and along the smaller veins. In the flowers they occur in the pedicel, sepals, filaments, ovary, style, and stigma (Figs. 3, 4), always associated to the vascular bundles. In the sepals and filaments they are smaller in diameter and inconspicuous (Figs. 3A-C, E, 4A, B, E). In the stigma and ovary they are more evident and follow the two stigmatic branches (Figs. 3D, 4D).

Morphology and origin

In both species, the laticifers are articulated (Fig. 1A-D). The laticifers arise from procambial cells in more differentiated tissues of the stem and inflorescence branches (Fig. 2A-C). In the differentiated tissues of the stem or inflorescence, the laticifers are parallelly grouped (arrow, Fig. 1). The laticifers are long and thick-walled (arrow, Fig. 1B, D). The walls are composed of pectin-cellulosic (positive reactions to Toluidine blue - purple, Figs. 1-4, and PAS - pink, Figs. 5A-B). No lignin was found. They are multinucleate, and each nucleus has fusiform shape (Figs. 1B, 3C, 4D).

Table 1. Distribution of laticifers in vegetative and floral organs of *Ampelocera glabra* and *Zelkova serrata* (Ulmaceae).

Part of the Plant	*Ampelocera glabra*	*Zelkova serrata*
Stem	+ (cortex)	+ (cortex)
Leaf	+ (petiole, midrib and blade veins)	+ (petiole, midrib and blade veins)
Pistillate flower	+ (pedicel, sepal, ovary, stigma)	+ (pedicel, sepal, ovary, stigma)
Staminate flower	+ (pedicel, sepal, stamens)	+ (pedicel, sepal, stamens)

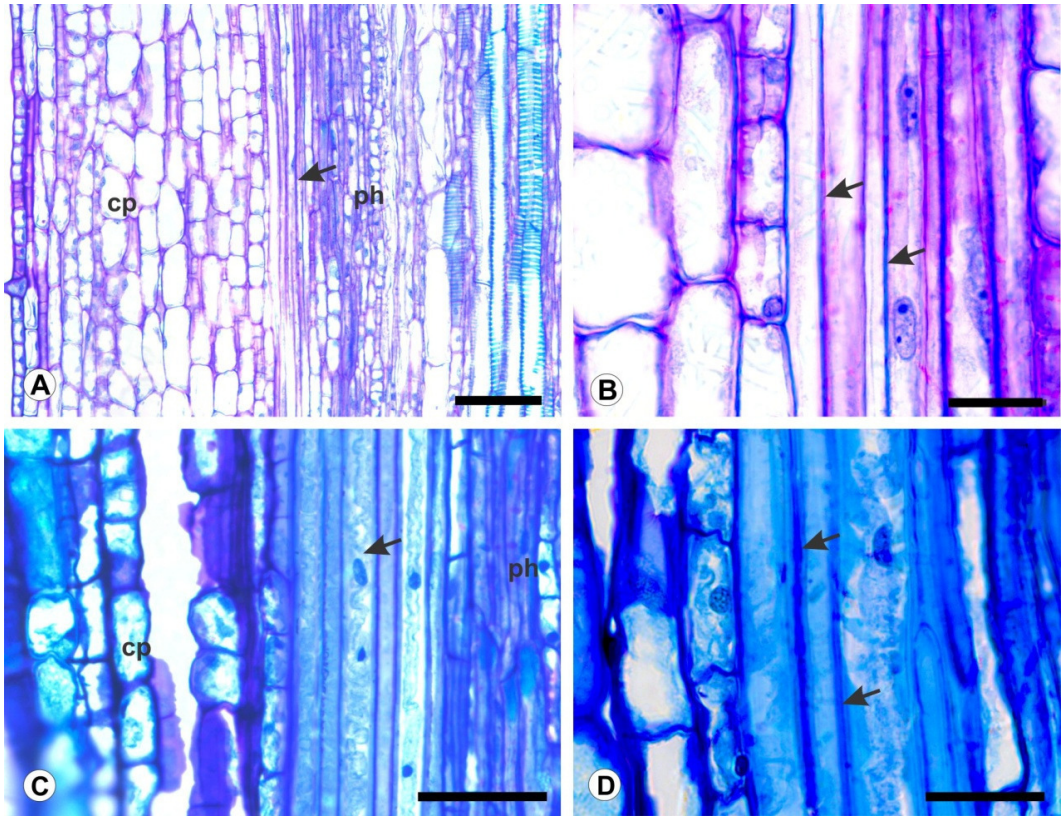

Figure 1. Articulated laticifers of the studied species of Ulmaceae (stained: Toluidine Blue). (A-B) Longitudinal sections of the stem of *Ampelocera glabra.* (A) Articulated laticifers (arrow); note the laticifers between the cortical parenchyma and phloem. (B) Laticifers with thick walls (arrow) and two nuclei, each nuclei with two nucleolus. (C-D) Longitudinal sections of the stem of *Zelkova serrata.* (C) Articulated laticifers (arrow); note the multinucleate laticifers between the cortical parenchyma and phloem. (D) Laticifers with thick walls (arrow). Scale bars: (A, C) 50 μm; (B, D) 20 μm.

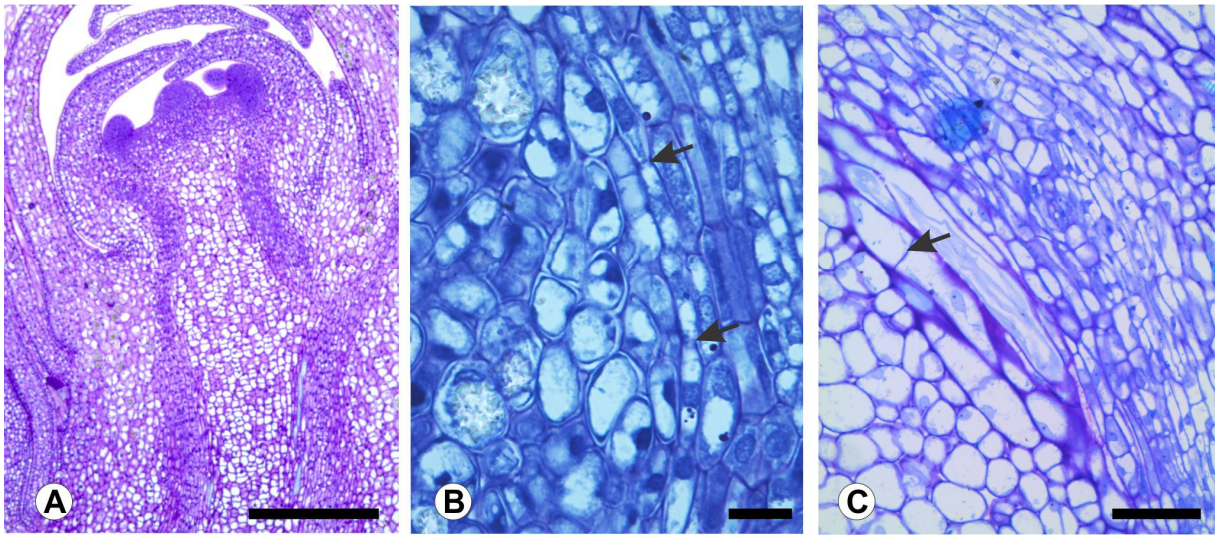

Figure 2. Origin of the laticifers of *Ampelocera glabra* (longitudinal sections stained with Toluidine Blue). (A) Flower meristem. Note undiferentiated cells close to the apex and differented cells below. (B) Note a serie of cells with disintegration of the terminal cell wall (arrow) forming the laticifer. (C) Thin terminal cell wall of the laticifer that desintegrates during its formation (arrow). Scale bars: (A) 200 μm; (B) 20 μm; (C) 50 μm.

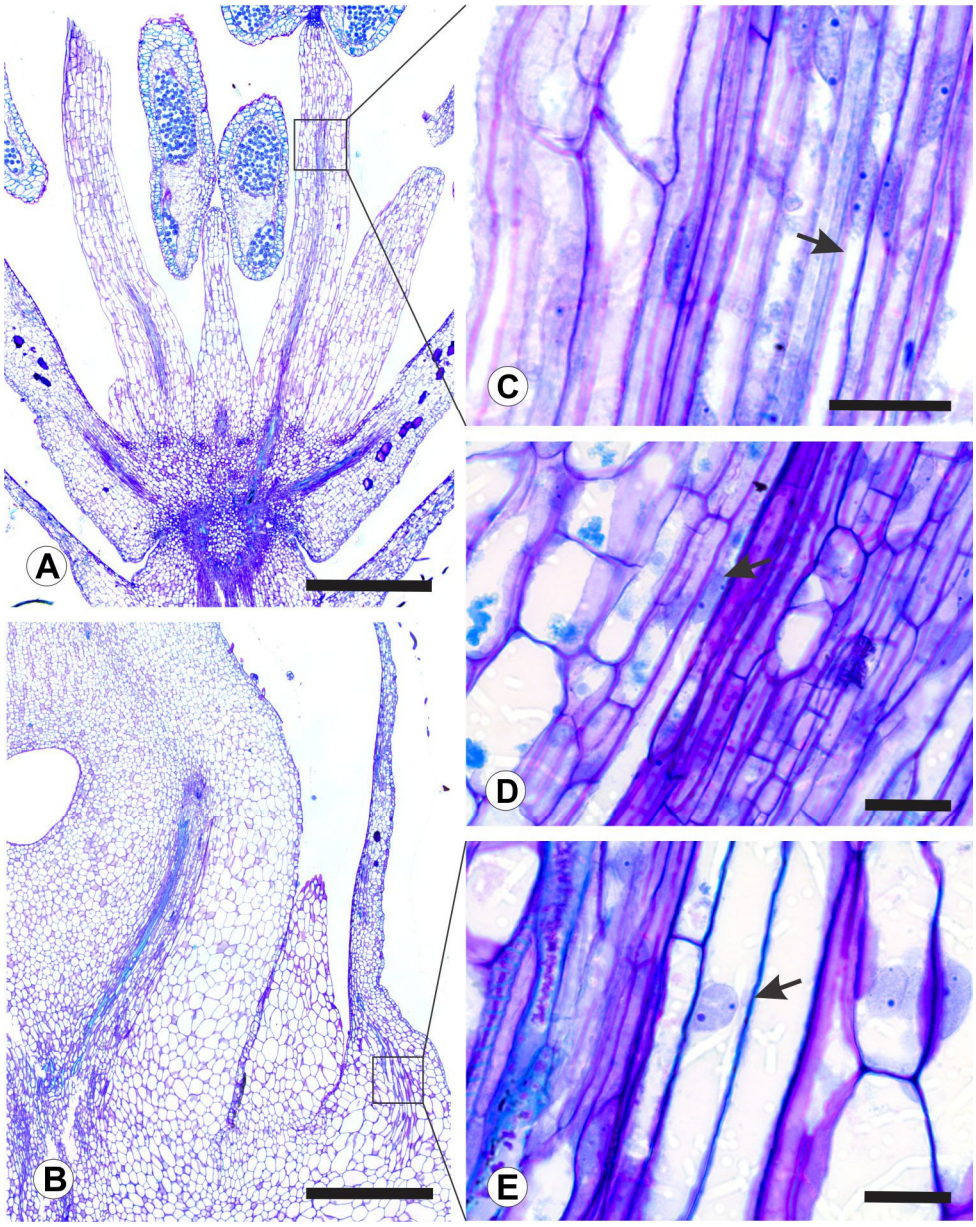

Figure 3. Laticifer distribution in the floral organs of *Ampelocera glabra* (longitudinal sections, stained: Toluidine Blue). (A) Staminate flower. (B) Pistillate flower. (C) Detail of the filament (image A) showing multinucleate laticifers. (D) Narrow laticifers in the stigma. (E) Detail of the sepal (image B) showing the laticifers. Scale bars: (A, B) 500 μm; (C, D, E) 20 μm.

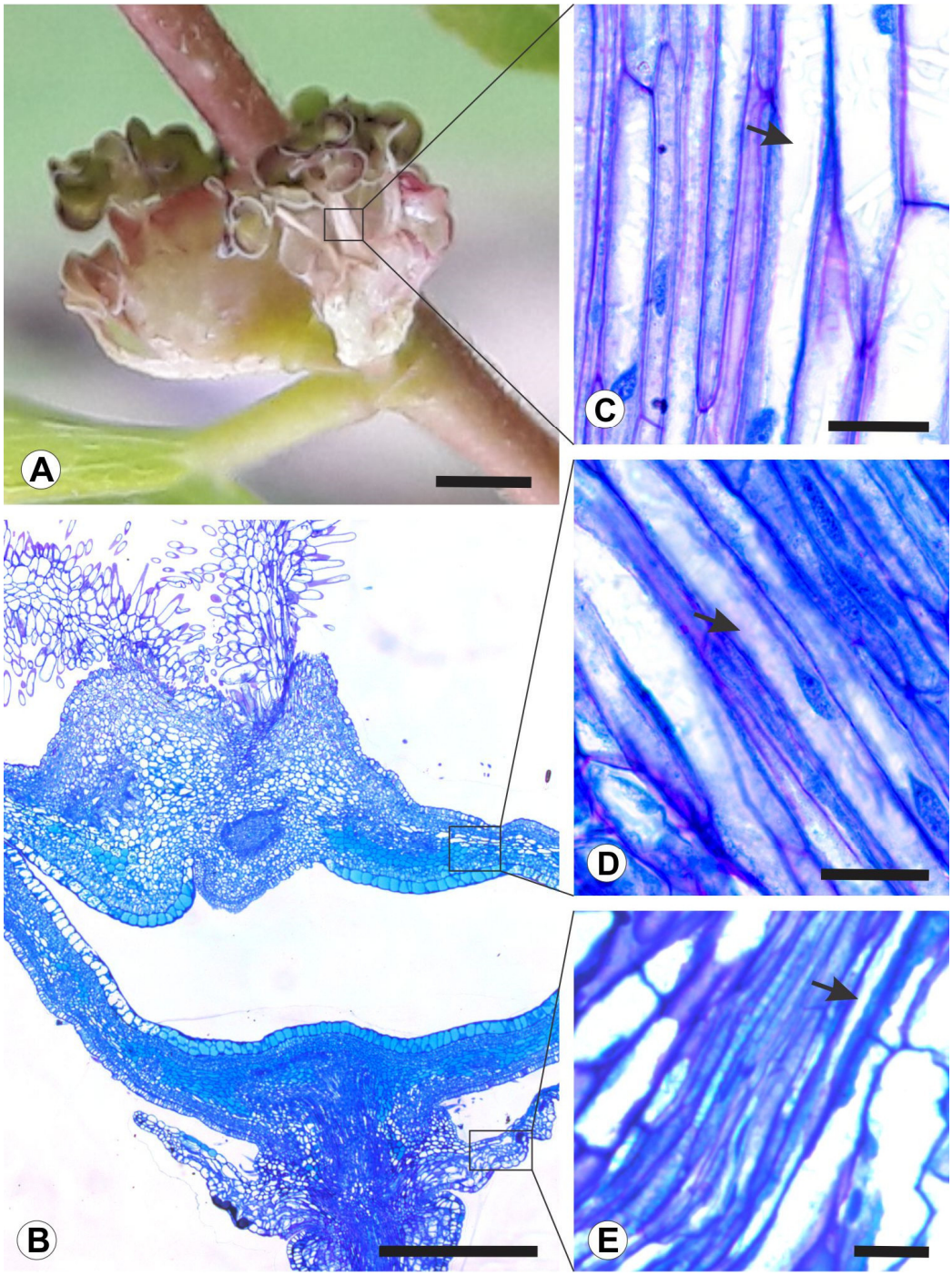

Figure 4. Laticifer distribution in the floral organs of *Zelkova serrata* (longitudinal sections, stained: Toluidine Blue). (A) Staminate flower. (B) Pistillate flower. (C) Detail of the filament (image A) showing laticifers (arrow). (D) Detail of the ovary wall (image B) showing laticifers (arrow). (E) Detail of the sepal (image B) showing narrow laticifers (arrow). Scale bars: (A, B) 500 μm; (C, D, E) 20 μm.

Histochemistry of the latex

The latex of both species seems to have the same composition (Table 2) and is apparently colorless and inconspicuous. The main components of the latex were neutral polysaccharides (positive reaction to PAS, Fig. 5A-B), and proteins (positive reaction to Xylidine Ponceau, Fig. 5C-D). Polysaccharides were found in the form of grains, which were grouped or dispersed in the latex (Fig. 5A-B). The proteins occur strongly reacting to the xylidine Ponceau test (Fig. 5C-D). Total lipids were also detected using Sudan III (Fig. 5E, F) and starch grains were detected using Lugol (Fig. 5G, H), but the lipid drops and starch grains were found in low quantity dispersed in the latex. The test performed for phenolic compounds were negative (Table 2).

Table 2. Histochemical data of the latex of *Ampelocera glabra* and *Zelkova serrata* (Ulmaceae).

Reagents	Target compound	Observed colour	*Ampelocera glabra*	*Zelkova serrata*
PAS	Polysaccharides	pink	+ (Fig. 5A)	+ (Fig. 5B)
Xylidine Ponceau	Proteins	red	+ (Fig. 5C)	+ (Fig. 5D)
Sudan III	Total lipids	orange	+ (Fig. 5E)	+ (Fig. 5F)
Lugol	Starch	black	+ (Fig. 5G)	+ (Fig. 5H)
Toluidine blue	Phenolic compounds	green	-	-
Ferric chloride	Phenolic compounds	brown	-	-

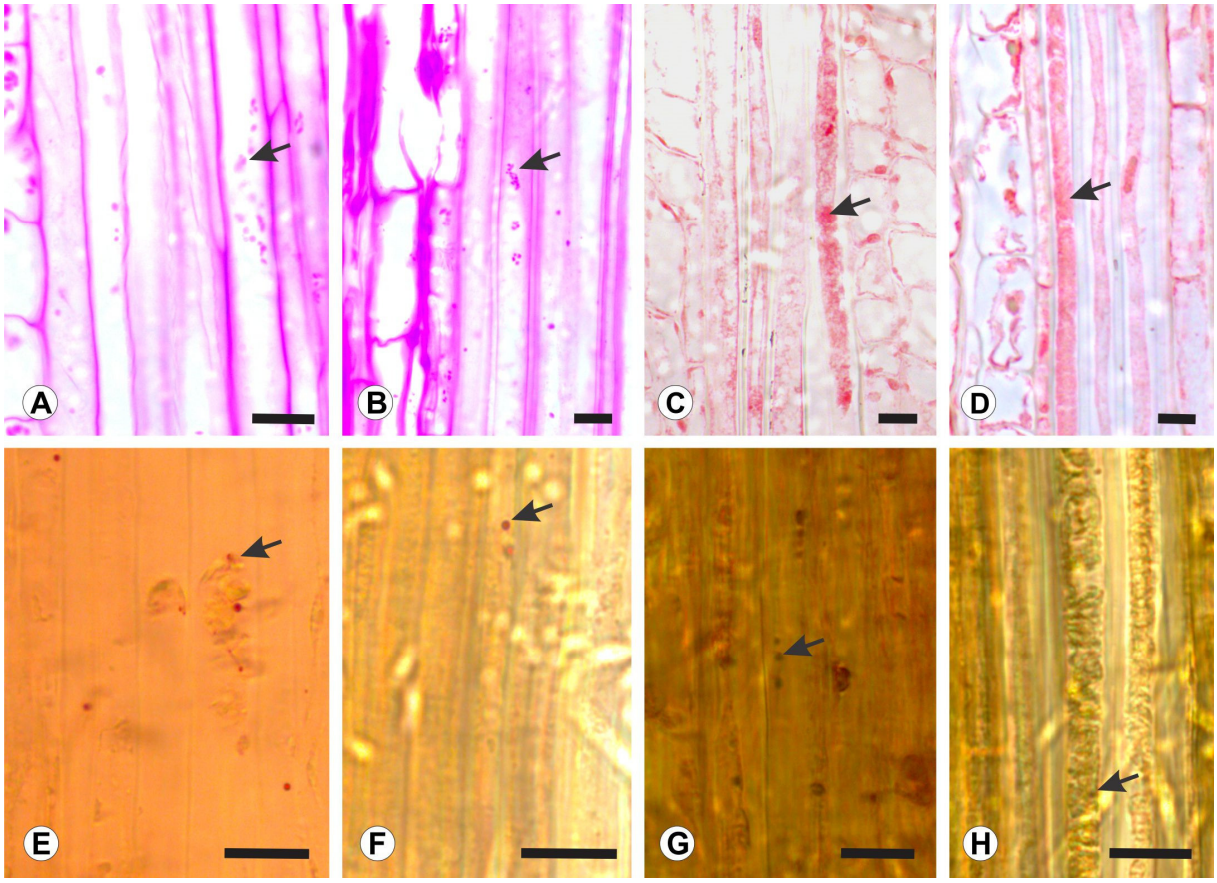

Figure 5. Histochemical tests performed in longitudinal sections of *Ampelocera glabra* (A, C, E, G) and *Zelkova serrata* (B, D, F, H) stem. (A-B) Neutral polysaccharides in the latex (positive reaction with PAS). (C-D) Proteins in the latex (positive reaction with xylidine Ponceau). (E-F) Total lipids in the latex (positive reaction with Sudan III). (G-H) Starch grains in the latex (positive reaction with Lugol). Scale bars: 10 μm.

4.5 Discussion

This is the first report of laticifers for the family Ulmaceae. Surprisingly, laticifers are widely distributed in the vegetative body of the plant and in the flowers of *Ampelocera glabra* and *Zelkova serrata*. It is interesting to emphasize that the two species have no apparent latex as other Urticalean rosids, Moraceae and Urticaceae (Fahn, 1979; Evert, 2006). Thus, anatomic analyses are extremely important in order to provide systematic and taxonomic features for Ulmaceae and for Urticalean rosids.

The laticifers of *A. glabra* and *Z. serrata* are morphologically similar to fibers, a fact that probably explains why they have gone unnoticed in anatomical studies so far (see Bechtel, 1921; Omori & Terabayashi, 1993). Their cell walls are thicker than

those of the surrounding parenchyma cells, and are composed of pectin-cellulose which seem to be deposited during the elongate of the organs.

The type (articulated), structure (thick wall) and latex composition of the laticifers found in *A. glabra* and *Z. serrata* are very similar. In Urticalean rosids, the laticifers are non-articulated in Moraceae (*Ficus pandurata* – Ramadan *et al.*, 2008; *Ficus*, *Broussonetia*, *Maclura* and *Morus* - Evert, 2006), Urticaceae (*Urtica* - Fahn, 179; Evert, 2006) and Cannabaceae (*Cannabis sativa* - Mesquita and Dias, 1984; *Humulus lupulus* - Hagel *et al.*, 2008), but they vary between branched and unbranched. They are unbranched in Cannabaceae species (*Cannabis sativa* and *Humulus lupulus*) (Meeuse, 1942; Mesquita and Dias, 1984; Evert, 2006; Hagel *et al.*, 2008) and in Urticaceae (*Urtica*). However, the laticifers have been reported to be articulated for *Ficus retusa* (Milanez 1954) and *Artocarpus kemando* (Topper and Koek-Noorman 1980) Moraceae. Thus, Urticalean rosids can showed a large variety in types of laticifers or the analyses need to be more thorough for to avoid misunderstanding.

In the Urticalean rosids the latex composition is diverse (neutral polysaccharides, proteins, phenolic compounds, lipids, alkaloids and starchs grains) (Furr & Mahlberg, 1981; Araújo *et al.*, 2014; C. R. Marinho - unpublished data), leading to a latex with different colors and densities in its species (see Mahlberg, 1993; Evert, 2006). The presence of proteins is a condition shared by all the families of the clade, whereas, surprisingly, the presence of large starch grains are exclusively found in Ulmaceae (see Furr & Mahlberg, 1981; Araújo *et al.*, 2014; Souza *et al.*, 2015).

The polysacharides and proteins found in the latex of Ulmaceae species may play a role in plant wound healing (Biesboer & Mahlberg, 1978; Souza *et al.*, 2011), an important mechanism of defence against herbivores and microorganisms (Fahn, 1979). Indeed, we found some galls in the ovary and in the floral receptacle of the studied species of Ulmaceae (personal observation), similar to *Ficus* species that suffer pressure exerted by non-pollinating fig wasps (Marinho *et al.*, 2018). Thus, the presence of laticifers in these parts of the plant could minimize the attack by galler animals.

The wide distribution of laticifers in the flowers of the studied species of Ulmaceae is remarkable, with ocurrence even in the stamens and stigma. Interesting is the presence of laticifers in the stigmatic region which is not very common, maybe due to the lack of such studies focusing on floral organs. However within the 18 species of Urticalean rosids recently studied in terms of laticifer distribution along the floral organs, only in *Castilla elastica* (Moraceae) laticifers were also found in the stigma (C. R. Marinho - unpublished data; Souza *et al.*, 2015). The ovary and stigmatic region are large in Ulmaceae and are exposed, as also observed in *Castilla elastica* (Moraceae); thus, the presence of laticifers could aid in the protection of these organs against herbivores. The performance of laticifers in plant-insect interactions deserves to be further studied in the future. We wonder whether the latex can play roles in pollination or pollen tube growth and guidance, thus not exhibiting so much toxicity as previously believed.

The discovery of laticifers in *Ampelocera glabra* and *Zelkova serrata* provides novel information about Ulmaceae, a family in which laticifers were previously considered to be absent (see Sytsma *et al.*, 2002; Judd *et al.*, 2009). Our study shows that the laticifers occur in all Urticalean rosid families (Evert, 2006; Fahn, 1979, 1999, Metcalfe 1966, Souza et al., 2015; Marinho et al., 2018) and can be probably a synapomorphy for this group.

4.6 References

APG IV. **2016**. An update of the Angiosperm Phylogeny Group classification for the orders and families of flowering plants: APG IV. *Botanical Journal of the Linnean Society* **181**: 1–20.

Araújo ND, Coelho VPM, Ventrella MC, Agra MF. **2014**. Leaf anatomy and histochemistry of three species of Ficus sect. Americanae supported by light and electron microscopy. *Microscopy and Microanalysis* **20**: 296–304.

Bechtel AR. **1921**. The Floral Anatomy of the Urticales. *American Journal of Botanical* **8**:

386–410.

Biesboer DD, Mahlberg PG. **1978**. Accumulation of Non-utilizable Starch in Laticifers of Euphorbia heterophylla and *E. myrsinites*. *Planta* **143**: 5–10.

Castelblanque L, Balaguer B, Martí C, Rodríguez JJ, Orozco M, Vera P. **2017**. Multiple facets of laticifer cells. *Plant Signaling and Behavior* **12**: 1–5.

Chae K, Lord EM. **2011**. Pollen tube growth and guidance: roles of small, secreted proteins. *Annals of Botany* 108: 627–636.

Demarco D, Castro MM. 2008. Laticíferos articulados anastomosados em espécies de Asclepiadeae (Asclepiadoideae, Apocynaceae) e suas implicações ecológicas. *Rev Bras Bot* 31:701–713.

Evert RF. 2006. *Esau's Plant Anatomy: meristems, cells, and tissues of the plant body: their structure, function, and development.* Ed. Wiley & Sons. New Jersey.

Fahn A. 1979. *Secretory tissues in plants*. London/New York/San Francisco.: Academic Press.

Fahn A. **1990**. *Plant Anatomy*. London: Butterworth-Heinemann.

Franklin-Tong V. **1999**. Signaling and the modulation of pollen tube growth. *The Plant cell* **11**: 727–38.

French JC. **1988**. Systematic occurrence of anastomosing laticifers in Araceae. *Botanical Gazette* **149**: 71–81.

Furr M, Mahlberg PG. **1981**. Histochemical analyses of laticifers and glandular trichomes in *Cannabis sativa*. *Journal of Natural Products* **44**: 153–159.

Gotelli MM, Lattar EC, Zini LM, Galati BG. **2017**. Style morphology and pollen tube pathway. *Plant Reproduction* **30**: 155–170.

Guérin P. **1923**. Les Urticées: cellules à mucilage, laticifères et canaux sécréteurs (suite et fin). *Bulletin de la Société Botanique de France* **70**: 255–263.

Hagel JM, Yeung EC, Facchini PJ. **2008**. Got milk ? The secret life of laticifers. *Trends in Plant Science*: 1360–1385.

Jensen WE. **1962**. *Botanical histochemistry: Principles and practice.* San Francisco: W. H. Freeman and Co.

Jiang L, Yang SL, Xie LF, *et al.* 2005. VANGUARD1 encodes a pectin methylesterase that enhances pollen tube growth in the Arabidopsis style and transmitting tract. *The Plant Cell* **17**: 584–596.

Johansen DA. **1940**. *Plant Microtechnique*. New York: McGraw-Hill Book Co. Inc.

Judd WS, Campbell CS, Kellogg EA, Stevens PF, Donoghue MJ. **2009**. *Sistemática vegetal. Um enfoque filogenético*. Porto Alegre, RS: Artmed.

Kraus JE, Arduin M. **1997**. *Manual básico de métodos em morfologia vegetal*.

Lillie RD. **1965**. *Histopathologic technic and practical histochemistry*. New York: McGraw-Hill Book Company.

Lewinsohn TM. 1991. The geographical distribution of plant latex. *Chemoecology* 2:64-68.

Mahlberg PG. **1993**. Laticifers: An Historical Perspective. *Botanical Review* **59**: 1–23.

Marinho CR, Pereira RAS, Peng Y-Q, Teixeira SP. **2018**. Laticifer distribution in fig inflorescence and its potential role in the fig-fig wasp mutualism. *Acta Oecologica* 90: 160-167.

Meeuse ADJ. **1942**. A study of intercellular relationships among vegetable cells with special reference to sliding growth'' and to cell shape. *Recueil Trav. Bot. Neerl* **38**: 18–140.

Mesquita JF, Dias JDS. **1984**. Ultrastructural and cytochemical study of the laticifers of *Cannabis sativa* L. *Bol. Soc. Brot.* **57**: 337–356.

Metcalfe CR. **1966**. Distribution of Latex in the Plant Kingdom. *Economic Botany* **21**: 115–127.

Mahlberg PG. 1993. Laticifers: an historical perspective. *Bot Rev* 59: 1-23.

Milanez FR. 1954. Sobre os laticíferos foliares de Ficus retusa. *Rodriguésia* 28-29:159-192.

Neubig K, Herrera F, Manchester SR, Abbott JR. 2012. Fossils, biogeography and dates in an expanded phylogeny of Ulmaceae. Botany 2012: *Annual Meeting of the Botanical Society of America in Columbus,* Ohio, USA

O'Brien TP, Feder N, McCully ME. **1964**. Polychromatic staining of plant cell walls by

toluidine blue O. *Protoplasma* **59**: 368–373.

Omori Y, Terabayashi S. **1993**. Gynoecial vascular anatomy and its systematic implications in Celtidaceae and Ulmaceae (Urticales). *Journal of Plant Research* **106**: 249–258.

Pearse AGE. **1985**. *Histochemistry: theoretical and applied.* Edinburgh: C. Livingstone.

Ramadan MA, Ahmad AS, Nafady AM, Mansour AI. 2008. Macro and micromorphology studies of the leaf, stem and stem bark of *Ficus pandurata* Hance. cultivated in Egypt. Bulletin of Pharmaceutical Sciences, Assiut University 31:1-28.

Rudall PJ. **1987**. Laticifers in Euphorbiaceae a conspectus. *Botanical Journal of the Linnean Society* **94**: 143–163.

Souza DP, Freitas CDT, Pereira DA, *et al.* 2011. Laticifer proteins play a defensive role against hemibiotrophic and necrotrophic phytopathogens. *Planta* **234**: 183–193.

Souza CD, Pereira RAS, Marinho CR, Kjellberg F, Teixeira SP. **2015**. Diversity of fig glands is associated with nursery mutualism in fig trees. *American Journal of Botany* **102**: 1–14.

Sytsma KJ, Morawetz J, Pires JC, *et al.* 2002. Urticalean Rosids: Circumscription, Rosid ancestry, and phylogenetics based on rbcL, trnL-F, and ndhF sequences. *Am J Bot* **89(9)**: 1531-1546.

Vidal BC. **1970**. Dichroism in collagen bundles stained with xylidine-Ponceau 2R. *Annales d´Histochimie* **15**: 289-296.

Wolters-Arts M, Lush WM, Mariani C. **1998**. Lipids are required for directional pollen-tube growth. *Nature* **392**: 818–821.

Zinkl GM, Zwiebel BI, Grier DG, Preuss D. **1999**. Pollen-stigma adhesion in Arabidopsis: a species-specific interaction mediated by lipophilic molecules in the pollen exine. *Development (Cambridge, England)* **126**: 5431–5440.

"As pessoas se convencem
De que a sorte me ajudou
Mas plantei cada semente
Que o meu coração desejou."

Nando - Aldir Blanc

CHAPTER 5: 'EXPANDING THE LATICIFER KNOWLEDGE IN CANNABACEAE:

DISTRIBUTION, MORPHOLOGY AND LATEX COMPOSITION'

Chapter 5: Expanding the laticifer knowledge in Cannabaceae: distribution, morphology and latex composition

5.1 Abstract

Cannabaceae is a known family because of the production of cannabinoids in laticifers and glandular trichomes in *Cannabis sativa*. Laticifers are secretory structures whose secreted product is denominated latex. In addition to *Cannabis sativa* laticifers were only reported for *Humulus lupulus* in Cannabaceae. Thus, the objectives of the present study were to check the occurrence and distribution of the laticifers in the stem, leaf and floral organs of four species of Cannabaceae (*Cannabis sativa*, *Celtis pubescens, Pteroceltis tatarinowii* and *Trema micrantha*), to detail the laticifer morphology and to identify the main classes of substances of the latex. The cellulase and pectinase activities were also analysed. Samples of shoot apices, stems, leaves and flowers were processed for anatomical, histochemical, ultrastructural and cytochemical analyses. Laticifers are articulated in all species. They occur in all vegetative organs (stem and leaves) and in almost all floral organs (pedicel, sepal, filament, ovary, style and stigma). They are thick-walled, multinucleate, with a large vacuole and a peripheral cytoplasm. The cytoplasm is composed of mitochondria, endoplasmic reticulum, plastids, dictyosomes and ribosomes. Plastids contain starch grains, oil drops and electron-dense material. Proteins, lipids and polysaccharides are detected in the latex. Phenolic compounds are exclusively found in *C. sativa* and terpenes in *C. pubescens* and *T. micrantha.* The endoplasmic reticulum is probably associated with the formation of vacuoles, the production of phenolics in *C. sativa* and of proteins in *C. pubescens* and *T. micrantha*. The pectinase and cellulase activities promot the dissolution of the terminal cell wall and the laticifers also elongate with the growth of the plant. In conclusion, the morphology and ontogeny showed that the laticifers in Cannabaceae are articulated and similar among the species corroborating the insertion of *Celtis, Pteroceltis* and *Trema* in Cannabaceae. The wide distribution of laticifers in the floral organs expands the knowledge about the laticifers and suggests that, despite the unclear presence of latex (colorless and low quantity) in the species, they have an important function in the protection of floral organs in Cannabaceae.

Keywords: *Canabis sativa*, cellulase, flowers, latex, pectinase, Urticalean rosids.

5.2 Introduction

The secretory structures or glands of Cannabaceae, especially of *Cannabis sativa* L., have aroused the interest of researchers because they are responsible for the production of a large amount of secondary metabolites of medicinal importance (Furr and Mahlberg 1981; Kim and Mahlberg 1991, 1997; Williamson and Evans 2000; Happyana et al. 2013). The latex of *C. sativa*, for example, is rich in cannabinoids and alkaloids (Furr and Mahlberg 1981), substances that have the medicinal potential to relieve symptoms related to the treatment of cancer, AIDS and sclerosis (Ashton 2001; Honório et al. 2006; Hill et al. 2010). The latex is produced in laticifers, internal secretory structures that form organized systems (Fahn 1990), composed of one specialized cell (non-articulated type) or several cells forming a tube (articulated type) that produce an emulsion of many small particles dispersed in a liquid with a different refractive index (Fahn 1979).

In Cannabaceae, laticifers have been found only in *Humulus lupulus* L. (Hagel et al. 2008) and *Cannabis sativa* (Furr and Mahlberg 1981; Mesquita and Dias 1984), a small number of species if we consider that Cannabaceae comprises ca. 109 species and 10 genera (Yang et al. 2013). The laticifers of *Cannabis sativa* (Furr and Mahlberg 1981; Mesquita and Dias 1984) and *Humulus lupulus* (Hagel et al. 2008) are non-articulated and unbranched.

Cannabaceae belongs to the Urticalean rosid clade that also comprises Moraceae, Ulmaceae and Urticaceae (Sytsma et al. 2002). In Cannabaceae and Moraceae, laticifers have been found throughout the whole plant body, unlike Urticaceae, in which the records indicate that they are restricted to the bark (Metcalfe 1966, Fahn 1979). Until recently, there were no records of laticifers for Ulmaceae. Thus, some authors consider that the laticifer distribution and occurrence constitute synapomorphies for these families (Judd et al. 2009). Another important issue related to laticifers is their classification among the Urticalean rosids. In Cannabaceae and Urticaceae, they were classified as non-articulated and unbranched (Metcalfe 1966,

Fahn 1979). In Moraceae, the classification is even more confusing. Some authors (Van Veenendaal and Den Outer 1990; Machado and Santos 2004; Quintanar et al. 2004; Jacomassi et al. 2007, 2010; Kitajima et al. 2012) have reported non-articulated branched laticifers, while others have reported articulated anastomosing laticifers (Milanez 1954; Topper and Koek-Noorman 1980) and non-articulated unbranched laticifers (Ramadan et al. 2008) depending on the species and organ analysed. The lack of studies on laticifer origin can be the cause of misinterpretations of the laticifer types; therefore, ontogenic studies are essential to a better laticifer classification (Fahn 1979, 1990). Even the latex exhibits different colors depending on the family, such as yellow-brown or colorless latex in Cannabaceae (Mahlberg 1993; Evert 2006), milky latex in Moraceae and colorless latex in Urticaceae (Evert 2006). Thus, there appears to be a diversity of types of laticifers and of latex in the Urticalean rosids that can be confirmed by further studies.

Therefore, the objectives of the present study were to check the occurrence and origin of laticifers, to analyse their morphology and distribution, and the main classes of compounds of the latex in four species of four different genera of Cannabaceae {*Cannabis sativa* L., *Celtis pubescens* (Kunth) Spreng., *Pteroceltis tatarinowii* Maxim. and *Trema micrantha* (L.) Blume}. The cytochemical localization of cellulase and pectinase was also tested to better understand the formation of laticifers. We intend to contribute new data to help reviewing the synapomorphies established for the Urticalean rosid clade.

5.3 Materials and methods

Samples of shoot and floral apices, stems, leaves and flowers were obtained in the field or from herbarium specimens (Table 1). Vouchers were deposited in the SPFR herbarium (FFCLRP / USP) and in the CGMS herbarium (INBIO/UFMS).

The samples collected in the field were fixed in buffered formalin (Lillie 1965) or in formalin – acetic acid – ethanol (70% FAA) for 48 h (Johansen 1940). The

herbarium samples were rehydrated in heated distilled water and then treated overnight with 2% KOH (Smith and Smith 1942). Both types of samples were dehydrated through an ethanolic series, embedded in histological resin (Historesin - Leica), and sectioned in longitudinal planes (5 μm), using a rotary microtome (Leica RM 2245). The sections were stained with 0.1% Toluidine Blue in phosphate buffer, pH 6.8 (O'Brien et al. 1964), mounted in immersion oil, and analysed under a light microscope.

Stem samples were also free-handed sectioned (in fresh material for *T. micrantha* and *C. pubescens* and fixed material for *C. sativa* and *P. tatarinowii*) and the main compounds of the latex were investigated using the following reagents: Sudan III for total lipids (Pearse 1985), Lugol for starch (Johansen 1940), ferric chloride for phenolic compounds (Johansen 1940) and Wagner's reagent (Furr and Mahlberg 1981) for alkaloids. Material embedded in historesin was stained with: Toluidine Blue O for detection of phenolic compounds (O'Brien et al. 1964), period acid-Schiff (PAS) for neutral polysaccharides (Jensen 1962), ruthenium red for pectins (Johansen 1940) and xylidine Ponceau for proteins (Vidal 1970). Terpenes and tannins were detected in *Celtis pubescens* and *Trema micrantha* using fresh samples cut by free hand. The Nadi reagent (David and Carde 1964) was employed for terpenes and vanillin hydrochloric acid was employed for tannins (Mace and Howell 1974). Photomicrographs were obtained using a Leica DFC 295 digital camera coupled to a Leica DM 5000 B light microscope.

For the ultrastructural analysis, small pieces of the shoot apex of *Celtis pubescens* and *Trema micrantha* were fixed in Karnovsky's solution (Karnovsky 1965) for 24 h, post-fixed in 1% osmium tetroxide in 0.1 M phosphate buffer, pH 7.2, washed in distilled water, dehydrated and embedded in Araldite. Sections cut with a Leica Reichert Ultracut S ultramicrotome at 60–70 nm were collected on copper grids and contrasted with 2% uranyl acetate and lead citrate for 15 min. Transmission electron micrographs were obtained using a Jeol 100CXII instrument.

Cytochemical localization of cellulase and pectinase at the ultrastructural level was performed for *Celtis pubescens* and *Trema micrantha.* The shoot apices were collected, fixed in Karnovsky's solution (Karnovsky 1965) for 24 h, washed 10 times in 0.1 M phosphate butter, pH 7.2, and stored overnight in the buffer at 4º C. For testing the cellulase activity, the samples were incubated in 0.05 M citrate buffer, pH 4.8, with 0.02% carboxymethylcellulase for 10 minutes at room temperature (Bal 1974). For pectinase activity, the samples were incubed in 0.1 M sodium acetate buffer, pH 5.0, with 0.5% pectin for 20 minutes at room temperature (Allen and Nessler 1984). Control samples were incubated in buffer respective of each test but without carboxymethylcellulase and pectin. The both samples treated and control samples were transferred to Benedict's reagent heated to 80º C for 10 minutes, washed in 0.1 M phosphate buffer and post-fixed in 1% osmium tetroxide for 2 h. Then, the samples continued to be processed using the usual method for ultrastructural analysis.

Table 1 Information about the Cannabaceae species sampled.

Species	Habitum	Sexual expression	Sample	Voucher
Cannabis sativa	herb	dioecious	Herbarium ESA, Piracicaba, SP, Brazil.	G.M Tenório nº 5 (123034), G.A Ogasawara nº 20 (119653), O. Marilia nº 13433 (68853), J.A. Zandoval nº 102 (13268) (ESA).
			Herbarium IAC, Campinas, SP, Brazil.	A.S. Lima s/nº (24827), A.P. Viégas s/nº (3881), C. Pacheco s/nº (18681) (IAC).
Celtis pubescens	shrub or tree	monoecious	USP, campus Ribeirão Preto, SP, Brazil.	F.M. Leme nº 98 (16046) and 107 (16047) (SPFR).
Pteroceltis tatarinowii	tree	monoecious	Botanical Garden, University of Vienna, Vienna, Austria.	F.M. Leme nº128 (CGMS).
Trema micrantha	tree	dioecious	USP, campus Ribeirão Preto, SP, Brazil.	F.M. Leme nº 92 (15959), 93 (15960). 94 (15957), 97 (16306) and 101 (15958) (SPFR).

5.4 Results

Laticifer Distribution, Origin and Morphology

Celtis pubescens, Pteroceltis tatarinowii and *Trema micrantha* exhibit laticifers in all the organs analysed (Fig. 1, Table 2), such as leaf blade, petiole, stem, pedicel, sepal, filament, ovary, style and stigma (Fig. 1a-h, Table 2), while in *Cannabis sativa* they are not found in sepals of pistillate flowers or in stamens of staminate flowers (Fig. 1a, b, Table 2) but are found in the large bract that covers the pistillate flowers (Fig. 1b).

Laticifers are located externally to the phloem (Fig. 2) and are organized into a set of three or more laticifers (Figs. 2 and 3). The laticifer are articulated begins as a serie of three or more cells in the apex (Fig. 3a, b) with the disintegration of the terminal cell wall (Fig. 3c, d). Then, it elongates with the growth of the plant between the phloem and parenchyma cells (Fig. 3b), or among other laticifers. The laticifers have thickened cell walls composed of pectin-cellulose (Figs. 2, 3b, 4e, f), and usualy possess nuclei of fusiform shape (Fig. 2).

Histochemistry of the latex

Under the microscope, the natural color of the latex is yellowish in *Cannabis sativa* (Fig. 4b) and colorless in the other species (Fig. 4a).

The latex of the four species is similar in chemical composition, except for the presence of phenolic compounds, terpenes and large starch grains (Table 3). It reacted positively for proteins with xylidine Ponceau (Fig. 4c, d), for neutral polysaccharides with PAS (Fig. 4e, f) and for total lipids with Sudan III (Fig. 4g, h). Large starch grains were detected with Lugol (Fig. 4a, b) in the latex of *C. pubescens, P. tatarinowii* and *Trema micrantha*, but not in *C. sativa.* Terpenes were detected with Nadi Reagent in the fresh samples of latex in *C. pubescens* and *T. micrantha* (Fig. 5c, d). No tannins were found for these species with vanillin hydrochloric acid (Table 3). Phenolic

compounds were only detected in the latex of *C. sativa* using ferric chloride (Fig. 5e) and Toluidine Blue (Fig. 5f).

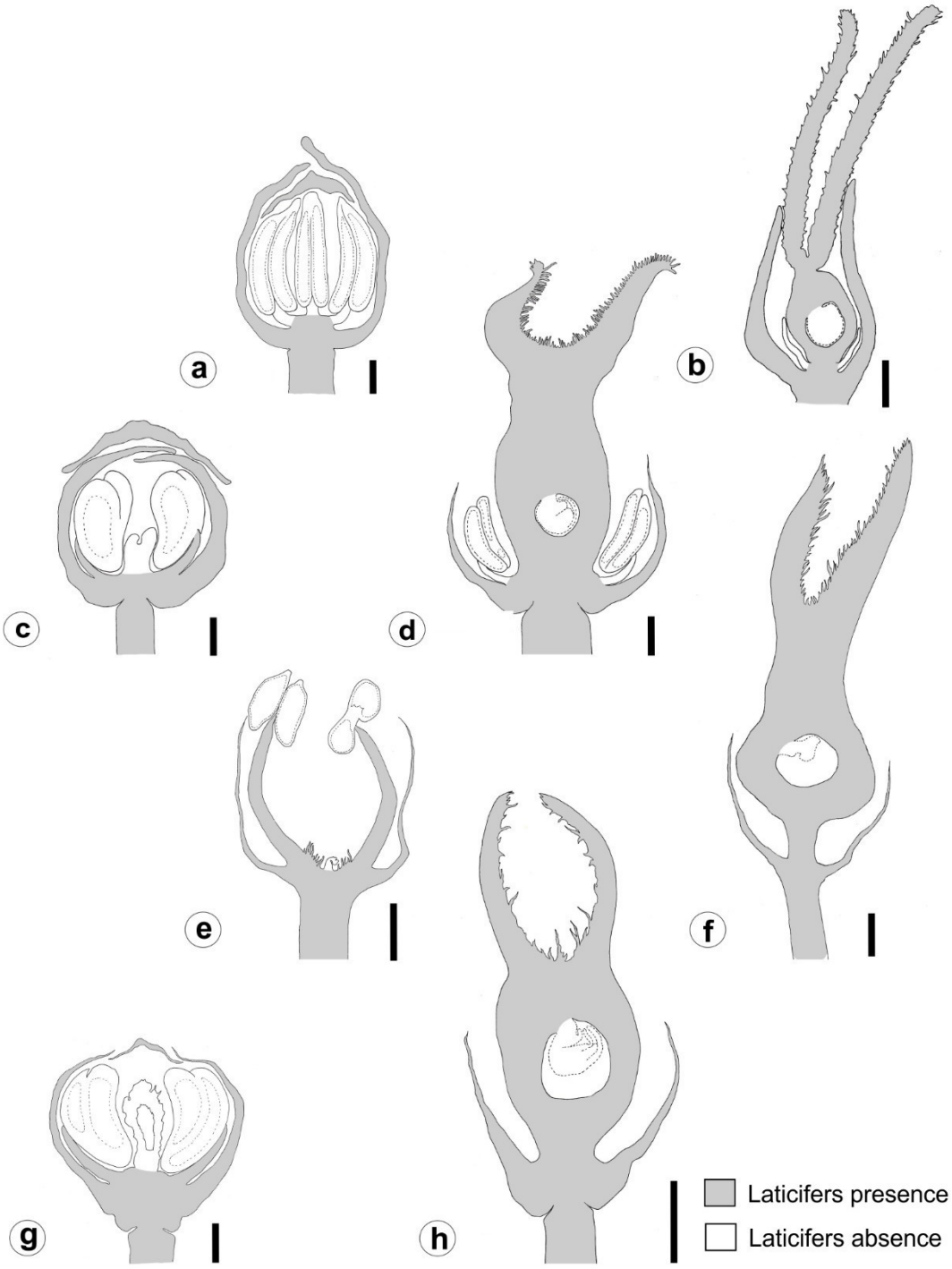

Fig. 1 Schematic drawings of longitudinal sections of flowers of Cannabaceae species showing the wide distribution of laticifers (hatched). **a, b** *Cannabis sativa*: staminate (a) and pistillate flowers (b). **c, d** *Celtis pubescens:* staminate (c) and pistillate flowers (d). **e, f** *Pteroceltis tatarinowii*: staminate (e) and pistillate flowers (f). **g, h** *Trema micrantha:* staminate (g) and pistillate flowers (h). Scale bars: (a) 1 mm; (b) 200 μm; (c, d) 500 μm; (e, f) 500 μm; (g, h) 500 μm.

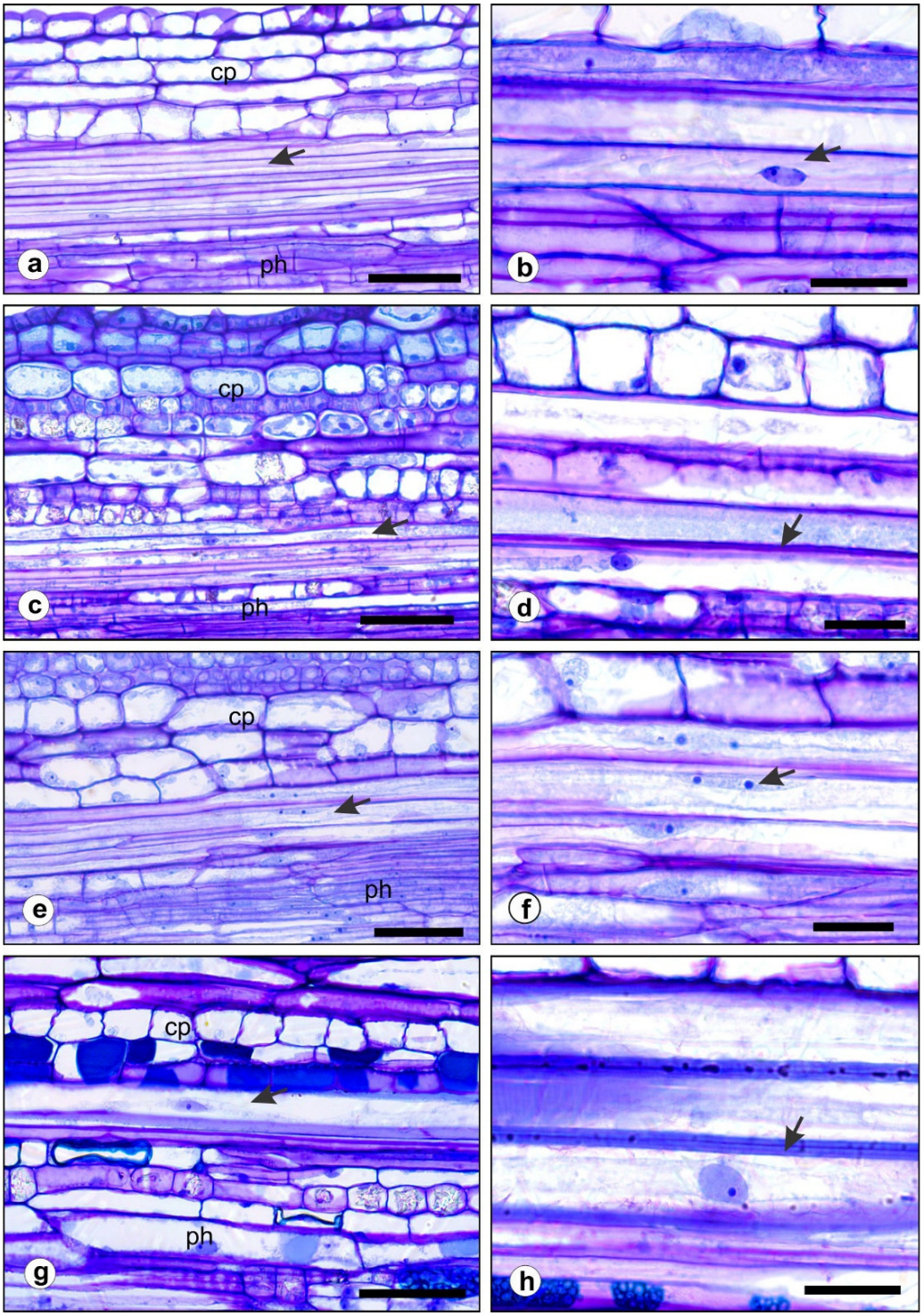

Fig. 2 Articulated laticifers of Cannabaceae species (longitudinal sections of the stem stained with Toluidine Blue). **a** Laticifers of *Cannabis sativa* (arrow) located between the cortical parenchyma and phloem. **b** Detail showing two laticifers; the arrow shows a nucleus. **c** Laticifers of *Celtis pubescens* (arrow) arranged into a set and located between the cortical parenchyma and phloem. **d** Detail of the laticifers showing a thick wall (arrow). **e** Multinucleate laticifers (arrow) of *Pteroceltis tatarinowii* located between the cortical parenchyma and phloem. **f** Detail showing laticifers with a nucleus and its nucleoli (arrow). **g** Laticifers of *Trema micrantha* (arrow) located between the cortical parenchyma and the phloem. **h** laticifers with a thick wall (arrow). Abbreviations: cp, cortical parenchyma; ph, phloem. Scale bars: (a, c, e, g) 50 μm, (b, d, f, h) 20 μm.

Table 2 Distribution of laticifers in the vegetative and floral organs of Cannabaceae species.

	Organ	*Cannabis sativa*	*Celtis pubescens*	*Pteroceltis tatarinowii*	*Trema micrantha*
	Stem	+	+	+	+
	Leaf	+	+	+	+
Pistillate flower	Pedicel	+	+	+	+
	Sepal	-	+	+	+
	Ovary	+	+	+	+
	Stigma	+	+	+	+
Staminate flower	Pedicel	+	+	+	+
	Sepal	+	+	+	+
	Filament	-	+	+	+
	Anther	-	-	-	-

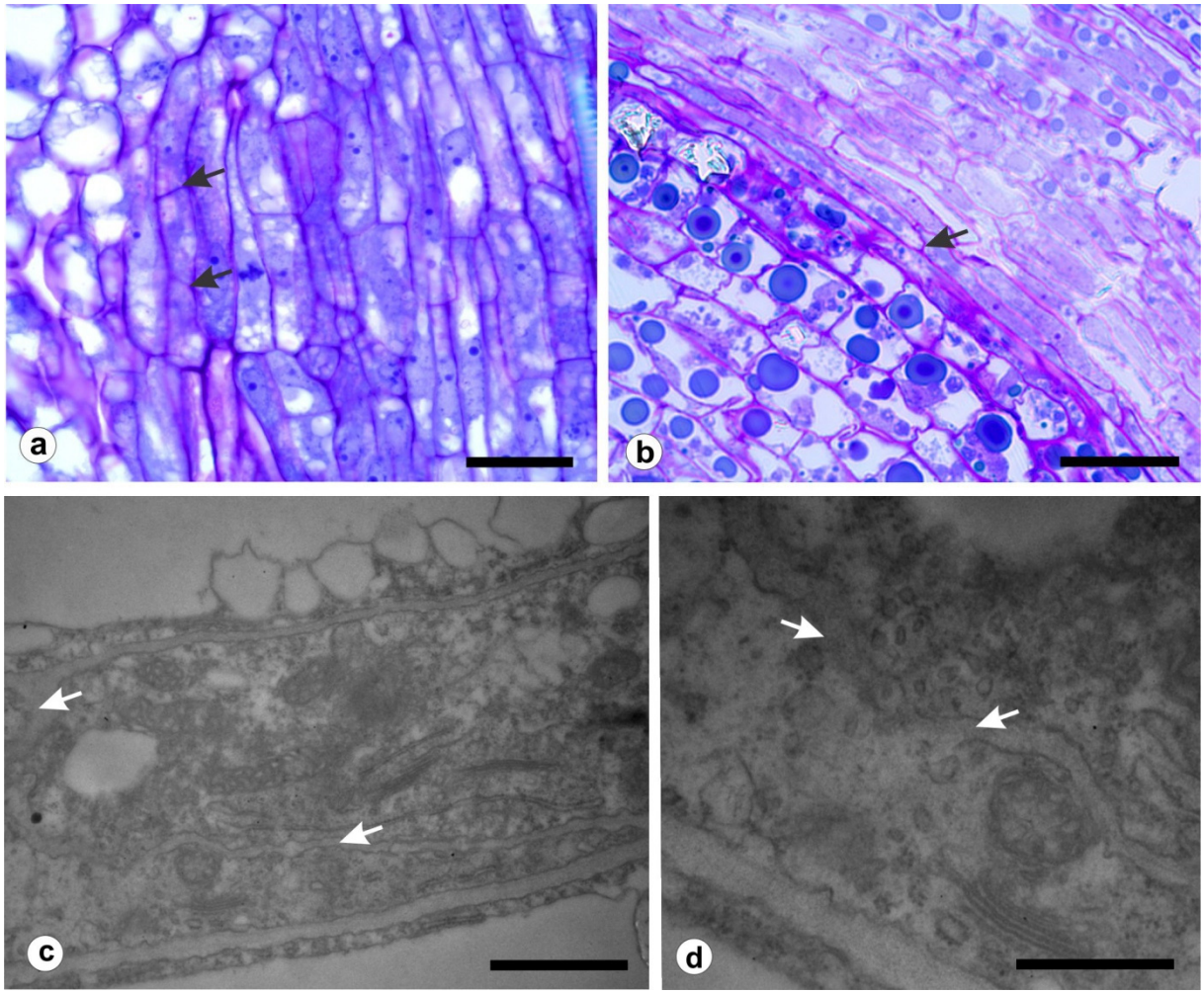

Fig. 3 Origin of the laticifers of Cannabaceae (longitudinal sections; a-b stained with Toluidine Blue; c-d transmission microscope). **a** Vegetative meristem of *Cannabis sativa*. Note a serie of laticifers cells with terminal cell wall still present (arrow). **b** Laticifers of *Celtis pubescens* that elongate with the growth of the plant. **c** Laticifers of *Celtis pubescens* showing the thin terminal cell wall. **d** Disintegration process of the cell wall for to form the articulated laticifer. Scale bars: (a-b) 20 µm, (c) 2 µm, (d) 1 µm.

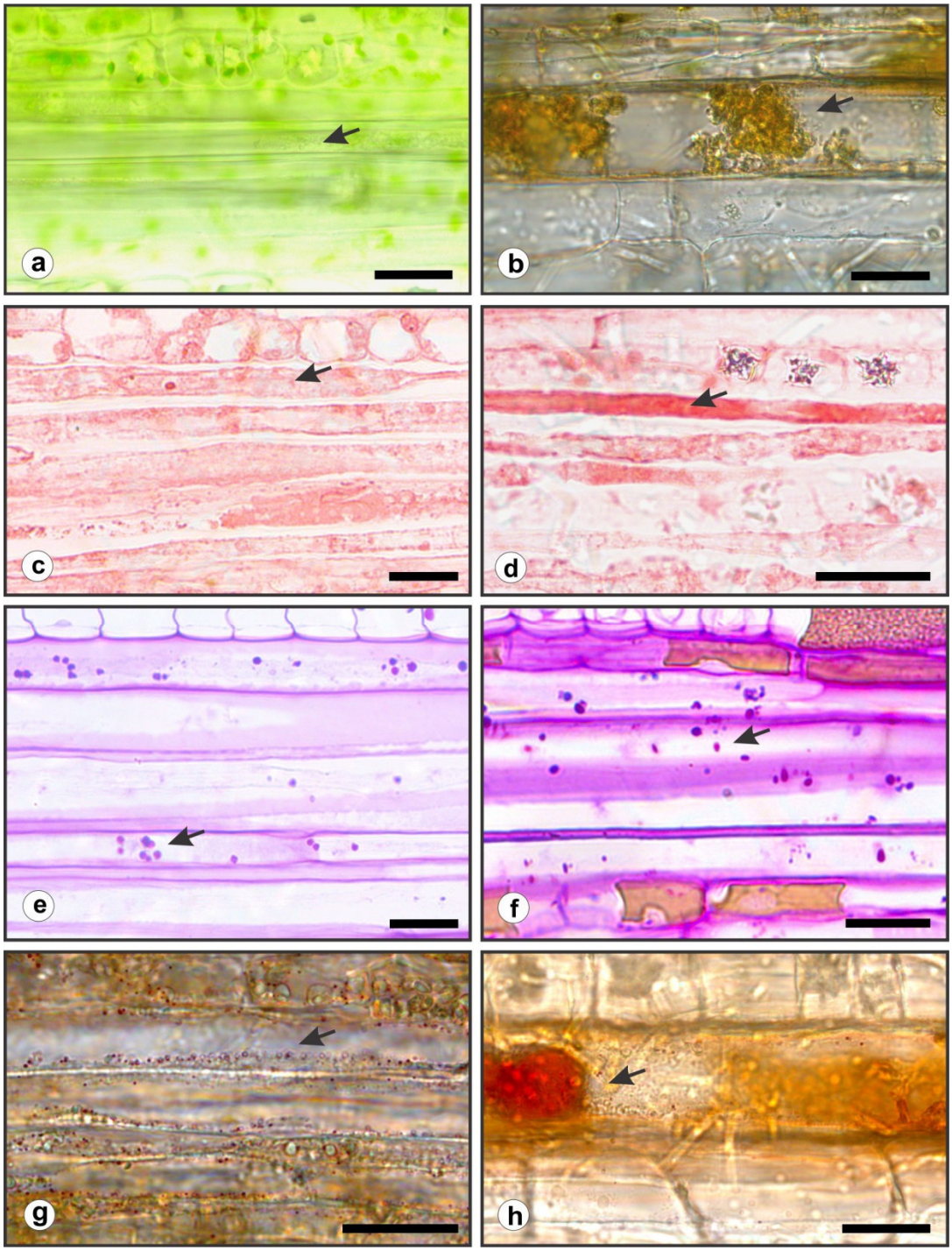

Fig. 4 Histochemical analyses of the latex of Cannabaceae species (longitudinal sections). **a** Laticifers of *Celtis pubescens* without staining; note the colorless latex. **b** Laticifers of *Cannabis sativa* without staining; note the yellowish latex. **c** Positive reaction of the latex of *Pteroceltis tatarinowii* for proteins (stain: xylidine Ponceau). **d** Positive reaction of the latex of *Celtis pubescens* for proteins (stain: Xylidine Ponceau). **e** Positive reaction of the latex of *Trema micrantha* for neutral polysaccharides (stain: PAS). **f** Positive reaction of the latex of *Cannabis sativa* for neutral polysaccharides (stain: PAS). **g** Positive reaction of the latex of *Pteroceltis tatarinowii* for total lipids (stain: Sudan III). **h** Positive reaction of the latex of *Cannabis sativa* for total lipids (stain: Sudan III). Scale bars: 20 μm.

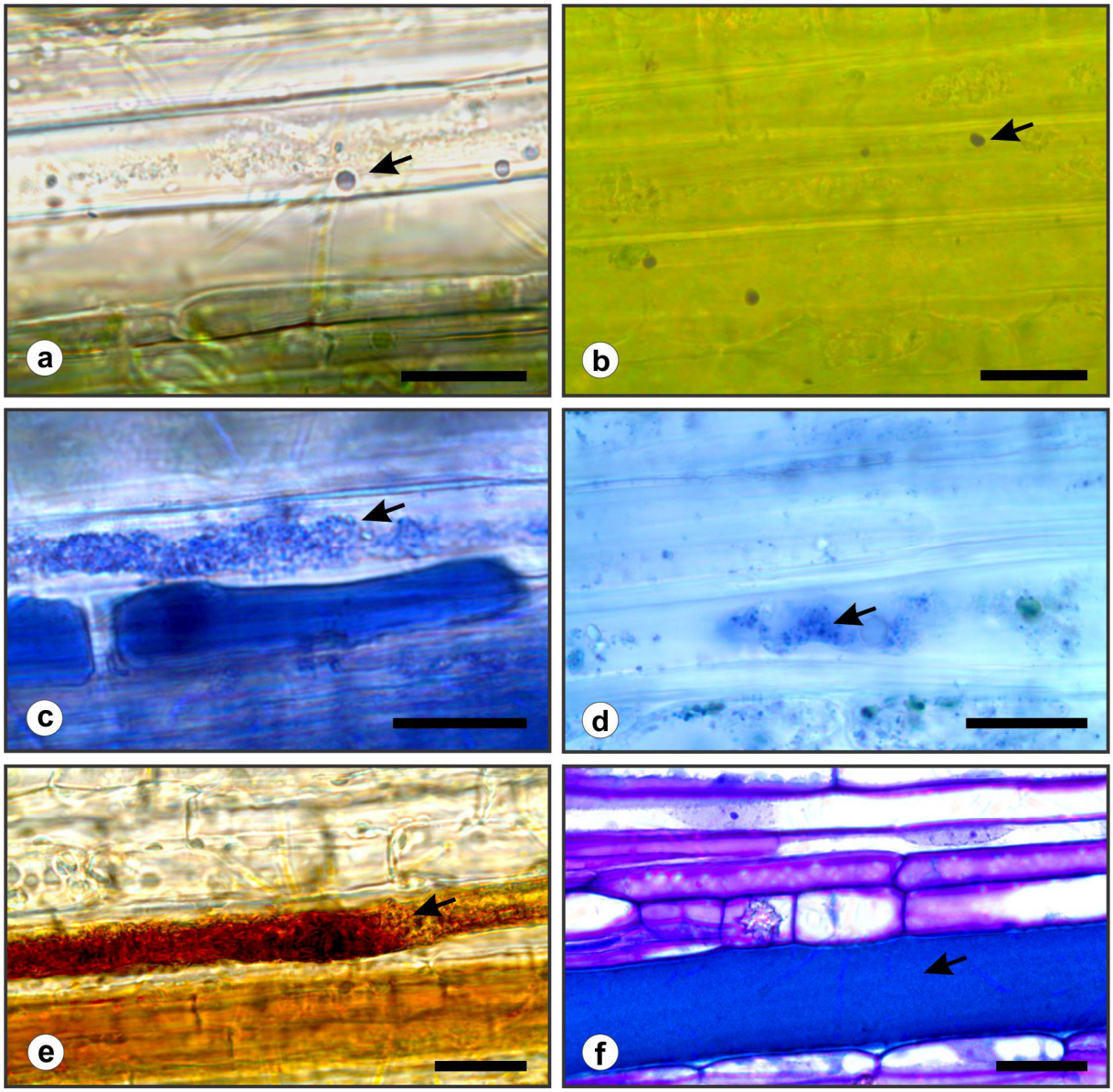

Fig. 5 Histochemical analyses of the latex of Cannabaceae species (longitudinal sections). **a** Positive reaction of the latex of *Trema micrantha* for starch (stain: lugol). **b** Positive reaction of the latex of C*eltis pubescens* for starch (stain: lugol). **c** Positive reaction of the latex of *Trema micrantha* for terpenes (stain: Nadi reagent). **d** Positive reaction of the latex of C*eltis pubescens* for terpenes (stain: Nadi reagent). **e, f** Positive reactions of the latex of *Cannabis sativa* for phenolic compounds with ferric chloride (e) and Toluidine Blue (f). Scale bars: 20 μm.

Table 3 Histochemical data obtained for the stem latex of Cannabaceae species. Simbols: (+) presence; (-) aubsence; (?) no analysed.

Reagents	Target compound	*Cannabis sativa*	*Celtis pubescens*	*Pteroceltis tatarinowii*	*Trema micrantha*
PAS	Total polysaccharides	+	+	+	+
Lugol	Amyloplast	-	+	+	+
Sudan III	Total lipids	+	+	+	+
Xylidine Ponceau	Protein	+	+	+	+
Wagner's reagent	Alkaloids	?	-	?	-
Toluidine Blue	Phenolic compounds	+	-	-	-
Ferric chloride	Phenolic compounds	+	-	-	-
Nadi reagent	Terpenes	?	+	?	+
Vanillin hydrochloric acid	Tannins	?	-	?	-

Ultrastructure

Subcellular characteristics of mature (Fig. 6a, 8a) and in differentiation (Figs. 6b-d, 7, 8c-d, 9) laticifers present in the stems of *Celtis pubescens* (Figs. 6, 7) and *Trema micrantha* (Figs. 8, 9) were compared and found to be similar for the two these species.

The laticifer walls are thicker when in contact with adjacent parenchymatous cells and thinner when in contact with another laticifer wall (Fig. 6a), mainly in the terminal wall whose are degraded in the formation of the laticifers (Fig. 6a).

The mature laticifer has a large central vacuole (Fig. 6a, 8a), a peripheral cytoplasm, and small vacuoles close to the large vacuole (Figs. 6a, 8a). Laticifers in differentiation show cytoplasm contains dictyosomes (Figs. 6c, 7a, 8c-d), and plastids with evident stacked thylakoids (Figs. 7a, b, 9c) and is rich in mitochondria with conspicuous cristae (Figs. 6a-c, 8c-d, 9a), free ribosomes and polyribosomes (Figs. 9a, b) as well as dilated rough endoplasmic reticulum (Figs. 6b, 9a, b).

The dictyosomes are formed of few cisterns (Fig. 7a, 8d) and are usually located close to cell wall (Figs. 7a, 8d). They are active and produce vesicles from the *trans* face of the *trans*-Golgi network (Figs. 7a) that are released into the remaining peripheral cytoplasm (arrow, Figs. 7a). Some dictyosomes were found surrounded by endoplasmic reticulum (Fig. 9a, b). Osmiophilic material is present in the cytoplasm

(6b, 7d, 9a, b, d) and vacuole (8a, b, 9d), where it appears around small vesicles or forms small globules. Plastids contain starch grains (Figs. 7a-b, 9c), oil droplets and electron-dense material (Fig. 7b). The plastid disintegrates and releases the oil droplets, electron-dense material and starch into the cytoplasm (Fig. 7a, b). Sometimes the starch is broken before the release (Fig. 7b), and is wrapped by vacuole membranes to compose the latex (Figs. 7a, b). The nucleus has one or two nucleoli (Figs. 7d).

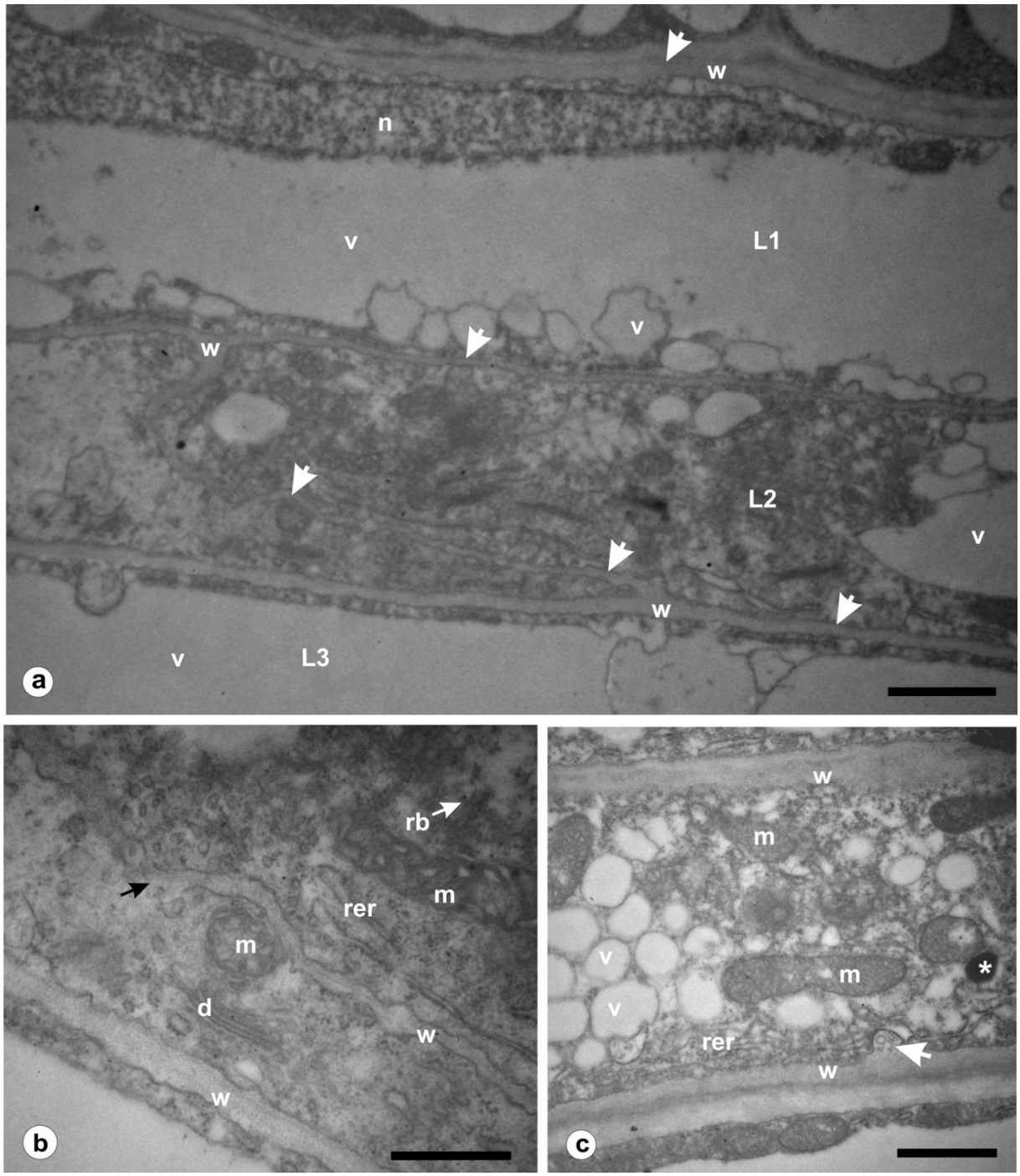

Fig. 6 Ultrastructure of articulated laticifers of *Celtis pubescens* (TEM). **a** Three laticifers; two mature laticifer (L1, L3) with peripheral cytoplasm showing a large vacuole (v) and other small vacuoles (v) near the wall (w), and part of the nuclei (n) in the first. Central laticifers in formation; note two cell with thin terminal wall (arrow) in degradation process (L2). **b** Cytoplasm rich in mitochondria (m), endoplasmic reticulum (er), and dictiossome (d) close to cell wall; note the disintegration processes of the terminal wall between the laticifers (black arrow). **c** Cytoplasm rich in mitochondria (m), small vacuoles (v), rough endoplasmic reticulum (rer) and osmiophilic bodies (*); note the thick wall (w) and vesicles being added to it (arrow). Scale bars: (a, c) 2 μm, (b) 1 μm.

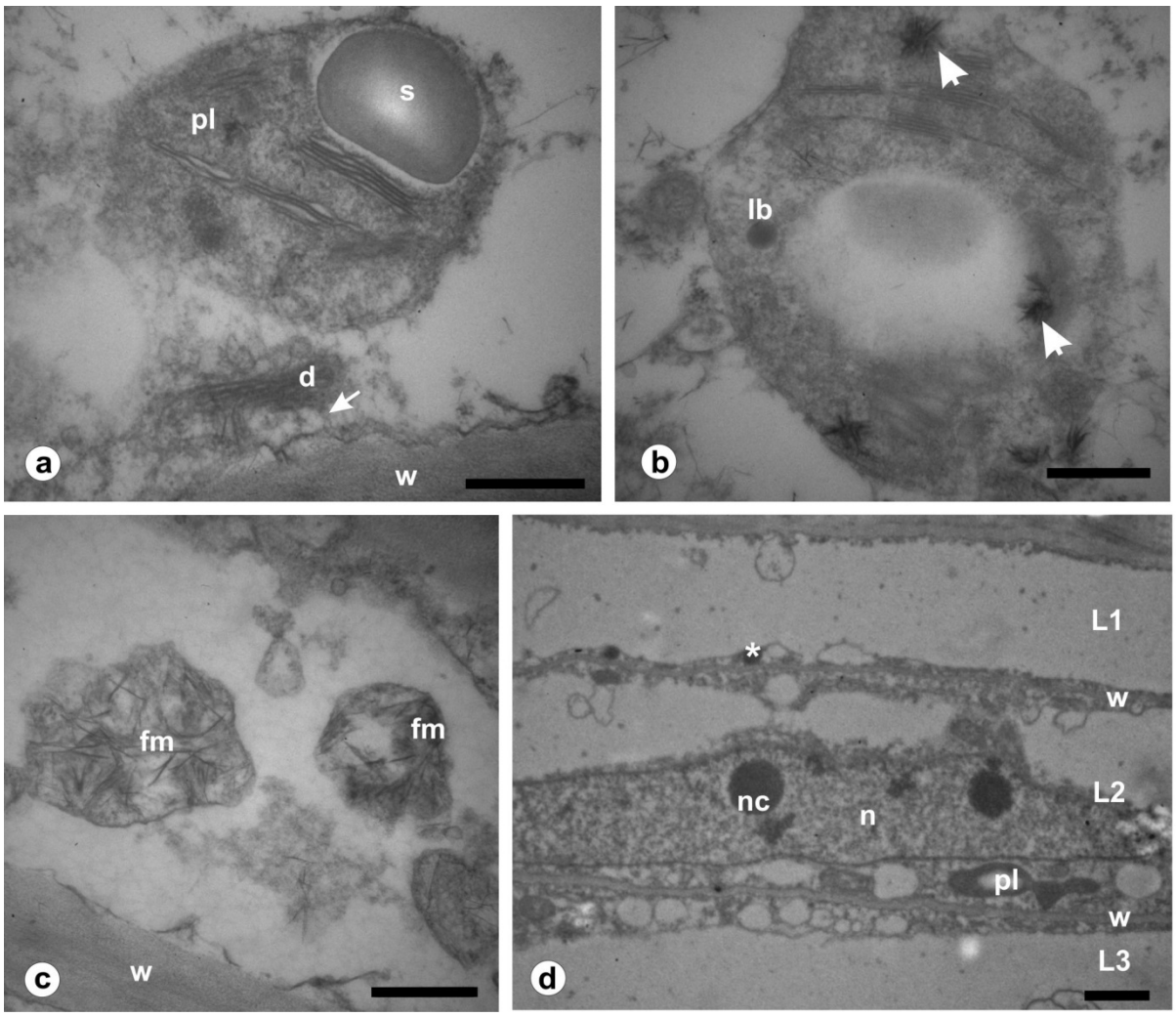

Fig. 7 Ultrastructure of articulated laticifers of *Celtis pubescens* (SEM). **a** Plastid (pl) with starch grains (s) and evident stacked thylakoids, and dictyosomes (d) near the wall (w). **b** Plastid (pl) with evident stacked thylakoids containing starch grains (s), lipid bodies (lb) and electron-dense material (arrows). **c** Detail of the electron-dense material (fm) inside the vacuole. **d** Three laticifers arranged in parallel (L1, L2, L3) showing their thin walls (w); note the peripheral cytoplasm with osmiophilic bodies (*), a plastid (pl), and the nucleus (n) with two nucleoli (nc). Scale bars: (a, c) 1 μm, (b) 2 μm, (d) 3 μm.

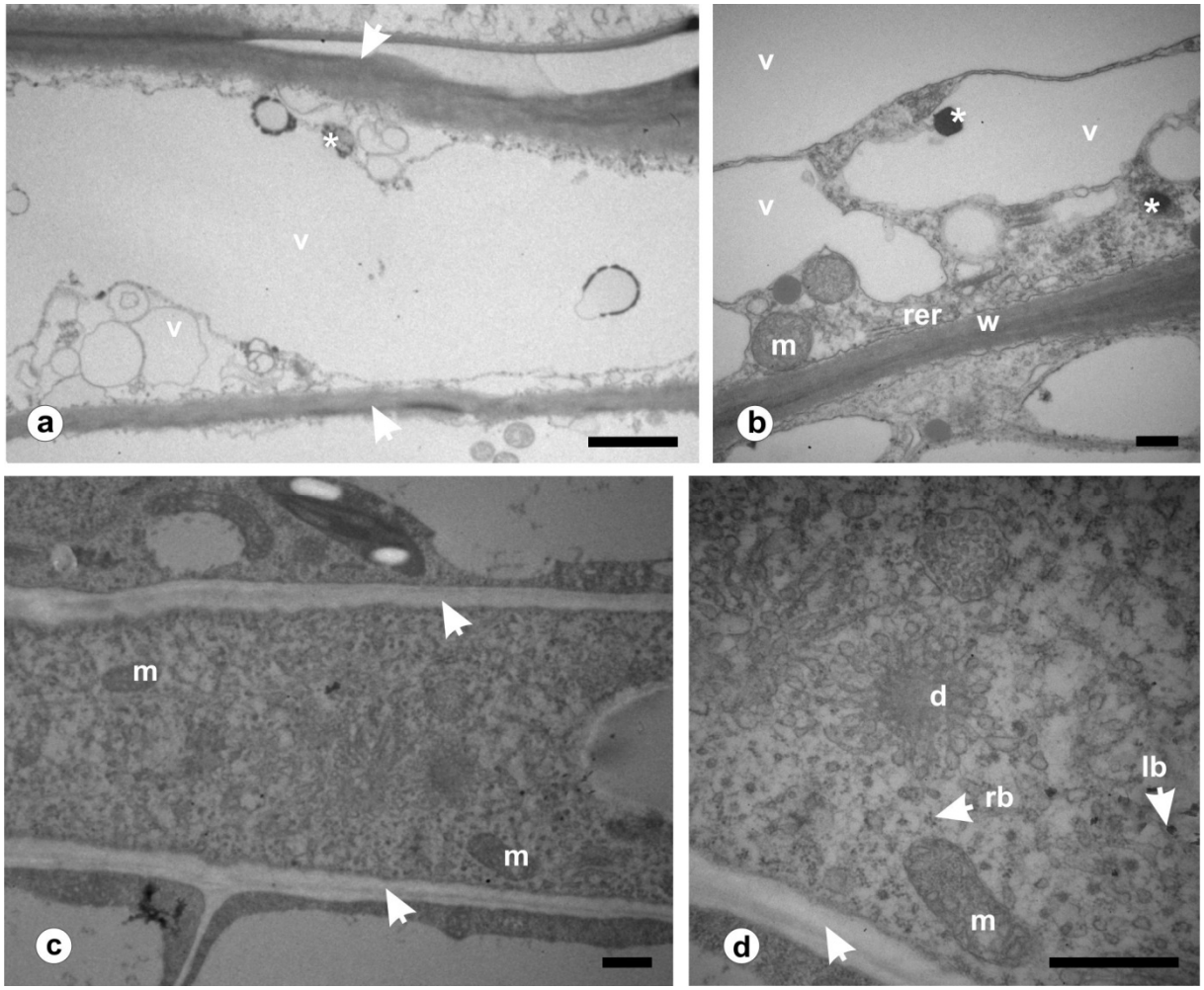

Fig. 8 Ultrastructure of articulated laticifers of *Trema micrantha* (TEM). **a** Peripheral cytoplasm of a mature laticifer (between arrows) showing a large vacuole and other small vacuoles with osmiophilic bodies (*). **b** Peripheral cytoplasm rich in mitochondria (m), rough endoplasmic reticulum (rer), vacuoles (v) formed by the endoplasmic reticulum, and osmiophilic bodies (*). **c-d** Laticifer in differentiation with active organelles. **d** Cytoplasm with mitochondria (m), dictyosomes (d), ribosomes (rb) and lipophilic bodies (lb); note the laticifer thick walls (arrow). Scale bars: (a) 3 μm, (b, c, d) 1 μm.

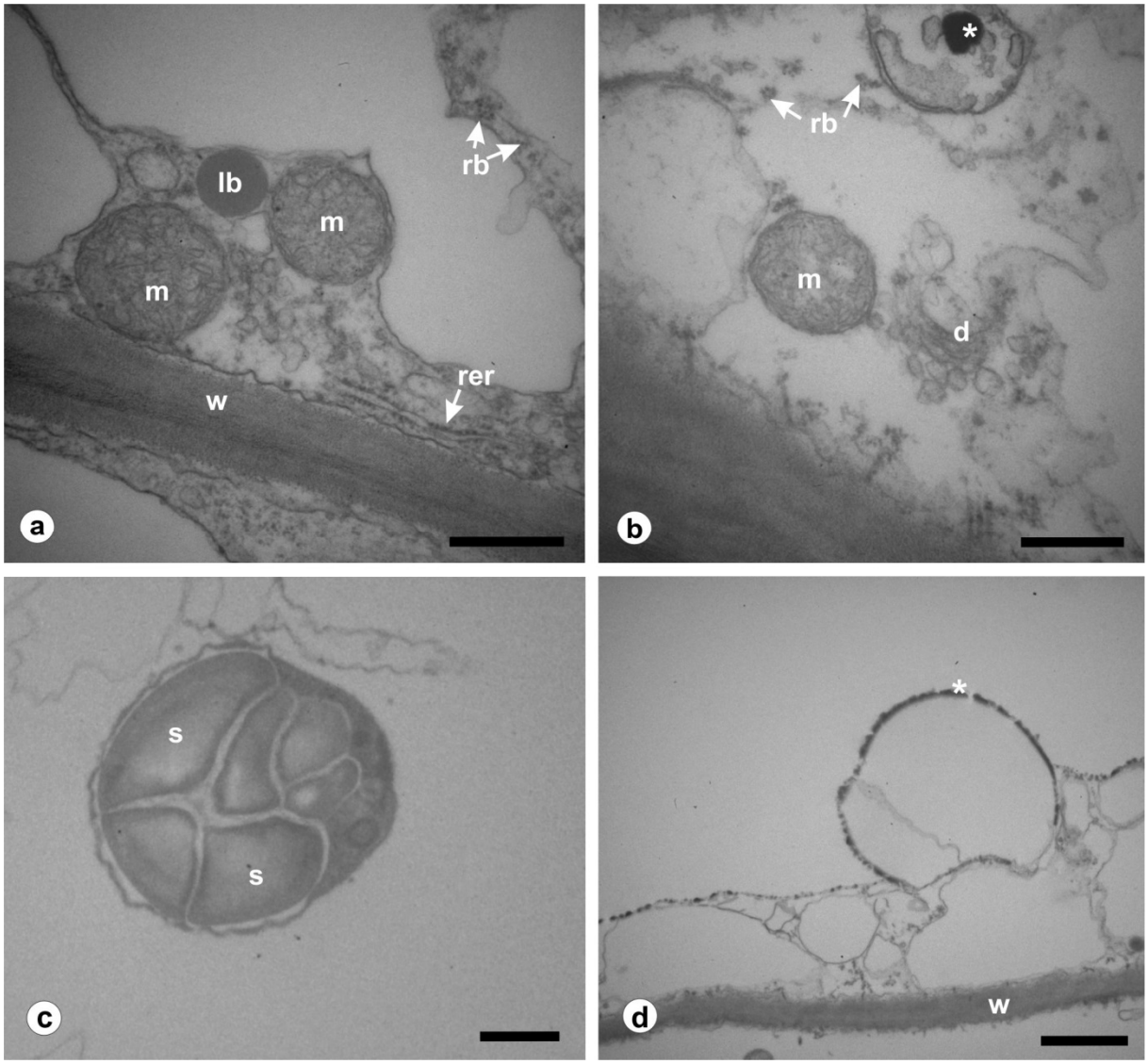

Fig. 9 Ultrastructure of articulated laticifers of *Trema micrantha* (SEM). **a** Cytoplasm with mitochondria (m), rough endoplasmic reticulum (rer), ribosomes (rb) and lipophilic bodies (lb); note the laticifer thick walls. **b** Cytoplasm with a mitochondria (m), dictyosomes (d) releasing vesicles in the trans-Golgi face, ribosomes (rb) and an osmiophilic body (*). **c** Plastid with starch grains (s). **d** osmiophilic material (*) around vesicles and tonoplast. Scale bars: (a, b, c) 1 μm, (d) 3 μm.

Cytochemical localization of cellulases and pectinases

Positive reactions for cellulase (Fig. 10) and pectinase (Fig. 11) activities were found in the cell wall close to middle lamella (Figs. 10a-c, 11a, c, d), vacuole (Figs. 10a, b, 11b) and endoplasmatic reticulum (Figs. 10a, 11b) by electron-dense crystalline inclusions. These electron-dense inclusions are reducing sugars, products of pectinase and cellulase activities in the laticifers that react with Benedict´s reagent. The reaction products apper widespread (Fig. 10a, b, 11a-c), or densely accumulated, forming groups in the vacuole (Figs. 10a, b, 11b) or in the cell wall (Figs. 10c, 11c, d). In the adjacent cells to the laticifers, positive reaction was also observed but less dense. In the control samples that were boiled without pectin or carboxymethylcellulase, the activity of cellulase was positive but less dense than the treated sample (Fig. 10d), however, the pectinase activity has positive reaction and was much similar to treated sample, located in the cell wall close to middle lamella (Fig. 11d).

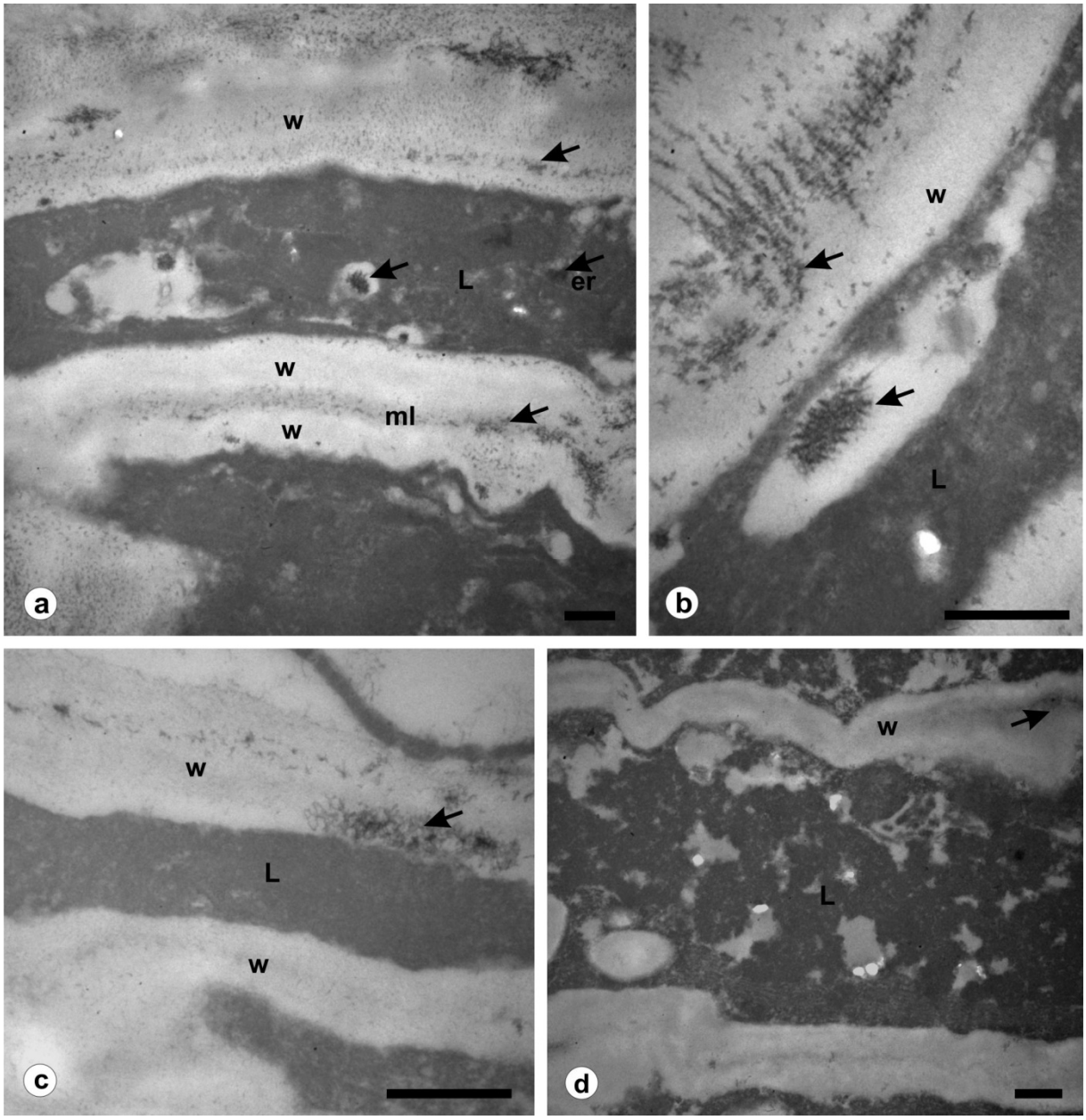

Fig. 10 Cytochemical localization of cellulase activity in the laticifers of *Celtis pubescens* (**a, b, d**) and *Trema micrantha* (**c**). **a-c** Laticifers incubated with carboxymethylcellulase. **a, b** Note the electron-dense reaction products in the middle lamella, protoplasmic and endoplasmic reticulum (positive reaction - arrow). **c** Reaction product of the cellulase close to cell wall of the laticifers (positive reaction - arrow). **d** Laticifer of control specimen incubated without cellulase. Note the absence of reaction product. There are only small electron-dense product in the middle lamella (arrow). Abreviations: (L) laticifers, (ml) middle lamellar, (w) cell walls. Scale bars: (a-d) 1 μm.

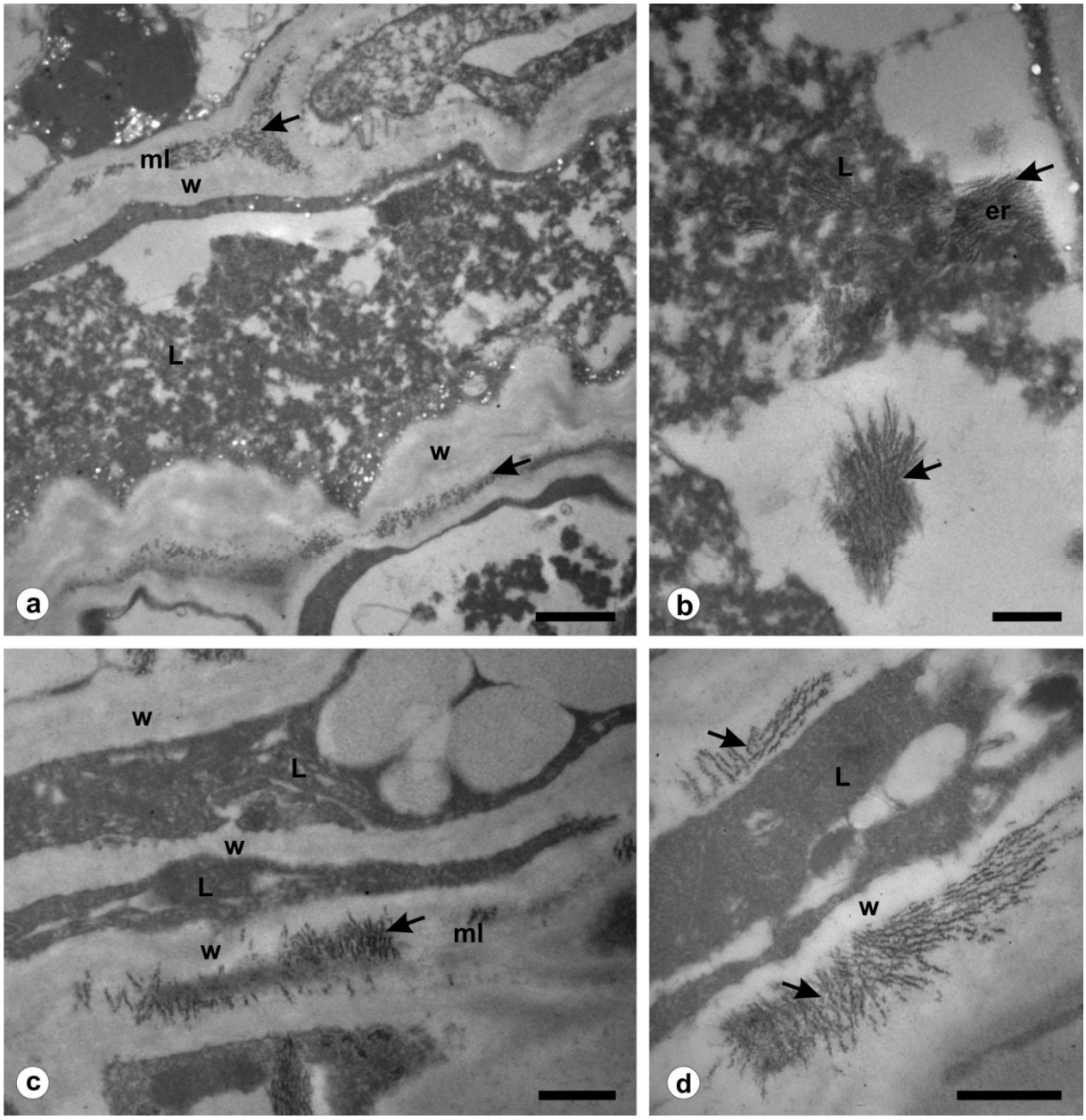

Fig. 11 Cytochemical localization of pectinase activity in the laticifers of *Celtis pubescens* (**a, b**) and *Trema micrantha* (**c, d**). **a-c** Laticifers incubated with pectin. **a** Electron-dense reaction products in the middle lamella (positive reaction - arrow). **b** Protoplasmic reaction product in the vacuole and in the endoplasmatic reticulum (positive reaction - arrow). **c** Reaction product of pectinase in the middle lamella (positive reaction - arrow). **d** Laticifer of control specimen incubated without pectin. Note that there are reaction product in the cell wall (positive reaction - arrow). Abreviations: (er) endoplasmatic reticulum, (L) laticifers, (ml) middle lamellar, (w) cell walls. Scale bars: (a) 2 μm, (b-d) 1 μm.

5.5 Discussion

The present report about the laticifers for *Celtis*, *Pteroceltis* and *Trema* is a great novelty for the family because in a previous study of Sytsma et al. (2002) laticifers were considered to be absent in these genera that were recently inserted into Cannabaceae. Therefore, our results corroborate the insertion of these genera into Cannabaceae together with *Cannabis* and *Humulus*, where the presence of laticifers throughout the plant has been described in previous studies (Meeuse 1942; Furr and Mahlberg 1981; Mesquita and Dias 1984; Hagel et al. 2008).

The laticifer structure of the Cannabaceae species studied so far is very similar. The study of laticifer origin showed that they are articulated different that previous studies that described non-articulated laticifers for *Cannabis sativa* and *Humulus lupulus* (Metcalfe 1966; Fahn 1979; Furr and Mahlberg 1981, Hagel et al. 2008), likely the lack of studies about laticifers ontogeny have took misundestood in the laticifers type. The classification of the laticifers type shows to need more attention, in Moraceae were described the both type of the laticifers (non-articulated - Van Veenendaal and Den Outer 1990; Machado and Santos 2004; Quintanar et al. 2004; Jacomassi et al. 2007, 2010; Kitajima et al. 2012; articulated -Milanez 1954; Topper and Koek-Noorman 1980).

The laticifer distribution along the plant body is also similar because they are widely distributed in the vegetative and floral organs, except for their absence in the sepals of the pistillate flower and stamens of the staminate flower of *Cannabis sativa*. An explanation for this absence could be related the reduced vasculature of these organs in *Cannabis sativa* (F. M. Leme, unpublished data) suggesting that the lack of the procambium not forms vascular bundles neither laticifers in the sepals.

Histochemical analyses showed that the main compounds of the latex of Cannabaceae species are polysaccharides, proteins and lipids (Furr and Mahlberg 1981; present study). Compounds such as starch grains (*P. tatarinowii*, *C. pubescens* and *T. micrantha*) and terpenes (*C. pubescens* and *T. micrantha*) are reported here for the first

time for the family. Alkaloids, previously found in *Cannabis sativa* by other researches (Furr and Mahlberg 1981), were not found in this study for the family, even when using fresh samples of *C. pubescens* and *T. micrantha*. Terpenes and phenols were found in the cytoplasm of glandular trichomes (Mahlberg and Kim 2004) and in the latex (Furr and Mahlberg 1981, present study) of *C. sativa.* It is likely that such terpenes and phenols constitute the cannabinoids that are defined as a group of terpenophenolic compounds and are exclusively found in *C. sativa* (Mechoulam and Gaoni 1967; Croteau et al. 2000; Andre et al. 2016). Recents studies showed two biosynthetic pathways that form the precursors of the cannabinoids: one is the plastid pathway (produce - methylerythritol 4-phosphate - MEP) and the other is the polyketide pathway (produce – olivetolic acid – OLA) (Andre et al. 2016, Sirikantaramas and Taura 2017). In *Trema micrantha* and *Celtis pubescens,* problably occurs the plastid pathway producing terpenes (present study). It is noteworthy that the polyketide pathway is still uncertain in terms of location; preliminary analyses indicate that it occurs in the cytoplasm (Gagne et al. 2012). Phenolic compounds may actually be absent or occur in an amount that it is not detectable by histochemical techniques. Thus, it is difficult to identify a potential cannabinoid production in the latex of *Celtis pubescens* and *Trema micrantha*.

Cannabis sativa (Mesquita and Dias 1984), *Celtis pubescens* and *Trema micrantha* (present study) are similar in the laticifer ultrastructure, while in Moraceae species it is different (see Heinrich 1970; Rachmilevitz and Fahn 1982; C. R. Marinho personal communication). The Cannabaceae species differ only in the amount of osmiophilic material that is larger in *Cannabis sativa* and lower in *C. pubescens* and *T. micrantha*, because of their different latex composition. Therefore, not only the distribution of the laticifers is a conserved character in the family but also the subcellular morphology of the laticifers.

The abundant mitochondria with conspicuous cristae detected in the analysed species are related to the energy supply for synthesis of compounds in the secretory structures (Wilson and Mahlberg 1980; Evert 2006). Dictyosomes act on the

secretion of polysaccharides (Fahn 1979, 1990; Dickison 2000; Evert 2006) and the plastids are involved in the production of terpenes and starch grains (Heinrich 1970; Wilson and Mahlberg 1978; Evert 2006). Beyond producing proteins and ribosomes (Evert 2006), the endoplasmic reticulum also participates in the formation of small vacuoles in the laticifers (Mesquita 1969; Nessler and Mahlberg 1977; Wilson and Mahlberg 1978; Mesquita and Dias 1984; Cai *et al.* 2009; present study).

The autophagy, the formation of a large vacuole from small vacuoles with participation of the endoplasmic reticulum followed by cytoplasm lysis, is usual in laticifers (i.e. *Lupinus albus* L., Mesquita 1969; *Papaver soniferum* L., Nessler and Mahlberg 1977; and *Asclepia syriaca* L., Wilson and Mahlberg 1978; *Ficus carica*, Rachmilevitz and Fahn 1982; *Cannabis sativa*, Mesquita and Dias 1984; *Euphorbia kansui* Liou, Cai et al. 2009, Zhang et al. 2018) and evident in the laticifers of Cannabaceae and Moraceae species (Heinrich 1970; Rachmilevitz and Fahn 1982; Mesquita and Dias 1984; present study), being considered an important process in the latex production and development of non-articulated laticifers (Zhang et al. 2018). The hydrolysis renders the cytoplasm more transparent and forms the small particles (Cai et al. 2009). Such particles, together with other compounds produced by the organelles such as starch, oil droplets, fibrillar material, proteins, and phenolics before cytoplasm hydrolysis, compose the latex (Cai et al. 2009; present study).

The latex composition of Cannabaceae species (Furr and Mahlberg 1981; present study) indicates that laticifers act in plant defense against herbivores. This defense includes preventing the insect from feeding on the plant and the accumulation of gums, gel or phenols that form tyloses, suggesting an increased resistance, as observed in elm trees (Ulmaceae, Dickison 2000). The laticifer distribution on the plant body is another criterion that cannot be neglected in the inference of functions for such an interesting and complex secretory structure. In *Ficus* species, laticifers have been considered to act in promoting the pollination by protecting the galled flowers (flowers where the wasp offspring emerges) against attack by non-pollinating wasps (Marinho et al. 2018). Cannabaceae consist of exclusively wind-pollinated species (Miller 1970;

Barth et al. 1975; Arruda and Sazima 1988; Culley et al. 2002), thus different selective pressures should act on laticifer distribution along the flower. Differently from *Ficus*, the flowers of Cannabaceae are exposed favoring wind pollination but also exposed to UV radiation, insects or other animals. Thus, protection appears to be the main function of laticifers in Cannabaceae. This can be illustrated by the finding of laticifers in the stigmatic region of the species studied, which is an important part of the flower for the reproductive success of wind-pollinated species (Culley et al. 2002; Friedman and Barrett 2009) with rare reports of laticifers.

The formation process of articulated laticifers of *Celtis pubescens* and *Trema micrantha* seems to be facilited by the dissolution of cellulose and pectin of the terminal cell wall and middle lamella by cellulase and pectinase enzymes (Nessler and Malhberg 1981; Allen and Nessler 1984). Pectinase and cellulase activities were reported for laticifers (Sheldrake 1969, Nessler and Mahlberg 1981; Allen and Nessler 1984; Marinho and Teixeira 2016) and are important in the process of dissolution of the cell wall.

The reaction product shows pectinase activity in the apical and lateral region of the laticifers wall; suggesting therefore that the pectinase activity also can be important in the lateral expansion of the laticifers (Allen and Nessler 1984; present study). Pectinase activity are found inclusive in the control test, indicate the saturation of the pectinase by endogenous pectin of the middle lamella and the addition of exogenous pectin not alter the density of reaction product in this region, as found in non-articulated laticifers (Allen and Nessler 1984).

The results suggest that cellulase and pectinase enzymes are synthesized on endoplasmatic reticulum and armazened in the vacuole and then are secreted to cell wall though exocytosis (Liang et al. 2009; Yu et al. 2004; Wang et al 1998).

5.6 Conclusion

In conclusion, we suggest that the presence of articulated laticifers can be a synapomorphy for Cannabaceae. The wide distribution of laticifers in vegetative and floral organs is reported here for the first time for the family, as well as the occurrence of large starch and terpenes in the latex. The similar laticifer ultrastructure of *C. sativa, C. pubescens* and *T. micrantha* should indicate that these species produce the same chemical classes of compounds but in different quantities. We emphasize the importance of more ecological studies to better understand the role of laticifers in the floral organs that in this first analysis appear to be involved in the protection of the flower.

5.7 References

Allen RD, Nessler CL (1984) Cytochemical localization of pectinase activity in laticifers of Nerium oleander L. Protoplasma 119:74-78

Andre CM, Hausman J-F, Guerriero G (2016) *Cannabis sativa*: The Plant of the Thousand and One Molecules. Front Plant Sci 7:1-17

Arruda VLV, Sazima M (1988) Polinização e reprodução de *Celtis iguanaea* (Jacq.) Sarg. (Ulmaceae), uma espécie anemófila. Rev Bras Bot 11:113-122

Ashton CH (2001) Pharmacology and effects of *Cannabis*: a brief review. Br J Psychiatry 178:101-106

Barth O, Macieira E, Corte-Real S (1975) Morfologia do polen anemofilo alergisante no Brasil. Mem Inst Oswaldo Cruz 73:141-150

Bal AK (1974) Cellulase. In: Haya MA (ed) Electron microscopy of enzymes, vol 3. Van Nostrand Reinhold, New York, pp 68-79

Cai X, Li W, Yin L (2009) Ultrastructure and cytochemical localization of acid phosphatase of laticifers in *Euphorbia kansui* Liou. Protoplasma 238:3-10

Croteau R, Kutchan TM, Lewis NG (2000) Natural products (secondary metabolites) In: Buchanan BB, Gruissem W, Jones RL, eds. Biochemistry and Molecular Biology

of Plants. Wiley, 1250-1318

Culley TM, Weller SG, Sakai AK (2002) The evolution of wind pollintion in angiosperms. Trends Ecol Evol 17:361-369

David R, Carde J (1964) Coloration différentielle des inclusions lipidiques et terpeniques des pseudophylles du pin maritime au moyen du reactif Nadi. Comptes Rendus Hebdomadaires des Séances de l'Academie des Sciences Paris D258:1338-1340

Dickison W (2000) Integrative plant anatomy. San Diego: Academic Press

Evert RF (2006) Esau's Plant Anatomy: meristems, cells, and tissues of the plant body: their structure, function, and development. Ed. Wiley & Sons. New Jersey

Fahn A (1979) Secretory tissues in plants. London: Academic Press

Fahn A (1990) Plant Anatomy. London: Butterworth-Heinemann

Friedman J, Barrett SCH (2009) Wind of change: New insights on the ecology and evolution of pollination and mating in wind-pollinated plants. Ann Bot 103:1515-1527

Furr M, Mahlberg PG (1981) Histochemical analyses of laticifers and glandular trichomes in *Cannabis sativa*. J Nat Prod 44:153-159

Gagnea SJ, Stouta JM, Liua E, Boubakira Z, Clarka SM, Page JE (2012) Identification of olivetolic acid cyclase from *Cannabis sativa* reveals a unique catalytic route to plant polyketides. PNAS, 31:12811-12816

Hagel JM, Yeung EC, Facchini PJ (2008) Got milk ? The secret life of laticifers. Trends Plant Sci 1360-1385

Happyana N, Agnolet S, Muntendam R, Dam A Van, Schneider B, Kayser O (2013) Analysis of cannabinoids in laser-microdissected trichomes of medicinal *Cannabis sativa* using LCMS and cryogenic NMR. Phytochemistry 87:51-59.

Heinrich G (1970) Elektronenmikroskopische Untersuchung der Milchrohren von Ficus elastica. Protoplasma 70:317-323

Hill MN, Patel S, Campolongo P, Tasker JG, Wotjak CT, Bains JS (2010) Functional interactions between stress and the endocannabinoid system: from synaptic

signaling to behavioral output. Journal Neurosci 30:14980-14986. https://doi.org/10.1523/JNEUROSCI.4283-10.2010

Honório KM, Arroio A, Silva ABF (2006) Aspectos terapêuticos de compostos da planta *Cannabis sativa*. Quim Nova 29:318-325

Jacomassi E, Moscheta IS, Machado SR (2007) Morfoanatomia e histoquímica de *Brosimum gaudichaudii* Trécul (Moraceae). Acta Bot Bras 21:575-597

Jacomassi E, Moscheta IS, Machado SR (2010) Morfoanatomia e histoquímica de órgãos reprodutivos de *Brosimum gaudichaudii* (Moraceae). Rev Bras Bot 33:115-129

Jensen WE (1962) Botanical histochemistry: Principles and practice. San Francisco: W. H. Freeman and Co.

Johansen DA (1940) Plant Microtechnique. New York: McGraw-Hill Book Co. Inc.

Walter S. Judd, Christopher S. Campbell, Elizabeth A. Kellogg, Peter F. Stevens, Michael J. Donoghue (2009) Sistemática Vegetal - 3.ed.: Um Enfoque Filogenético. Ed. Artmed

Karnovsky MJ (1965) A formaldehyde-glutaraldehyde fixative of hight osmolality for use in electron microscopy. J Cell Biol 27:137-138

Kim E-S, Mahlberg PG (1991) Secretory cavity development glandular trichomes of *Cannabis sativa* L. (Cannabaceae). Am J Bot 78:220-229

Kim E-S, Mahlberg PG (1997) Immunochemical localization of tetrahydrocannabinol of (THC) in cryofixed glandular trichomes of *Cannabis* (Cannabaceae). Am J Bot 84:336-342

Kitajima S, Taira T, Oda K, Yamato KT, Inukai Y, Hori Y (2012) Comparative study of gene expression and major proteins function of laticifers in lignified and unlignified organs of mulberry. Planta 235:589-601

Liang S, Wang H, Yang M, Wu H (2009) Sequential actions of pectinases and cellulases during secretory cavity formation in Citrus fruits. Trees 23:19-27

Lillie RD (1965) *Histopathologic technic and practical histochemistry*. New York: McGraw-Hill Book Company

Mace M, Howell C (1974) Histochemistry and identification of condensed tannin

precursors in roots of cotton seedlings. Can J Bot 52:2423-2426

Mahlberg PG (1993) Laticifers: An Historical Perspective. Bot Rev 59:1-23

Mahlberg PG, Kim ES (2004) Accumulation of Cannabinoids in Glandular Trichomes of Cannabis (Cannabaceae). J lnd Hemp 9(1):15-35

Marinho CR, Pereira RAS, Peng Y-Q, Teixeira SP (2018) Laticifer distribution in fig inflorescence and its potential role in the fig-fig wasp mutualism. Acta Oecol 90:160-167

Marinho CR, Teixeira SP (2016) Cytochemical localization of pectinases and cellulases in developing laticifers of *Maclura tinctoria* and *Ficus montana* (Moraceae). European Microscopy Congress 2016

Mechoulam R, Gaoni Y (1967) Recent advances in the chemistry of hashish. Fortschritte der Chemie Organischer Naturstoffe 25, 175-213

Meeuse ADJ (1942) A study of intercellular relationships among vegetable cells with special reference to sliding growth'' and to cell shape. Recueil Trav Bot Neerl 38:18-140

Mesquita JF (1969) Electron microscope study of the origin and development of the vacuoles in root-tip cells of *Lupinus albus* L. J Ultrastruct Res 26:242-250

Mesquita JF, Dias JDS (1984) Ultrastructural and cytochemical study of the laticifers of *Cannabis sativa* L. Bol Soc Brot 57:337-356

Metcalfe CR (1966) Distribution of latex in the plant kingdom. Economic Botany 21:115-127

Milanez FR (1954) Sobre os laticíferos foliares de *Ficus retusa*. Rodriguésia 28/29:159-192

Miller N (1970) The genera of Cannabaceae in the southeastern United States. J Arnold Arbor 51:185-203

Nessler C, Mahlberg P (1977) Ontogeny and cytochemistry of alkaloidal vesicles in laticifers of *Papaver somniferum* L. (Papaveraceae). Am J Bot 64:541-551

Nessler CL, Mahlberg PG (1981) Cytochemical localization of cellulase activity in articulated, anastomosing laticifers of *Papaver somniferum* L. (Papaveraceae). Am J

Bot 68:730-732

O'Brien TP, Feder N, McCully ME (1964) Polychromatic staining of plant cell walls by toluidine blue O. Protoplasma 59:368-373

Pearse AGE (1985) Histochemistry: theoretical and applied. Edinburgh: C. Livingstone

Quintanar A, Castrejón JLZ, Lopéz C, Salgado-Ugarte IH (2004) Anatomía e histoquímica de la corteza de cinco especies de Moraceae. Polibotánica 15-38

Rachmilevitz T, Fahn A (1982) Ultrastructure and development of the laticifers of *Ficus carica* L. Ann Bot 49:13-22

Ramadan MA, Ahmad AS, Nafady AM, Mansour AI (2008) Macro and micromorphology studies of the leaf, stem and stem bark of *Ficus pandurata* Hance. cultivated in Egypt. Bull. Pharm. Sci., Assiut University 31:1-28

Smith FH, Smith EC (1942) Anatomya of the inferior ovary of *Darbya*. Am J Bot 29(6):464-471

Sirikantaramas S, Taura F (2017) Cannabinoids: Biosynthesis and Biotechnological Applications. In: Chandra S., Lata H., ElSohly M. (eds) *Cannabis sativa* L. - Botany and Biotechnology. Springer, Cham pp 183-206

Sheldrake AR (1969) Cellulase in Latex and its Possible Significance in Cell Differentiation. Planta 89:82-84

Sytsma KJ, Morawetz J, Pires JC et al (2002) Urticalean Rosids: Circumscription, Rosid ancestry, and phylogenetics based on rbcL, trnL-F, and ndhF sequences. Am J Bot 89(9): 1531–1546.

Topper SMC, Koek-Noorman J (1980) The occurrence of axial latex tubes in the secondary xylem of some species of Art. IAWA Bulletin I:113-119

Van Veenendaal WLH, Den Outer RW (1990) Distribution and development of the non-articulated branched laticifers on *Morus nigra* L. (Moraceae). Acta Bot Neerl 39:285-296

Vidal BC. 1970. Dichroism in collagen bundles stained with xylidine-Ponceau 2R. Annales d´Histochimie 15:289-296

Zhang Q, Wang D, Zhang H, Wang M, Li P, Fang X, Cai X (2018) Detection of

autophagy processes during the development of nonarticulated laticifers in *Euphorbia kansui* Liou. Planta 247:845-861. https://doi.org/10.1007/s00425-017-2835-0

Wang XY, Guo GQ, Nie XW, Zheng GC (1998) Cytochemical localization of cellulase activity in pollen mother cells of David lily during meiotic prophase I and its relation to secondary formation of plasmodesmata. Protoplasma 204:128-138

Williamson EM, Evans FJ (2000) Cannabinoids in clinical practice. Drugs 60:1303-1314

Wilson KJ, Nessler CL, Mahlberg PG (1976) Pectinase in *Asclepias* Latex and its Possible Role in Laticifer Growth and Development. Am J Bot 63(8):1140-1144

Wilson K, Mahlberg P (1978) Ultrastructure of non-articulated laticifers in mature embryos and seedlings of *Asclepias syriaca* L. (Asclepiadaceae). Am J Bot 65:98-109

Yang M-Q, Velzen R Van, Bakker FT, Sattarian A, Li D, Yi T (2013) Molecular phylogenetics and character evolution of Cannabaceae. Taxon 62:473-485

Yu CH, Guo GQ, Nie XW, Zheng GC (2004) Cytochemical localization of pectinase activity in pollen mother cells of Tobacco during meiotic prophase I and its relation to the formation of secondary plasmodesmata and cytoplasmic channels. Acta Bot Sin 46:1443-1453

Final considerations

The present study clarified the development of the flower in some Cannabaceae and Ulmaceae species. Our data contribute to the knowledge of floral construction and the occurrence of laticifers in the group, adding new information to the families that had changed in the latest phylogenetic analyses (Sytsma et al., 2002; Yang et al., 2013).

1. The floral development of Cannabaceae and Ulmaceae species show that the follow possesses are involved in the floral reduction: (1) absence of whorls from inception resulting in apetaly and dicliny (androecium or gynoecium) and (2) abortion of organs or whorls (carpels or stamens) resulting in dicliny and in a pseudomonommerous gynoecium. The pseudomonomerous gynoecium is formed by abortion of one of the carpels, and the reduced carpel exhibits reduced vascularization and does not form an ovule.
2. The interpretation of the floral ontogeny of Cannabaceae species supports the current phylogeny of the family and the relationship between *Celtis* and *Trema*, and *Cannabis* and *Humulus* (Yang et al., 2013). *Celtis* and *Trema* share a robust calyx, diclinous flowers formed by the initiation and subsequent abortion of organs, inflexed stamens and a bifacial stigma. *Cannabis* and *Humulus* share diclinous flowers characterized by the complete absence of androecium or gynoecium, straight stamens, and a unifacial stigma.
3. The flowers of Ulmaceae have no hypanthium. The atypical merism (increase or decrease of organs numbers) is a result of the space left by reduction of the whorls and/or of organs in *Ampelocera glabra*. The features found for *Ampelocera glabra* such as monoecy, diclinous flowers, tetramerous calyx, polyandry, and a suppressed carpel with fewer vascular bundles suggest that the flowers of the species of the tropical clade of Ulmaceae have acquired features more recently than temperate ones.

4. *Celtis* was classified as monoecious, with two floral morph types, pistillate and staminate flowers in the same individual. Flowers previously considered as perfect are actually structurally perfect but functionally pistillate, the staminodes have no pollen or atypical pollen and the wall anthers have no typical endothecium. The floral features are important for the characterization of the clades and species of *Celtis* and additional studies with Asian and African species would be important for the systematics of the group.
5. The discovery of laticifers in *Ampelocera glabra*, *Zelkova serrata* (Ulmaceae), *Celtis pubescens*, *Pteroceltis tatarinowii* and *Trema micrantha* (Cannabaceae) provides novel information for these families, mainly in Ulmaceae in which laticifers were previously considered to be absent (see Sytsma et al., 2002). Now we can attest that the laticifers widely occurs in Urticalean rosids and can be considered as a putative synapomorphy for this group.
6. The wide distribution of laticifers mainly in floral organs is reported by the first time for Cannabaceae and Ulmaceae, as well as the occurrence of large starch and terpenes in the latex. Laticifers appear to be related with protection of floral organs.
7. The process of degradation of cellulose and pectin by the cellulase and pectinase activity promote the dissolution of cell wall between the terminal walls of the cells that form the articulated laticifers in *Celtis pubescens* and *Trema micrantha*.
8. The processes that take to floral reduction and the presence of laticifers showed a connection with the anemophily. Floral reduction becomes the flowers inconspicuous and the laticifers assist them in the defense against phytophagous.

Our data help to characterize genera or subclades of Cannabaceae and Ulmaceae and contribute to a more comprehensive understanding of the floral diversity and evolution in these families and in Rosales. However, ecological studies are still important to better understand the role of laticifers in the flower that in this first analysis appear to be involved in the protection.

References

Sytsma KJ, Morawetz J, Pires JC et al (2002) Urticalean Rosids: Circumscription, Rosid ancestry, and phylogenetics based on rbcL, trnL-F, and ndhF sequences. Am J Bot 89(9): 1531–1546.

Yang M-Q, Velzen R Van, Bakker FT, Sattarian A, Li D, Yi T (2013) Molecular phylogenetics and character evolution of Cannabaceae. Taxon 62:473-485

Anexo 1

COORDENADORIA DE PÓS-GRADUAÇÃO
INSTITUTO DE BIOLOGIA
Universidade Estadual de Campinas
Caixa Postal 6109. 13083-970, Campinas, SP, Brasil
Fone (19) 3521-6378. email: cpgib@unicamp.br

DECLARAÇÃO

Em observância ao **§5º do Artigo 1º da Informação CCPG-UNICAMP/001/15**, referente a Bioética e Biossegurança, declaro que o conteúdo de minha Tese de Doutorado, intitulada "***DESENVOLVIMENTO FLORAL E LATICÍFEROS EM ESPÉCIES DE CANNABACEAE MARTINOV E ULMACEAE MIRB.***", desenvolvida no Programa de Pós-Graduação em Biologia Vegetal do Instituto de Biologia da Unicamp, não versa sobre pesquisa envolvendo seres humanos, animais ou temas afetos a Biossegurança.

Assinatura: Flávia Maria Leme

Nome do(a) aluno(a): Flávia Maria Leme

Assinatura: Teixeira

Nome do(a) orientador(a): Simone de Pádua Teixeira

Data: 12/09/2018

Anexo 2

Declaração

As cópias de artigos de minha autoria ou de minha co-autoria, já publicados ou submetidos para publicação em revistas científicas ou anais de congressos sujeitos a arbitragem, que constam da minha Dissertação/Tese de Mestrado/Doutorado, intitulada **Floral development and laticifers in species de Cannabaceae Martinov and Ulmaceae Mirb.**, não infringem os dispositivos da Lei n.° 9.610/98, nem o direito autoral de qualquer editora.

Campinas, 12/09/2018

Assinatura : Flávia Maria Leme

Nome do(a) autor(a): **Flávia Maria Leme**

RG n.° 1459713

Assinatura : Teixeira

Nome do(a) orientador(a): **Simone de Pádua Teixeira**

RG n.° 20.267.105-7